

Charles University  
Faculty of Science

Developmental and Cell Biology



Mgr. Aleshkina Daria

**Non-coding RNAs in oocyte and early embryo  
Nekódující RNA v oocytu a časném embryu**

Doctoral thesis

Supervisor: Ing. Andrej Susor, Ph.D.

Institute of Animal Physiology and Genetics, Czech Academy of Sciences

Prague, 2022

**Prohlášení:**

Prohlašuji, že jsem závěrečnou práci zpracovala samostatně a že jsem uvedla všechny použité informační zdroje a literaturu. Tato práce ani její podstatná část nebyla předložena k získání jiného nebo stejného akademického titulu.

I hereby declare that I wrote this thesis independently, using the cited literature. This work or a substantial part of it has not been submitted elsewhere to obtain any other academic degree.

18. 2. 2022 v Praze

Aleshkina Daria

## **Acknowledgment**

Foremost, I would like to express my deepest gratitude to my supervisor Ing. Andrej Susor, Ph.D. for the priceless guidance on every step of my studies and help with all questions or doubts. Valuable discussions and provided opportunities allowed me to successfully complete my dissertation and gain rich knowledge about the topic. I am also very grateful to Ph.D. Rajan Iyyappan for the endless support, insight about the project and explanations of complicated molecular methods which definitely improved my scientific competence.

I would like to thank my lab colleagues for excellent work atmosphere and outdoor lab events, especially Barbara Schmidtova, Michal Dvořan, Anna Jindrova, Edgar Del Llano and Ph.D. Denisa Jansova. Also I appreciated a lot help from Jaroslava Šupolíková and Markéta Hančová with experiments, including early morning oocyte isolations. Moreover, I thank Anatol Marta, Ph.D. Zuzana Majtanova, Katerina Nemes and Yaroslav Nemes for the wonderful time at IAPG.

Moreover, I thank my friend, family, and particularly my husband Ph.D. Dmytro Didukh for support, discussions and helpful comments about my project.

## **Contents**

Abstrakt (česky).....	4
Abstract.....	5
1. Introduction.....	6
1.1 Role of ncRNAs in the eukaryotic cell .....	7
1.1.1 Role of ncRNAs in transcription and RNA processing .....	8
1.1.2 Role of ncRNAs in translation.....	9
1.2 Mammalian oocyte, early embryo and transcriptome.....	11
1.2.1 Translational control in mammalian oocyte and early embryo.....	13
1.3 LncRNAs in the germ cells.....	14
2. Aims of the thesis .....	16
3. Comments on publications.....	17
3.1 NcRNA <i>BCI</i> influences translation in the oocyte .....	17
3.2 Oocyte specific lncRNA variant <i>Rose</i> influences oocyte and embryo development.....	19
3.3 Single Molecule RNA Localization and Translation in the Mammalian Oocyte and Embryo .....	21
4. Discussion.....	24
5. Conclusions.....	27
6. References.....	28
7. Abbreviations.....	36
8. Curriculum Vitae .....	38
9. Research papers .....	40



## **Abstrakt (česky)**

Nekódující RNA (ncRNA), které byly dříve považovány za „transkripční šum“, jsou dnes známé jako klíčové molekuly v hlavních buněčných procesech. ncRNA jsou exprimovány ve vysokých hladinách – pouze 2 % transkribovaného genomu u vyšších eukaryot odpovídá proteinům kódujícím RNA. Je známo, že řada různých ncRNA má strukturní, funkční či regulační role, ale vliv většiny nekódujících transkriptů zůstává nejasný. Mezi ncRNA jsou obzvláště zajímavé dlouhé ncRNA (lncRNAs, delší než 200 bp). LncRNA nemají jednotnou funkci, ale v mnoha studiích byly pozorovány regulace na transkripční a translační úrovni, které jsou založené na regulaci lncRNA. Proto by nové lncRNA mohly pomoci vylepšit syntézu proteinů ve vysoce diferencovaných buněčných typech. Zejména plně dorostlý savčí oocyt a rané embryo vyžadují přesně kontrolovanou translaci maternálních transkriptů k tomu, aby mohla být koordinována meiotická progresse a časný vývoj embrya, zatímco je transkripce umlčena. Zaměřili jsme se tedy na studium zapojení ncRNA do syntézy proteinů a následného vlivu na fyziologii oocyty a raného embrya.

Nejdříve jsme analyzovali expresi a distribuci několika ncRNA během meiotického zrání a časného vývoje embrya – jmenovitě *BCI* (*Brain cytoplasmic RNA 1*), *Rose* (*lncRNA in Oocyte Specific Expressed*), *Rn7sk* (*RNA Component of 7SK Nuclear Ribonucleoprotein*), *Neat2* (*Nuclear Enriched Abundant Transcript 2*) a *IAPLtrla* (*Intracisternal A Particle Long terminal repeat*). Zjistili jsme, že tyto ncRNA měly ve stádiu GV jasně danou jadernou či cytoplazmatickou lokalizaci. Jejich exprese klesala během maturace a následného vývoje. Jelikož jsou funkce ncRNA přímo spojeny s jejich subcelulárním umístěním, tak jsme pro další analýzu vybrali dvě cytoplazmatické ncRNA – *BCI* a *Rose*. Pozorovali jsme, že *BCI* a *Rose* jsou s ribozomy asociované ncRNA, což naznačuje jejich roli v translační regulaci a fyziologii savčího oocyty. Naše výsledky naznačují, že ncRNA *BCI* potlačuje cap-dependentní iniciaci translace v GV, což je v souladu s její navrhovanou úlohou v dendritech. Prokázali jsme však také, že *BCI* inhibuje translaci specifických mRNA, *Dlg4* a *Actb*, prostřednictvím interakcí s 3'UTR. Tato interakce vyžaduje proteinovou souhru podobně jako mnoho regulačních ncRNA, které působí jako součást ribonukleoproteinových komplexů. Navíc jsme vyvinuli nový RNA-PLA přístup, který nám umožňuje detekovat lokalizovat jednotlivé komponenty, RNA a proteinu. RNA-PLA nám tedy umožnila vizualizovat v GV oocytech interakci *BCI* s vazebným partnerem Fragile X Mental Retardation Protein (FMRP). Dále bylo zjištěno, že shlukování proteinu FMRP v cytoplazmě je způsobeno nadměrnou expresí *BCI* v MII oocyty. Potvrdili jsme tedy, že ncRNA *BCI* reguluje translaci specifických maternálních mRNA.

Dále jsme se zaměřili na druhou s ribozomy asociovanou lncRNA *Rose*, která je v oocyty exprimována ve dvou variantách – jedna z nich je specifická pro oocyt. *Rose* je u transkripčně aktivních stádií lokalizovaná v cytoplazmě a jádře, kdežto u transkripčně neaktivních buněk je lokalizována pouze v cytoplazmě. Ačkoliv nadměrná exprese *Rose* nijak neovlivňuje zrání oocytů, tak její snížená exprese má za následek abnormality v cytokinezi oocytů a zhoršený preimplantační vývoj embrya.

Studovali jsme tedy celou řadu ncRNA, jejich expresi a lokalizaci v subcelulárním kontextu během meiotického zrání a raného embryonálního vývoje. Kromě toho jsme identifikovali ncRNA, které přispívají k buněčné fyziologii oocyty a časnému vývoji embrya. Naše výsledky přispívají k lepšímu pochopení regulačních procesů během vývojových událostí v savčích oocytech a embryích, které jsou založené na ncRNA.

## **Abstract**

Once considered as ‘transcriptional noise’ noncoding RNAs (ncRNAs) nowadays are known to be key molecules in major cellular processes. ncRNAs are expressed at very high levels as only 2% of transcribed genome corresponds to protein-coding RNAs in higher eukaryotes. Various ncRNAs are known to have structural, functional, or regulatory roles, but the influence of the majority of non-coding transcripts is still unclear. Among ncRNAs, long ncRNAs (lncRNAs, longer than 200 bp) are of particular interest. lncRNAs do not have a uniform function but many studies observed lncRNA-based regulations at the transcriptional and translational levels. Therefore, novel lncRNAs could specifically fine-tune protein synthesis in the highly differentiated cell types. Particularly, fully-grown mammalian oocyte and early embryo require precisely controlled translation of maternal transcripts to coordinate meiotic progression and early embryo development while transcription is silent. We aimed to study the involvement of ncRNAs in protein synthesis and consequent influence on the oocyte and early embryo physiology.

For the first time, we analysed the expression and distribution of several ncRNAs, namely *Brain cytoplasmic RNA 1 (BCI)*, *lncRNA in Oocyte Specifically Expressed (Rose)*, *RNA Component of 7SK Nuclear Ribonucleoprotein (Rn7sk)*, *Nuclear Enriched Abundant Transcript 2 (Neat2)* and *Intracisternal A Particle Long terminal repeat RNA (IAPLtr1a)* during meiotic maturation and early embryo development. We found that selected ncRNAs exhibited defined nuclear or cytoplasmic localization on the GV stage. The expression pattern of selected ncRNAs declined during maturation and development. As ncRNAs functions are directly connected to their subcellular location, we selected for further analysis two cytoplasmic ncRNAs: *BCI* and *Rose*. We observed that *BCI* and *Rose* are ribosome-associated ncRNAs which hint at their role in translational regulation and physiology of the mammalian oocyte.

Our results indicated that ncRNA *BCI* represses cap-dependent translational initiation in GV in accordance with its proposed role in dendrites. However, we also demonstrated that *BCI* inhibits translation of specific mRNAs, *Dlg4* and *Actb* via interaction with 3’UTR. We showed that such interaction requires a protein interplay similarly to many regulatory ncRNAs which act as a part of ribonucleoprotein complexes. Moreover, we developed a new RNA-PLA approach enabling us to detect proximity of target RNA and protein. RNA-PLA allowed us to visualize multiple spots of interaction in the GV oocyte between *BCI* and its proposed binding partner Fragile X Mental Retardation Protein (FMRP). Furthermore, clustering of the FMRP protein in the cytoplasm was induced by overexpression of *BCI* in MII oocyte. Thus, we confirmed that ncRNA *BCI* is modulating translation of maternal mRNA pool in the oocyte.

Next, we focused on second ribosome-associated lncRNA *Rose* expressed in two variants in the oocyte and one is oocyte-specific. *Rose* is localized in the cytoplasm and nucleus at transcriptionally active stages and only in the cytoplasm during transcriptionally silent stages. Although overexpression of *Rose* did not affect oocyte maturation downregulation of *Rose* resulted in abnormalities in oocyte cytokinesis and impaired preimplantation embryo development.

Altogether, we studied a number of ncRNAs and their expression and localization within subcellular context during meiotic maturation and early development. Moreover, we identified ncRNAs that contribute to the cellular physiology of the oocyte and early embryo development. Our results improve understanding of ncRNA-based regulatory networks during developmental events in the mammalian oocyte and embryo.

## **1. Introduction**

RNAs are vital for every cell in any organism. RNA molecule is assembled as a copy of the sequence of DNA in the nucleus but unlike DNA, RNA is found as a single strand of nucleotides, rather than a double strand. Many variants of RNA molecules have been described, however, the most important classification feature is protein-coding potential. So-called messenger RNAs (mRNAs) serve as a unidirectional vector transmitting information from the nucleus to the cytoplasm where they become templates for protein synthesis (Jackson, Hellen and Pestova, 2010). Variable sets of three nucleotides in the mRNA specifically code for one amino acid, thus forming a particular protein. This is usually referred to as the central dogma of molecular biology and explains the flow of genetic information: "DNA makes RNA, and RNA makes protein"(Crick, 1970).

However, other types of functional RNAs have been identified which do not code for any proteins and therefore are referred to as non-coding RNAs (ncRNAs). The first discovered ncRNAs were transfer RNAs (tRNAs) and ribosomal RNAs (rRNAs) which act in protein synthesis (Holley *et al.*, 1965; Attardi and Amaldi, 1970). Arbitrarily ncRNAs are divided into three large groups according to their sequence length and structure. There are small ncRNAs that are shorter than 200 nucleotides. These ncRNAs include several defined classes such as microRNAs (miRNAs), small interfering RNAs (siRNAs), piwi-interacting RNAs (piRNAs), small nuclear RNAs (snRNAs), small nucleolar RNAs (snoRNAs), and etc. which have particular and well-studied functional and/or regulatory roles (Dieci, Preti and Montanini, 2009; Valadkhan, 2010; Fischer, 2015; Ozata *et al.*, 2019). On the other hand, ncRNAs longer than 200 nucleotides are referred to as long non-coding RNAs (lncRNAs). Unlike small ncRNA, lncRNAs exhibit no functional uniformity. Lately, many ncRNAs have been considered to be master regulators or structural components in major cellular processes, including transcription, posttranscriptional gene regulation, and translation (Kaikkonen, Lam and Glass, 2011; Statello *et al.*, 2021). Another group of ncRNAs includes circular RNAs (circRNAs) which form a covalently closed continuous loop and often are conserved across species (Qu *et al.*, 2015). CircRNAs have key roles in the regulation of gene expression and splicing in physiological and pathological processes, such as cancer and neurodegenerative diseases (Qu *et al.*, 2017). Moreover, some types of ncRNAs are found to have functions in the extracellular matrix (Zhou and Chen, 2019) (Fig. 1).

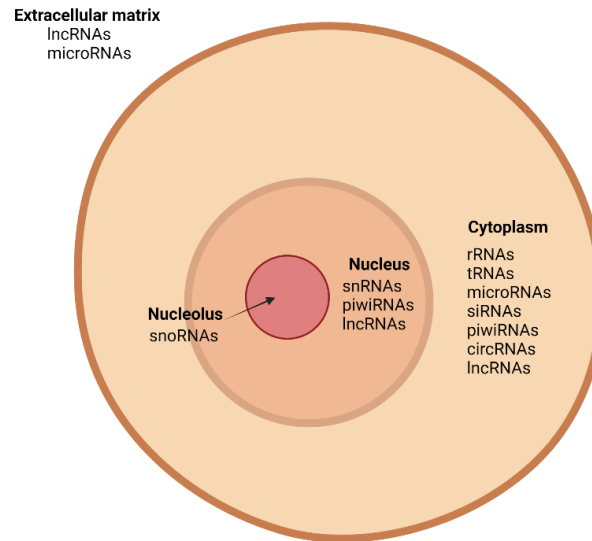


**Figure 1. Localization of functionally important types of ncRNAs in the eukaryotic cell.** Cytoplasmic ncRNAs include rRNAs and tRNAs, necessary for protein synthesis; regulatory ncRNAs such as microRNAs, siRNAs, piRNAs, circRNAs, lncRNAs. Nuclear ncRNAs include snRNAs involved in splicing and pre-mRNA processing; piRNAs in the regulation of transposon expression; structural and regulatory lncRNAs. Nucleolar snoRNAs guide modifications of other RNAs. LncRNAs and microRNAs are present in the extracellular matrix and are involved in intracellular communications.

Several structural advantages of lncRNA were highlighted in recent years. LncRNAs efficiently perform sequence-specific nucleic acid recognition. For example, proteins involved in sequence-specific binding require 100 times more sequence space than an RNA with the same affinity (Geisler and Coller, 2013). Furthermore, the ability of lncRNAs to fold into compound three-dimensional structures provides complex recognition surfaces with high affinity and specificity (Graf and Kretz, 2020). Moreover, lncRNAs often organize multiprotein complexes and are found to guide RNA Binding Proteins (RBPs) (Ferrè, Colantoni and Helmer-Citterich, 2016).

### 1.1 Role of ncRNAs in the eukaryotic cell

NcRNAs are abundantly transcribed in the eukaryotic cells and participate in multiple cellular mechanisms (P. Zhang *et al.*, 2019). NcRNAs appear to be a previously elusive level of signalling that controls gene expression in both nucleus and cytoplasm, including transcription, processing, translation and decay, and etc. Functions of ncRNAs in the cell could be divided into two categories: housekeeping and regulatory. While housekeeping ncRNAs are abundantly and ubiquitously expressed and regulate generic cellular functions, regulatory ncRNAs are implicated in more stringent control of gene expression (P. Zhang *et al.*, 2019). Moreover, an important regulatory ncRNAs subgroup, lncRNAs frequently exhibit more species- and cell-specific expression patterns than mRNAs suggesting execution of very precise regulatory functions (Gloss and Dinger, 2016; Ganesh *et al.*, 2020).

However, the majority of ncRNAs presented by lncRNAs remain poorly characterized without well-defined roles in cellular processes. Therefore, it is still an open question for a vast fraction of lncRNAs if they are truly functional or represent only inconsequential ‘transcriptional noise’ or have some translational potential. Sequencing data indicated purifying selection on lncRNA genes which

supports the functionality of the transcripts (Ponjavic, Ponting and Lunter, 2007). Other studies highlight that lncRNA secondary structures are more important from an evolutionary point of view than sequence (Johnsson *et al.*, 2014). On the other hand, lncRNAs are often associated with ribosomes suggesting their possible regulatory interaction with translational machinery or uncharacterized cryptic translational events (Zaheed *et al.*, 2021). In the latter case, transcripts initially misclassified as lncRNAs can code small peptides which are assumed to be highly unstable (Erhard *et al.*, 2018).

### **1.1.1 Role of ncRNAs in transcription and RNA processing**

Both small and long ncRNAs have important functions in the cell nucleus. Their roles have been recently linked to the regulation of many transcription-associated processes and splicing. For example, universal for all metazoans is *Rn7sk* snRNA that controls the elongation of nascent transcripts (Diribarne and Bensaude, 2009). Housekeeping snRNAs, for example, U1 and U2 snRNA, orchestrate mRNA splicing and form spliceosome, while snoRNAs chemically modify rRNAs, tRNAs, and snRNAs in the nucleolus. A completely different group of small RNAs include regulatory microRNAs, piRNAs and siRNAs. These short ncRNAs are processed from single- or double-stranded RNAs act in post-transcriptional events, however, recent data indicate their involvement in transcriptional regulations (Malecová and Morris, 2010; Iwasaki, Siomi and Siomi, 2015; Dana *et al.*, 2017; Seeley *et al.*, 2018; Gebert and MacRae, 2019).

lncRNAs are considered to be regulatory ncRNAs and appear to be a hidden layer of molecular networks in chromatin architecture/epigenetic memory, transcription, pre-mRNA splicing, editing. For example, transcription of an antisense lncRNA itself can influence transcription of the sense mRNA (Santoro *et al.*, 2013). Some lncRNAs display enhancer-like activity (eRNAs) (Santoro *et al.*, 2013) or directly interact with RNA polymerase II (Yakovchuk, Goodrich and Kugel, 2009). Moreover, lncRNAs regulate chromatin configuration and can specifically target histone-modifying activities (Pandey *et al.*, 2008; Tsai *et al.*, 2010; Congrains *et al.*, 2013). One of the well-known examples of lncRNAs role in epigenetic modifications is the involvement of *Xist* lncRNA in the dosage compensation mechanism in female placental animals (Sado and Brockdorff, 2013; Loda and Heard, 2019). *Xist* inactivates one of the X chromosomes by tethering polycomb repressive complex 2 (PRC2) and therefore inducing the formation of stable heterochromatin. Other known examples are *HOTTIP* and *HOTAIR* lncRNAs which directly affect morphogenesis by regulating gene expression of Homeobox (HOX) genes, HOXA cluster and HOXD cluster respectively (Rinn *et al.*, 2007; Wang *et al.*, 2011).

lncRNAs are also linked to both gene activation and repression through the organization of nuclear subdomains (Song *et al.*, 2021). Abundantly expressed and conserved throughout mammalian lineage *nuclear enriched abundant transcript 2 (Neat2)* lncRNA (also known as *Malat1*) specifically localizes in nuclear speckles (Arun, Aggarwal and Spector, 2020; Hasenson and Shav-Tal, 2020). Firstly, *Neat2* is retained in the nucleus and localizes to nuclear speckles where pre-mRNAs are processed. Therefore, it was suggested to regulate alternative splicing. Secondly, it is associated with chromatin and affect transcription of specific genes. Other lncRNA found in the nuclear subdomains is *nuclear enriched abundant transcript 1 (Neat1)* lncRNA which localizes to paraspeckles - protein-rich nuclear organelles built around a specific lncRNA scaffold (Yamazaki and Hirose, 2015). *Neat1* plays a structural role and is essential for organization and integrity of nuclear paraspeckles which influence gene regulation (Fox *et al.*, 2018).

Thus, ncRNA and specifically lncRNAs are considered to be important regulators of transcription and RNA processing. While some ncRNAs have housekeeping nucleus-associated functions in all

eukaryotes (e.g. snoRNAs or snRNAs), most of the lncRNAs act selectively on certain genes. This implies that functional annotation of novel lncRNAs is necessary for the understanding of complex nuclear regulations.

### 1.1.2 Role of ncRNAs in translation

A number of housekeeping ncRNAs play irreplaceable roles in protein synthesis. rRNAs are essential components of both small and large subunits of the ribosome and facilitate the translation of mRNA codons into amino acids. tRNAs carry an amino acid to the translation machinery and recognise a complement codon on mRNA. Interaction of rRNA with mRNA and tRNA ensures proper protein synthesis based on mRNA code (Bastide and David, 2018).

Moreover, ncRNAs participate not only in ongoing translation but also tightly regulate gene expression on various post-transcriptional levels. MiRNAs and siRNAs are small regulatory ncRNAs containing around 20-24 nucleotides that have similar functions in translational repression. However, they are produced through different biogenesis pathways: miRNAs are derived from hairpins in RNA transcripts whereas siRNAs are processed from longer regions of double-stranded RNA. Both miRNAs and siRNAs are involved in the RNA-silencing mechanism together with Argonaute proteins. They form RNA-induced silencing complexes (RISC) which lead to inhibition of translation or decay of target mRNA (Fischer, 2015). Another group of small RNAs involved in gene silencing with the formation of RISC are piRNAs. PiRNAs are mostly known for their role in germline transposon silencing during gametogenesis where they direct piwi proteins to the transposon targets (Ozata *et al.*, 2019).

lncRNAs are important modulators of post-transcriptional control in the cytoplasm (Rashid, Shah and Shan, 2016) (Fig. 2). lncRNAs can drive the formation of Ribonucleoprotein (RNP) complexes and guide them to protein synthesis machinery (Briata and Gherzi, 2020). Many lncRNA-based regulations involve direct or indirect interactions with *cis*-acting regulatory sequences in 5' and 3' untranslated regions (5'UTRs and 3'UTRs) of target mRNAs. (Peng *et al.*, 2019; Priyanka *et al.*, 2021). Such sequences are referred to as zip codes and can interact with ncRNAs or proteins via the primary sequence or secondary structure (Singh *et al.*, 2015). *Cis*-elements are also required for the formation of RNPs involved in the localization, translational silencing, and stability of the RNA (Mayr, 2019).

lncRNAs can either repress or promote protein synthesis via binding to 5'UTRs and 3'UTRs of mRNAs. For example, *lincRNA-p21* is a lncRNA expressed in cancer cells which is negatively influencing translation of several mRNAs by imperfect base pairing with untranslated regions (Yoon *et al.*, 2012). Some antisense lncRNAs directly bind parts of their complementary mRNA targets and promote protein synthesis (Carrieri *et al.*, 2012). Currently, such antisense lncRNAs are referred to as SINEUPs since an embedded inverted SINEB2 sequence is necessary for upregulation of translation (Zucchelli *et al.*, 2015). One of the first described SINEUPs is Antisense (AS) *Uchl1* lncRNA which is transcribed from the opposite strand of *Uchl1* mRNA. AS *Uchl1* lncRNA enhances translation of *Uchl1* mRNA in stress conditions (Carrieri *et al.*, 2012).

Besides their role in translation, lncRNAs have also been implicated in both positive and negative regulation of mRNA stability (Rashid, Shah and Shan, 2016). Antisense lncRNA stabilize their coding partners, for example, *FGFR3-AS1* lncRNA interacted with 3'UTR of *FGFR3* mRNA and increased *FGFR3* mRNA stability in tumorigenic tissue (Sebastian-Delacruz *et al.*, 2021). On the contrary, *1/2-sbsRNAs* are required for degradation via Staufen 1 and STAU1-mediated mRNA

decay. *1/2-sbsRNAs* complementary bind 3'UTR of target mRNAs and create a double-stranded RNA binding site for STAU1 and thus initiate degradation (Gong and Maquat, 2011).

Moreover, aside from competing with small RNAs for binding sites on target mRNAs, lncRNAs and circRNAs can act as sponges for miRNAs and sequester their action (Qu *et al.*, 2015; Chen *et al.*, 2017; Zhang *et al.*, 2018).

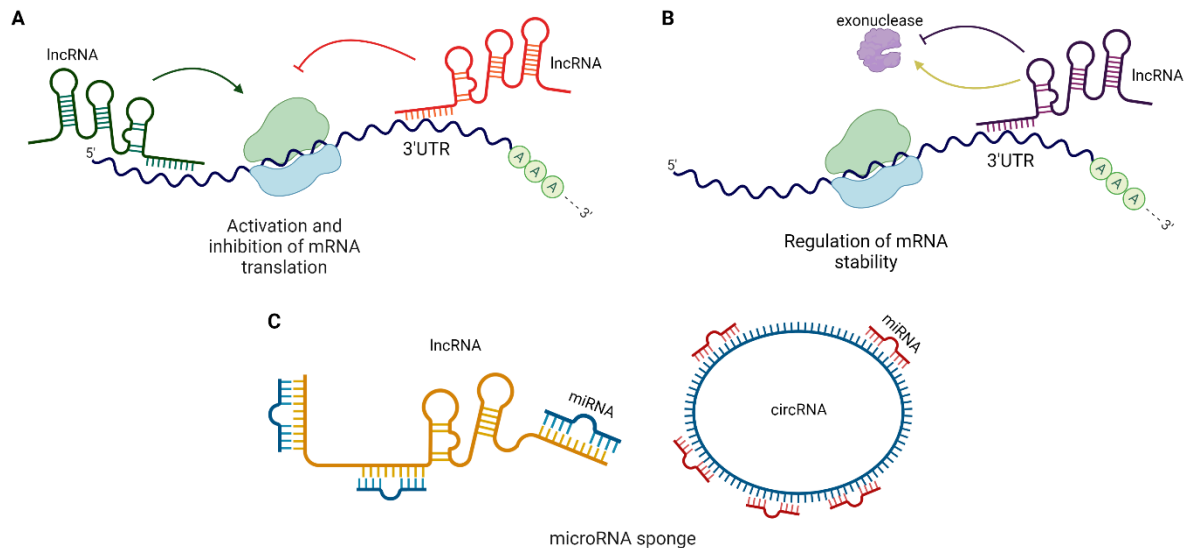


**Figure 2. Functions of lncRNAs and circRNA in the translational regulation.** *Sequence-specific interactions of lncRNAs with mRNA lead to either translational activation or repression (A) or affect stability of mRNA (B). Both lncRNA and circRNA can act as miRNA sponges and sequester miRNA activity (C).*

Various lncRNAs regulate cap-dependent translation by obstructing the formation of translation initiation complex (Karakas and Ozpolat, 2021). In lymphoma cells, lncRNA *GAS5* binds eIF4E and decreases the translation of c-Myc (Hu, Lou and Gupta, 2014) and in breast cancer cells lncRNA *RPI* interacts with eIF4E repressing translation (Jia *et al.*, 2019). Similarly, rodent-specific *Brain Cytoplasmic RNA 1 (BCI)* was shown to prevent the formation of 48S preinitiation complex in dendrites (Tiedge *et al.*, 1991). *BCI* ncRNA is a 154nt-long Pol III-derived transcript that binds to eIF4B, eIF4A, and Poly(A)-binding protein (PABP) via 3'-stem-loop and the adjacent A-rich region (Rozhdestvensky *et al.*, 2001; Eom *et al.*, 2011; Lee *et al.*, 2020). Reportedly, *BCI* acts together with RNA-binding Fragile-X Mental Retardation Protein (FMRP) leading to the assembly of large messenger RNPs but this link is still being discussed (Zalfa *et al.*, 2003; Iacoangeli *et al.*, 2008) (Fig. 3).

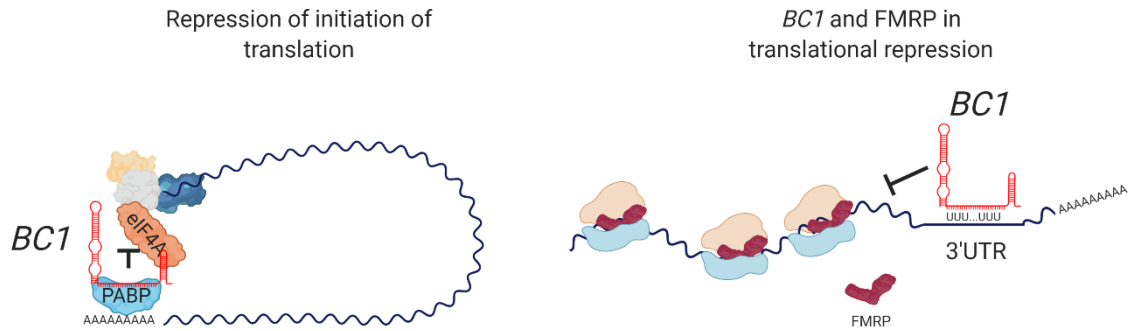


**Figure 3. Proposed mechanism of action of ncRNA *BC1* in dendrites.** *BC1* interacts with *PABP* and *eIF4B*, *eIF4A* and prevents the formation of initiation complex and translational initiation. Moreover, *BC1* acts together with a translational repressor *FMRP* and selectively inhibits translation of specific mRNAs.

Thus, ncRNAs regulate gene expression in both nucleus and cytoplasm and are well suited for multiple functions. The functional versatility of ncRNAs explains why they act in many cell types and processes, including complex multicellular development. The abovementioned examples represent only a portion of already annotated lncRNAs but the majority of them remain poorly understood. In addition, many lncRNAs are expressed at low levels and exhibit developmental stage or cell-specific expression which suggests their particular and unique molecular roles. Moreover, a growing number of reports implicate ncRNAs in the control of post-transcriptional events and therefore could be engaged in the cell types highly dependent on post-transcriptional regulations, such as mammalian oocyte.

## 1.2 Mammalian oocyte, early embryo and transcriptome

One of the cell types in which the role of RNA regulatory networks cannot be underestimated is the mammalian oocyte and early embryo. The main reason for such dependence on RNA is the way how oocyte develops and performs meiotic maturation, which includes a period of active transcription and a long period of silent transcription.

In developing embryo, undifferentiated primordial germ cells (PGCs) initiate meiosis after rounds of mitotic divisions but are arrested at the diplotene stage until the female reaches puberty. After birth and before puberty, primary oocytes are stored in dormant state in a layer of pre-granulosa cells forming a primary follicle. During puberty, meiosis is resumed upon stimuli from hypothalamus-anterior pituitary axis mediated by follicle-stimulating and luteinizing hormone. This results in a growth and high transcriptional activity which leads to the accumulation of RNA content in oocyte, one of the largest cells. This is followed by the formation of the fully grown oocyte, so called ‘germinal vesicle’ (GV), at which transcription is ceased (Christou-Kent *et al.*, 2020). GV oocyte can then undergo meiotic maturation, become fully matured in the metaphase II (MII) stage and await fertilization (Fig. 4; Fig. 5).



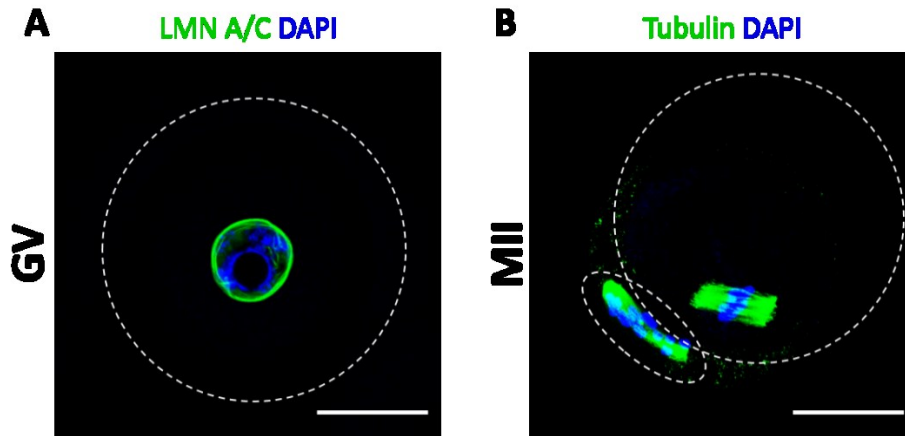


**Figure 4. Mammalian oocyte.** (A) On the GV stage, nuclear lamina labelled by LMN A/C (green) is intact and the oocyte is transcriptionally silent. (B) After NEBD oocyte extracts first polar body, forms the second spindle labelled by Tubulin (green) and becomes arrested at MII stage awaiting for fertilization. Scale bars 25  $\mu\text{m}$ .

In the case of mammalian oocytes transcription is restored in the 2-cell (mouse) or 8-16 cell (human, bovine) embryo when the zygotic genome activation (ZGA) occurs (De La Fuente *et al.*, 2004; Clarke, 2012). Therefore, during its growth, the oocyte must produce all the transcripts needed to fulfil its protein requirements during the active period of meiotic completion, fertilization, and ZGA. During maturation, the oocyte relies only on previously synthesized and accumulated components as well as on mRNA stabilization and translation repression mechanisms (Susor and Kubelka, 2017) (Fig. 6).

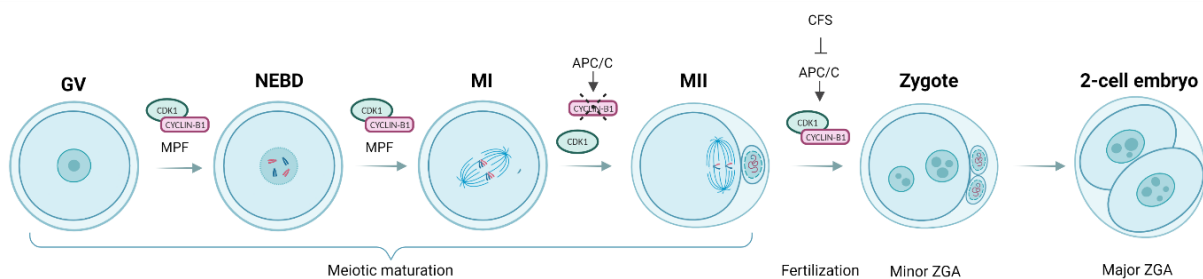


**Figure 5. Molecular mechanisms of meiotic maturation in mouse oocyte.** Active MPF – a complex of CDK1 and Cyclin B (CCNB) leads to NEBD and MI. In anaphase, MPF is inhibited by APC/C which results in polar body (PB) extrusion. After MPF becomes active again and oocyte is arrested in MII stage until fertilization. When MII oocyte is fertilized second PB is extruded and minor ZGA occurs. The major ZGA occurs in the 2 cell embryo.

Meiotic oocyte maturation is a complex process with unique mechanisms leading to the reduction of the genomic content to the haploid state. After the resumption of meiosis selective maternal mRNA decay is initiated (Su *et al.*, 2007). The main component of the events leading to nuclear envelope break down (NEBD) and completion of meiotic maturation is maturation-promoting factor (MPF, Fig. 5; Fig. 6) – a complex of cyclin-dependent kinase 1 (CDK1) and Cyclin B (Tripathi, Prem Kumar and Chaube, 2010). The activity of MPF reaches maximum level during metaphase I stage (MI) and afterward is reduced via the action of the anaphase-promoting complex (APC/C) (Pesin and Orr-Weaver, 2008). During MII stage arrest so-called cytotstatic factor (CSF) prevents

exit from the metaphase II stage via the stabilization of cyclin B (Tripathi, Prem Kumar and Chaube, 2010). Thus, at this moment MPF activity is again restored and oocyte awaits for the fertilization. Fertilization results in the extrusion of the second polar body and the formation of zygote. After the first mitotic cleavage, major ZGA takes place in 2 cell embryo and transcription is completely restored (Svoboda, 2018). Furthermore, massive clearance of maternal transcripts accompanies ZGA (Sha, Zhang and Fan, 2019) (Fig. 5; Fig. 6).

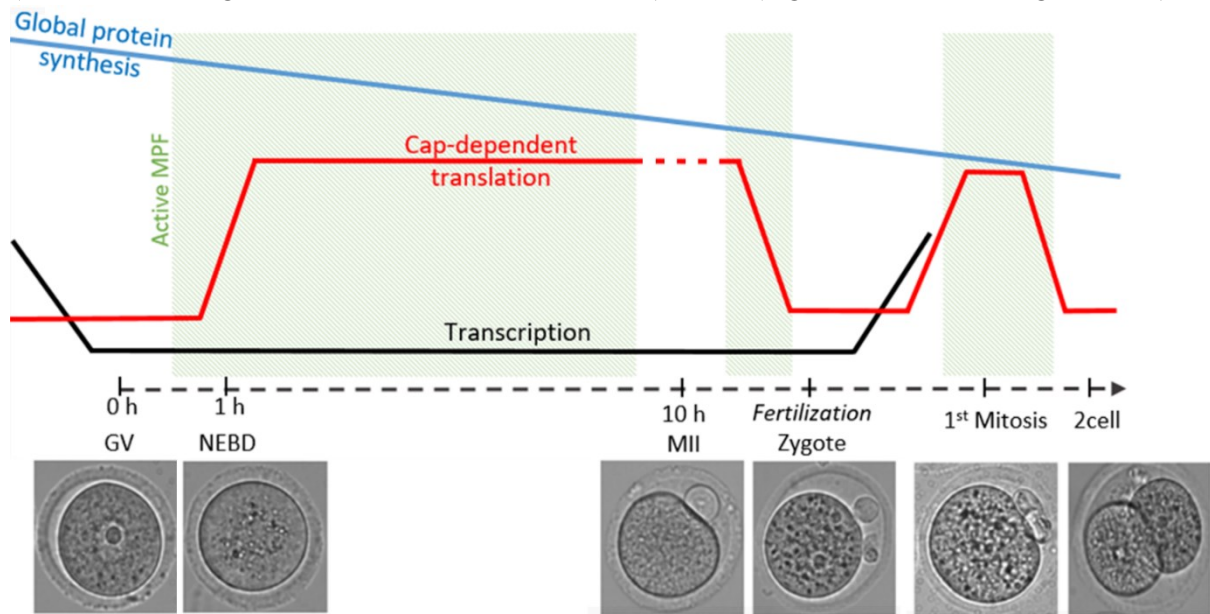


**Figure 6. Translation during meiosis in mammalian oocytes.** *Transcription is silenced after the resumption of meiosis and global protein synthesis decreases during oocyte maturation and early embryo development. Nevertheless, the level of cap-dependent translation is upregulated after NEBD with active involvement of MPF. Used from Susor and Kubelka 2017.*

### 1.2.1 Translational control in mammalian oocyte and early embryo

The meiotic maturation and early embryo development require time-dependent translation of the MPF components, phosphorylation targets and many other proteins. Significant mechanisms regulating the fate of the mRNAs in the fully grown oocyte and early embryo have been described: RNA localization, cytoplasmic RNA polyadenylation, regulation of cap-dependent initiation (Bettegowda and Smith, 2007; Susor *et al.*, 2015; Susor and Kubelka, 2017), endogenous siRNAs pathway (Stein *et al.*, 2015) and RNA modifications (Brachova *et al.*, 2019). These processes are usually guided by specific RBPs and RNAs that exist in the form of RNP complexes where mRNA is masked to escape from translation or degradation (Christou-Kent *et al.*, 2020; Voronina and Pshennikova, 2021).

Proper temporal and spatial RNA localization provides advantages over transport of protein products in both germ- and non-germline cells (Blower, 2013). The crucial role of RNA localization in the oocytes was described firstly in various non-mammalian species (Wang and Lehmann, 1991; Bashirullah, Cooperstock and Lipshitz, 2001; Tadros *et al.*, 2007; Semotok *et al.*, 2008; Sindelka *et al.*, 2018). In contrast to non-mammalian species, much less is known about mRNA localization in mammalian oocytes (Oh and Houston, 2017). However, recent data suggested a sequestering mechanism of poly(A) RNAs storage in the nucleus of fully-grown GV oocyte allowing physical separation of mRNAs and translational machinery (Susor *et al.*, 2015; Jansova *et al.*, 2018).

The overall level of protein produced from an mRNA depends on translation efficiency. In the mammalian oocyte after mRNAs are exported from the nucleus, they undergo deadenylation and are stored in the cytoplasm with short poly(A) tails in loop form. This prevents interaction with translation initiation factors and transcript degradation machinery, allowing long-term storage of mRNA. The oocyte utilizes cytoplasmic polyadenylation to initiate stage-specific translation of selected transcripts during meiotic maturation (Dai *et al.*, 2019). Key regulatory components in cytoplasmic polyadenylation involve polyadenylation element (CPE) and polyadenylation signal (PAS) in the 3'UTR of target mRNA (Radford, Meijer and de Moor, 2008) which interact with an RBP - CPE-binding protein (CPEB) (Hake and Richter, 1994; Stebbins-Boaz, Hake and Richter, 1996).

Furthermore, mTOR-eIF4F signalling is crucial for the control of translation in the mammalian oocyte (Dowling *et al.*, 2010; Susor *et al.*, 2015). mTOR-eIF4F affects phosphorylation of 4E-binding proteins (4E-BPs) and the ribosomal protein S6 kinases and therefore activation protein synthesis in the oocyte.

Nevertheless, suggested mechanisms of translational control in mammalian oocyte do not cover the dynamics of all maternal transcripts. As mentioned above, many lncRNAs are shown to regulate mRNAs post-transcriptionally through interaction with 3'UTRs, well-known regulatory elements in meiotic maturation. Furthermore, the ability of lncRNAs to assemble RNPs, perform efficient sequence-specific nucleic acid recognition, and facilitate repression or activation of translation makes this group promising candidates for modulation of maternal mRNA pool in the oocyte. Currently, our understanding of the role of lncRNAs in the translational regulation of meiotic maturation is far from complete.

### 1.3 LncRNAs in the germ cells

The role of lncRNAs in development of the reproductive system has only recently begun to be discovered and specific lncRNAs have been annotated. Emerging evidence indicated the involvement of lncRNAs in germ cell differentiation in mammals, particularly Spga-lncRNA1/2 in spermatogonial stem cells (Joshi and Rajender, 2020). Furthermore, several lncRNAs were shown to be important after the switch from mitotic proliferations to meiotic mode in spermatogenesis. For example, *Tsx* (testis-specific X-linked) is expressed in the nucleus of pachytene spermatocytes and its knockout causes increase in apoptosis (Anguera *et al.*, 2011). Another spermatogenic antisense lncRNA *Tbca13* was shown to participate in posttranscriptional regulation of the sense *Tbca16* mRNA which is required for microtubule re-arrangement (Nolasco *et al.*, 2012).

On the other hand, the role of a large portion of expressed ncRNAs and lncRNAs in the oogenesis is still not understood. While a major pathway of miRNA in mouse oocytes was shown to be inactive and dispensable for development (Kataruka *et al.*, 2020), in oocytes of other mammalian species, for example, bovine or human, miRNAs may have regulatory roles (Battaglia *et al.*, 2016; Sinha *et al.*, 2017). Data about the role of lncRNA in meiotic maturation are scarce and enigmatic.

Several lncRNAs were recently functionally characterized in the mammalian oocyte. The most abundant cytoplasmic lncRNA *Sirenal* slightly impacts mitochondrial distribution in the perinuclear area without known reproductive consequences in the laboratory mouse (Ganesh *et al.*, 2020). Moreover, *Sirenal* harbours CPE element in the 3'UTR and undergoes cytoplasmic polyadenylation. This is an unexpected feature for lncRNA that is not protein-coding and is usually observed in translationally controlled maternal mRNAs. Another interesting lncRNA which was discovered to be essential in the early development of mouse embryo is *lincGET* (Wang *et al.*, 2016). Nevertheless, it was widely accepted that the first two blastomeres of mammalian embryos are

equally totipotent recent data challenge that hypothesis including distribution of *lincGET* lncRNA (Wang *et al.*, 2018; Casser *et al.*, 2019). *lincGET* expression starts after ZGA and is more abundant in one blastomere in 2-cell embryo. Such asymmetric distribution predisposes blastomeres fate toward the inner cell mass or trophectoderm. On the contrary, some of the abundant and well-studied lncRNAs are often nonessential for meiotic maturation and embryonic development. *Neat1* lncRNA is the main structural component of nuclear paraspeckles and knock-out of *Neat1* leads to a complete lack of paraspeckles (Nakagawa *et al.*, 2011). Surprisingly, depletion of *Neat1* does not affect viability and fertility in mice. In the same manner, knock-out of *Neat2* lncRNA (*Malat1*) does not influence fertility of mice, however, nuclear speckles form even in the absence of *Neat2* (Nakagawa *et al.*, 2012).

Thus, lncRNAs contribute to both mammalian oocyte maturation and early embryo development, however role of the majority of lncRNAs still remains to be elucidated. Identification of particular lncRNAs and analysis of their localization pattern will shed light on the complex molecular processes in such highly differentiated cells.

## **2. Aims of the thesis**

The objective of this thesis is to study the involvement of ncRNAs in the molecular physiology of mammalian oocyte and preimplantation embryo development.

I analysed the expression and localization of specific ncRNAs during oocyte maturation and early embryo development. Moreover, I characterized their role in the oocyte development with the emphasis on their role in processes associated with protein synthesis.

The specific aims of this work were:

- Analysis of RNA-Seq datasets during oocyte development and selection of specific ncRNAs.
- Analysis of candidate ncRNAs during oocyte and early embryo development. Elucidation of the physiological relevance of novel ncRNAs related to meiotic and embryo development.
- Establishment of RNA and translation detection *in situ* in the oocyte and early embryo.

### **To study involvement of *BCI* ncRNA in the regulation of translation in the mammalian oocyte**

- To analyse expression of *BCI* during meiotic maturation and early development.
- To study if *BCI* functions as a translational repressor and promotes maternal mRNAs translational dormancy in the mammalian oocyte.
- To reveal specific targets of *BCI* translational repression in the mammalian oocyte.
- To investigate if *BCI* functions as an intermediate link inside FMRP mRNPs inhibiting translation of selected proteins.

### **To investigate role of novel unannotated lncRNA *Rose (lncRNA in Oocyte Specifically Expressed)* in mammalian oocyte and early embryo**

- To analyse expression of *ROSE* meiotic maturation and early development.
- Describe and visualize localization of *Rose (lncRNA in Oocyte Specifically Expressed)* lncRNA.
- To analyse role of *ROSE* in the oocyte development using downregulation experiments.

### **To visualize selected ncRNAs during meiotic maturation and early embryo development**

- To localize LTR retrotransposon-derived *IAPLtr1a* and *Neat2* lncRNAs in the mammalian oocyte and embryo.
- To visualize novel uncharacterized ncRNAs in the mammalian oocyte.

### **3. Comments on publications**

This thesis is based on research presented in three published scientific papers, all listed chronologically below with detailed description of my contribution.

3.1 **D. Aleshkina**, R. Iyyappan, C.J. Lin, T. Masek, M. Pospisek, A. Susor, ncRNA BCI influences translation in the oocyte, **RNA Biol.** (2021). <https://doi.org/10.1080/15476286.2021.1880181>  
ncRNA BCI influences translation in the oocyte

D. A. performed collection of the samples, RNA isolation and cDNA preparation, overexpression experiments, RNA fluorescence *in situ* hybridization (FISH), RNA-proximity ligation assay (RNA-PLA) and immunocytochemistry (ICC) experiments, live cell imaging, <sup>35</sup>S-Methionine incorporation, lncRNA pull down, prepared most of the figures and contributed to writing of the manuscript.

3.2 R. Iyyappan, **D. Aleshkina**, L. Zhu, Z. Jiang, V. Kinterova, A. Susor, Oocyte specific lncRNA variant Rose influences oocyte and embryo development, **Non-Coding RNA Res.** (2021). <https://doi.org/10.1016/j.ncrna.2021.06.001>

D. A. contributed with visualization of the RNA, downregulation experiments, preparation of presented figures, and writing of the manuscript.

3.3 D. Jansova, **D. Aleshkina**, A. Jindrova, R. Iyyappan, Q. An, G. Fan, A. Susor, Single Molecule RNA Localization and Translation in the Mammalian Oocyte and Embryo, **J. Mol. Biol.** (2021). <https://doi.org/10.1016/j.jmb.2021.167166>

D.A. contributed with sample collection, RNA isolation and cDNA preparation, RNA FISH experiments and participated in preparation of the figures and manuscript editing.

During my PhD studies I also participated in another scientific project which resulted in following scientific publication. This project is not directly links to the topic of my PhD thesis thus not included to the list of thesis manuscripts (but listed in the attachments).

E. Llano, R. Iyyappan, **D. Aleshkina**, T. Masek, M. Dvoran, Z. Jiang, M. Pospisek, M. Kubelka, A. Susor, SGK1 is essential for meiotic resumption in mammalian oocytes. **European Journal of Cell Biology**, *accepted*.

#### **3.1 ncRNA *BCI* influences translation in the oocyte**

Translation in the mammalian oocyte is a tightly regulated process. Various mechanisms are suggested to affect the translation rate of maternal mRNA pool in it including shortening of polyA tail and cap-dependent regulation. However, additional regulators may be involved among which possible candidate ncRNAs are known to play roles in post-transcriptional events. One of such ncRNAs is *Brain Cytoplasmic 1 (BCI)* which represses translation in dendrites.

The main objective of the presented study was to shed light on the role of *BCI* in mammalian oocyte and early embryo and analyse possible involvement of *BCI* in the translational regulations of the maternal mRNA pool.

We analysed the expression of *BCI* in GV and MII oocytes as well as in 2-cell embryo. We found that *BCI* is abundantly expressed on GV stage with a decrease on MII and 2cell stages. Moreover, quantitative polymerase chain reaction (qPCR) analysis of cDNA samples obtained from

cytoplasmic and nuclear fractions showed exclusive cytoplasmic localization for *BCI*. Interestingly, Scarce Sample Polysome profiling (SSP-profiling) showed a high association of *BCI* with polyribosomes in GV oocyte suggesting *BCI* interaction with translational machinery.

To understand the role of *BCI* in the mammalian oocyte we applied an overexpression (OE) approach using microinjection of *BCI* RNA into the oocyte cytoplasm. Firstly, we evaluated OE effect on the global translation rate and performed <sup>35</sup>S-Methionine labelling in both GV and MII stages. We found that *BCI* only slightly, however significantly, repressed global translation in the GV stage but not in the MII stage. Such a limited effect on overall translation suggested that *BCI* represses translation of a subset of mRNAs rather than whole mRNA pool. Moreover, *BCI* has been reported to interact with PABP and eIF4 causing translational repression. Thus, we analysed the effect of *BCI* OE on the translation of 5' TOP mRNAs and microinject luciferase reporters with 5' TOP motif along with *BCI*. Our results demonstrated that *BCI* OE decreases translation of 5'TOP reporter and therefore indicates that *BCI* influences translation of a subset of mRNAs.

Previous studies suggested a functional link between *BCI* and mRNAs coding for actin  $\beta$  (*ACTB*) and postsynaptic density protein 95 (*DLG4*, also known as PSD95). Moreover, *in silico* analysis predicted a base-pairing interaction between A-rich region of *BCI* and polyU sequence in 3'UTR of *Actb* and *Dlg4* mRNAs. We examined whether *BCI* OE influences the translation of these mRNAs with the Immunoblot approach. We detected a significant decrease in the level of both *ACTB* and *DLG4* proteins in the GV oocyte but not in MII oocyte. In the same manner, we analysed the level of Survivin protein which mRNA contains TOP motif in 5'UTR. The level of Survivin decreased after the *BCI* OE only on the GV stage. Hence, data about global translation and luciferase reporters we concluded that *BCI* negatively influences cap-dependent translation of specific mRNAs only in the GV stage oocyte.

However, it was still unknown if *BCI* interacts with candidate mRNAs directly or via a protein interplay. We applied lncRNA pull-down approach with *BCI* anti-sense oligonucleotides for two sample types from GV stage oocytes: complete cell lysate and isolated total RNA. We found that both *Actb* and *Dlg4* mRNAs were enriched after pull-down procedure in cell lysate sample but not in the total RNA sample. *Survivin* mRNA was enriched in neither of those samples. These results showed that *BCI* physically interacts with *Actb* and *Dlg4* mRNAs through a protein interplay. Previously, FMRP protein was proposed to be a binding partner of *BCI* which facilitates the interaction of *BCI* with mRNAs destined for translational repression. To analyse the potential interaction of *BCI* and FMRP we performed *in situ* RNA-PLA in mouse oocytes with addition of a hybridization step of a target RNA and anti-sense biotinylated oligonucleotide probes. For proximity detection, we used anti-biotin antibody and specific antibodies for protein of interest. We observed multiple spots of interaction on the GV stage and almost none in the MII stage. In addition, we found that *BCI* OE leads to clustering of FMRP protein and polyA mRNA in the MII oocyte.

In conclusion, in this work we analysed the role of *BCI* ncRNA in the mammalian oocyte and early embryo and found that it represses translation of specific mRNAs on GV stage. We showed, that *BCI* negatively influences cap-dependent translation and translation of *Actb* and *Dlg4* mRNAs via protein interplay. Moreover, we confirmed a physical link between *BCI* ncRNA and FMRP protein (Fig. 7).

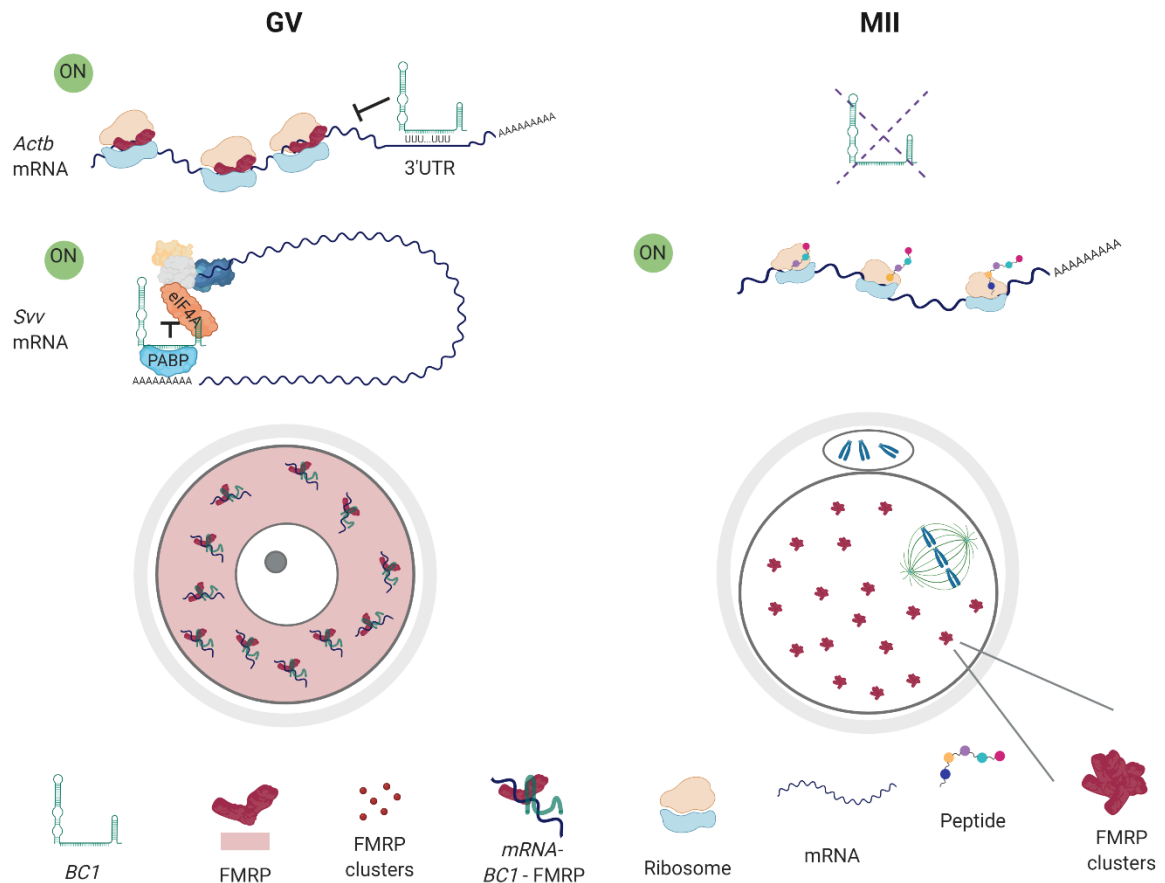


**Figure 7. Role of *BC1* ncRNA in the mammalian oocyte.** *BC1* represses translation of specific mRNAs via interaction with target 3'UTR. *BC1* inhibits cap-dependent initiation of translation in the GV oocyte. *BC1* physically interacts with FMRP in GV oocyte and affects clustering of FMRP in MII oocyte.

### 3.2 Oocyte specific lncRNA variant *Rose* influences oocyte and embryo development

In terms of the absence of transcription in mammalian oocyte the role of RNA is vital. However, not only important mRNAs are stored and utilized during the maturation and development but also many ncRNAs. These ncRNAs and especially lncRNAs may be a hidden layer of regulatory control in the mammalian oocyte and elucidation of the functional significance of each is a challenging task.

The objective of this work was to unveil the role of an enigmatic lncRNA transcript *Gm32743* named *lncRNA Oocyte Specifically Expressed (Rose)*.

First of all, we analysed the expression of *Gm32743* in somatic tissues and the oocyte. According to Ensembl databases, *Gm32743* lncRNA consists of three noncoding exons (NCE) thus we checked whether this lncRNA undergoes alternative splicing. We found that *Gm32743* is highly expressed in somatic tissues, especially in brain and heart, however, with different splicing pattern in comparison to the oocyte. In the case of oocytes *Gm32743* was presented in two variants: one contained all three exons (*Rose 1*; NCE1-3) and the second only exons 1 and 3 (*Rose 2*; NCE1&3). We found that *Rose* was abundant in the GV oocyte and its expression decreased gradually till 2 cell stage of embryo.



Secondly, we studied the localization pattern of *Rose* lncRNA (Fig. 8). During transcriptionally active stages (growing oocyte and 2 cell embryo) *Rose* was observed in both nucleus and cytoplasm. In contrast to that, during transcriptionally inactive stages such as fully-grown GV and zygote *Rose* was present exclusively in the cytoplasm. Localization of *Rose* lncRNA may be directly linked with its functions and might manifest its involvement into transcription-associated processes in transcriptionally active stages.

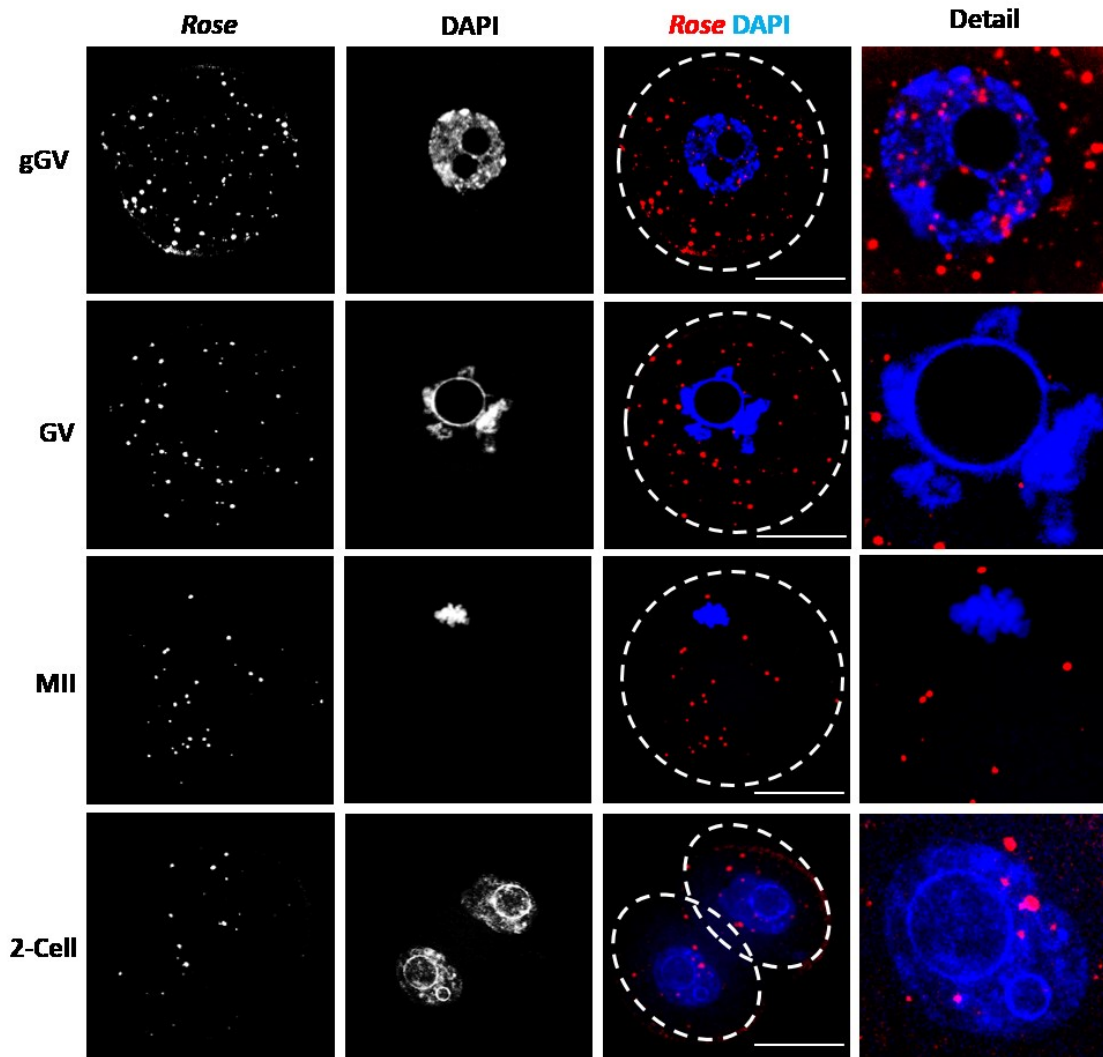


**Figure 8. Localization of *Rose* lncRNA in mammalian oocyte and early embryo.** *On transcriptionally active stages including growing GV (gGV) and 2 cell embryo *Rose* lncRNA localizes both to the nucleus and cytoplasm. On transcriptionally silent stages, GV and MII, *Rose* lncRNA is dispersed exclusively in the cytoplasm.*

Moreover, performed SSP-profiling (Masek *et al.*, 2020) showed that *Rose* was associated with polysomal fraction rather than with non-polysomal. To analyse the non-coding status of *Rose* we used Coding Potential Assessment Tool (CPAT) which confirmed that *Rose* has no protein-coding potential. Thus, presence in polysomal fractions might indicate role of *Rose* in posttranscriptional regulations.

To understand the importance of *Rose* during meiotic maturation we performed overexpression and downregulation experiments via microinjection of *Rose* to the GV oocyte. No abnormalities in the oocyte meiotic progression were observed during time-lapse experiments in case of overexpression

of *Rose*. However, in the case of downregulation of *Rose* lncRNA through microinjections of short double-stranded RNA (dsRNA) fragments against *Rose* abnormalities were found. The formation of spindle was impaired and major aberrancies happened during chromosome segregation. Moreover, the majority of oocytes failed to extrude polar body. Next, we followed our study by downregulation of *Rose* lncRNA in zygotes and analysis of the downregulation effect in early embryo development. We did not observe any significant impact on the progression to 2 cell stage however downregulation of *Rose* substantially reduced embryonic development to blastocyst in comparison to control.

Thus, in this study we analysed the expression and functional importance of a novel lncRNA *Rose* in the mammalian oocyte and early embryo. We found that *Rose* undergoes alternative splicing and its variant is specifically expressed in the oocyte and early embryo. Moreover, the association of *Rose* with polysomal fraction suggests regulatory functions. The downregulation approach by dsRNA injections allowed us to unravel functional significance of *Rose* in the mammalian oocyte and early embryo.

### **3.3 Single Molecule RNA Localization and Translation in the Mammalian Oocyte and Embryo**

As oocyte relies only on previously synthesized transcripts spatial and temporal distribution of RNA and local translation is important for oocyte physiology. Despite well-known facts about the asymmetric distribution of RNAs in oocytes of many non-mammalian species, data about single-molecule RNA localisation in the mammalian oocyte is scarce. Thus, analysis of ncRNA and mRNA distribution in the oocyte may give hints about the fate of the RNA in the single-cell environment. Moreover, direct visualisation and demonstration of protein synthesis are beneficial for understanding dynamic processes which take place during oocyte maturation.

The objective of this work was to examine the expression and localization patterns of various non-coding and coding RNAs and develop a novel approach for visualization of a single mRNA together with its translational event.

We started this study with a selection of ncRNA and mRNA targets. We selected the following ncRNA candidates: *nuclear enriched abundant transcript 2 (Neat2)*, small nuclear RNA, *RNA Component of 7SK Nuclear Ribonucleoprotein (Rn7sk)*, and *Intracisternal A Particle Long terminal repeat RNA (IAPLtr1a)* (Fig. 9). Using RNA FISH we observed that all selected ncRNAs are present in the nucleus of a fully grown GV oocyte and after NEBD become dispersed in the cytoplasm in the MII stage. After fertilization *Neat2* and *IAPLtr1a* become almost absent in the zygote however the presence of *Rn7sk* in both zygotic pronuclei is restored but not in the nucleus of the polar body. Furthermore, we selected coding mRNA targets that play important roles in oocyte physiology: *Actin  $\beta$  (Actb)* and *Cyclins (Ccnb2, Ccnb3)*. RNA FISH demonstrated that target mRNAs were localized in the cytoplasm and their level decreased throughout meiotic maturation and development. For the quantification of RNA FISH signals, we used equatorial z-sections and to validate this approach we also quantified the number of *Ccnb3*, a candidate mRNA, in the entire oocyte and zygote volume. We observed positive correlation between quantification from single equatorial Z-section and whole volume which confirmed the reliability of simplified scoring.

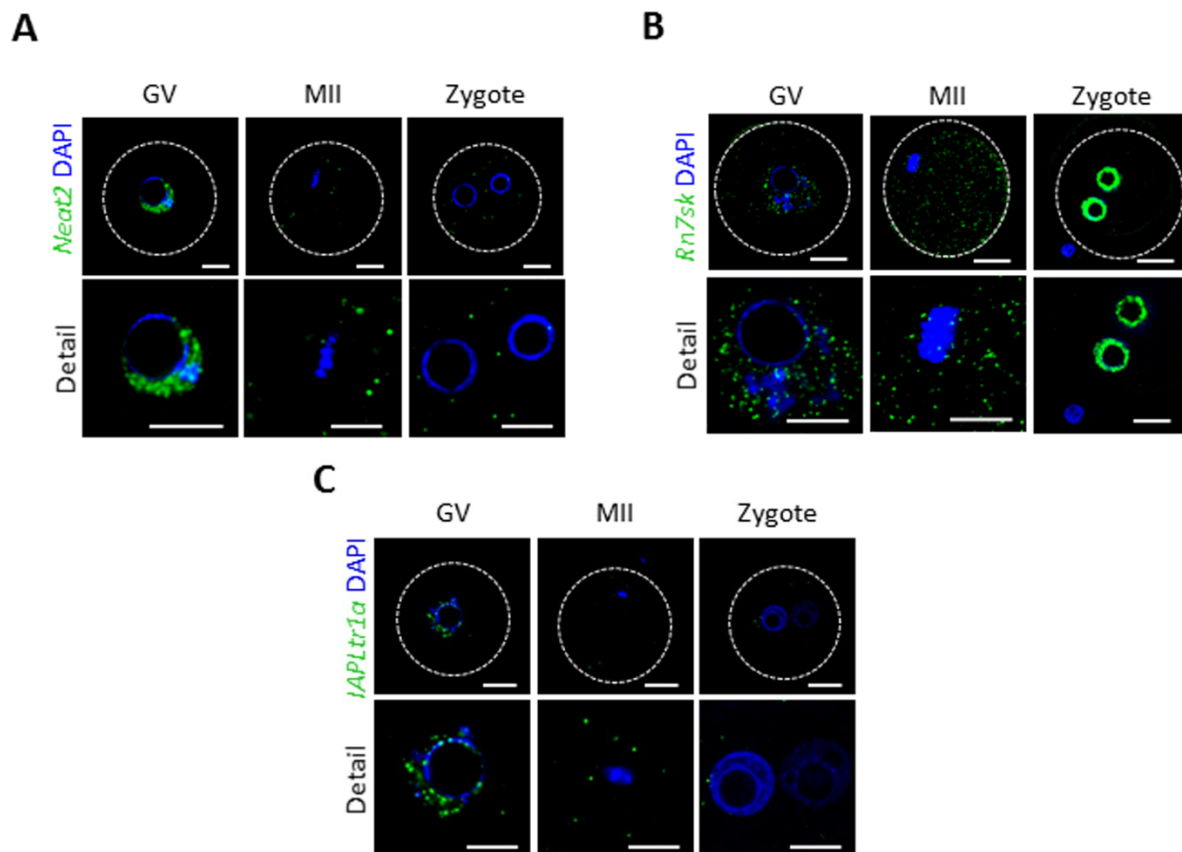


**Figure 9. Localization of ncRNAs in mammalian oocyte and early embryo.** *Neat2* (A), *Rn7sk* (B), and *IAPLtr1a* (C) are present in the nucleus of GV oocyte and after NEDB on MII stage are dispersed in the cytoplasm. While *Neat2* and *IAPLtr1a* are almost absent in the zygote, *Rn7sk* snRNA become again accumulates in zygotic pronuclei.

Moreover, we used qPCR to validate and confirm the quantification obtained from RNA FISH experiments. To do so, we firstly collected samples of fully-grown GV and MII oocytes and zygotes, isolated RNA and performed cDNA synthesis. Trends of expression of candidate RNAs positively correlated between RNA FISH and qPCR approaches. Based on that, we were able to reliably detect localization and expression patterns of selected coding and noncoding RNAs during meiotic maturation and early embryo development.

Simultaneously performed RNA FISH and ICC allowed us to stain single RNA molecules along with protein markers for specific subcellular structures. Particularly, we detected *Neat2* localization in the nucleus of GV oocyte and visualized nuclear envelope via ICC with LMN A/C antibody. Furthermore, we stained the spindle of MII oocyte using anti-tubulin antibody and analysed *Ccnb2* mRNA distribution.

Next, we proceeded with the visualization of a translational event of specific mRNA candidate in the oocytes and zygotes. In order to do that we combined RNA FISH approach which allowed us to label single-molecule mRNAs and PLA using anti-puromycin and anti-ACTB antibodies (RNA-puro-PLA). To perform RNA-puro-PLA we first treated the cells with puromycin which was incorporated into a newly synthesized protein in case of ongoing translation. As mRNA candidates, we selected *Actb*, *Ccnb1*, and *Mos*. Obtained results showed that *Actb* is translated in all studied stages, however more actively on the GV stage in comparison to MII oocyte and zygote. In the case of *Ccnb1* and *Mos* it is known that selected mRNAs are translationally dormant on the GV stage and

become actively translated only later on MII stage. Using RNA-puro-PLA we confirmed that translation of *Ccnbl* and *Mos* was absent on the GV stage but elevated drastically on MII stage. Moreover, obtained results correlated with the level of polysomal occupancy of *Ccnbl* and *Mos* mRNAs on GV and MII stages.

To sum up, we visualized and quantified several selected ncRNAs and mRNAs in the mammalian oocyte and early embryo and confirmed obtained data with an additional approach, qPCR. We were able to detect both single-molecule RNA candidates as well as subcellular structures such as nuclear envelope and meiotic spindle by ICC. To further study the fate of mRNAs during oocyte maturation and early embryo development we developed a new approach called RNA-puro-PLA enabling detection and visualization of translational events of a single mRNA. RNA-puro-PLA results showed distinct patterns of translation on different stages for selected candidates. Thus, here we reliably localized endogenous RNA candidates and their translation within a biological context.

## **4. Discussion**

In this dissertation, my main goal was to unravel the role of selected ncRNAs in the mammalian oocyte. Numerous ncRNAs and especially lncRNAs are transcribed in the mammalian oocyte suggesting their important roles in meiotic maturation and further embryonic development (Ernst *et al.*, 2018; Wang, Koganti and Yao, 2020). Considering that ncRNAs and especially lncRNAs are known to act in post-transcriptional regulations (Rashid, Shah and Shan, 2016; P. Zhang *et al.*, 2019; Karakas and Ozpolat, 2021; Sebastian-Delacruz *et al.*, 2021) they can influence mechanisms of mRNA translation and stabilization in transcriptionally silent mammalian oocyte (Susor and Kubelka, 2017).

I detected several ncRNAs in the oocyte from which *BCI*, *Rose*, and *IAPLtr1a* were not identified in the oocyte previously. I also evaluated the expression of known nuclear ncRNAs *Neat2* and *Rn7sk* (Diribarne and Bensaude, 2009; Yu and Shan, 2016). I found that selected ncRNAs are expressed in GV oocyte and subsequently decline during maturation and early embryo development. Moreover, I observed that one of the selected lncRNA *Rose* is expressed in the oocyte in two variants one of which is oocyte-specific. Specificity of expression is one of the main characteristics which distinguishes lncRNAs from mRNAs because lncRNA expression usually is more cell type specific than the expression of protein-coding genes (Mercer, Dinger, Sunkin, *et al.*, 2008; Pauli *et al.*, 2012). LncRNAs are frequently expressed in developmental-stage, tissue-, and cell-specific manner suggesting their certain regulatory functions. Moreover, such expression pattern provides lncRNAs with great potential to be biomarkers of specific diseases. Another selected ncRNA *BCI* was firstly described in rodents' brain (Tiedge *et al.*, 1991), however later was observed in other tissues. Moreover, I studied ncRNAs *Neat2* and *Rn7sk* which are ubiquitously expressed in all cell types as they have generic roles (Diribarne and Bensaude, 2009; Yu and Shan, 2016).

Gene knockout (KO) is one of the main techniques for analysis of a selected gene's role in an organism or a specific cell type (Hall, Limaye and Kulkarni, 2009). There is a lack of knock-out studies for poorly annotated lncRNAs such as *Rose* and *IapLTR1a*. Recently, knock-out studies were made for several known ncRNAs which I analysed in the presented work. Depletion of *Rn7sk* affected transcription of cell cycle regulators and caused cell cycle arrest (Bandiera *et al.*, 2021). Unexpectedly, a knock-out of very abundant nuclear lncRNA *Neat2* did not lead to problems in viability or fertility (Nakagawa *et al.*, 2012). *Neat2* is considered to be an important component of nuclear speckles, however in cells that lacked *Neat2* nuclear speckle markers were correctly localized. In the same manner, *BCI*-KO animals showed no apparent phenotypes but had reduced exploratory activity (Skryabin *et al.*, 2003). Such mice were fertile and oocyte maturation and early embryo development were not affected. Therefore, in my work, I selected overexpression as the main approach to study the function of *BCI*.

Via comparisons of nucleus and cytoplasmic fractions, I found that two ncRNAs *BCI* and *Rose* exhibit cytoplasmic localization in GV oocyte. Only recently vital roles of cytoplasmic lncRNAs were unravelled and described in posttranscriptional regulations (Zhang *et al.*, 2014; Rashid, Shah and Shan, 2016; Noh *et al.*, 2018). Furthermore, both *BCI* and *Rose* appeared to be ribosome-associated suggesting their interaction with translational machinery (Pircher, Gebetsberger and Polacek, 2014). It is known that ncRNAs often specifically bind structural features and regulatory sequences within the UTRs mRNAs. Therefore, ncRNAs can co-sediment with translating ribosomes during fine-tuning the specificity of translation of complementary mRNA. However, recent advancements in the genetic and proteomic approaches showed the association of lncRNAs

with ribosomes and can indicate actual encoding of proteins or short peptides by these lncRNAs. Many lncRNAs have been found to contain short open reading frames (ORFs) and code for micropeptides which actually perform biological functions (X. Zhang *et al.*, 2019). However, performed computational analysis did not reveal any cryptic ORF in ncRNAs *BCI* and *Rose*.

lncRNAs are known to carry out important functions in the translational regulation (Chekulaeva and Rajewsky, 2019) and therefore can play a role in the modulation and control of maternal mRNA pool (Battaglia *et al.*, 2017). I analysed the functional role of selected ncRNAs and found that ncRNA *BCI* is negatively regulating translation in mammalian oocytes. *BCI* is known to inhibit the formation of 48S initiation complex in the rodent dendrites via binding to eIF4B, eIF4A and PABP (Rozhdestvensky *et al.*, 2001; Eom *et al.*, 2011; Lee *et al.*, 2020). I found that *BCI* is associated with polysomal fraction affecting cap-dependent translational initiation machinery in mammalian oocyte. Also, our results showed that *BCI* interacts with 3'UTR sequences of specific mRNAs and represses their translation. The ability of lncRNAs to obstruct or facilitate formation of translation initiation complex recently has been discovered (Karakas and Ozpolat, 2021). In the oocyte inhibition of untimely initiation of translation might be crucial for controlled protein synthesis and prevention of premature decay of the mRNA. Furthermore, 3'UTRs-mediated regulations are common for mRNA localization or control of protein abundance in many cellular processes (Mayr, 2019). In mammalian oocytes cytoplasmic polyadenylation is based on interactions of RNA-binding proteins with specific signals, CPEs and PASs, in 3'UTR of target mRNAs (Sha, Zhang and Fan, 2019). Thus, direct physical interaction of ncRNA *BCI* and 3'UTRs of selected ncRNAs might disrupt attachment of other RPBs such as PABP and hence translation of single mRNAs.

Moreover, I and others showed that *BCI* interacts with FMRP – a translational repressor known to drive the formation of RNP complexes (Zalfa *et al.*, 2003). Moreover, I observed that *BCI* overexpression affects localization pattern of FMRP and poly(A) RNA in MII oocyte. Many other oocyte RNPs have been identified in mammalian oocyte, however, exact mechanisms of mRNA regulation in such RNPs have not been yet fully elucidated. For example, Y-box-binding protein MSY2 or Pumilio (PUM) proteins recognise the PUM-binding element (PBE) (Christou-Kent *et al.*, 2020). Germlines of many model organisms (*Xenopus*, *Drosophila*, *C. elegans*, and zebrafish) have well-conserved membrane-free RNPs. Among them, an equivalents of somatic P-bodies are called 'germ granules'. In mouse, such granules have been described to exist only in primordial follicle oocytes of mice under two weeks of age (Voronina *et al.*, 2011). However, the absence of distinct P-bodies and stress granules in the mammalian oocyte suggests other mechanisms of mRNA decay and storage (Flemer *et al.*, 2010). The formation of *BCI*-FMRP complexes affects gene expression and might present a new RNP complex in mammalian oocyte with repressed translational activity.

In contrast to *BCI*, another selected ribosome-associated lncRNA *Rose* did not affect translational rate in the oocyte. On the other hand, the knockdown experiments showed that *Rose* has an important regulatory role in oocyte cytokinesis and the embryonic cleavages after ZGA. Other lncRNAs were also shown to participate in chromosome segregation, microtubule dynamics cytokinesis (Stojic *et al.*, 2020). For example, Pei *et al.*, in 2018 showed that lncRNA *CRYBG3* directly binds G-actin to repress its polymerization and resulting in M-phase cell arrest (Pei *et al.*, 2018). Therefore, lncRNAs are implicated in cell cycle control during mitosis and meiosis. Observed phenotype suggests that *Rose* lncRNA is indispensable for female germ cell and embryonic development.

As ncRNAs perform their functions without being translated to the protein their localization is directly connected with their regulatory roles and thus is highly informative. For example, proper

localization of ncRNAs is important for long-term memory formation including stabilization of mRNAs or regulation of the local translation (Mercer, Dinger, Mariani, *et al.*, 2008). In the oocytes of non-mammalian species localization of RNA is crucial for the following embryonic development but data about ncRNA and mRNA localization in mammalian oocyte are scarce. There are a few ways how to study localization of RNA through RNA extraction from single cells or specific compartments, but in general those are laborious and crude approaches. RNA FISH is the main approach for visualization of single or multiple RNAs in fixed cells (Raj *et al.*, 2008; Xie, Timme and Wood, 2018). Combination of RNA FISH with other methods, such as ICC staining and PLA (Tom Dieck *et al.*, 2015; Moissoglu *et al.*, 2019) enables detection of selected ncRNAs along with quantitative and spatial-subcellular context adding information about colocalization with possible binding partners. Moreover, RNA FISH is a very convenient method for RNAs with tissue-specific expression patterns as it excludes the possibility of sample contamination.

Altogether, we have shown that lncRNAs play an important role in oocyte physiology. Novel and uncharacterized molecules are important for solving the puzzle of complex molecular mechanisms in the cell. Moreover, the identification of lncRNA-mediated regulatory mechanisms and their malfunctions might shed light on the problem of infertility (Battaglia *et al.*, 2017; Joshi and Rajender, 2020; Zhou and Wang, 2020). Importantly, some lncRNAs (e.g. *AFAPI-ASI*, *HOTAIR*, *AACSPI*) are not expressed in normal adult tissues but specifically contribute in both oogenesis and carcinogenesis suggesting that reactivation of an embryonic lncRNA program may contribute to human malignancies (Bouckenheimer *et al.*, 2016).

Germline or embryonic specific ncRNAs might be used as quality markers used in biotechnology or assisted reproductive technologies thus their study requires further effort (Robles, Valcarce and Riesco, 2019).

## **5. Conclusions**

- I have shown that ncRNA *BCI*, snRNA *Rn7sk* and lncRNAs *Neat2*, *Rose*, *IAPLtr1a* are expressed in the mouse oocyte and early embryo.
- I have demonstrated that snRNA *Rn7sk* and lncRNAs *Neat2* are localized in the nucleus of GV mouse oocyte with a significant decrease during meiotic maturation and early embryo development. The same pattern of expression exhibited earlier unknown retrotransposon-derived *IAPLtr1a* lncRNA which might indicate nucleus associated functions.
- I have detected an association of *BCI* ncRNA and *Rose* lncRNA with polyribosomes in the GV mouse oocyte which indicates their involvement in translational machinery. Particularly, *BCI* slightly represses the mechanism of translational initiation.
- I have observed that translation of specific mRNA targets is inhibited by *BCI* ncRNA via a protein interplay. In addition, *BCI* ncRNA interacts with FMRP protein in the GV oocyte and influences clustering of FMRP and polyA mRNA in MII oocyte. Therefore, *BCI* might function as a platform for complex interactions between RBP and mRNAs.
- I have shown that *Rose* lncRNA is alternatively spliced in mammalian oocyte and is expressed in two forms one of which is oocyte-specific. Oocyte-specific form of *Rose* lncRNA has a role in embryo cleavage after ZGA in 2-cell embryo.
- We established RNA FISH (RNA Scope) approach for localization of individual RNA molecules. We found that it is suitable for quantitative spatio-temporal analysis of specific RNAs in the mammalian oocyte and early embryo.
- We developed a new RNA-puro-PLA approach for visualization of *in situ* translation with single-molecule resolution.

My thesis provides new insights into ncRNA-based regulatory networks in mouse oocyte and early embryo development. Moreover, here I present novel methods which I believe can contribute to studies about ncRNA molecular pathways and expand our knowledge about cellular physiology and pathology related to the reproduction of mammals.



## **6. References**

- Anguera, M. C. *et al.* (2011) 'Tsx produces a long noncoding RNA and has general functions in the germline, stem cells, and brain', *PLoS Genetics*. doi: 10.1371/journal.pgen.1002248.
- Arun, G., Aggarwal, D. and Spector, D. L. (2020) 'MALAT1 long non-coding RNA: Functional implications', *Non-coding RNA*. doi: 10.3390/NCRNA6020022.
- Attardi, G. and Amaldi, F. (1970) 'Structure and synthesis of ribosomal RNA.', *Annual review of biochemistry*. doi: 10.1146/annurev.bi.39.070170.001151.
- Bandiera, R. *et al.* (2021) 'RN7SK small nuclear RNA controls bidirectional transcription of highly expressed gene pairs in skin', *Nature Communications*. doi: 10.1038/s41467-021-26083-4.
- Bashirullah, A., Cooperstock, R. L. and Lipshitz, H. D. (2001) 'Spatial and temporal control of RNA stability', *Proceedings of the National Academy of Sciences of the United States of America*. doi: 10.1073/pnas.111145698.
- Bastide, A. and David, A. (2018) 'Interaction of rRNA with mRNA and tRNA in translating mammalian ribosome: Functional implications in health and disease', *Biomolecules*. doi: 10.3390/biom8040100.
- Battaglia, R. *et al.* (2016) 'MicroRNAs are stored in human MII oocyte and their expression profile changes in reproductive aging', *Biology of Reproduction*. doi: 10.1095/biolreprod.116.142711.
- Battaglia, R. *et al.* (2017) 'Non-coding RNAs in the ovarian follicle', *Frontiers in Genetics*. doi: 10.3389/fgene.2017.00057.
- Bettogowda, A. and Smith, G. W. (2007) 'Mechanisms of maternal mRNA regulation: Implications for mammalian early embryonic development', *Frontiers in Bioscience*. doi: 10.2741/2346.
- Blower, M. D. (2013) 'Molecular Insights into Intracellular RNA Localization', in *International Review of Cell and Molecular Biology*. doi: 10.1016/B978-0-12-407699-0.00001-7.
- Bouckenheimer, J. *et al.* (2016) 'Long non-coding RNAs in human early embryonic development and their potential in ART', *Human Reproduction Update*. doi: 10.1093/humupd/dmw035.
- Brachova, P. *et al.* (2019) 'Inosine RNA modifications are enriched at the codon wobble position in mouse oocytes and eggs', *Biology of Reproduction*. doi: 10.1093/biolre/ioz130.
- Briata, P. and Gherzi, R. (2020) 'Long non-coding RNA-ribonucleoprotein networks in the post-transcriptional control of gene expression', *Non-coding RNA*. doi: 10.3390/NCRNA6030040.
- Carrieri, C. *et al.* (2012) 'Long non-coding antisense RNA controls Uchl1 translation through an embedded SINEB2 repeat', *Nature*. doi: 10.1038/nature11508.
- Casser, E. *et al.* (2019) 'Differences in blastomere totipotency in 2-cell mouse embryos are a maternal trait mediated by asymmetric mRNA distribution', *Molecular Human Reproduction*. doi: 10.1093/molehr/gaz051.
- Chekulaeva, M. and Rajewsky, N. (2019) 'Roles of long noncoding rnas and circular rnas in translation', *Cold Spring Harbor Perspectives in Biology*. doi: 10.1101/cshperspect.a032680.
- Chen, S. *et al.* (2017) 'LncRNA TUG1 sponges microRNA-9 to promote neurons apoptosis by up-regulated Bcl2l11 under ischemia', *Biochemical and Biophysical Research Communications*. doi: 10.1016/j.bbrc.2017.02.043.
- Christou-Kent, M. *et al.* (2020) 'Diversity of RNA-Binding Proteins Modulating Post-Transcriptional Regulation of Protein Expression in the Maturing Mammalian Oocyte', *Cells*. doi:

10.3390/cells9030662.

Clarke, H. J. (2012) 'Post-transcriptional control of gene expression during mouse oogenesis', *Results and Problems in Cell Differentiation*. doi: 10.1007/978-3-642-30406-4\_1.

Congrains, A. *et al.* (2013) 'ANRIL: Molecular mechanisms and implications in human health', *International Journal of Molecular Sciences*. doi: 10.3390/ijms14011278.

Crick, F. (1970) 'Central dogma of molecular biology', *Nature*. doi: 10.1038/227561a0.

Dai, X. X. *et al.* (2019) 'A combinatorial code for mRNA 3'-UTR-mediated translational control in the mouse oocyte', *Nucleic Acids Research*. doi: 10.1093/nar/gky971.

Dana, H. *et al.* (2017) 'Molecular Mechanisms and Biological Functions of siRNA.', *International journal of biomedical science : IJBS*.

Dieci, G., Preti, M. and Montanini, B. (2009) 'Eukaryotic snoRNAs: A paradigm for gene expression flexibility', *Genomics*. doi: 10.1016/j.ygeno.2009.05.002.

Diribarne, G. and Bensaude, O. (2009) '7SK RNA, a non-coding RNA regulating P-TEFb, a general transcription factor', *RNA Biology*. doi: 10.4161/rna.6.2.8115.

Dowling, R. J. O. *et al.* (2010) 'mTORCI-mediated cell proliferation, but not cell growth, controlled by the 4E-BPs', *Science*. doi: 10.1126/science.1187532.

Eom, T. *et al.* (2011) 'Dual Nature of Translational Control by Regulatory BC RNAs', *Molecular and Cellular Biology*. doi: 10.1128/mcb.05885-11.

Erhard, F. *et al.* (2018) 'Improved Ribo-seq enables identification of cryptic translation events', *Nature Methods*. doi: 10.1038/nmeth.4631.

Ernst, E. H. *et al.* (2018) 'Transcriptome analysis of long non-coding RNAs and genes encoding paraspeckle proteins during human ovarian follicle development', *Frontiers in Cell and Developmental Biology*. doi: 10.3389/fcell.2018.00078.

Ferrè, F., Colantoni, A. and Helmer-Citterich, M. (2016) 'Revealing protein-lncRNA interaction', *Briefings in Bioinformatics*. doi: 10.1093/bib/bbv031.

Fischer, S. E. J. (2015) 'RNA interference and microRNA-mediated silencing', *Current Protocols in Molecular Biology*. doi: 10.1002/0471142727.mb2601s112.

Flemer, M. *et al.* (2010) 'P-body loss is concomitant with formation of a messenger RNA storage domain in mouse oocytes', *Biology of Reproduction*. doi: 10.1095/biolreprod.109.082057.

Fox, A. H. *et al.* (2018) 'Paraspeckles: Where Long Noncoding RNA Meets Phase Separation', *Trends in Biochemical Sciences*. doi: 10.1016/j.tibs.2017.12.001.

Ganesh, S. *et al.* (2020) 'The most abundant maternal lncRNA Sirena1 acts post-transcriptionally and impacts mitochondrial distribution', *Nucleic Acids Research*. doi: 10.1093/nar/gkz1239.

Gebert, L. F. R. and MacRae, I. J. (2019) 'Regulation of microRNA function in animals', *Nature Reviews Molecular Cell Biology*. doi: 10.1038/s41580-018-0045-7.

Geisler, S. and Collier, J. (2013) 'RNA in unexpected places: Long non-coding RNA functions in diverse cellular contexts', *Nature Reviews Molecular Cell Biology*. doi: 10.1038/nrm3679.

Gloss, B. S. and Dinger, M. E. (2016) 'The specificity of long noncoding RNA expression', *Biochimica et Biophysica Acta - Gene Regulatory Mechanisms*. doi: 10.1016/j.bbgrm.2015.08.005.

Gong, C. and Maquat, L. E. (2011) 'LncRNAs transactivate STAU1-mediated mRNA decay by duplexing with 3' UTRs via Alu element', *Nature*. doi: 10.1038/nature09701.

- Graf, J. and Kretz, M. (2020) 'From structure to function: Route to understanding lncRNA mechanism', *BioEssays*. doi: 10.1002/bies.202000027.
- Hake, L. E. and Richter, J. D. (1994) 'CPEB is a specificity factor that mediates cytoplasmic polyadenylation during *Xenopus* oocyte maturation', *Cell*. doi: 10.1016/0092-8674(94)90547-9.
- Hall, B., Limaye, A. and Kulkarni, A. B. (2009) 'Overview: Generation of Gene Knockout Mice', *Current Protocols in Cell Biology*. doi: 10.1002/0471143030.cb1912s44.
- Hasenson, S. E. and Shav-Tal, Y. (2020) 'Speculating on the Roles of Nuclear Speckles: How RNA-Protein Nuclear Assemblies Affect Gene Expression', *BioEssays*. doi: 10.1002/bies.202000104.
- Holley, R. W. *et al.* (1965) 'Structure of a ribonucleic acid', *Science*. doi: 10.1126/science.147.3664.1462.
- Hu, G., Lou, Z. and Gupta, M. (2014) 'The long non-coding RNA GAS5 cooperates with the eukaryotic translation initiation factor 4E to regulate c-Myc translation', *PLoS ONE*. doi: 10.1371/journal.pone.0107016.
- Iacoangeli, A. *et al.* (2008) 'On BC1 RNA and the fragile X mental retardation protein', *Proceedings of the National Academy of Sciences of the United States of America*. doi: 10.1073/pnas.0710991105.
- Iwasaki, Y. W., Siomi, M. C. and Siomi, H. (2015) 'PIWI-interacting RNA: Its biogenesis and functions', *Annual Review of Biochemistry*. doi: 10.1146/annurev-biochem-060614-034258.
- Jackson, R. J., Hellen, C. U. T. and Pestova, T. V. (2010) 'The mechanism of eukaryotic translation initiation and principles of its regulation', *Nature Reviews Molecular Cell Biology*. doi: 10.1038/nrm2838.
- Jansova, D. *et al.* (2018) 'Localization of RNA and translation in the mammalian oocyte and embryo', *PLoS ONE*. doi: 10.1371/journal.pone.0192544.
- Jia, X. *et al.* (2019) 'KLF5 regulated lncRNA RP1 promotes the growth and metastasis of breast cancer via repressing p27kip1 translation', *Cell Death and Disease*. doi: 10.1038/s41419-019-1566-5.
- Johnsson, P. *et al.* (2014) 'Evolutionary conservation of long non-coding RNAs; Sequence, structure, function', *Biochimica et Biophysica Acta - General Subjects*. doi: 10.1016/j.bbagen.2013.10.035.
- Joshi, M. and Rajender, S. (2020) 'Long non-coding RNAs (lncRNAs) in spermatogenesis and male infertility', *Reproductive Biology and Endocrinology*. doi: 10.1186/s12958-020-00660-6.
- Kaikkonen, M. U., Lam, M. T. Y. and Glass, C. K. (2011) 'Non-coding RNAs as regulators of gene expression and epigenetics', *Cardiovascular Research*. doi: 10.1093/cvr/cvr097.
- Karakas, D. and Ozpolat, B. (2021) 'The role of lncRNAs in translation', *Non-coding RNA*. doi: 10.3390/nrna7010016.
- Kataruka, S. *et al.* (2020) 'MicroRNA dilution during oocyte growth disables the microRNA pathway in mammalian oocytes', *Nucleic Acids Research*. doi: 10.1093/nar/gkaa543.
- De La Fuente, R. *et al.* (2004) 'Major chromatin remodeling in the germinal vesicle (GV) of mammalian oocytes is dispensable for global transcriptional silencing but required for centromeric heterochromatin function', *Developmental Biology*. doi: 10.1016/j.ydbio.2004.08.028.
- Lee, Y. *et al.* (2020) 'Brain cytoplasmic RNAs in neurons: From biosynthesis to function', *Biomolecules*. doi: 10.3390/biom10020313.

- Loda, A. and Heard, E. (2019) 'Xist RNA in action: Past, present, and future', *PLoS Genetics*. doi: 10.1371/journal.pgen.1008333.
- Malecová, B. and Morris, K. (2010) 'Transcriptional gene silencing mediated by non-coding RNAs', *Current opinion in molecular therapeutics*.
- Masek, T. *et al.* (2020) 'Identifying the transcriptome of mouse NEBD-stage oocytes via SSP-profiling; a novel polysome fractionation method', *International Journal of Molecular Sciences*. doi: 10.3390/ijms21041254.
- Mayr, C. (2019) 'What are 3' utrs doing?', *Cold Spring Harbor Perspectives in Biology*. doi: 10.1101/cshperspect.a034728.
- Mercer, T. R., Dinger, M. E., Mariani, J., *et al.* (2008) 'Noncoding RNAs in long-term memory formation', *Neuroscientist*. doi: 10.1177/1073858408319187.
- Mercer, T. R., Dinger, M. E., Sunkin, S. M., *et al.* (2008) 'Specific expression of long noncoding RNAs in the mouse brain', *Proceedings of the National Academy of Sciences of the United States of America*. doi: 10.1073/pnas.0706729105.
- Moissoglu, K. *et al.* (2019) 'Translational regulation of protrusion-localized RNAs involves silencing and clustering after transport', *eLife*. eLife Sciences Publications Ltd, 8. doi: 10.7554/eLife.44752.
- Nakagawa, S. *et al.* (2011) 'Paraspeckles are subpopulation-specific nuclear bodies that are not essential in mice', *Journal of Cell Biology*. doi: 10.1083/jcb.201011110.
- Nakagawa, S. *et al.* (2012) 'Malat1 is not an essential component of nuclear speckles in mice', *RNA*. doi: 10.1261/rna.033217.112.
- Noh, J. H. *et al.* (2018) 'Cytoplasmic functions of long noncoding RNAs', *Wiley Interdisciplinary Reviews: RNA*. doi: 10.1002/wrna.1471.
- Nolasco, S. *et al.* (2012) 'The expression of tubulin cofactor A (TBCA) is regulated by a noncoding antisense TbcA RNA during testis maturation', *PLoS ONE*. doi: 10.1371/journal.pone.0042536.
- Oh, D. and Houston, D. W. (2017) 'RNA localization in the vertebrate oocyte: Establishment of oocyte polarity and localized mRNA assemblages', in *Results and Problems in Cell Differentiation*. doi: 10.1007/978-3-319-60855-6\_9.
- Ozata, D. M. *et al.* (2019) 'PIWI-interacting RNAs: small RNAs with big functions', *Nature Reviews Genetics*. doi: 10.1038/s41576-018-0073-3.
- Pandey, R. R. *et al.* (2008) 'Kcnq1ot1 Antisense Noncoding RNA Mediates Lineage-Specific Transcriptional Silencing through Chromatin-Level Regulation', *Molecular Cell*. doi: 10.1016/j.molcel.2008.08.022.
- Pauli, A. *et al.* (2012) 'Systematic identification of long noncoding RNAs expressed during zebrafish embryogenesis', *Genome Research*. doi: 10.1101/gr.133009.111.
- Pei, H. *et al.* (2018) 'Long noncoding RNA CRYBG3 blocks cytokinesis by directly binding G-Actin', *Cancer Research*. doi: 10.1158/0008-5472.CAN-18-0988.
- Peng, W. X. *et al.* (2019) 'lncRNA RMST Enhances DNMT3 Expression through Interaction with HuR', *Molecular Therapy*. doi: 10.1016/j.ymthe.2019.09.024.
- Pesin, J. A. and Orr-Weaver, T. L. (2008) 'Regulation of APC/C activators in mitosis and meiosis', *Annual Review of Cell and Developmental Biology*. doi: 10.1146/annurev.cellbio.041408.115949.

- Pircher, A., Gebetsberger, J. and Polacek, N. (2014) 'Ribosome-associated ncRNAs: An emerging class of translation regulators', *RNA Biology*. doi: 10.1080/15476286.2014.996459.
- Ponjavic, J., Ponting, C. P. and Lunter, G. (2007) 'Functionality or transcriptional noise? Evidence for selection within long noncoding RNAs', *Genome Research*. doi: 10.1101/gr.6036807.
- Priyanka, P. *et al.* (2021) 'The lncRNA HMS recruits RNA-binding protein HuR to stabilize the 3'-UTR of HOXC10 mRNA', *Journal of Biological Chemistry*. doi: 10.1016/j.jbc.2021.100997.
- Qu, S. *et al.* (2015) 'Circular RNA: A new star of noncoding RNAs', *Cancer Letters*. doi: 10.1016/j.canlet.2015.06.003.
- Qu, S. *et al.* (2017) 'The emerging landscape of circular RNA in life processes', *RNA Biology*. doi: 10.1080/15476286.2016.1220473.
- Radford, H. E., Meijer, H. A. and de Moor, C. H. (2008) 'Translational control by cytoplasmic polyadenylation in *Xenopus* oocytes', *Biochimica et Biophysica Acta - Gene Regulatory Mechanisms*. doi: 10.1016/j.bbagr.2008.02.002.
- Raj, A. *et al.* (2008) 'Imaging individual mRNA molecules using multiple singly labeled probes', *Nature Methods*. doi: 10.1038/nmeth.1253.
- Rashid, F., Shah, A. and Shan, G. (2016) 'Long Non-coding RNAs in the Cytoplasm', *Genomics, Proteomics and Bioinformatics*. doi: 10.1016/j.gpb.2016.03.005.
- Rinn, J. L. *et al.* (2007) 'Functional Demarcation of Active and Silent Chromatin Domains in Human HOX Loci by Noncoding RNAs', *Cell*. doi: 10.1016/j.cell.2007.05.022.
- Robles, V., Valcarce, D. G. and Riesco, M. F. (2019) 'Non-coding RNA regulation in reproduction: Their potential use as biomarkers', *Non-coding RNA Research*. doi: 10.1016/j.ncrna.2019.04.001.
- Rozhdestvensky, T. S. *et al.* (2001) 'Neuronal BC1 RNA structure: Evolutionary conversion of a tRNAAla domain into an extended stem-loop structure', *RNA*. doi: 10.1017/S1355838201002485.
- Sado, T. and Brockdorff, N. (2013) 'Advances in understanding chromosome silencing by the long non-coding RNA Xist', *Philosophical Transactions of the Royal Society B: Biological Sciences*. doi: 10.1098/rstb.2011.0325.
- Santoro, F. *et al.* (2013) 'Imprinted *Igf2r* silencing depends on continuous airn lncRNA expression and is not restricted to a developmental window', *Development (Cambridge)*. doi: 10.1242/dev.088849.
- Sebastian-Delacruz, M. *et al.* (2021) 'The role of lncRNAs in gene expression regulation through mRNA stabilization', *Non-coding RNA*. doi: 10.3390/ncrna7010003.
- Seeley, J. J. *et al.* (2018) 'Induction of innate immune memory via microRNA targeting of chromatin remodelling factors', *Nature*. doi: 10.1038/s41586-018-0253-5.
- Semotok, J. L. *et al.* (2008) 'Drosophila Maternal Hsp83 mRNA Destabilization Is Directed by Multiple SMAUG Recognition Elements in the Open Reading Frame', *Molecular and Cellular Biology*. doi: 10.1128/mcb.00037-08.
- Sha, Q. Q., Zhang, J. and Fan, H. Y. (2019) 'A story of birth and death: mRNA translation and clearance at the onset of maternal-To-zygotic transition in mammals', *Biology of Reproduction*. doi: 10.1093/biolre/i0z012.
- Sindelka, R. *et al.* (2018) 'Asymmetric distribution of biomolecules of maternal origin in the *Xenopus laevis* egg and their impact on the developmental plan', *Scientific Reports*. doi: 10.1038/s41598-018-26592-1.

- Singh, G. *et al.* (2015) 'The clothes make the mRNA: Past and present trends in mRNP fashion', *Annual Review of Biochemistry*. doi: 10.1146/annurev-biochem-080111-092106.
- Sinha, P. B. *et al.* (2017) 'MicroRNA-130b is involved in bovine granulosa and cumulus cells function, oocyte maturation and blastocyst formation', *Journal of Ovarian Research*. doi: 10.1186/s13048-017-0336-1.
- Skryabin, B. V. *et al.* (2003) 'Neuronal Untranslated BC1 RNA: Targeted Gene Elimination in Mice', *Molecular and Cellular Biology*. doi: 10.1128/mcb.23.18.6435-6441.2003.
- Song, Z. *et al.* (2021) 'The nuclear functions of long noncoding RNAs come into focus', *Non-coding RNA Research*. doi: 10.1016/j.ncrna.2021.03.002.
- Statello, L. *et al.* (2021) 'Gene regulation by long non-coding RNAs and its biological functions', *Nature Reviews Molecular Cell Biology*. doi: 10.1038/s41580-020-00315-9.
- Stebbins-Boaz, B., Hake, L. E. and Richter, J. D. (1996) 'CPEB controls the cytoplasmic polyadenylation of cyclin, Cdk2 and c-mos mRNAs and is necessary for oocyte maturation in *Xenopus*', *EMBO Journal*. doi: 10.1002/j.1460-2075.1996.tb00616.x.
- Stein, P. *et al.* (2015) 'Essential Role for Endogenous siRNAs during Meiosis in Mouse Oocytes', *PLoS Genetics*. doi: 10.1371/journal.pgen.1005013.
- Stojic, L. *et al.* (2020) 'A high-content RNAi screen reveals multiple roles for long noncoding RNAs in cell division', *Nature Communications*. doi: 10.1038/s41467-020-14978-7.
- Su, Y. Q. *et al.* (2007) 'Selective degradation of transcripts during meiotic maturation of mouse oocytes', *Developmental Biology*. doi: 10.1016/j.ydbio.2006.09.008.
- Susor, A. *et al.* (2015) 'Temporal and spatial regulation of translation in the mammalian oocyte via the mTOR-eIF4F pathway', *Nature Communications*. doi: 10.1038/ncomms7078.
- Susor, A. and Kubelka, M. (2017) 'Translational regulation in the mammalian oocyte', in *Results and Problems in Cell Differentiation*. doi: 10.1007/978-3-319-60855-6\_12.
- Svoboda, P. (2018) 'Mammalian zygotic genome activation', *Seminars in Cell and Developmental Biology*. doi: 10.1016/j.semcdb.2017.12.006.
- Tadros, W. *et al.* (2007) 'SMAUG Is a Major Regulator of Maternal mRNA Destabilization in *Drosophila* and Its Translation Is Activated by the PAN GU Kinase', *Developmental Cell*. doi: 10.1016/j.devcel.2006.10.005.
- Tiedge, H. *et al.* (1991) 'Dendritic location of neural BC1 RNA', *Proceedings of the National Academy of Sciences of the United States of America*. doi: 10.1073/pnas.88.6.2093.
- Tom Dieck, S. *et al.* (2015) 'Direct visualization of newly synthesized target proteins in situ', *Nature Methods*. Nature Publishing Group, 12(5), pp. 411–414. doi: 10.1038/nmeth.3319.
- Tripathi, A., Prem Kumar, K. V. and Chaube, S. K. (2010) 'Meiotic cell cycle arrest in mammalian oocytes', *Journal of Cellular Physiology*. doi: 10.1002/jcp.22108.
- Tsai, M. C. *et al.* (2010) 'Long noncoding RNA as modular scaffold of histone modification complexes', *Science*. doi: 10.1126/science.1192002.
- Valadkhan, S. (2010) 'Role of the snRNAs in spliceosomal active site', *RNA Biology*. doi: 10.4161/rna.7.3.12089.
- Voronina, A. S. and Pshennikova, E. S. (2021) 'mRNPs: Structure and role in development', *Cell Biochemistry and Function*. doi: 10.1002/cbf.3656.
- Voronina, E. *et al.* (2011) 'RNA granules in germ cells', *Cold Spring Harbor Perspectives in Biology*. doi: 10.1101/cshperspect.a002774.

- Wang, C. and Lehmann, R. (1991) 'Nanos is the localized posterior determinant in *Drosophila*', *Cell*. doi: 10.1016/0092-8674(91)90110-K.
- Wang, J. *et al.* (2016) 'A novel long intergenic noncoding RNA indispensable for the cleavage of mouse two-cell embryos', *EMBO reports*. doi: 10.15252/embr.201642051.
- Wang, J. *et al.* (2018) 'Asymmetric Expression of LincGET Biases Cell Fate in Two-Cell Mouse Embryos', *Cell*. doi: 10.1016/j.cell.2018.11.039.
- Wang, J., Koganti, P. P. and Yao, J. (2020) 'Systematic identification of long intergenic non-coding RNAs expressed in bovine oocytes', *Reproductive Biology and Endocrinology*. doi: 10.1186/s12958-020-00573-4.
- Wang, K. C. *et al.* (2011) 'A long noncoding RNA maintains active chromatin to coordinate homeotic gene expression', *Nature*. doi: 10.1038/nature09819.
- Xie, F., Timme, K. A. and Wood, J. R. (2018) 'Using Single Molecule mRNA Fluorescent in Situ Hybridization (RNA-FISH) to Quantify mRNAs in Individual Murine Oocytes and Embryos', *Scientific Reports*. doi: 10.1038/s41598-018-26345-0.
- Yakovchuk, P., Goodrich, J. A. and Kugel, J. F. (2009) 'B2 RNA and Alu RNA repress transcription by disrupting contacts between RNA polymerase II and promoter DNA within assembled complexes', *Proceedings of the National Academy of Sciences of the United States of America*. doi: 10.1073/pnas.0810738106.
- Yamazaki, T. and Hirose, T. (2015) 'The building process of the functional paraspeckle with long non-coding RNAs', *Frontiers in Bioscience - Elite*. doi: 10.2741/E715.
- Yoon, J. H. *et al.* (2012) 'LincRNA-p21 Suppresses Target mRNA Translation', *Molecular Cell*. doi: 10.1016/j.molcel.2012.06.027.
- Yu, B. and Shan, G. (2016) 'Functions of long noncoding RNAs in the nucleus', *Nucleus*. doi: 10.1080/19491034.2016.1179408.
- Zaheed, O. *et al.* (2021) 'Exploring Evidence of Non-coding RNA Translation With Trips-Viz and GWIPS-Viz Browsers', *Frontiers in Cell and Developmental Biology*. doi: 10.3389/fcell.2021.703374.
- Zalfa, F. *et al.* (2003) 'The Fragile X syndrome protein FMRP associates with BC1 RNA and regulates the translation of specific mRNAs at synapses', *Cell*. doi: 10.1016/S0092-8674(03)00079-5.
- Zhang, K. *et al.* (2014) 'The ways of action of long non-coding RNAs in cytoplasm and nucleus', *Gene*. doi: 10.1016/j.gene.2014.06.043.
- Zhang, P. *et al.* (2019) 'Non-Coding RNAs and their Integrated Networks', *Journal of integrative bioinformatics*. doi: 10.1515/jib-2019-0027.
- Zhang, X. *et al.* (2019) 'Mechanisms and functions of long non-coding RNAs at multiple regulatory levels', *International Journal of Molecular Sciences*. doi: 10.3390/ijms20225573.
- Zhang, Z. K. *et al.* (2018) 'A newly identified lncRNA MAR1 acts as a miR-487b sponge to promote skeletal muscle differentiation and regeneration', *Journal of Cachexia, Sarcopenia and Muscle*. doi: 10.1002/jcsm.12281.
- Zhou, G. and Chen, X. (2019) 'Emerging role of extracellular microRNAs and lncRNAs', *ExRNA*. AME Publishing Company, 1(February-March), pp. 1–6. doi: 10.1186/S41544-019-0012-2/TABLES/1.
- Zhou, Z. and Wang, B. (2020) 'Identification of male infertility-related long non-coding RNAs and their functions based on a competing endogenous RNA network', *Journal of International*

*Medical Research*. doi: 10.1177/0300060520961277.

Zucchelli, S. *et al.* (2015) 'SINEUPs: A new class of natural and synthetic antisense long non-coding RNAs that activate translation', *RNA Biology*. doi: 10.1080/15476286.2015.1060395.



## **7. Abbreviations**

3'UTRs	3' untranslated regions
4E-BPs	4E-binding proteins
5'UTRs	5' untranslated regions
<i>Actb</i>	<i>Actin β</i>
ACTB	Actin β
APC/C	Anaphase-promoting complex
AS	Antisense
<i>BC1</i>	<i>Brain cytoplasmic RNA 1</i>
CCNB	Cyclin B
CDK1	Cyclin-dependent kinase 1
circRNAs	Circular RNAs
CPAT	Coding Potential Assessment Tool
CPE	Cytoplasmic polyadenylation element
CPEB	CPE-binding protein
CSF	Cytostatic factor
DLG4	Postsynaptic density protein 95
dsRNA	Double-stranded RNA
eRNAs	Enhancer long noncoding RNAs
FISH	Fluorescence <i>in situ</i> hybridization
FMRP	Fragile X Mental Retardation Protein
gGV	Growing GV
GV	Germinal vesicle/Oocytes in germinal vesicle stage
HOX	Homeobox
<i>IAPLtr1a</i>	<i>Intracisternal A Particle Long terminal repeat RNA</i>
ICC	Immunocytochemistry
KO	Knockout
LMN A/C	Lamin A/C
lncRNAs	Long noncoding RNAs
MI	Metaphase I/Oocytes in metaphase I stage
MII	Metaphase II/Oocytes in metaphase II stage
miRNAs	Micro RNAs
MPF	Maturation-promoting factor
mRNAs	Messenger RNAs
NCE	Noncoding exons
ncRNAs	Noncoding RNAs
<i>Neat1</i>	<i>Nuclear Enriched Abundant Transcript 1</i>
<i>Neat2</i>	<i>Nuclear Enriched Abundant Transcript 2</i>
NEBD	Nuclear envelope break down/Oocytes after nuclear envelope break down
OE	Overexpression
ORFs	Open reading frames
PABP	Poly(A)-binding protein
PAS	Polyadenylation signal
PGCs	Primordial germ cells
piRNAs	Piwi-interacting RNAs
PLA	Proximity ligation assay
PRC2	Polycomb repressive complex 2
qPCR	Quantitative polymerase chain reaction
RBPs	RNA Binding Proteins
RISC	RNA-induced silencing complexes
<i>Rn7sk</i>	<i>RNA Component of 7SK Nuclear Ribonucleoprotein</i>
RNA-PLA	RNA- proximity ligation assay

RNA-puro-PLA	Puromycilation proximity ligation assay
RNP	Ribonucleoprotein
<i>Rose</i>	<i>LncRNA in Oocyte Specifically Expressed</i>
rRNAs	Ribosomal RNAs
siRNAs	Small interfering RNAs
snoRNAs	Small nucleolar RNAs
snRNAs	Small nuclear RNAs
SSP-profiling	Scarce Sample Polysome profiling
tRNAs	Transfer RNAs
ZGA	Zygotic genome activation

## **8. Curriculum Vitae**

### **Aleshkina Daria**

📍 Libechov, Czech Republic 27721

☎ +420774035703 @aleshkina@iapg.cas.cz

#### **Education:**

**2018 - 2022** Charles University, Prague, Czech Republic

PhD Program Developmental and Cell Biology

Thesis title: Impact of long non-coding RNAs on translation in the mammalian germ cells

**2014 - 2016** Saint Petersburg State University, Saint Petersburg, Russia

Master Degree Program

Thesis title: Karyotype characteristics of the littoral mollusc *Littorina saxatilis*

**2010 - 2014** Saint Petersburg State University, Saint Petersburg, Russia,

Bachelor Degree Program

Thesis title: Molecular and cytogenetic analysis of 15q11-q13 region in patients with Prader-Willy syndrome

#### **Work History:**

**2018 – Present** PhD student

Laboratory of Biochemistry and Molecular Biology of Germ Cells, Institute of Animal Physiology and Genetics Czech Academy of Sciences, Libechov, Czech Republic

#### **Key Skills:**

- RNA and DNA FISH
- Microinjection-mouse oocyte & embryo
- Bright field, fluorescent and confocal microscopy
- Immunocytochemistry
- RNA isolation
- PCR and qPCR
- RNA pull-down assay
- Luciferase assay
- Chromosome isolation
- Mendeley, Graph Pad
- Basic skills in RStudio, LasX

#### **Publications:**

**Aleshkina D**, Iyyappan R, Lin Ch. J, Masek T, Pospisek M, Susor A. ncRNA BC1 influences translation in the oocyte, **RNA Biol.** 2021

Iyyappan R, **Aleshkina D**, Zhu L, Jiang Z, Kinterova V, Susor A. Oocyte specific lncRNA *Rose* variant influences oocyte and embryo development, **Non-coding RNA Research** 2021

Jansova D, **Aleshkina D**, Jindrova A, Iyyappan R, Qin A, Fan G, Susor A. Single molecule RNA localization and translation in the mammalian oocyte and embryo. **Journal of Molecular Biology**

2021

Llano E, Iyyappan R, **Aleshkina D**, Masek T, Dvoran M, Jiang Z, Pospisek M, Kubelka M, Susor A. SGK1 is essential for meiotic resumption in mammalian oocytes. **European Journal of Cell Biology**, *accepted*.

### **Conferences:**

**2020** Virtual Regulatory & Non-coding RNAs meeting, Cold Spring Harbor, USA. Poster: ‘Non-coding RNA *BCI* affects translation of specific targets in mammalian oocyte’

**2019** 3rd International Symposium on Frontiers in Molecular Science: RNA regulatory Networks, Lisbon, Portugal. Oral talk: ‘ncRNA in mammalian oocyte and early embryo development’

**2019** EMBO Workshop Awakening of the genome: The maternal-to-zygotic transition, Prague, Czech Republic. Poster: ‘ncRNA role in mammalian oocyte and early embryo development’

**2019** DevCellBio PhD Conference, Prague. Short talk.

**2018** DevCellBio PhD Conference, Prague. Poster presentation.

**2018** Visegrad Group Society for Developmental Biology, Inaugural Meeting. 6. – 9. 9. 2018. Brno.

### **Grants:**

**2021-2022** Internal Grant Agency of Institute of Animal Physiology and Genetics Czech Academy of Sciences, Grant title: Visualization of novel lncRNAs in mammalian oocyte. Principal investigator. Budget 4 500 USD.

**2021-2023** The Charles University Grant Agency (GA UK), Grant title: Molecular role of ncRNAs in oocyte and embryo development. Principal investigator. Budget 27 000 USD.

### **Other experiences:**

**2021** Internship at Marine Biological laboratory (The University of Chicago), Woods Hole, MA. Dr. Rosenthal’s laboratory. HCR RNA FISH on *Doryteuthis pealeii* embryos

**2016 – 2017** Bioinformatics Institute, Saint-Petersburg, Russia.

**2015** AB-321 Ecology of Arctic Marine Benthos Course, University Centre in Svalbard, Norway

**2015** Established and Emerging Model Organisms for Marine Science Course, Pierre and Marie Curie University, Roscoff, France

## **9. Research papers**

**D. Aleshkina**, R. Iyyappan, C.J. Lin, T. Masek, M. Pospisek, A. Susor, ncRNA BC1 influences translation in the oocyte, **RNA Biol.** (2021). <https://doi.org/10.1080/15476286.2021.1880181>  
ncRNA BC1 influences translation in the oocyte

R. Iyyappan, **D. Aleshkina**, L. Zhu, Z. Jiang, V. Kinterova, A. Susor, Oocyte specific lncRNA variant Rose influences oocyte and embryo development, **Non-Coding RNA Res.** (2021). <https://doi.org/10.1016/j.ncrna.2021.06.001>


D. Jansova, **D. Aleshkina**, A. Jindrova, R. Iyyappan, Q. An, G. Fan, A. Susor, Single Molecule RNA Localization and Translation in the Mammalian Oocyte and Embryo, **J. Mol. Biol.** (2021). <https://doi.org/10.1016/j.jmb.2021.167166>

E. Llano, R. Iyyappan, **D. Aleshkina**, T. Masek, M. Dvoran, Z. Jiang, M. Pospisek, M. Kubelka, A. Susor, SGK1 is essential for meiotic resumption in mammalian oocytes. **European Journal of Cell Biology**, *accepted*.

RESEARCH PAPER



## ncRNA BC1 influences translation in the oocyte

D. Aleshkina<sup>a</sup>, R. Iyyappan<sup>a</sup>, Ch. J. Lin<sup>b</sup>, T. Masek<sup>c</sup>, M. Pospisek<sup>c</sup>, and A. Susor <sup>a</sup>

<sup>a</sup>Laboratory of Biochemistry and Molecular Biology of Germ Cells, Institute of Animal Physiology and Genetics of the Czech Academy of Sciences, Libechev, Czech Republic; <sup>b</sup>MRC Centre for Reproductive Health, The University of Edinburgh, Edinburgh, UK; <sup>c</sup>Department of Genetics and Microbiology, Faculty of Science, Charles University in Prague, Prague, Czech Republic

### ABSTRACT

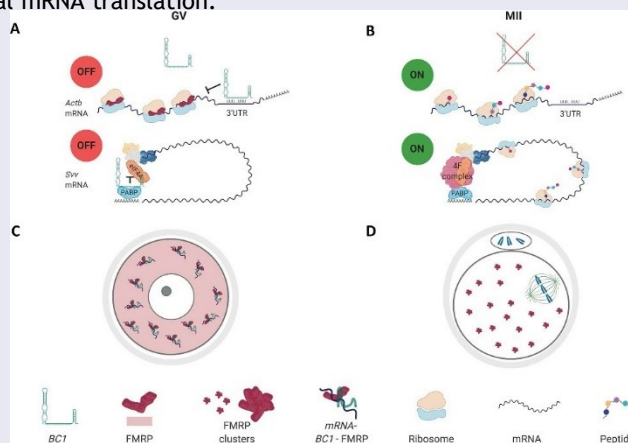
Regulation of translation is essential for the diverse biological processes involved in development. Particularly, mammalian oocyte development requires the precisely controlled translation of maternal transcripts to coordinate meiotic and early embryo progression while transcription is silent. It has been recently reported that key components of mRNA translation control are short and long noncoding RNAs (ncRNAs). We found that the ncRNA *Brain cytoplasmic 1 (BC1)* has a role in the fully grown germinal vesicle (GV) mouse oocyte, where is highly expressed in the cytoplasm associated with polysomes. Overexpression of *BC1* in GV oocyte leads to a minute decrease in global translation with a significant reduction of specific mRNA translation via interaction with the Fragile X Mental Retardation Protein (FMRP). *BC1* performs a repressive role in translation only in the GV stage oocyte without forming FMRP or Poly(A) granules. In conclusion, *BC1* acts as the translational repressor of specific mRNAs in the GV stage via its binding to a subset of mRNAs and physical interaction with FMRP. The results reported herein contribute to the understanding of the molecular mechanisms of developmental events connected with maternal mRNA translation.

### ARTICLE HISTORY

Received 15 October 2020  
Revised 17 December 2020  
Accepted 15 January 2021

### KEYWORDS

Non-coding RNA; translation; oocyte; embryo; development



### Introduction

Non-coding RNAs (ncRNAs) represent a major part of the transcriptome and exhibit a variety of structures and functions. Despite numerous ncRNAs having emerged and evolved rapidly, they are poorly conserved among mammalian species compared with protein-coding genes [1,2]. Also, whilst the number of reported ncRNAs is rapidly increasing [3], we still only have little data about their cellular functions. Moreover, it is still puzzling as to which ncRNAs are truly functional and which of them represent only ‘transcriptional noise’.

A phylogenetically heterogeneous group of mammalian non-coding Brain Cytoplasmic (BC) RNAs was originally described as controlling translation in dendrites [4]. While *BC1* ncRNA is

restricted to rodents and *BC200* is found in primates, they independently gained translational repression function at a later stage of mammalian evolution when more stringent gene expression control mechanisms were acquired [5]. *BC1* ncRNA, which is a 154nt-long Pol III-derived transcript, is a phylogenetic descendant of tRNA<sub>Ala</sub> [6]. *BC1* contains a 5'-stem-loop domain followed by a single-stranded central homopolymeric A-rich region and a 3'-stem-loop domain [7]. *BC1* was shown to obstruct the formation of the 48S preinitiation complex in cap-dependent translation. This is mediated by a 3'-stem-loop and the adjacent A-rich region through which *BC1* interacts with eIF4B, eIF4A and PABP [8–11]. Thus, *BC1* negatively modulates translation initiation.

Moreover, in 2003, Zalfa and colleagues reported *BC1* acts together with RNA-binding Fragile X Mental Retardation Protein (FMRP) leading to the assembly of large messenger RNPs, in which translation repression of specific mRNA targets occurs [12–16]. FMRP has been shown to orchestrate particular mRNAs by regulating their stability, localization and translation [14]. However, *BC1*-FMRP interaction is still being described and discussed, as several groups suggest direct physical association of *BC1* and FMRP in the rodent brain [12,17] while others propose a sequential model of action of these molecules in the same translational pathway [9,18–20]. *BC1* is reported to bind mRNAs which bear U-rich regions through a one-stranded A22 central domain [19]. Phenocopy detected in single *BC1* and FMRP knock-outs (KOs), and more severe but still phenocopy observed in double KO animals indicate that the target mRNAs partially overlaps [20–22].

In many mammalian cell types, ncRNA functions remain poorly understood. One significant example is the oocyte. In recent years, the expression of ncRNAs in oogenesis and oocyte maturation has become a focus of attention [23–26]. Meiotic oocyte maturation is a complex process with unique mechanisms leading to the reduction of the genomic content to the haploid state. The fully grown oocyte (‘germinal vesicle (GV)’ oocyte) is transcriptionally silent and utilizes only transcripts synthesized in earlier developmental stages [27]. Thus, reliance on translational control mechanisms throughout the maturation is a key feature of the oocyte [reviewed in 28], including the involvement of ncRNAs in mRNA stabilization and translation repression [29].

Here, we analysed the expression and distribution of *BC1* ncRNA in the mouse oocyte and its role in the modulation of the translation of the maternal mRNA pool. Our results demonstrate that *BC1* plays a role in the regulation of the translation of specific maternal mRNAs in the GV stage without contributing to oocyte developmental competence.

## Results

### *BC1* ncRNA is abundant in the GV oocyte with polysomal association

At first, we analysed the expression of *BC1* ncRNA (*BC1*) in GV and MII oocytes and 2-cell embryos. We found that *BC1* is highly expressed in the GV stage with a subsequent significant decrease in the MII stage and 2-cell embryo (Fig. 1A). For comparison, we determined levels of *Gapdh* mRNA and *Neat2* lncRNA. Both of them also declined from the GV to 2-cell stage, however, not as dramatically as *BC1* (Fig. 1A). Next, we focused on *BC1* cellular localization in the GV-stage oocyte. We performed qPCR analysis of cDNA samples prepared from nuclear and cytoplasmic fractions and found out that *BC1* exhibited exclusive cytoplasmic localization. *Gapdh* mRNA was present in both the nucleus and cytoplasm in sharp contrast to the strict and well-known nuclear localization of *Neat2* lncRNA (Fig. 1B and Figure S1) [30,31].

Several previous studies found that *BC1* ncRNA acts as a suppressor of translation of specific mRNAs in the brain [22,32]. To test whether *BC1* directly impacts translation in the mouse oocyte, we implemented a recently optimized approach for Scarce Sample Polysome profiling (SSP-profiling) – an established method to study active translation [33]. In order to analyse the polysomal association of *BC1*, we performed qPCR of non-polysomal (NP) and polysomal fractions (P) of GV and MII oocytes. SSP-profiling was validated by qRT-PCR for association 18S and 28S rRNAs with each of profiling fraction (Figure S2) [33]. To our surprise we detected a significant enrichment of *BC1* ncRNA in the polysomal fraction of GV oocytes, meaning this RNA is bound to ribosomes despite not coding for a protein (Fig. 1C). In MII oocytes *BC1* demonstrated equal and very low polysomal association (Fig. 1C). Polysomal occupancy of *Gapdh* mRNA was high in both oocyte stages (Fig. 1C) and nucleus abundant lncRNA *Neat2* [31] was absent in polysomal fractions (Fig. 1C).

In conclusion, we found that *BC1* is highly abundant in the cytoplasm of the GV oocyte with enrichment at polysomes indi-

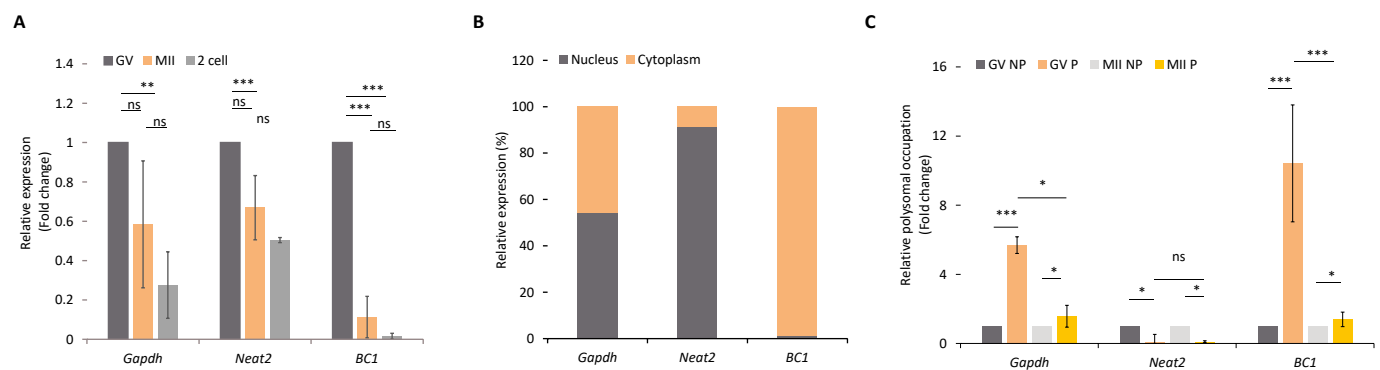


**Figure 1.** *BC1* ncRNA is abundant in the GV oocyte with polysomal association.

(A) qRT-PCR analysis of *BC1* expression in the GV, MII oocytes and 2-cell embryo. Values obtained for GV stage were set as 1. *Gapdh* mRNA and *Neat2* lncRNA were used as controls. Relative expression; mean  $\pm$  SD; Student's *t*-test: \*\**p* < 0.01; \*\*\**p* < 0.001, ns for non-significant, *n* = 3. (B) Expression of *BC1* in the nucleus and cytoplasm of oocyte. Values obtained from qPCR of the nucleus and cytoplasm combined as 100%. *Gapdh* mRNA and *Neat2* lncRNA were used as controls. See also Figure S1. (C) Polysomal association of RNAs coding for *Gapdh*, *Neat2* and *BC1* in the GV and MII oocyte. Expression in the GV stage was set as 1. *Gapdh* mRNA and *Neat2* lncRNA were used as controls. Relative expression, mean  $\pm$  SD; Student's *t*-test: \**p* < 0.05; \*\*\**p* < 0.001, ns for non-significant, *n*  $\geq$  2. NP, non-polysomal; P, polysomal. See Figure S2 for validation of polysomal fractionation.

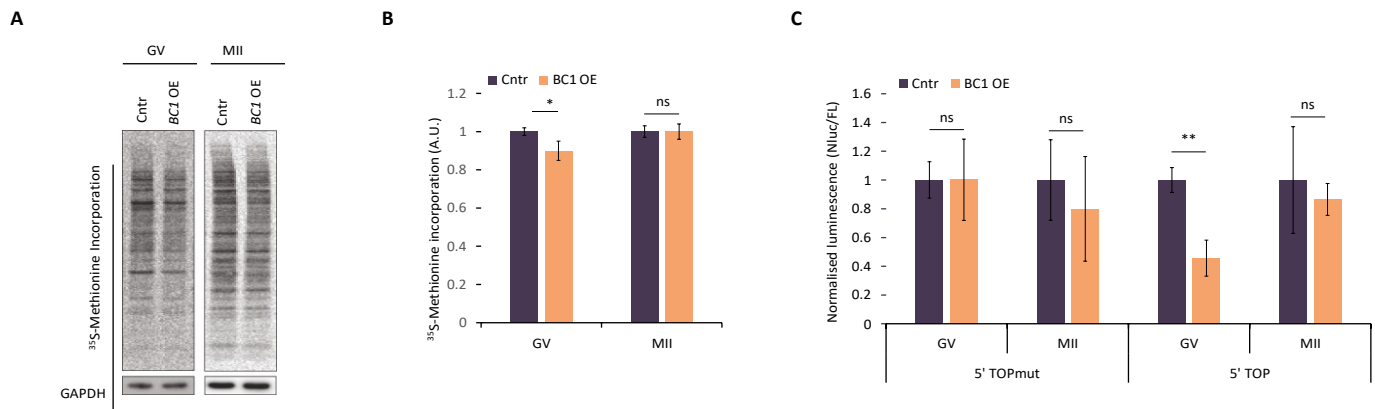


**Figure 2.** *BC1* overexpression leads to decrease of global translation and TOP RNA reporter in the GV oocytes.

(A) <sup>35</sup>S-Methionine incorporation in mouse oocytes with overexpression (OE) of *BC1* RNA. Expression GAPDH protein was used as a loading control. Representative images from at least three independent replicates. See Figure S3 for validation of overexpression. (B) Quantification of <sup>35</sup>S-Methionine incorporation. Values obtained for the control (Cnr) group were set as 1. Data from four independent experiments; mean ± SD; Student's *t*-test: \**p*<0.05; ns, non-significant, *n*≥4. (C) Analysis of NanoLuc expression of RNA reporters in oocytes contains mutation in 5'UTR (mut) and with canonical 5'TOP motive in the control and OE of *BC1* RNA. Chemiluminescence values obtained for the Cnr group were set as 1 and Firefly Chemiluminescence was used as a microinjection control for normalization (Nluc/FL); mean ± SD; Student's *t*-test: \*\**p*<0.01; ns, non-significant, *n*≥5.

cating its involvement in the regulation of maternal RNAs metabolism.

### ***BC1* overexpression leads to decrease of global translation and TOP RNA reporter in GV oocytes**

We found *BC1* ncRNA was localized in cytoplasm and associated with polysomes in the GV oocyte (Fig. 1B, Fig. 1C and Figure S1) indicating its possible involvement in translational control in the oocyte. As there was no effect of *BC1* knock-down on female fertility [34] we applied an overexpression (OE) approach using microinjection of *BC1* RNA into the oocyte cytoplasm (Figure S3). Additionally, to detect global translation rate we performed <sup>35</sup>S-Methionine labelling in both GV and MII stages. We found only a mild, but statistically significant, decrease of global translation in the GV stage with *BC1* OE (Fig. 2A). Nevertheless, there was no influence on total translation in the MII stage despite overexpressed *BC1* transcript accumulation compared with the GV stage (Figure S3). Moreover, we analysed whether *BC1* OE impedes translation by stress-activated phosphorylation of eIF2 $\alpha$  [35]. Using immunoblot we did not detect an increased level of phosphorylated eIF2 $\alpha$  (Ser51) (Figure S4), therefore we conclude that *BC1* OE does not cause stress-induced translation arrest.

The diminutive decrease of global translation in the GV oocyte might be explained by *BC1*-mediated translational repression of just a subset of mRNAs. It was reported that *BC1* binds PABP and eIF4 in dendrites leading to the repression of cap-dependent translation and therefore 5' TOP mRNAs [8,32] could be the target of *BC1*-mediated regulation. In order to verify this phenomenon in oocytes, we applied luciferase reporters with 5' TOP motif in the presence of *BC1* [36]. We microinjected two RNAs derived from NanoLuc reporter constructs to fully grown GV oocytes with *BC1* OE. The first construct contained a mutated 5'TOP motif in 5' UTR while the second one bore a strong canonical 5'TOP sequence. Subsequently, we measured the luminescence signal in both oocyte developmental

stages. Obtained results demonstrated no influence of *BC1* OE on the control 5'TOPmut reporter translation (Fig. 2C). Contrarily, we detected a decrease of NanoLuc activity of the canonical 5'TOP reporter RNA in GV-stage oocyte, while a lack of influence of *BC1* OE was observed in the MII stage (Fig. 2C).

Taken together, obtained data might indicate that *BC1* is able to influence the translation of a specific subset of mRNAs in the GV stage oocyte as demonstrated by the 5'TOP reporter construct.

### ***BC1* ncRNA influences translation of specific targets in the GV mouse oocyte**

Several studies associated *BC1* ncRNA function with mRNAs coding for ACTIN B (ACTB) and DLG4 (PSD95) [12,19]. We tested whether *BC1* OE influences the production of these proteins. Immunoblot analysis clearly showed that *BC1* OE significantly decreased levels of ACTB and DLG4 proteins in the GV stage oocyte while had no effect in the MII stage (Fig. 3). This finding is consistent with the observed, GV-stage oocyte restricted decrease of 5'TOP NanoLuc reporter translation after *BC1* OE (Fig. 2C). Thus, we aimed to study the translation of endogenous 5'TOP mRNA coding for Survivin (SVV) protein [37]. Similarly, the level of SVV protein declined exclusively in *BC1* OE GV oocytes (Fig. 3); with no significant change in both control GV-stage oocytes, nor in the MII stage (Fig. 3).

Our data clearly show that *BC1* ncRNA negatively influences the translation of specific mRNAs only in the GV stage oocyte in agreement with the analysis of global translation and NanoLuc reporter (Fig. 2).

### ***BC1* physically interacts with candidate mRNAs via protein interplay**

In connection with the discovered translational repression of candidate mRNAs coding for ACTB, DLG4 and SVV, we examined potential molecular interactions of selected mRNAs (Fig. 3) and *BC1* in the mouse oocyte. Due to the fact that the



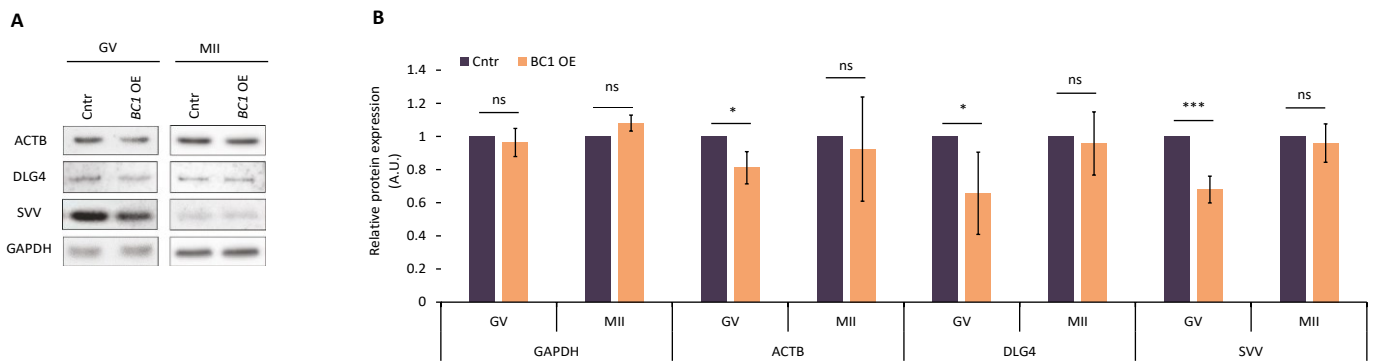


**Figure 3.** *BC1* ncRNA influences translation of specific targets in the GV mouse oocyte.

(A) Western blot analysis of ACTB, DLG4 and SVV in GV and MII oocytes with OE of *BC1*RNA. GAPDH was used as a loading control. Representative images from at least three independent replicates. (B) Quantification of western blot analysis. Values obtained for the control groups injected with *H2b:gfp* RNA were set as 1. Data from three independent experiments; mean  $\pm$  SD; Student's *t*-test: \* $p$ <0.05; \*\*\* $p$ <0.001; ns, non-significant.

3'UTRs of mRNAs are considered to play major regulatory roles in mRNA fate [38], we focused preferentially on the *BC1* interactions with the 3'UTR of the candidate mRNAs. We performed *in silico* prediction of RNA–RNA interaction using open-source IntaRNA 2.0 software [39]. We found that *BC1* and 3'UTRs of *Actb*, *Dlg4* and *Svv* mRNAs could form heteroduplexes with *BC1* (displayed as different negative values of minimum free energy (MFE), which consist of hybridization energy subtracted by the energy needed to unfold *BC1* and target mRNA; Figure S5A). Contrarily, *Gapdh* mRNA, which is not influenced by *BC1* OE, does not contain any region able to interact with *BC1* in its 3'UTR (Figure S5). Additionally, as a reference *Anln* mRNA was analysed. *Anln* mRNA, which interacts with lncRNA *Uca1* [40], displayed a high negative MFE (Figure S5A). *Actb* and *Dlg4*

mRNAs also exhibited relatively high negative MFE values (high binding affinity). In contrast to *Gapdh* 3'UTR, they both contain U-rich stretches, which were predicted to interact with the 22-nucleotide-long stretch of adenosines in *BC1* ncRNA (Figure S5B). Analysis of binding efficiency of TOP mRNA SVV shows low MFE (Figure S5).

*In silico* analysis of the 3'UTR of candidate transcripts revealed their interaction with *BC1* ncRNA. Next, we tested whether *BC1* – target mRNA interactions are based only on direct RNA-RNA base pairing or are mediated/facilitated by some auxiliary protein/s. To answer this question, we performed RNA pull-down with *BC1* anti-sense biotinylated oligonucleotide probes and streptavidin-coupled beads (Fig. 4A) [41]. In relation to the known function of *BC1* in the GV oocyte

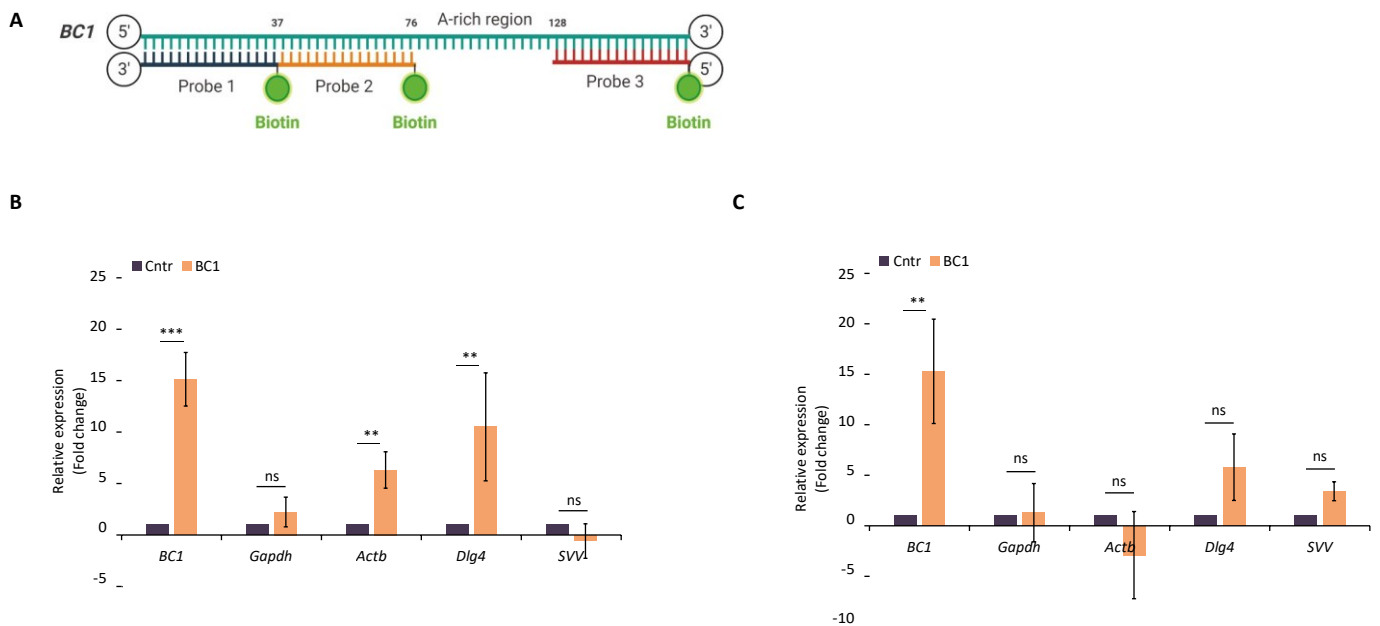


**Figure 4.** *BC1* physically interacts with candidate mRNAs via protein interplay.

(A) Scheme of *BC1* anti-sense DNA 5'-biotinylated oligonucleotide probes related to *BC1*. (B) Pull-down from whole oocytes lysate with three probes complementary to *BC1* ncRNA (*BC1*) and without probes as a negative control (Cntr). Endogenous *BC1* and *Gapdh* RNAs were used as additional controls. Values obtained from control were set as 1. Relative expression; mean  $\pm$  SD; Student's *t*-test: \* $p$ <0.05; \*\* $p$ <0.01, \*\*\* $p$ <0.001, ns for non-significant,  $n \geq 2$ . (C) Pull-down from purified total RNA with three probes complementary to *BC1* ncRNA (*BC1*) and without probes as a negative control (Cntr). Endogenous *BC1* and *Gapdh* RNAs were used as additional controls. Values obtained from control were set as 1. Relative expression; mean  $\pm$  SD; Student's *t*-test: \* $p$ <0.05; ns for non-significant,  $n=3$ .

(Figs 1–3) we focused on this stage. Firstly, we pulled down *BC1* with associated molecular partners from whole oocyte lysates. Following qRT-PCR analysis, we found significant enrichment of *BC1* (Fig. 4B) indicating its efficient capture. Almost equal amounts of *Gapdh* mRNA were detected in samples without (Cntr) and those containing three (*BC1*) oligonucleotide probes excluding non-specific pull-down (Fig. 4B). Importantly, *Actb* and *Dlg4* candidate mRNAs were considerably enriched after *BC1* pull-down (Fig. 4B), however, without statistical significance in the case of *Svv* mRNA (Fig. 4B). Additionally, we performed *BC1* ncRNA pull-down from purified total RNA isolated from GV oocytes to test whether *BC1* binds target mRNA through a protein intermediate partner. Similarly as in Fig. 4B the qPCR analysis showed high enrichment of the input *BC1* ncRNA (Fig. 4C) but the absence of the non-target *Gapdh* mRNA (Fig. 3). No significant enrichment was detected of target *Actb*, *Dlg4* and *Svv* mRNAs in *BC1* pull-down (Fig. 4C).

Comparison of *BC1* pull-down results obtained from cell lysate and total RNA indicates that an unspecified protein partner/s mediates or at least facilitate (in contribution with the proposed base pairing) *BC1* interaction with *Actb* and *Dlg4* mRNAs in the mouse GV oocyte.

### *BC1* interacts with FMRP protein in the GV oocyte

As fragile X mental retardation protein (FMRP [9,15,16,19]; has previously been identified as partnering *BC1* we were prompted to determine its role in the oocyte. Similarly to FMRP, *BC1* ncRNA has been described as a translational repressor, but its exact mechanism of action has not yet been detailed [14,42]. Firstly, we analysed FMRP expression in the mouse oocyte and early embryo (Figure S6). FMRP was present in all stages of oocyte maturation with a significant decrease in the 2-cell embryo (Figure S6). To investigate physical *BC1* interaction with FMRP we performed *in situ* RNA–proximity ligation assay (RNA-PLA) in the mouse oocyte [43,44] with the addition of a hybridization step to target RNA followed by proximity detection by anti-biotin antibody and specific antibodies for protein of interest. Using confocal microscopy we observed multiple interaction sites of *BC1* ncRNA with FMRP in the GV-

oocyte cytoplasm (Figure 5AB) with a significant reduction of their number in the MII stage (Fig. 5A). As a positive control for PLA, we used known interaction of *eEF2* mRNA with RPL24 in polysomes [43] (Figure S7) and as a negative technical control used LMN A/C phosphorylated at Ser22 (does not interact with *eEF2* mRNA) (Figure S7).

Here, we confirmed that *BC1* ncRNA physically interacts with its protein partner FMRP in the GV oocyte.

### *BC1* overexpression does not lead to clustering of FMRP and RNA in GV oocyte

It is known that inhibition of mRNA translation is associated with the formation of cytoplasmic RNP [45]. FMRP was identified to promote and regulate the assembly of RNP granules including RNP transport granules, P-bodies and stress granules in various cell types [46,47]. Accordingly, we expected that *BC1* OE will also induce RNP clusters in the mouse oocyte. Thus, we performed immunocytochemistry (ICC) and RNA FISH in order to examine the localization of FMRP (Fig. 6A) and poly(A) mRNA (Fig. 6C) in oocytes with *BC1* overexpression. *BC1* OE did not induce the formation of either FMRP-containing or Poly(A)-containing RNP granules in the GV stage (Fig. 6). In contrast, MII-stage oocytes contained both FMRP and poly(A) in distinct cytoplasmic clusters (foci) regardless of *BC1* overexpression (Fig. 6). Localization of the *BC1*-FMRP complex positively correlates with detected *BC1* ncRNA localization in the cytoplasm (Fig. 1B and Figure S1). Quantification of FMRP-containing and poly(A)-containing foci in MII oocytes showed a significant increase in their number in the *BC1* OE group suggesting a positive effect of *BC1* on their formation (Fig. 6). Additionally, we performed RNA FISH of *Actb* mRNA and, intriguingly, we did not observe any clustering pattern in either oocyte group (Figure S8A). Moreover, quantification of the *Actb* mRNA signal showed a significant increase of the mRNA in the MII stage (Figure S8B); which was independently confirmed by qRT-PCR (Figure S8C).

Further, we wanted to test whether the FMRP foci seen in GV oocytes can be related to stress granules (SGs), in other words, whether FMRP is a constituent of SG in GV-stage oocytes (Fig. 6 and Figure S8A). We induced translational stress [48] by 0.5 mM

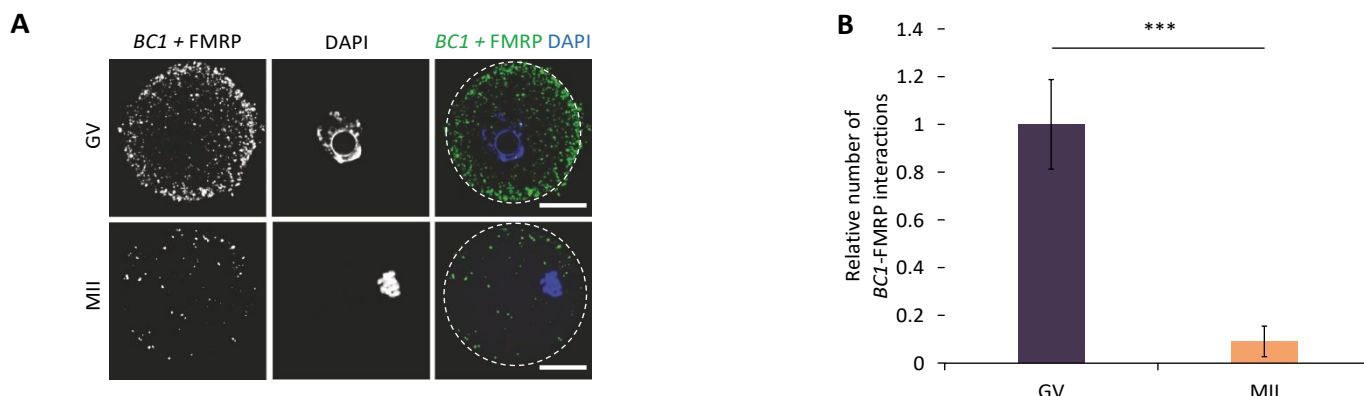


**Figure 5.** *BC1* interacts with FMRP protein in the GV oocyte.

(A) RNA-protein proximity ligation assay (RNA-PLA) detecting *BC1* ncRNA-FMRP interactions. Representative confocal images of GV and MII oocytes; scale bars 25  $\mu$ m; PLA green; DNA blue;  $n \geq 7$ . (B) Quantification of *BC1*-FMRP interactions in GV and MII oocytes. Values obtained for the GV oocytes were set as 1. Relative number of *BC1*-FMRP interactions; mean  $\pm$  SD; Student's *t*-test: \*\*\* $p < 0.001$ ,  $n \geq 7$ .

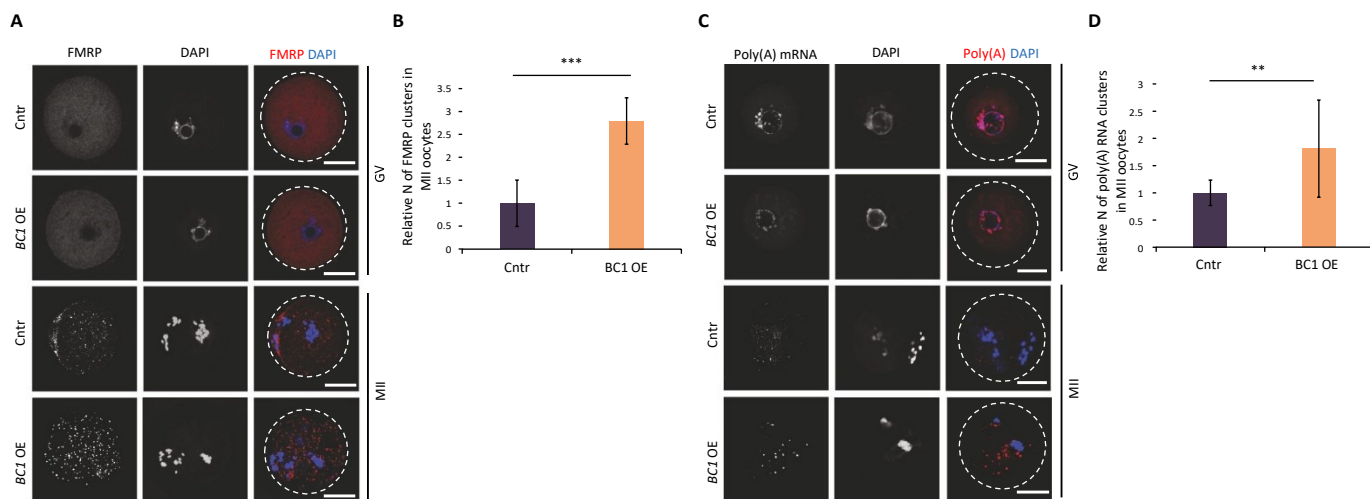


**Figure 6.** *BC1* overexpression does not lead to clustering of FMRP and RNA in GV oocyte.

(A) Representative confocal images of GV and MII oocytes labelled with FMRP antibodies in the absence (Cntr) or presence (*BC1* OE) of *BC1*; scale bars 25  $\mu$ m; FMRP red; DNA blue;  $n \geq 30$ . (B) Quantification of FMRP clusters in MII oocyte. Values obtained for the Cntr group were set as 1. Relative number of FMRP clusters; mean  $\pm$  SD; Student's *t*-test:  $***p < 0.001$ ,  $n \geq 30$ . (C) Representative confocal images of GV and MII oocytes labelled with Oligo(dT) Probe for poly(A) RNA in the absence (Cntr) or presence (*BC1* OE) of *BC1*; scale bars 25  $\mu$ m; FMRP red; DNA blue;  $n \geq 10$ . (D) Quantification of poly(A) RNA clusters in MII oocyte. Values obtained for the Cntr groups were set as 1. Relative number of poly(A) RNA clusters; mean  $\pm$  SD; Student's *t*-test:  $**p < 0.01$ ,  $n \geq 10$ .

sodium arsenite (arsenite;  $\text{NaAsO}_2$ ) treatment. Arsenite is a well-established SGs elicitor, which induces eIF2 $\alpha$  phosphorylation at Serine51 and causes translation arrest and polysome disassembly [49] (Figure S9A). Although arsenite treatment of GV oocytes revealed no formation of FMRP clusters, we did however observe a distinct pattern of FMRP localization in perinuclear area (Figure S9B). MII oocytes showed similar FMRP localization clustering pattern in both arsenite-treated and untreated groups (Figure S9B and S9C).

Altogether our results suggest that *BC1* OE inhibits the translation of specific mRNAs in the GV stage by mechanisms that do not depend on the formation of protein or RNA foci.

### Overexpression of *BC1* does not alter oocyte or early embryo development

We observed that *BC1* OE leads to the mild downregulation of the translation of specific mRNAs only in the GV oocyte (Figs 2 and Figs 3). Thus, we asked whether *BC1* OE might

cause any developmental defects during mouse oocyte maturation. We did not find any effect on the oocyte physiology nor on meiotic progression after *BC1* OE (Fig. 7). Moreover, we performed parthenogenic activation of MII oocytes matured *in vitro* from GV oocytes with *BC1* OE to analyse developmental oocyte competence. Similarly to oocyte maturation, no abnormalities in the embryo development were observed (Fig. 7).

To sum up, we saw that the *BC1* OE alone did not have an influence over mouse oocyte maturation nor early embryo development.

In conclusion, we propose an overall scheme how *BC1* might contribute to the translational regulation of specific mRNAs in the GV and MII stages (Graphical abstract).

### Discussion

In this study, we analysed the role of *BC1*, a maternal ncRNA which is involved in mRNA metabolism in the mammalian

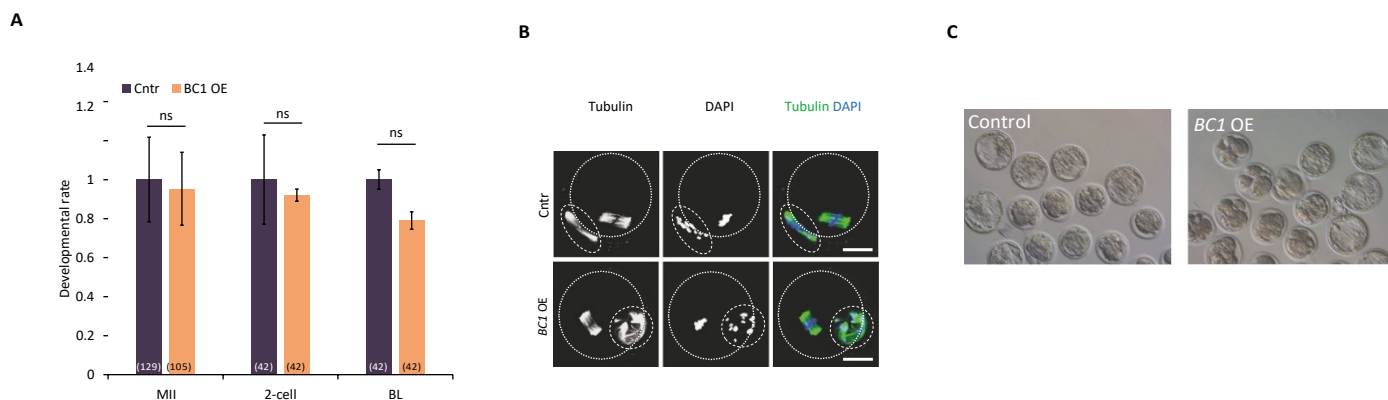


**Figure 7.** Overexpression of *BC1* does not alter oocyte or early embryo development.

(A) Analysis of the maturation and developmental competence of the oocyte with *BC1* overexpression. Relative number of oocytes; mean  $\pm$  SD; Student's *t*-test: ns for non-significant,  $n \geq 42$ . See Figure S3 for validation of overexpression. (B) Analysis of the morphology of the MII oocyte with overexpression of *BC1*. Representative confocal images of MII oocytes labelled with tubulin antibodies in the control (Cntr) and OE of *BC1*; scale bars 25  $\mu$ m; Tubulin green; DNA blue;  $n \geq 20$ . (C) Bright-field images of blastocyst development in control and *BC1* OE groups.

oocyte. Functional analysis of ncRNAs is challenging and roles have only been assigned to a small fraction of ncRNAs, while it is not clear what fraction of ncRNAs has a measurable effect beyond being transcribed and processed through the RNA metabolism. mRNA translation has been shown to be essential for regulating a number of cellular processes during development [50]. This is especially true in the mammalian oocyte which, after a transcriptionally active growth period, resumes meiosis during a period of transcriptional quiescence with a store of maternally synthesized RNAs. Progression through meiosis and early embryo development is therefore regulated at the level of mRNA stabilization, translation and post-translational modification. The storage of ribosomal components and maternal mRNA is a prerequisite for the meiotic and developmental competence of the oocyte [51].

*BC1* ncRNA has been shown as a negative regulator of translation in neuronal synapses [9]. We found that *BC1* has high expression in the GV stage oocyte and almost disappears in the MII oocyte and post-fertilization. Here we studied the role of *BC1* in oocyte protein synthesis via its overexpression. Importantly, overexpression of *BC1* does not cause stress leading to global translation decrease as is the case with arsenite treatment. Cytoplasmic localization of *BC1* and association with polysomes [our results and 4] lead us to the suggestion that *BC1* is involved in translational regulation. Polysomal occupation in the oocyte shows the increased translation of specific mRNAs [33,52]; however, a certain portion of polysomes might be translationally inactive and belong to cytoplasmic ribosomal lattices; a storage form of ribosomes known in oocyte [53,54]. The presence of *BC1* in polysomal fraction and *BC1* physical interaction with FMRP indicate direct interplay with translational machinery of GV oocyte. Colocalisation of *BC1* with FMRP in the cytoplasm is consistent with roles in mRNA translation/stabilization. FMRP had been shown to interact with ribosomal protein L5 in *Drosophila* [55,56] but, on the other hand, it was associated with stress granules and P bodies [57,58]. Moreover, in neuronal cell FMRP is associated with polyribosomes [59–61], stalled ribosomes and messenger ribonucleoproteins (mRNPs) which sediment in the same fractions [62, 63] where functions as a translational repressor of subset mRNAs [64]. Ribosome stalling is linked to translational repression mechanism where mRNA is repressed at elongation/termination awaiting translational reactivation upon appropriate signals [60,63]. However, to our knowledge, nothing is known about stalling polysomes in mammalian oocyte but endogenous decay of *BC1* in the MII oocyte might lead to the release of stalled polysomes or mRNPs from translational inhibition. *BC1* appears to promote the interaction between FMRP and other mRNAs that are known to interact with FMRP, possibly via base-pairing interactions, and thereby regulate the translation of a subset of mRNAs at synapses [15,16]. FMRP, involved in regulating the translation of mRNPs, combines with *BC1* in the GV oocyte to form the *BC1*-FMRP complex. This complex can inhibit the translation of a certain subset of FMRP-targeted mRNAs. *BC1*-FMRP forms in the GV where *BC1* is abundant which leads to a mild negative effect on translation only in fully grown GV oocytes. As an example of *BC1* negative influence on translation in the GV oocyte is target *Actb* mRNA which moreover promotes its stability. Experimental expression of *BC1* promoted stabilization of target mRNA in the matured oocyte which might indicate that i)

translational repression leads to mRNA stabilization or ii) involvement of *BC1* in the stabilization of mRNA during oocyte development. In connection, *BC1* has possibly more a potent effect during oocyte growth with suppression of newly transcribed mRNAs to exclude them from translational machinery thus promoting their storage and stability for further cellular development.

Interestingly in the GV oocyte both *BC1*-FMRP and poly(A) RNA distribute evenly without clustering suggesting no formation of large RNP structures (foci) for translational suppression of candidate mRNAs in the GV oocyte. Despite translational stress by arsenite treatment this similarly does not promote the formation of FMRP foci but FMRP instead becomes localized to the perinuclear area where the ER is localized [65–68] suggesting that the clustering or formation of granular structures in the GV oocyte is in some extent inhibited. Flemer et al. [69] similarly show no formation of granular structures related to P-bodies in the fully grown mouse oocyte. P-bodies are distinctive foci in the cytoplasm of eukaryotic cells which have a functional role in mRNA decay and miRNA-mediated translational repression [70–72]. Related to the non-functional miRNA pathway in the mouse oocyte [73,74] might suggest that *BC1* could take a role as a translational repressor in the fully grown oocyte however substituted by another mechanism after the resumption of meiosis. Possibly *BC1* ncRNA might substitute the miRNA pathway in transitional repression in the growing and fully grown oocyte where the target mRNAs are suppressed therefore promoting their translational dormancy and stability to form ribosomal lattices [53,54,75]. Our results suggest the role of *BC1*-FMRP complex in the mechanism of promoting translational dormancy and stability of specific maternal mRNAs at cytoplasmic polysomal-mRNP structures in the GV oocyte.

*In silico* analysis of *BC1* binding motifs showed to some extent an affinity to the target mRNAs containing a poly(U) stretch on 3'UTR. Direct mRNA-ncRNA binding in the 3'UTR region may disrupt PABP attachment and hence the initiation of translation at a single mRNA level. We found that binding efficiency is debilitated with the absence of protein/organelles-ribosomes, mRNPs suggesting a *BC1*-protein interplay in the translational inhibition. Additionally, our dual-luciferase reporter assay and candidate mRNA demonstrated that translational suppression of *BC1* influences RNA belonging to the TOP motif class [37].

As *BC1* naturally disappears from the maturing oocyte and its experimental overexpression does not influence translation globally or specifically (candidate mRNAs) we speculated on an increased formation of FMRP and RNA foci. However, we discovered that FMRP clusters form naturally in the MII oocyte when *BC1* becomes naturally decreased. Despite ectopic overexpression *BC1* in the mature oocyte increases the clustering of FMRP and RNA without any effect on translation of the candidate mRNA targets. We, therefore, propose that FMRP and polyA RNA clustering is independent of a *BC1* role in translational repression in this stage. We suggest that FMRP and PolyA clustering in the MII oocyte lead to the attenuation of an ectopically overexpressed translational repressor that promotes translation.

Apart from a mild effect on the translation of candidate mRNAs, there were no abnormalities in meiotic progression and early embryo development. In summary, *BC1* ncRNA is not necessary for terminal mouse oocyte development. Observed result linked with *BC1* interaction with the 3'UTR



of newly transcribed mRNAs during oocyte growth suggesting suppression their translation directly on the ribosome-mRNP structures to promote maternal mRNA storage and stability. Further research is needed to investigate the involvement of ncRNAs in the regulation of translation in the mammalian oocyte and early embryo.

## Methods

### Oocyte isolation, cultivation and treatment

Oocytes were acquired from ICR mice of a minimum of 6 weeks old. The females were stimulated 46 h prior to oocyte isolation using 5 IU of pregnant mare serum gonadotropin (PMSG; Folligon; Merck Animal Health) per mouse. All animal experiments were performed in accordance to guidelines and protocols approved by the Laboratory of Biochemistry and Molecular Biology of Germ Cells at the Institute of Animal Physiology and Genetics in Czech Republic. All animal work was conducted according to Act No. 246/1992 on the protection of animals against cruelty, issued by experimental project #215/2011, certificate #CZ02389, issued by the Ministry of Agriculture. Fully grown GV oocytes were isolated into transfer medium (TM) supplemented with 100  $\mu$ M 3-isobutyl-1-methylxanthine (IBMX; Sigma Aldrich) for prevention of spontaneous meiotic resumption. Selected oocytes were denuded and cultivated in M16 medium (Millipore) without IBMX at 37°C, 5% CO<sub>2</sub> for 0 (GV) or 12 h (MII). For induction of SGs oocytes were treated with 0.5 mM sodium arsenite in M16 medium (arsenite; NaAsO<sub>2</sub>). Parthenogenetic activation was carried out as previously described [76]. In brief, *in vitro* matured MII-stage oocytes were cultured in calcium-free CZB medium with 10 mM strontium and supplemented with 5  $\mu$ g/ml cytochalasin B for 5 hours. Embryos were then cultured in KSOM-AA medium at 37°C, 5%CO<sub>2</sub> and 5%O<sub>2</sub>.

### Nuclei isolation

The zona pellucida was removed using Tyrode acid solution (Sigma). The oocytes were disrupted by hand using a pulled glass pipette in PBS drop (cytoplasm) and nuclei were washed in three drops of PBS. Pipette wash (W) from oocyte disruption was used as a control of the isolation protocol.

### PCR and RT-PCR

RNeasy Plus Micro kit (Qiagen) was used for RNA extraction following the manufacturer's instructions. Reverse transcription was performed with qPCR BIO cDNA Synthesis Kit (PCR Biosystems). PCR was performed with PPP master mix (TOP-Bio). The following program was used: 94°C 1 min; 94°C 18 sec; 58°C 15 sec; 72°C for *Gapdh*; 94°C 1 min; 94°C 18 sec; 60°C 15 sec; 72°C for *Neat2* and *BC1*. Products were separated on 1.5% agarose gel with GelRed (41,003, Biotinum) staining. RT-PCR was then carried out using the QuantStudio13 and the Luna® Universal qPCR Master Mix (New England BioLabs) according to manufacturer's protocols with an annealing temperature of 60°C. Primers are listed in Table S2A.

### Polysome fractionation

Polysome fractionation followed by RNA isolation was carried out according to Scarce Sample Polysome profiling (SSP-profiling) method by Masek et al. [33]. Briefly, cycloheximide-treated oocytes (CHX, Sigma Aldrich) were lysed and resulting samples were loaded onto 10–50% sucrose gradients. Centrifugation was performed in SW55Ti rotor (Beckman Coulter) at 45,000 RPM (246,078 x g) for 65 min at 4°C (Optima L-90 ultracentrifuge, Beckman Coulter). Ten equal fractions were collected from each polysome profile and subjected to RNA isolation by Trizol reagent (Sigma-Aldrich). qRT-PCR-based quantification of 18S and 28S rRNAs in each fraction was applied to visualize individual polysome profiles [33]. Then, non-polysomal (NP; fractions 1–5) and polysomal fractions (P; fractions 6–10) were pooled and subjected to qRT-PCR (QuantStudio 3 cycler, Applied Biosystems) using *BC1*, *Neat2* and *Gapdh* gene-specific primers. Sequencing libraries were prepared using SMART-seq v4 ultra-low input RNA kit (Takara Bio). Sequencing was performed with HiSeq 2500 (Illumina) as 150-bp paired-ends. Reads were trimmed using Trim Galore v0.4.1 and mapped onto the mouse GRCm38 genome assembly using Hisat2 v2.0.5. Gene expression was quantified as fragments per kilobase per million (FPKM) values in Seqmonk v1.40.0.

### Measurement of overall protein synthesis

To measure the overall protein synthesis, 50 mCi of <sup>35</sup>S-methionine (Perkin Elmer) was added to methionine-free culture medium. An exact number of oocytes per sample (5–10) were labelled for 12 h, then lysed in SDS-buffer and subjected to SDS-polyacrylamide gel electrophoresis (PAGE). The labelled proteins were visualized by autoradiography on BasReader (Fuji) and quantified by Aida software (RayTest). *Gapdh* was used as a loading control.

### In silico prediction

RNA–RNA interactions were predicted by using the IntaRNA tool with default settings (<http://rna.informatik.uni-freiburg.de/IntaRNA/Input.jsp>) [39]. Accession numbers of analysed mRNA targets and 3'UTR coordinates are listed in Table S1. Visualization of interactions was created with BioRender.com.

### Cell lysate and total RNA-lncRNA pull-down

RNA-lncRNA pull-down procedures were done according to Torres et al. [41] with slight changes. Cell lysate pull-down included a cross-linking step: fixation of the cells in 1% PFA and quenching by 1/10 volume of glycine 1.25 M. After 2 × 5 min washes in PBS cells were frozen and stored at –80. In the case of total RNA pull-down cells were frozen without a cross-linking step with subsequent RNA isolation by Trizol reagent (Sigma-Aldrich). Using described lysis (cell lysate) and hybridization buffers, samples were lysed and subsequently incubated on RT for 6 hours with following *BC1* anti-sense DNA 5'-biotinylated oligonucleotide probes (GENERI BIOTECH) designed to bind

three distinct regions of the *BC1* (Fig. 4A): probe 1 GGCAAGCGCTCTACCACTGAGCTAAATCCCCAACCCC; probe 2 CCAGAGCTGAGGACCGAACCCAGGGCCTTGCGCTTGCTA; probe 3 TCTTTGAAAATGAAAAAGGTTGTGTGTGCCAGTTACCTTG. Samples were incubated overnight with Dynabeads M-280 Streptavidin (Themofisher). The RNA-protein complex was washed and separated from the beads by Proteinase K. RNA was isolated by Trizol reagent with subsequent analysis by RT-PCR with specific primers.

### RNA FISH

RNA FISH was performed according to Tetkova et al. [31]. Briefly, fixed oocytes (15 min in 4% PFA) were pre-treated with protease III provided in RNAScope H<sub>2</sub>O<sub>2</sub> and Protease Reagents kit (diluted 1:15 in nuclease-free water; Cat. No. 322,381, ACD) for 10 min. Each sample was then incubated with RNAScope probe (Table S2C) at 2 h in 40°C to detect *Actb* mRNA. RNA FISH protocol for amplification was followed using reagents in RNAScope Multiplex Fluorescent Detection Reagents v2 kit (Cat. No. 323,110, ACD), with extended washing: 2 × 10 min washing after probe hybridization (1x wash buffer diluted in nuclease-free water; RNAScope Wash Buffer Reagents, Cat. No. 310,091, ACD); v2 Amp1 30 min, 40°C, 2 × 5 min 1x wash buffer; v2 Amp2 30 min, 40°C, 2 × 5 min 1x wash buffer; v2 Amp3 15 min, 40°C, 2 × 5 min 1x wash buffer. After amplification, HRP-C1/C2/C3 was used on the corresponding channels of specific probe, for 15 min, 40°C. Oocytes were washed again 2 × 5 min in 1x wash buffer. TSA Cy5 dye (Perkin Elmer) diluted to 1:1500 in TSA buffer (ACD) was used for fluorescent labelling of the amplified signal. After washing and application of HRP blocker (30 min in 40°C), samples were washed a final time 2 × 5 min in 1x wash buffer and mounted in Prolong Gold Antifade with DAPI (Life Technologies) on epoxy coated slides (Thermo Scientific). PolyA RNA FISH was performed according to 43. Briefly, oocytes were fixed for 10 min in 4% paraformaldehyde and permeabilized in 0.1% Triton X-100 in PBS with 40 units/20 μL of RNaseOut (Invitrogen). Oocytes were washed in Wash Buffer A (Biosearch Technologies) and incubated overnight at 30°C in hybridization buffer (Biosearch Technologies) with 75 nM oligo-dT(22) labelled with Cy5 probe (Generi Biotech). Oocytes were then washed 3x in Wash Buffer A and 2x in SSC (Biosearch Technologies). Images were obtained using a confocal microscope (Leica SP5). Image quantification was performed using ImageJ software (<http://rsbweb.nih.gov/ij/>). Bacterial *DapB* RNA (*Bacillus subtilis*, str. SMY; EF191515.1) was used as a negative control.

### RNA-protein *in situ* proximity ligation assay (RNA-PLA)

Oocytes were cultivated then fixed for 15 min in 4% PFA and pre-treated with protease III provided in RNAScope H<sub>2</sub>O<sub>2</sub>, washed in PBS and incubated with *BC1* (mentioned above) or *eEF2* (GGACTTAACACTTGAAGTCCGTTGGGAGTG) anti-sense DNA 5'-biotinylated oligonucleotide probes 2 h in 40°C. After washes in PBS (2 × 5 min), cells were then incubated with mouse anti-biotin antibody (1:150; 03-3700; Invitrogen) together with corresponding primary antibodies: rabbit anti-FMRP (1:150; cs4317; Cell signalling) or anti-RPL24 (1:150; PAS-62,450, Thermo Fisher) at 4°C overnight (primary antibodies are listed

in Table S2B). For negative control mouse, anti-biotin antibody and anti-pLMN A/C (1:150; cs2026; Cell signalling) antibody were used. PLA was performed following instructions of PLA Duolink kits (DUO92006 and DUO92008, Sigma Aldrich) and a previously published protocol [43]. The samples were washed using PBS and then in Wash Buffer A (Sigma Aldrich) and incubated with 40 μL of the probe reaction mix for 1 h at 37°C. Next, the samples were washed in 1x Wash Buffer A for 2 × 5 min and the following ligation reaction was performed for 30 min at 37°C. After washing (2 × 5 min) in Wash Buffer A, 40 μL of amplification reaction reagent was added to each sample and incubated for 100 min at 37°C. The samples were then washed for 2 × 10 min in 1x Wash Buffer B (Sigma Aldrich) and for 2 min in 0.01x Wash Buffer B and mounted on a slide using Prolong Mounting Medium with DAPI (H-1500, Vector Laboratories). Inverted confocal microscope (Leica SP5) was used for sample visualization. Image quantification of interactions was analysed in ImageJ software (<http://rsbweb.nih.gov/ij/>).

### Immunocytochemistry

Fixed oocytes (15 min in 4% PFA; Sigma Aldrich) were permeabilized in 0.1% Triton X-100 for 10 min, washed in PBS supplemented with polyvinyl alcohol (PVA, Sigma Aldrich) and incubated with primary antibodies (Table S2B) diluted in PVA/PBS overnight at 4°C. Oocytes were then washed 2 × 15 min in PVA/PBS and primary antibodies were detected using relevant Alexa Fluor 488/594/647 conjugates (Invitrogen) diluted to 1:250 for 1 h at room temperature. Washed oocytes (2 × 15 min in PVA/PBS) were mounted onto slides using ProLong Mounting Medium with DAPI. Inverted confocal microscope (Leica SP5) was used for sample visualization. Image quantification and assembly were performed using ImageJ and Adobe Photoshop CS3. Experiments were repeated 3x with 20–30 oocytes per group/experiment.

### Microinjection of oocytes and live-cell imaging

Isolated NE oocytes were microinjected in TM with IBMX using inverted microscope Leica DMI 6000B, TransferMan NK2 (Eppendorf) and FemtoJet (Eppendorf). Solution used for oocyte injection contained: 20 ng/μL of *in vitro* transcribed H2b:gfP RNA (mMessage, Ambion) from plasmid (provided by Dr. Martin Anger, Laboratory of Cell Division Control, IAPG CAS) in combination with 20 ng/μL of *in vitro* transcribed *BC1* RNA (mMessage, Ambion) from Puc57 plasmid (Generi biotech). 1 h after microinjection oocytes were selected and either washed from IBMX and cultivated to MII stage or stored at GV stage overnight. Microinjected oocytes were placed into 4-well culture chamber (Sarstedt) in 10 μL of equilibrated M16 media (37.5°C, 5% CO<sub>2</sub>) covered with mineral oil (M8410; Sigma Aldrich). The cells were imaged using inverted microscope Leica DMI 6000B equipped with a controlled chamber system (Tempcontroller 2000–2 Pecon, and a CO<sub>2</sub> controller, Pecon). Time-lapse movies (LAS X, Leica microsystems) of meiotic maturation of microinjected oocytes with chromatin marker (H2b:gfP) were used for phenotype evaluation (nuclear envelope breakdown, polar body extrusion).

### Luciferase reporter assay

GV oocytes were microinjected with Nanoluc and Firefly reporter constructs using micromanipulator Leica DMI 6000B, TransferMan NK2 (Eppendorf) and FemtoJet (Eppendorf). 5'TOP and 5'TOPmut sequence were cloned into pNL1.2 vector (Promega). NheI-T7 overhanged forward primer and BglIII reverse primers used to amplify 5'TOP and 5'TOPmut sequence from plasmids which contained conventional and mutated 5'UTR TOP sequence of *Eef2* mRNA: pIS1-Eef25UTR-renilla (Addgene #38,235), pIS1-Eef25UTR-TOPmut-renilla (Addgene #38,236) [77] vector and cloned into pNL1.2 vector. Combination with Firefly Luciferase (Addgene #18,964) was used as an injection control. Samples were analysed by Dual-Glo Luciferase Assay System (Promega). Luminescence was measured by Synergy HTX Plate Reader (BioTek Instruments).

### Immunoblotting

An exact number of cells (15–30 oocytes) was washed in PVA/PBS and frozen to  $-80^{\circ}\text{C}$ . Prepared samples were lysed in NuPAGE LDS Sample Buffer (NP0007, Thermo Fisher Scientific) and NuPAGE Sample Reducing Agent (NP0004, Thermo Fisher Scientific) and heated at  $100^{\circ}\text{C}$  for 5 min. Proteins were separated on precast gradient 4–12% SDS-PAGE gel (Thermo Fisher Scientific) and blotted to Immobilon P membrane (Millipore) in a semidry blotting system (Biometra GmbH) at  $5\text{ mA cm}^2$  for 25 min. Membranes were then blocked in 5% skimmed milk dissolved in 0.05% Tween-Tris buffer saline (TTBS), pH 7.4 for 1 h. Membranes were incubated overnight at  $4^{\circ}\text{C}$  with the primary antibodies (Table S2B) diluted in 1% milk/TTBS. Secondary antibodies with Peroxidase were used (711–035-152 Anti-Rabbit Donkey or 715–035-151 Anti-Mouse Donkey, both Jackson ImmunoResearch), diluted 1:7500 in 1% milk/TTBS for 1 h at room temperature. ECL (Amersham) was used for visualization of immunodetected proteins on X-ray films. The films were scanned by calibrated densitometer (GS-800, Bio-Rad Laboratories) and quantified in ImageJ. Presented images were cropped from membranes, contrast and brightness were adjusted using Adobe Photoshop CS3.

### Acknowledgments

We thank Jaroslava Supolikova and Marketa Hancova for assistance with experiments.

### Disclosure statement

No potential conflict of interest was reported by the authors.

### Funding

This research was funded by GACR18-19395S and Institutional Research Concept RVO67985904. The funders had no role in study design, data collection and analysis, decision to publish or preparation of the manuscript; Grantová Agentura České Republiky [GACR18-19395S].

### Ethical approval

All animal work was conducted according to Act No 246/1992 for the protection of animals against cruelty; from 25.09.2014 number CZ02389, issued by the Ministry of Agriculture.

### ORCID

A. Susor  <http://orcid.org/0000-0003-2926-4096>

### References

- [1] Kutter C, Watt S, Stefflova K, et al. Rapid turnover of long noncoding RNAs and the evolution of gene expression. *PLoS Genet.* 2012;8:e1002841.
- [2] Ponting CP, Oliver PL, Reik W. Evolution and functions of long noncoding RNAs. *Cell.* 2009;136:629–641.
- [3] Frankish A, Diekhans M, Ferreira AM, et al. GENCODE reference annotation for the human and mouse genomes. *Nucleic Acids Res.* 2019;47:766–773.
- [4] Tiedge H, Freneau RT, Weinstock PH, et al. Dendritic location of neural BC1 RNA. *Proc Natl Acad Sci U S A.* 1991;88:2093–2097.
- [5] Taft RJ, Pheasant M, Mattick JS. The relationship between non-protein-coding DNA and eukaryotic complexity. *BioEssays.* 2007;29:288–299.
- [6] Rozhdestvensky TS, Kopylov AM, Brosius J, et al. Neuronal BC1 RNA structure: evolutionary conversion of a tRNAAla domain into an extended stem-loop structure. *Rna.* 2001;7:722–730.
- [7] Lin D, Pestova TV, Hellen CUT, et al. Translational control by a small RNA: dendritic BC1 RNA targets the eukaryotic initiation factor 4A helicase mechanism. *Mol Cell Biol.* 2008;28:3008–3019.
- [8] Eom T, Berardi V, Zhong J, et al. Dual nature of translational control by regulatory BC RNAs. *Mol Cell Biol.* 2011;31:4538–4549.
- [9] Lee Y, Lee HS, Kim M, et al. Brain cytoplasmic RNAs in neurons: from biosynthesis to function. *Biomolecules.* 2020;10:11–15.
- [10] Muddashetty RS, Khanam T, Kondrashov A, et al. Poly(A)-binding protein is associated with neuronal BC1 and BC200 ribonucleoprotein particles. *J Mol Biol.* 2002;321:433–445.
- [11] Wang H, Iacoangeli A, Popp S, et al. Dendritic BC1 RNA: functional role in regulation of translation initiation. *J Neurosci.* 2002;22:10232–10241.
- [12] Briz V, Restivo L, Pasciuto E, et al. The non-coding RNA BC1 regulates experience-dependent structural plasticity and learning. *Nat Commun.* 2017;8:1–15.
- [13] Lacoux C, Di Marino D, Boyl PP, et al. BC1-FMRP interaction is modulated by 2'-O-methylation: RNA-binding activity of the tudor domain and translational regulation at synapses. *Nucleic Acids Res.* 2012;40:4086–4096.
- [14] de Rubeis S, Bagni C. Regulation of molecular pathways in the Fragile X Syndrome: insights into Autism Spectrum Disorders. *J Neurodev Disord.* 2011;3:257–269.
- [15] Zalfa F, Giorgi M, Primerano B, et al. The Fragile X syndrome protein FMRP associates with BC1 RNA and regulates the translation of specific mRNAs at synapses. *Cell.* 2003;112:317–327.
- [16] Zalfa F, Adinolfi S, Napoli I, et al. FMRP binds specifically to the brain cytoplasmic RNAs BC1/BC200 via a novel RNA binding motif. *J Biol Chem.* 2005;280:33403–33410.
- [17] Zhang T, Pang P, Fang Z, et al. Expression of BC1 impairs spatial learning and memory in Alzheimer's disease via APP translation. *Mol Neurobiol.* 2018;55:6007–6020.
- [18] Eom T, Muslimov IA, Iacoangeli A, et al. Dendritic targeting and regulatory RNA control of local neuronal translation. *Oxford Handb Neuronal Protein Synth.* 2018;1–29.



- [19] Iacoangeli A, Rozhdestvensky TS, Dolzhanskaya N, et al. On BC1 RNA and the fragile X mental retardation protein. *Proc Natl Acad Sci U S A*. 2008;105:734–739.
- [20] Zhong J, Chuang SC, Bianchi R, et al. Regulatory BC1 RNA and the fragile X mental retardation protein: convergent functionality in brain. *PLoS One*. 2010;5:e15509.
- [21] Darnell JC, Van Driesche SJ, Zhang C, et al. FMRP stalls ribosomal translocation on mRNAs linked to synaptic function and autism. *Cell*. 2011;146:247–261.
- [22] Iacoangeli A, Tiedge H. Translational control at the synapse: role of RNA regulators. *Trends Biochem Sci*. 2013;38:47–55.
- [23] Battaglia R, Vento ME, Borzi P, et al. Non-coding RNAs in the ovarian follicle. *Front Genet*. 2017;8:57.
- [24] Ganesh S, Horvat F, Drutovic D, et al. The most abundant maternal lncRNA *Sirena1* acts post-transcriptionally and impacts mitochondrial distribution. *Nucleic Acids Res*. 2020;48:3211–3227.
- [25] Karlic R, Ganesh S, Franke V, et al. Long non-coding RNA exchange during the oocyte-to-embryo transition in mice. *DNA Res*. 2017;24:129–141.
- [26] Kataruka S, Modrak M, Kinterova V, et al. MicroRNA dilution during oocyte growth disables the microRNA pathway in mammalian oocytes. *Nucleic Acids Res*. 2020;48:8050–8062.
- [27] De La Fuente R, Viveiros MM, Burns KH, et al. Major chromatin remodeling in the germinal vesicle (GV) of mammalian oocytes is dispensable for global transcriptional silencing but required for centromeric heterochromatin function. *Dev Biol*. 2004;275:447–458.
- [28] Susor A, Kubelka M. Translational regulation in the mammalian oocyte. In: Results and problems in cell differentiation. Results. 2017;63:257–295. Springer Verlag
- [29] Carrieri C, Cimatti L, Biagioli M, et al. Long non-coding antisense RNA controls *Uchl1* translation through an embedded SINEB2 repeat. *Nature*. 2012;491:454–457.
- [30] Hutchinson JN, Ensminger AW, Clemson CM, et al. A screen for nuclear transcripts identifies two linked noncoding RNAs associated with SC35 splicing domains. *BMC Genomics*. 2007;8:1–16.
- [31] Tetkova A, Jansova D, Susor A. Spatio-temporal expression of *ANK2* promotes cytokinesis in oocytes. *Sci Rep*. 2019;9:1–13.
- [32] Wang H, Iacoangeli A, Lin D, et al. Dendritic BC1 RNA in translational control mechanisms. *J Cell Biol*. 2005;171:811–821.
- [33] Masek T, Del Llano E, Gahurova L, et al. Identifying the translome of mouse NEBD-stage oocytes via SSP-profiling; a novel polysome fractionation method. *Int J Mol Sci*. 2020;21:1254.
- [34] Skryabin BV, Sukonina V, Jordan U, et al. Neuronal untranslated BC1 RNA: targeted gene elimination in mice. *Mol Cell Biol*. 2003;23:6435–6441.
- [35] Dever TE. Gene-specific regulation by general translation factors. *Cell*. 2002;108:545–556.
- [36] England CG, Ehlerding EB, Cai W. NanoLuc: a small luciferase is brightening up the field of bioluminescence. *Bioconjug Chem*. 2016;27:1175–1187.
- [37] Gandin V, Masvidal L, Hulea L, et al. NanoCAGE reveals 5' UTR features that define specific modes of translation of functionally related MTOR-sensitive mRNAs. *Genome Res*. 2016;26:636–648.
- [38] Mayr C. What are 3' UTRs doing? *Cold Spring Harb. Perspect Biol*. 2019;11(10):a034728.
- [39] Mann M, Wright PR, Backofen R. IntaRNA 2.0: enhanced and customizable prediction of RNA-RNA interactions. *Nucleic Acids Res*. 2017;45:435–439.
- [40] Barbagallo C, Brex D, Caponnetto A, et al. LncRNA *UCA1*, upregulated in CRC biopsies and downregulated in serum exosomes, controls mRNA expression by RNA-RNA interactions. *Mol Ther Nucleic Acids*. 2018;12:229–241.
- [41] Torres M, Becquet D, Guillen S, et al. RNA pull-down procedure to identify RNA targets of a long non-coding RNA. *J Vis Exp*. 2018;2018:e57379.
- [42] Chen E, Joseph S. Fragile X mental retardation protein: a paradigm for translational control by RNA-binding proteins. *Biochimie*. 2015;114:147–154.
- [43] Jansova D, Tetkova A, Koncicka M, et al. Localization of RNA and translation in the mammalian oocyte and embryo. *PLoS One*. 2018;13:1–25.
- [44] Söderberg O, Leuchowius KJ, Gullberg M, et al. Characterizing proteins and their interactions in cells and tissues using the in situ proximity ligation assay. *Methods*. 2008;45:227–232.
- [45] Erickson SL, Lykke-Andersen J. Cytoplasmic mRNP granules at a glance. *J Cell Sci*. 2011;124:293–297.
- [46] Lai A, Valdez-Sinon AN, Bassell GJ. Regulation of RNA granules by FMRP and implications for neurological diseases. *Traffic*. 2020;21:454–462.
- [47] Rosario R, Filis P, Tessyman V, et al. FMRP associates with cytoplasmic granules at the onset of meiosis in the human oocyte. *PLoS One*. 2016;11:1–14.
- [48] Wheeler JR, Matheny T, Jain S, et al. Distinct stages in stress granule assembly and disassembly. *Elife*. 2016;5:e18413.
- [49] Pakos-Zebrucka K, Koryga I, Mnich K, et al. The integrated stress response. *EMBO Rep*. 2016;17:1374–1395.
- [50] Shi Z, Barna M. Translating the genome in time and space: specialized ribosomes, RNA regulons, and RNA-binding proteins. *Annu Rev Cell Dev Biol*. 2015;31:31–54.
- [51] Monti M, Zanoni M, Calligaro A, et al. Developmental arrest and mouse antral not-surrounded nucleolus oocytes. *Biol Reprod*. 2013;88:1–7.
- [52] Del Llano E, Masek T, Gahurova L, et al. Age-related differences in the translational landscape of mammalian oocytes. *Aging Cell*. 2020;19:e13231.
- [53] Burkholder GD, Comings DE, Okada TA. A storage form of ribosomes in mouse oocytes. *Exp Cell Res*. 1971;69:361–371.
- [54] Yurttas P, Vitale AM, Fitzhenry RJ, et al. Role for *PADI6* and the cytoplasmic lattices in ribosomal storage in oocytes and translational control in the early mouse embryo. *Development*. 2008;135:2627–2636.
- [55] Chen E, Sharma MR, Shi X, et al. Fragile X mental retardation protein regulates translation by binding directly to the ribosome. *Mol Cell*. 2014;54:407–417.
- [56] Ishizuka A, Siomi MC, Siomi H. A *Drosophila* fragile X protein interacts with components of RNAi and ribosomal proteins. *Genes Dev*. 2002;16:2497–2508.
- [57] Didiot MC, Subramanian M, Flatter E, et al. Cells lacking the fragile X mental retardation protein (FMRP) have normal RISC activity but exhibit altered stress granule assembly. *Mol Biol Cell*. 2009;20:428–437.
- [58] Lee EK, Kim HH, Kuwano Y, et al. HnRNP C promotes APP translation by competing with FMRP for APP mRNA recruitment to P bodies. *Nat Struct Mol Biol*. 2010;17:732–739.
- [59] Feng Y, Absher D, Eberhart DE, et al. FMRP associates with polyribosomes as an mRNP, and the I304N mutation of severe fragile X syndrome abolishes this association. *Mol Cell*. 1997;1:109–118.
- [60] Khandjian EW, Huot ME, Tremblay S, et al. Biochemical evidence for the association of fragile X mental retardation protein with brain polyribosomal ribonucleoproteins. *Proc Natl Acad Sci U S A*. 2004;101:13357–13362.
- [61] Stefani G, Fraser CE, Darnell JC, et al. Fragile X mental retardation protein is associated with translating polyribosomes in neuronal cells. *J Neurosci*. 2004;24:7272–7276.
- [62] Davidson EH. *Gene Activity in Early Development*. 3rd Edition. Academic Press, Inc; 1986. p. 158–159.
- [63] Graber TE, Hébert-Seropian S, Khoutorsky A, et al. Reactivation of stalled polyribosomes in synaptic plasticity. *Proc Natl Acad Sci U S A*. 2013;110:16205–16210.
- [64] Shah S, Molinaro G, Liu B, et al. FMRP control of ribosome translocation promotes chromatin modifications and alternative splicing of neuronal genes linked to autism. *Cell Rep*. 2020;30:4459–4472.e6.



- [65] Dalton CM, Carroll J. Biased inheritance of mitochondria during asymmetric cell division in the mouse oocyte. *J Cell Sci.* **2013**;126:2955–2964.
- [66] FitzHarris G, Marangos P, Carroll J. Changes in endoplasmic reticulum structure during mouse oocyte maturation are controlled by the cytoskeleton and cytoplasmic dynein. *Dev Biol.* **2007**;305:133–144.
- [67] Schlaitz AL, Thompson J, Wong CCL, et al. REEP3/4 ensure endoplasmic reticulum clearance from metaphase chromatin and proper nuclear envelope architecture. *Dev Cell.* **2013**;26:315–323.
- [68] Susor A, Jansova D, Cerna R, et al. Temporal and spatial regulation of translation in the mammalian oocyte via the mTOR-eIF4F pathway. *Nat Commun.* **2015**;6:1–12.
- [69] Flemr M, Ma J, Schultz RM, et al. P-body loss is concomitant with formation of a messenger RNA storage domain in mouse oocytes. *Biol Reprod.* **2010**;82:1008–1017.
- [70] Chan SP, Slack FJ. microRNA-mediated silencing inside P-bodies. *RNA Biol.* **2006**;3:97–100.
- [71] Jakymiw A, Pauley KM, Li SL, et al. The role of GW/P-bodies in RNA processing and silencing. *J Cell Sci.* **2007**;120:1702.
- [72] Parker R, Sheth U. P bodies and the control of mRNA translation and degradation. *Mol Cell.* **2007**;25:635–646.
- [73] Ma J, Flemr M, Stein P, et al. MicroRNA activity is suppressed in mouse oocytes. *Curr Biol.* **2010**;20:265–270.
- [74] Suh N, Baehner L, Moltzahn F, et al. MicroRNA function is globally suppressed in mouse oocytes and early embryos. *Curr Biol.* **2010**;20:271–277.
- [75] Sternlicht AL, Schultz RM. Biochemical studies of mammalian oogenesis: kinetics of accumulation of total and poly(A)-containing RNA during growth of the mouse oocyte. *J Exp Zool.* **1981**;215:191–200.
- [76] Lin CJ, Koh FM, Wong P, et al. Hira-mediated H3.3 incorporation is required for DNA replication and ribosomal RNA transcription in the mouse zygote. *Dev Cell.* **2014**;30:268–279.
- [77] Thoreen CC, Chantranupong L, Keys HR, et al. A unifying model for mTORC1-mediated regulation of mRNA translation. *Nature.* **2012**;485:109–113.

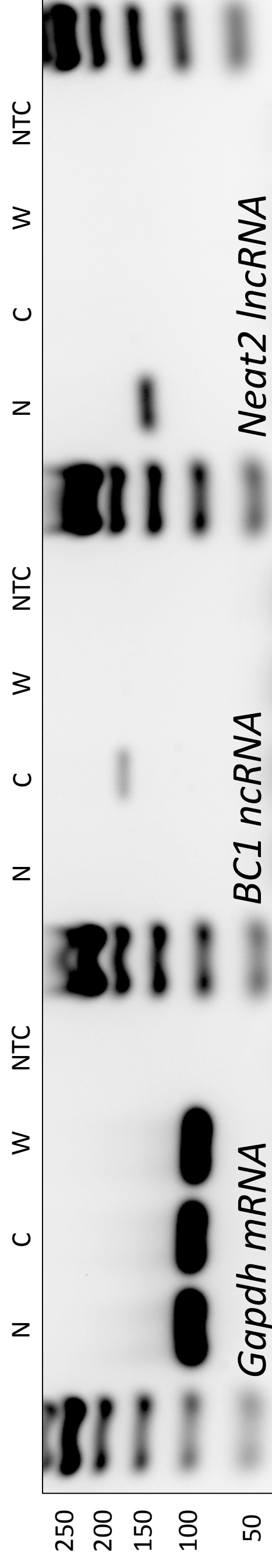


**Figure S1: Localization of *Gapdh* mRNA, *BC1* ncRNA and *Neat2* lncRNA in mammalian oocyte.**

PCR analysis of oocyte Nuclei (N), Cytoplasm (C) for *Gapdh* mRNA, *Bc1* ncRNA and lncRNA *Neat2* expression in nucleus and cytoplasmic fractions of GV oocyte. Nucleus isolation pipette wash (W) and PCR reaction without cDNA (NTC) were used as negative technical controls. Note, abundant *Gapdh* mRNA persist in all samples. See **Figure 1A**.

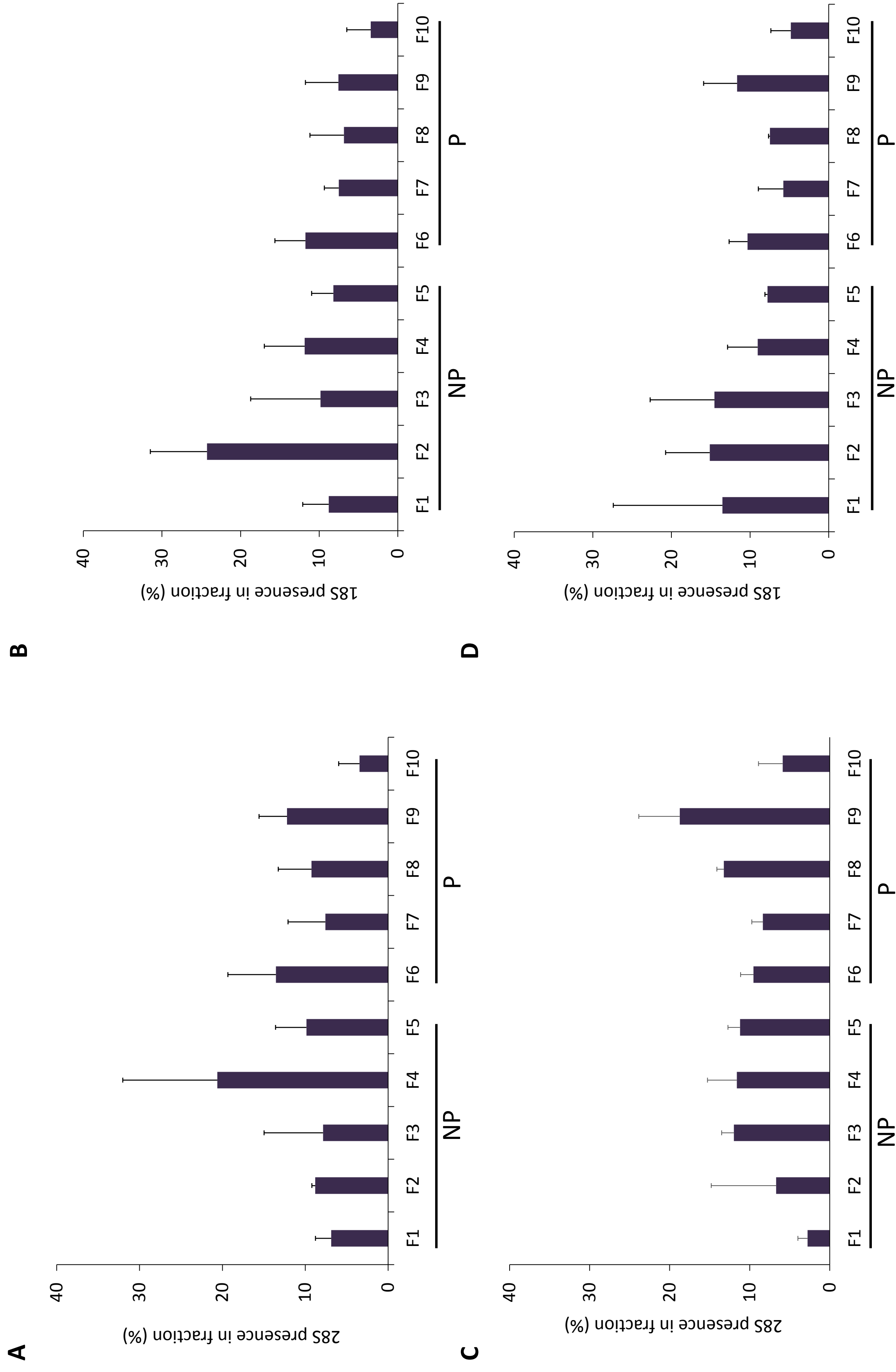


**Figure S2: qRT-PCR of Scarce Sample Polysome (SSP) profiling, where fractions (F1-F5) represent non-polysomal and F6-F10 polysomal associated rRNAs.**

- A)** qRT-PCR analyses of 28S rRNA levels in SSP profiling fractions obtained from GV oocytes. Relative association; mean  $\pm$  SD;  $n \geq 3$ .  
**B)** qRT-PCR analyses of 18S rRNA levels in SSP profiling fractions obtained from GV oocytes. Relative association; mean  $\pm$  SD;  $n \geq 3$ .  
**C)** qRT-PCR analyses of 28S rRNA levels in SSP profiling fractions obtained from MII oocytes. Relative association; mean  $\pm$  SD;  $n \geq 3$ .  
**D)** qRT-PCR analyses of 28S rRNA levels in SSP profiling fractions obtained from MII oocytes. Relative association; mean  $\pm$  SD;  $n \geq 3$ .

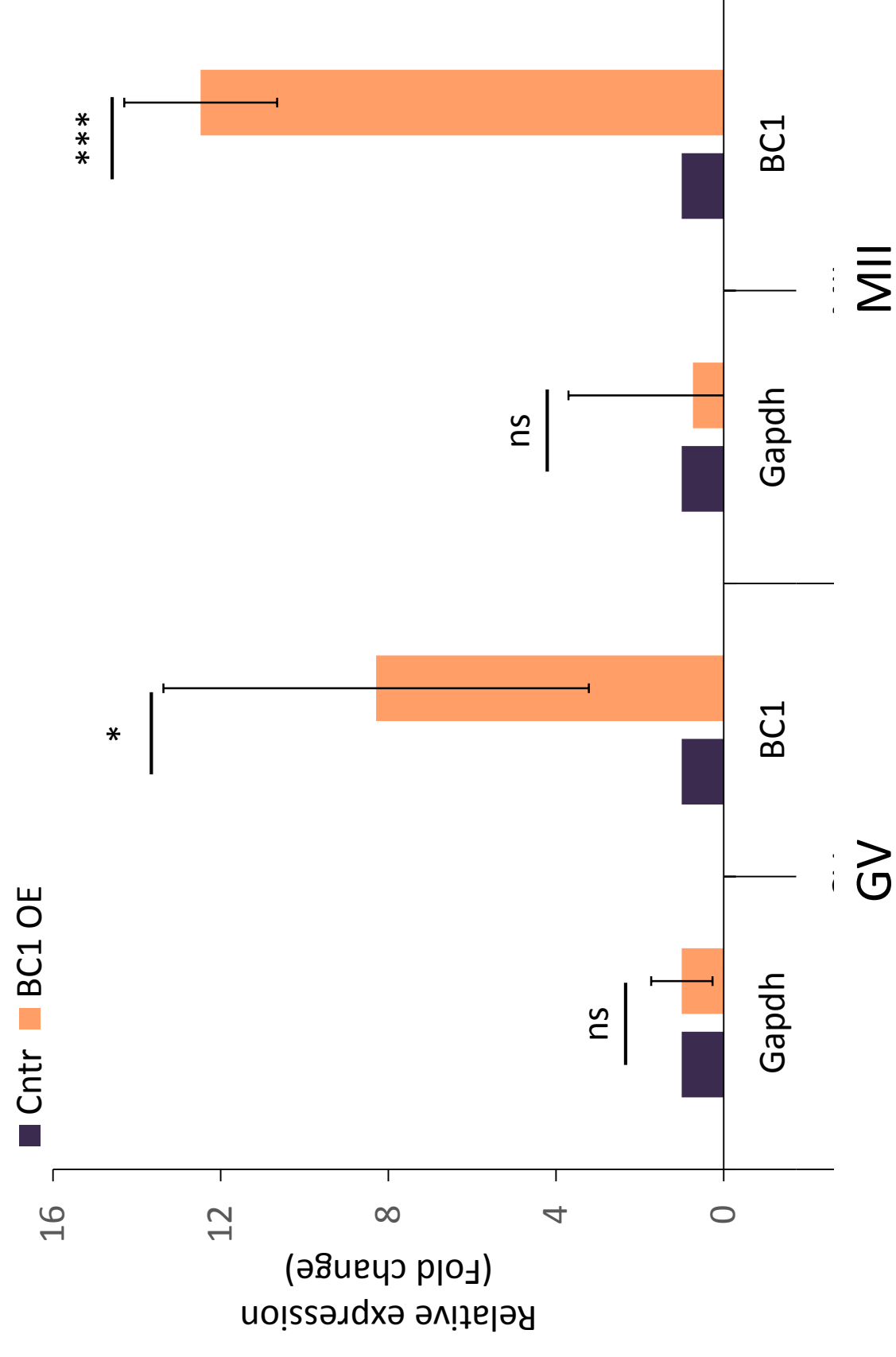


**Figure S3: Validation of BC1 ncRNA overexpression in the GV and MII stage oocytes.**

qRT PCR analysis of *Gapdh* mRNA and *BC1* ncRNA expression in GV and MII oocytes in the injection with control (Cntr) or BC1 (OE) RNAs. Values obtained for the Cntr group were set as 1. *Gapdh* mRNA was used as a control. Relative expression, mean  $\pm$  SD; Student's *t*-test, \* $p < 0.05$ , \*\* $p < 0.001$ , ns for non-significant,  $n=3$ .

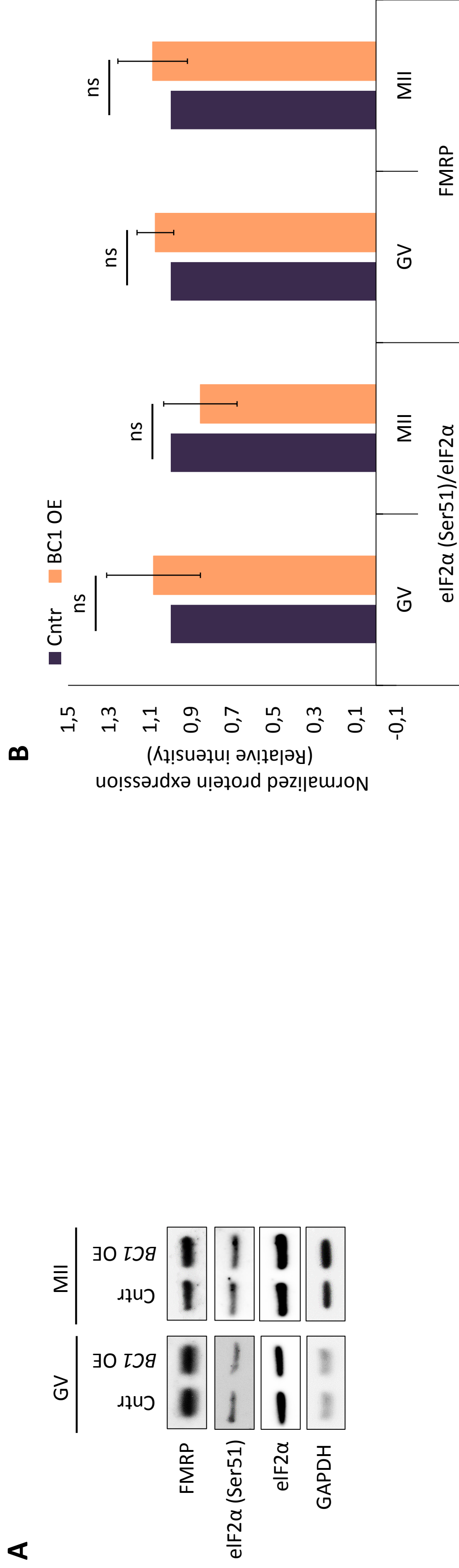


**Figure S4: BC1 overexpression does not influence translational stress or FMRP expression.**

**A)** Western blot analysis of FMRP, p-eIF2α (Ser51), eIF2α in GV and MII oocytes injected with control or BC1 RNAs.

**B)** GAPDH was used as a loading control. Representative images from at least three independent replicates. Quantification of western blot analysis normalized to GAPDH. Values obtained for the Cntr group were set as 1.

Data from three independent experiments; mean ± SD; Student's *t*-test: ns for non-significant.

**A**

3'UTR of target mRNA - ncRNA	Minimum Free Energy (MFE; kcal/mol)
<i>Gapdh</i> – <i>BC1</i>	No interaction
<i>Anln</i> – <i>UCA1</i>	-23.29
<i>Actb</i> – <i>BC1</i>	-24.2
<i>Dlg4</i> – <i>BC1</i>	-11.8
<i>SVV</i> – <i>BC1</i>	-7.7

**B**

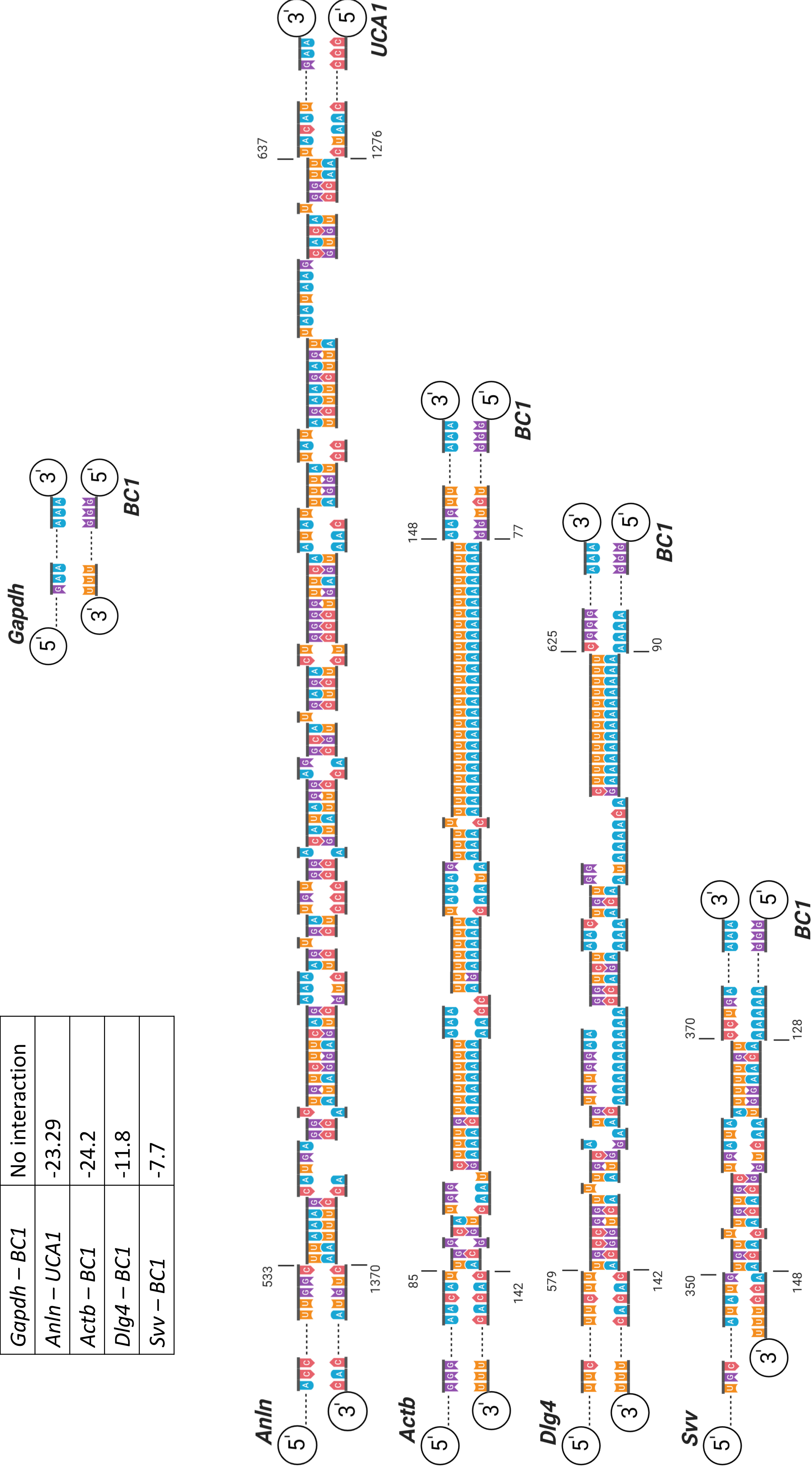
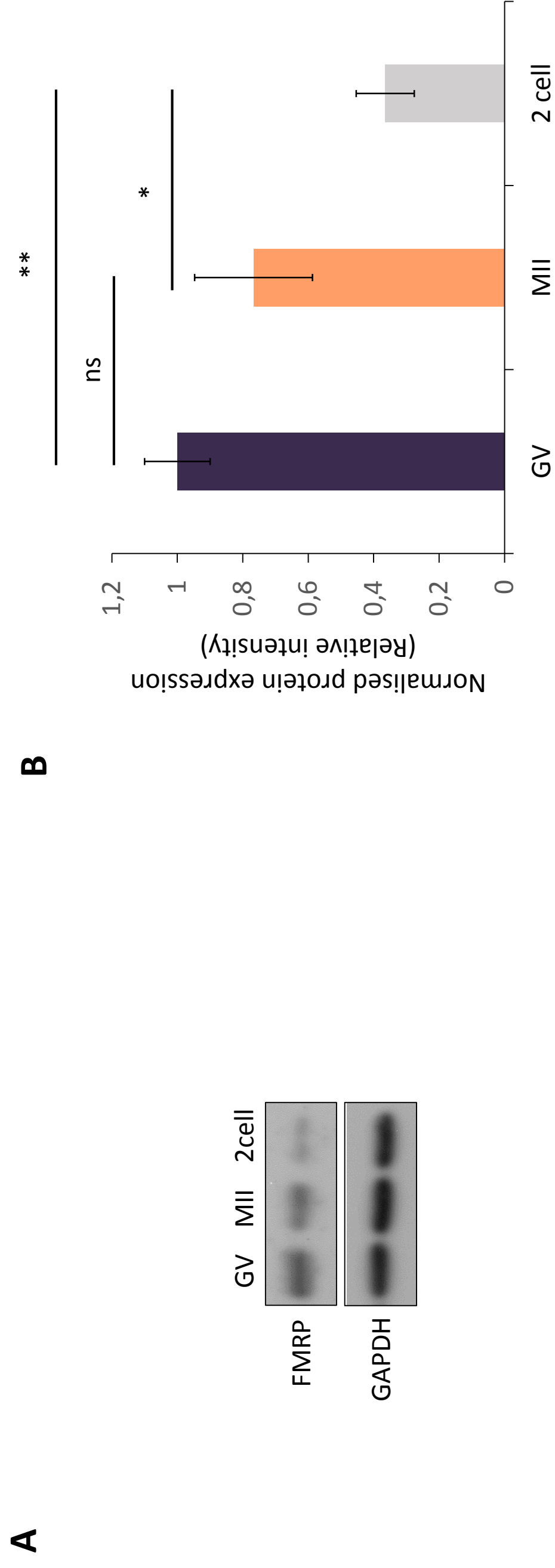


**Figure S5: Analysis of *BC1* complementarity with 3'UTR of target mRNAs.**

**A)** Values of prediction using IntaRNA 2.0 software of RNA – RNA interaction between *BC1* and 3'UTRs of *Gapdh*, *SVV*, *Actb* and *Dlg4* mRNAs. Known interaction of *Anln* mRNA with *Uca1* lncRNA (Barbagallo et al. 2018) was used as positive control.

**B)** *In silico analysis* using IntaRNA 2.0 software for prediction of minimum free energy for *BC1*– target mRNA 3'UTR interactions.

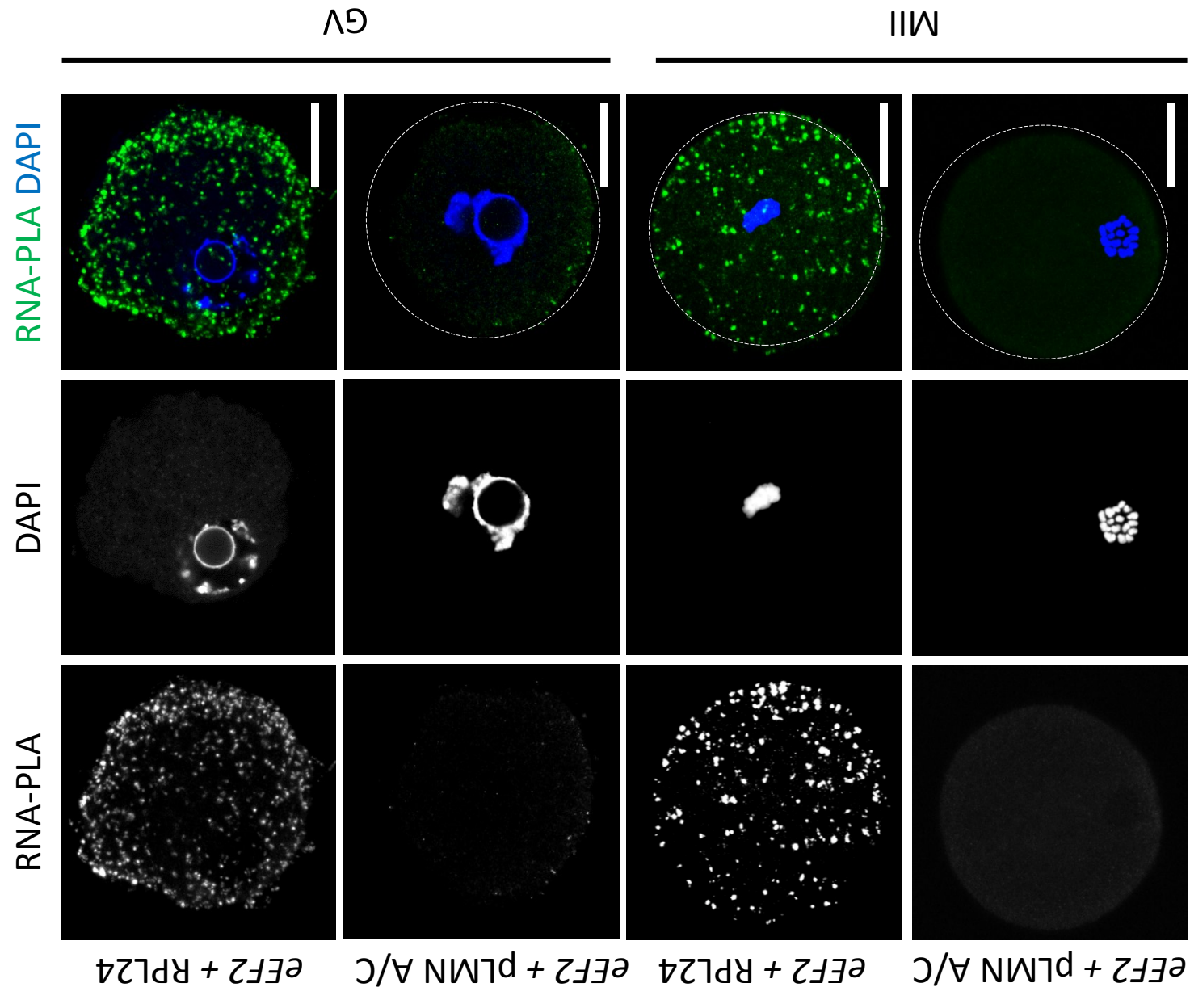
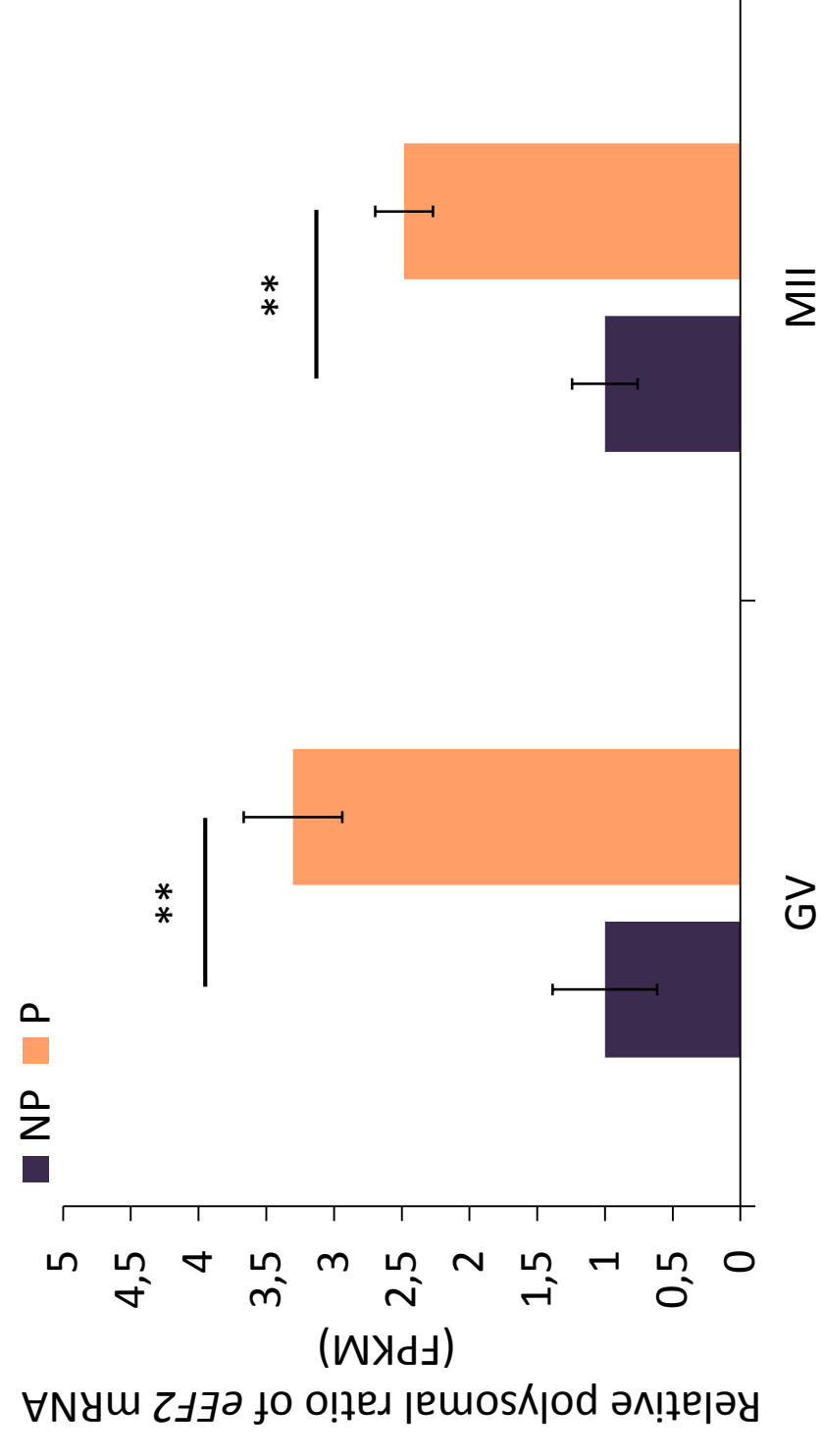




**Figure S6: FMRP expression decreases in the MII oocyte and early embryo.**

**A)** Western blot analysis of FMRP in the GV and MII oocytes and 2-cell embryo. GAPDH was used as a loading control. Representative images from at least three independent replicates.

**B)** Quantification of western blot analysis normalized to GAPDH. Values obtained for the GV stage was set as 1. Data from three independent experiments; mean  $\pm$  SD; Student's *t*-test: \* $p < 0.05$ , \*\* $p < 0.01$ , ns for non-significant.

**A****B**

**Figure S7: Controls for RNA-protein *in situ* proximity ligation assay (RNA-PLA).**

**A)** Known interaction (Zhang 2016) eEF2 mRNA with RPL24 was used as a positive control in the GV and MII oocytes. Non interacting eEF2 mRNA with phosphorylated LMN A/C on serine 22 was used as a negative RNA-PLA control. Representative confocal images of the GV and MII oocytes; scale bars 25  $\mu$ m; interactions, green; DNA, blue;  $n \geq 10$ .

**B)** Abundance of eEF2 mRNA in polyribosome fraction (P) in GV and MII oocyte. Values obtained for the non-polyribosome fraction (NP) were set as 1. Relative FPKM value, mean  $\pm$  SD; Student's *t*-test: ns for non-significant,  $n = 3$ .



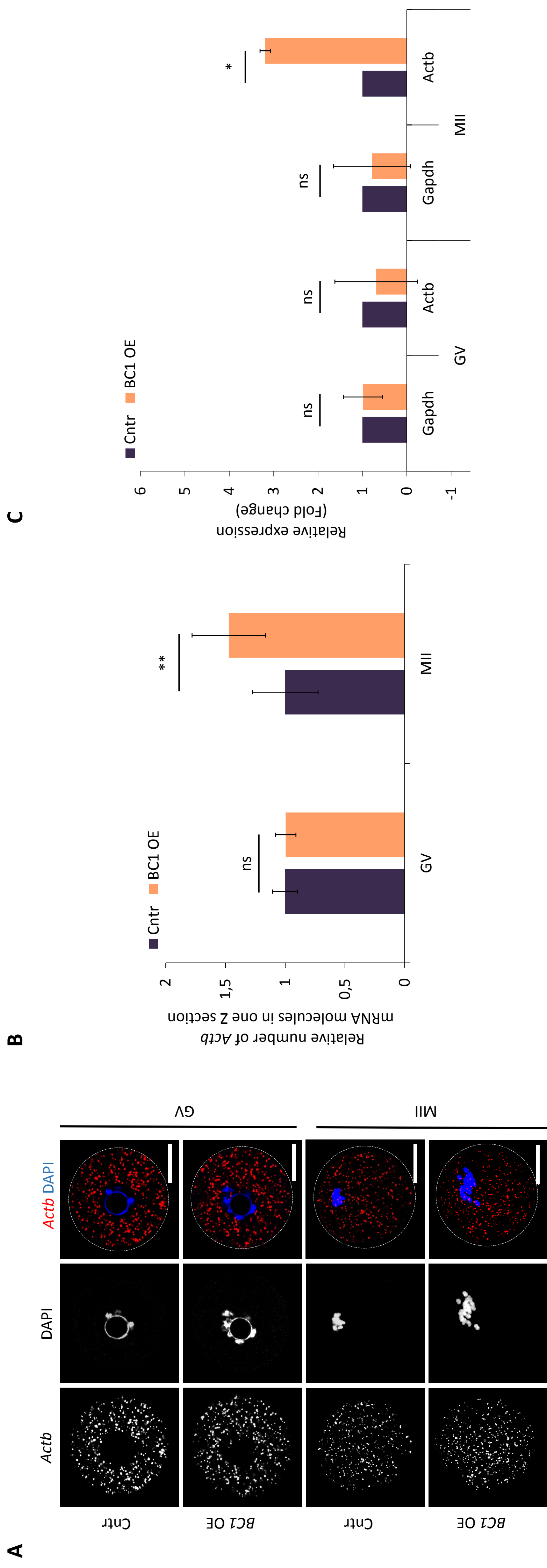


**Figure S8: BC1 overexpression does not influence clustering of target mRNA but does influence the stability.**

**A)** *Actb* RNA FISH of representative confocal images of the control or *BC1* overexpression (OE) in the GV and MII oocytes. Scale bars 25  $\mu$ m; *Actb* mRNA grey and red; DNA blue;  $n \geq 13$ .

**B)** Quantification of *Actb* mRNA molecules in equatorial Z section in the GV and MII oocyte. Values obtained for the Cntr group were set as 1. Relative number of *Actb* mRNA molecules in one Z section; mean  $\pm$  SD; Student's t-test: \*\* $p < 0.01$ , ns for non-significant,  $n \geq 13$ .

**C)** qRT PCR analysis of *Gapdh* and *Actb* mRNAs expression in GV and MII oocytes in the injection with control (Cntr) or *BC1* (OE) RNAs. Values obtained for the Cntr group were set as 1. *Gapdh* mRNA was used as a control. Relative expression; mean  $\pm$  SD; Student's t-test: \* $p < 0.05$ , ns for non-significant,  $n \geq 2$ .

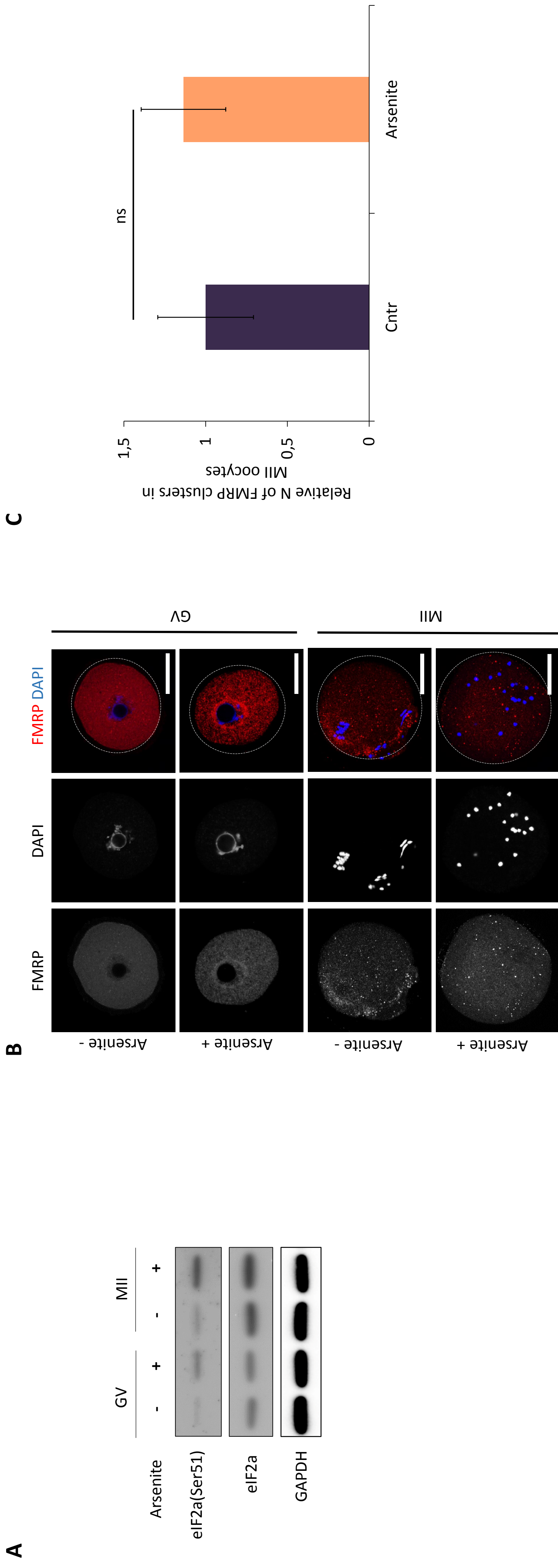


**Figure S9: Chemically induced stress does not copy FMRP clustering via BC1 OE.**

**A)** Western blot analysis of eIF2a(Ser51) and eIF2a in the GV and MII oocytes in the absence (-) or presence (+) of arsenite. GAPDH was used as a loading control. Representative images from at least three independent replicates.

**B)** Representative confocal images of the GV and MII oocytes labelled with FMRP antibodies in the absence or presence of arsenite. Scale bars 25  $\mu$ m; FMRP grey and red; DNA blue;  $n \geq 20$ .

**C)** Quantification of FMRP clusters in MII oocyte. Values obtained for the Cntr group were set as 1. Relative number of FMRP clusters; mean  $\pm$  SD; Student's *t*-test: ns for non-significant,  $n \geq 10$ .

<b>Official symbol (mRNA)</b>	<b>Accession No.</b>	<b>3'UTR target region</b>
<i>Gapdh</i>	NM_001289726.1	1095-1272
<i>Anln</i>	NM_001284301.3	3429-4620
<i>UCA1</i>	NR_015379.3	NA
<i>Actb</i>	NM_007393.5	1237-1920
<i>Dlg4</i>	NM_001109752.1	2481-3315
<i>Svv</i>	NM_009689.2	537-971

**Table S1:** Supplementary table of targets used for IntaRNA 2.0 *in silico* prediction.

Official symbol (Gene)	Forward 5´-3´	Reverse 5´-3´	Gene Bank ID	product size (bp)
<i>BC1</i>	GCTCAGTGGTAGAGCGCTTG	GGTTGTGTGCCAGTTACC	NR_038088.1	136
<i>Neat2</i>	AGGGAAAAGGGGAAAGC	AGGGGTGAAGGGTCTGTGAT	NR_002847.2	133
<i>Actb</i>	TCCTTCTTGGGTATGGAATCCT	GTCCTTACGGATGTCAACGTCAC	NM_007393.5	84
<i>Dlg4</i>	TCTCCTCCCTCAAGGCCAAT	TGGAACCCGCCCTTTGAG	NM_001109752	335
<i>Svv</i>	AGAACAAAATTGCAAAGGAGACCA	GGCATGTCACCTCAGGTCCAA	NM_009689.2	138
<i>Gapdh</i>	TGGAGAAACCTGCCAAGTATG	GGTCCTCAGTGTAGCCCAAG	NM_001289726.1	93
<i>18S</i>	CGCTCCACCAACTAAGAAGC	CTCAACACGGGAAACCTCAC	NR_003278	110
<i>28S</i>	CTAAATACCGGCACGAGACC	TTCACGCCCTCTTGAACCTCT	NR_003279	88

A

Official symbol (Protein)	Cat. No	Host animal	Manufacture	Size (kDa)
ACTB	BS-0061R	Rabbit	Bioss	42
DLG4 (PSD95)	51-6900	Rabbit	Invitrogen	100
SVV	cs2808P	Rabbit	Cell Signalling	16
FMRP	cs4317	Rabbit	Cell Signalling	80
eIF2	cs9722	Rabbit	Cell Signalling	38
p-eIF2	cs3398	Rabbit	Cell Signalling	38
TUBB	2128	Rabbit	Cell Signalling	55
RPL24	PA562450	Rabbit	ThermoFischer	24
Biotin	03-3700	Mouse	Invitrogen	0.2
p-LMN A/C	cs2026	Rabbit	Cell Signalling	69, 78
GAPDH	G9545	Rabbit	Sigma Aldrich	36

B

Official symbol (Gene)	Accession No.	Target region	No. of ZZ pairs	Channel	Cat. No.
<i>Actb</i>	NM_007393.5	2 - 406	6	C1	316741

C

**Table S2: Supplementary tables of primers, primary antibodies and RNA FISH probe.**

A) Primers designed for PCR and qRT-PCR.

B) Primary antibodies used in Immunoblotting, Immunocytochemistry, RNA-PLA.

C) Probe used in RNA FISH (RNAScope). Bacterial *DapB* RNA (*Bacillus subtilis*, str. SMY; EF191515.1) was used as a negative control.





## Oocyte specific lncRNA variant *Rose* influences oocyte and embryo development

Rajan Iyyappan<sup>a</sup>, Daria Aleshkina<sup>a</sup>, Linkai Zhu<sup>b</sup>, Zongliang Jiang<sup>b</sup>, Veronika Kinterova<sup>c</sup>, Andrej Susor<sup>a,\*</sup>

<sup>a</sup> Laboratory of Biochemistry and Molecular Biology of Germ Cells, Institute of Animal Physiology and Genetics of the Czech Academy of Sciences, Rumburska 89, 277 21, Libechev, Czech Republic

<sup>b</sup> School of Animal Sciences, AgCenter, Louisiana State University, Baton Rouge, LA, 70820, United States

<sup>c</sup> Laboratory of Developmental Biology, Institute of Animal Physiology and Genetics of the Czech Academy of Sciences, Rumburska 89, 277 21, Libechev, Czech Republic

### ARTICLE INFO

#### Keywords:

lncRNA  
Oocyte  
Early embryo  
Polysome  
Meiosis

### ABSTRACT

Fully grown mammalian oocytes store a large amount of RNA synthesized during the transcriptionally active growth stage. A large part of the stored RNA belongs to the long non-coding class which contain either transcriptional noise or important contributors to cellular physiology. Despite the expanding number of studies related to lncRNAs, their influence on oocyte physiology remains enigmatic. We found an oocyte specific anti-sense, long non-coding RNA, “*Rose*” (*lncRNA in Oocyte Specifically Expressed*) expressed in two variants containing two and three non-coding exons, respectively. *Rose* is localized in the nucleus of transcriptionally active oocyte and in embryo with polysomal occupancy in the cytoplasm. Experimental overexpression of *Rose* in fully grown oocyte did not show any differences in meiotic maturation. However, knocking down *Rose* resulted in abnormalities in oocyte cytokinesis and impaired preimplantation embryo development. In conclusion, we have identified an oocyte-specific maternal lncRNA that is essential for successful mammalian oocyte and embryo development.

### 1. Introduction

Long non-coding RNAs (lncRNAs) are stretches of RNA of at least 200 nucleotides which are not translated into protein. The vast majority of human and mouse transcriptome belongs to this noncoding class. Bre-schi et al., 2017 annotated 15,767 and 9989 lncRNAs in the human and the mouse [1]. Whilst the major part of all transcribed RNA belongs to ncRNA, they have not been well characterized so far. ncRNAs present in various tissues and cells are mostly alternatively spliced or processed into smaller RNA [2]. Recent evidence shows that lncRNAs are engaged in all aspects of cellular activity with lncRNAs predominantly playing specific roles inside the nucleus and regulating transcriptional and posttranscriptional processes [3,4], as well as epigenetics [2]. Moreover, accumulating evidence shows that lncRNAs form complexes with diverse structural and regulatory functions in the cytoplasm along with RNA binding proteins and mRNAs [5]. lncRNAs display different sub-cellular localization and possess distinct regulatory impacts at their particular site of action [6,7].

Although there have been studies into the functions of lncRNAs in

mammalian cells, their roles in germ cells are largely unknown. Recently there were just a few studies stating the importance of lncRNA in germ cells [8,9] and its evolutionary significance [10]. Fully grown mammalian oocytes store a large amount of RNA synthesized during the transcriptionally active growth stage, most of which belong to a non-coding class, contributing to cell physiology, and yet, also merely transcriptional noise.

In this study, we characterised mouse *lncRNA in Oocyte Specifically Expressed* (“*Rose*”) in the mouse oocyte and early embryo. We investigated the expression and localization of *Rose* at the various stages of oocyte and early embryo development. Moreover, we elucidated the function of *Rose* by gain- and loss-of-function approaches in order to study its contribution to cell physiology.

### 2. Materials and methods

#### 2.1. Oocyte isolation and cultivation

The females of 6-week-old ICR mice were stimulated with 5 IU

\* Corresponding author.

E-mail address: [susor@iapg.cas.cz](mailto:susor@iapg.cas.cz) (A. Susor).

<https://doi.org/10.1016/j.ncrna.2021.06.001>

Received 26 April 2021; Received in revised form 11 June 2021; Accepted 23 June 2021

Available online 26 June 2021

2468-0540/© 2021 The Authors. Publishing services by Elsevier B.V. on behalf of KeAi Communications Co. Ltd. This is an open access article under the CC BY

license (<http://creativecommons.org/licenses/by/4.0/>).

pregnant mare serum gonadotropin (PMSG; Folligon; Merck Animal Health) per mouse. After 46 h, the oocytes were isolated from the ovaries. Fully grown germinal vesicle (GV) oocytes were isolated into transfer medium (TM) supplemented with 100  $\mu$ M 3-isobutyl-1-methyl-xanthine (IBMX; Sigma Aldrich) for the prevention of spontaneous meiotic resumption. Selected oocytes were denuded and cultivated in M16 medium (Millipore) without IBMX at 37 °C, 5% CO<sub>2</sub> for 0 h (GV) or 16 h during second metaphase arrest (MII). For embryo collection, the stimulated mice were again injected with 5 IU hCG before being mated overnight with males of the same strain. After 16 h, zygotes were recovered from the excised oviducts and cultured in EmbryoMax Advanced KSOM Embryo Medium (Sigma-Aldrich).

All animal experiments were performed in accordance to guidelines and protocols approved by the Laboratory of Biochemistry and Molecular Biology of Germ Cells at the Institute of Animal Physiology and Genetics in Czech Republic. All animal work was conducted according to Act No. 246/1992 on the protection of animals against cruelty, issued by experimental project #215/2011, certificate #CZ02389, issued by the Ministry of Agriculture.

## 2.2. PCR and RT-PCR

RNA was extracted using TRI reagent (Sigma). The equal amount of RNA was used for cDNA synthesis using both hexamers and oligo-d(T) primers (qPCR BIO cDNA Synthesis Kit, PCR Biosystems). For PCR (PPP master mix, TOP-Bio) the following program was used: 94 °C 5 min; 94 °C 15 s; 58–60 °C 15 s; 72 °C and then the products were separated on 0.8% agarose gel with GelRed (41003, Biotinum) staining. RT-PCR (Luna Universal qPCR Master Mix, New England BioLabs) was carried out using QuantStudio3. qPCR data were normalized to GAPDH expression by the  $\Delta\Delta$ Ct approach. Primers are listed in [Supplementary Table 1](#). RNA extraction, PCR and RT-PCR were all performed according to the manufacturer's instructions.

## 2.3. RNA FISH

RNA FISH was performed following Tetkova et al. [11]. Briefly: oocytes were fixed (15 min in 4% PFA) and pre-treated with protease III (diluted 1:15 in nuclease-free water; Cat. No. 322381, ACD) for 10 min. Each sample was then incubated with corresponding RNAScope probes ([Supplementary Table 1](#)) at 2 h in 40 °C to detect *Rose*. RNA FISH protocol for amplification was followed using RNAScope Multiplex Fluorescent Detection Reagents v2 kit (Cat. No. 323110, ACD), with extended washing. After amplification, HRP-C1/C2/C3 was used on the corresponding channels of specific probe, for 15 min, 40 °C. Oocytes were washed again 2.5 min in 1x wash buffer. TSA Cy5 dye (Perkin-Elmer) diluted to 1:1500 in TSA buffer (ACD) was used for fluorescent labelling of the amplified signal. After washing and application of HRP blocker (30 min in 40 °C), samples were washed a final time 2  $\times$  5 min in 1x wash buffer and mounted in Prolong Gold Antifade with DAPI (Life Technologies) on epoxy coated slides (Thermo Scientific). Images were obtained using a confocal microscope (Leica SP5). Image quantification of single equatorial Z was performed by ImageJ software (<http://rsbweb.nih.gov/ij/>). Images were converted to the binary type and threshold range was set to distinguish fluorescent RNA signals from the background. Quantification was performed via standard 'Analyze particles' tool. Bacterial *DapB* RNA (*Bacillus subtilis*, str. SMY; EF191515.1) was used as a negative control.

## 2.4. Polysome fractionation

Polysome fractionation followed by RNA isolation was carried out according to the Scarce Sample Polysome profiling (SSP-profiling) method by Masek et al. [12]. Briefly, at the time of oocyte collection, 200 oocyte/embryos were treated with 100  $\mu$ g/mL cycloheximide for 10 min and collected in 350  $\mu$ L lysis buffer (10 mM Hepes, pH 7.5; 62.5

mM KCl, 5 mM MgCl<sub>2</sub>, 2 mM DTT, 1% TritonX-100) containing 100  $\mu$ g/mL CHX and 20 U/ml Ribolock (Thermo Fisher Scientific). After disruption of the zona pellucida with 250  $\mu$ L of zirconia-silica beads (BioSpec), lysates were centrifuged at 8000 g for 5 min at 4 °C. Supernatants were loaded onto 10–50% sucrose gradients. Centrifugation was performed at 45,000 RPM (246,078 $\times$ g) for 65 min at 4 °C (Optima L-90 ultracentrifuge, Beckman Coulter). Ten equal fractions were collected from each polysome profile and subjected to RNA isolation. These RNA and its profile were validated using the primer for 18s and 28s rRNA by qPCR [12]. Then, non-polysomal (NP; fractions 1–5) and polysomal fractions (P; fractions 6–10) were pooled and subjected to qRT-PCR (QuantStudio 3 cyclor, Applied Biosystems) using *Rose* NCE1 specific primers.

## 2.5. Immunocytochemistry

Oocytes were fixed (15 min in 4% PFA; Sigma Aldrich), permeabilized (10 min in 0.1% Triton X-100) and washed in PBS supplemented with polyvinyl alcohol (PVA, Sigma Aldrich) and incubated with anti-acetylated  $\alpha$ -tubulin (T7451, Sigma Aldrich) diluted in PVA/PBS, overnight at 4 °C. Oocytes were then washed 2  $\times$  15 min in PVA/PBS and primary antibodies were detected using relevant Alexa Fluor 488/594/647 conjugates (Invitrogen) diluted to 1:250 for 1 h at room temperature. Washed oocytes (2  $\times$  15 min in PVA/PBS) were mounted onto slides using Vectashield with DAPI. An inverted confocal microscope (Leica SP5) was used for sample visualization. Morphology of the spindles (anti-acetylated  $\alpha$ -tubulin) and chromosomes (DAPI) were defined by spindle morphology and chromosomal alignment. Spindles were analysed as maximum intensity projection Z-stack images using LAS X (Leica) software. Experiments were repeated 3x with 20–30 oocytes per group/experiment.

## 2.6. In vitro transcription, microinjection and live-cell imaging

*H2b:gfp* RNA from plasmid (provided by Dr Martin Anger, Laboratory of Cell Division Control, IAPG CAS) and *Rose* cRNA for overexpression was prepared using T7 mMessage, Ambion kit. The dsRNA against *Rose* was prepared using a MEGAscript RNAi Kit. These dsRNA were digested by ShortCut<sup>R</sup> RNase III (New England Biolabs) for making small and efficient dsRNA [13]. As a negative control, we used MISSION<sup>®</sup> esiRNA (control) targeting Renilla luciferase (RLUC, Sigma Aldrich).

Isolated fully grown oocytes/Zygotes were microinjected in TM with/without IBMX using a Leica DMI 6000B inverted microscope, TransferMan NK2 (Eppendorf) and FemtoJet (Eppendorf). Solution used for oocyte/embryo injection contained: 20 ng/ $\mu$ L of *in vitro* transcribed *H2b:gfp* RNA in combination with 100 ng/ $\mu$ L (overexpression) or 1000 ng/ $\mu$ L esiRenilla (dsRenilla) or dsRose. 24 h after microinjection, oocytes were washed from IBMX and cultivated to MII stage. In case of zygotes, after 4 h of microinjection, the embryos were transferred into KSOM (Sigma-Aldrich, Merck) media for further development. Microinjected oocytes were placed into a 4-well culture chamber (Sarstedt) in 10  $\mu$ L of equilibrated M16 media (37.5 °C, 5% CO<sub>2</sub>) covered with mineral oil (M8410; Sigma Aldrich). The cells were imaged using a Leica DMI 6000B inverted microscope equipped with a controlled chamber system (Temp controller 2000–2 Pecon, and a CO<sub>2</sub> controller, Pecon). Time lapse recordings (LAS X, Leica microsystems) of meiotic maturation of microinjected oocytes were used for phenotype evaluation (nuclear envelope breakdown, polar body extrusion).

## 2.7. In silico prediction

RNA-RNA interactions were predicted by using the IntaRNA tool with default settings (<http://rna.informatik.uni-freiburg.de/IntaRNA/Input.jsp>) [14]. Results are presented in [Supplementary Table 3](#). Non-coding potential analysis was predicted using the Coding Potential

Assessment Tool (CPAT) (<http://lilab.research.bcm.edu/cpat/>) [15].

## 2.8. Statistical analysis

Experiments were repeated at least 3 times unless stated. Mean and SD values were calculated using MS Excel, statistical significance of the differences between the groups was tested using Student's t-test and we applied one way ANOVA for comparisons of more than two groups then Tukey's multiple comparisons test as a post-hoc test (PrismaGraph5).  $p < 0.05$  was considered as statistically significant.

## 3. Results

### 3.1. *Rose* lncRNA variant expressed only in the mouse oocyte and early embryo

The gene coding for *Gm32743* is located on chromosome 9 and is transcribed as linear, antisense RNA 1611 nucleotides (nt) in length (Fig. 1A). According to the mouse ENCODE database, *Gm32743* lncRNAs present in almost all mouse tissues and is highly expressed in the heart and brain (Supplementary Fig. 1). *Gm32743* contains three non-coding exons: NCE1 (312 nt), NCE2 (112 nt), and NCE3 (170 nt) (Fig. 1A and Supplementary Figs. 2A–C). We found that only the oocyte and embryo expresses two variants of *Rose* lncRNA (Fig. 1A and B) which contains exons NCE1-3 (variant 1) and exons NCE1&3 (variant 2) (Fig. 1A and Supplementary Figs. 2A and B), respectively. Interestingly, our semi quantitative and qPCR data shows that neither variants of *Rose* are found in other mouse tissues (Fig. 1B and C). However, upstream NCEs exist only in other tissues whereas downstream NCEs have been found in all analysed tissues, including oocytes (Fig. 1B). Alignment of *Gm32743* showed no significant similarity with other organism. Next, we analysed

the expression of both *Rose* lncRNA variants using primers specific to NCE1 in the fully grown GV, matured MII oocyte and 1- & 2-cell embryo. We found that *Rose* has the highest expression in the GV oocyte with a significant decrease in the 2-cell embryo (Figs. 1D and 2A and B). In order to exclude possibility of genomic DNA contamination in the samples, as a control, *Dazl* exon 3 and 4 specific primers were used to amplify the expected PCR product (Supplementary Fig. 3).

In conclusion, we found that *Gm32743* is spliced and its variant exclusively expressed in the mouse oocyte and early embryo generating *Rose* lncRNA.

### 3.2. Cytoplasmic localised *Rose* is present in the polysomal fraction in oocyte and early embryo

As it might predict the RNA's role in the cell [16], we examined the localization of *Rose* in the oocyte and early embryo. Using RNA FISH approach, we found that the transcriptionally active growing oocyte (growing GV; gGV) and 2-cell embryo have *Rose* lncRNA distributed in both the nucleus and the cytoplasm (Fig. 2A and B). Contrastingly, *Rose* was not present in the nucleus of the transcriptionally inactive fully grown GV oocyte and Zygote (Fig. 2A and Supplementary Fig. 4A). Similar to the qRT PCR analysis, RNA FISH showed a significant decrease of *Rose* in the matured MII oocyte, zygote and 2-cell embryo (Figs. 1D and 2A and B). As a negative control for RNA FISH we used a probe specific for bacterial RNA *Dab8* and it was not detected in oocytes and early embryos (Supplementary Fig. 4B). Previously we detected ncRNA in the cytoplasm and polysomal fractions [17] so we asked if *Rose* is present in non-polysomal (NP) and polysomal (P) fractions from fully grown GV, MII oocytes and 2-cell embryos. Interestingly, we found that *Rose* was enriched in the polysomal fraction which was confirmed by qRT PCR (Fig. 2C). *Rose* is annotated as lncRNA, however we detected

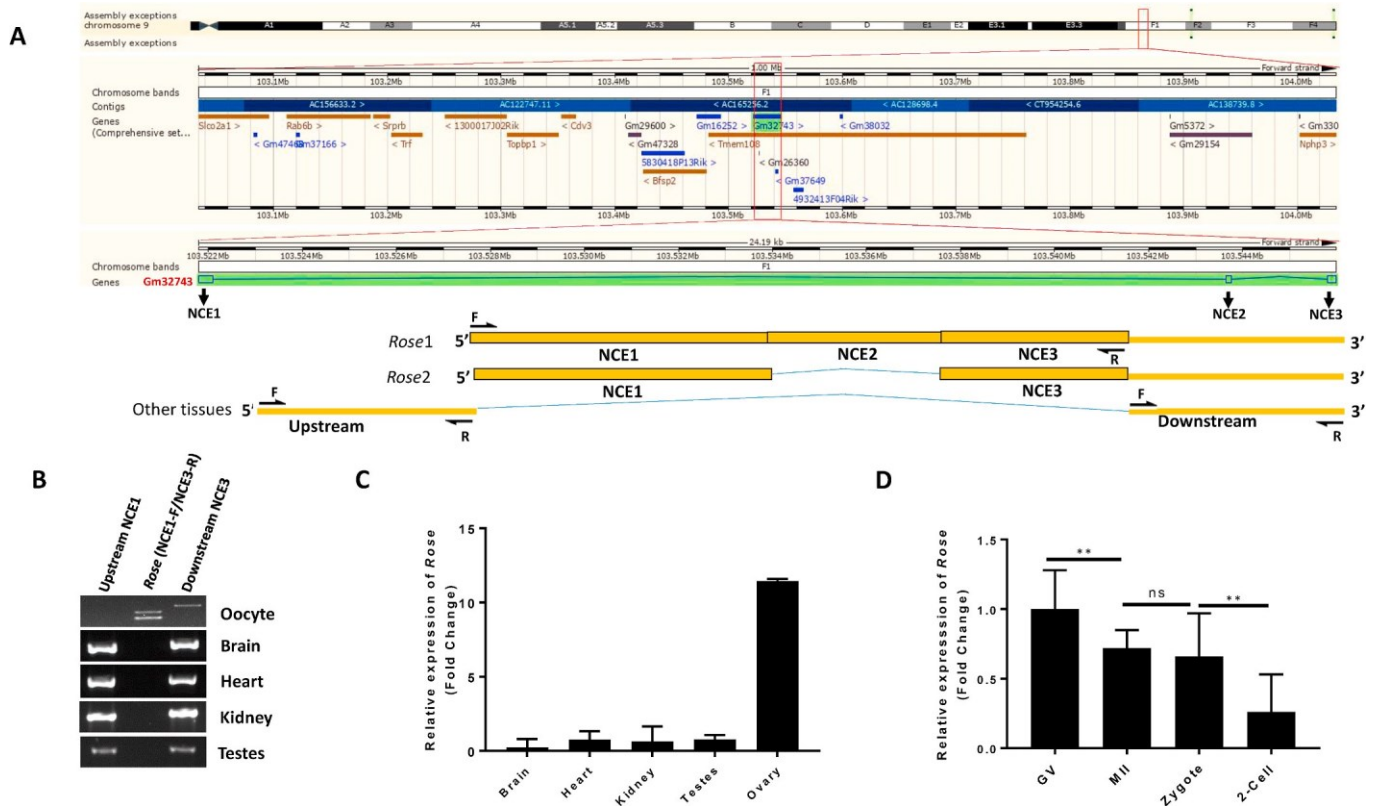


**Fig. 1.** *Rose* lncRNA variant expressed only in the mouse oocyte and early embryo. (A) Scheme of genome organisation of *Gm32743* from Ensembl browser. Also see Supplementary Fig. 1. (B) PCR detection of *Rose* lncRNA in oocyte and mouse tissues. Also see Supplementary Fig. 2. (C) qRT-PCR detection of *Rose* expression in various mouse tissues. Also see Supplementary Fig. 4A. (D) Expression of *Rose* lncRNA in GV, MII, zygote and 2-cell stage embryo. Mean  $\pm$  SD; One-way ANOVA:  $F(2, 3) = 66.07$ ,  $p < 0.01$ . Tukey's multiple comparisons test: \*\* $p < 0.01$ , ns - non-significant;  $n = 2$ . Also see Supplementary Fig. 4A.

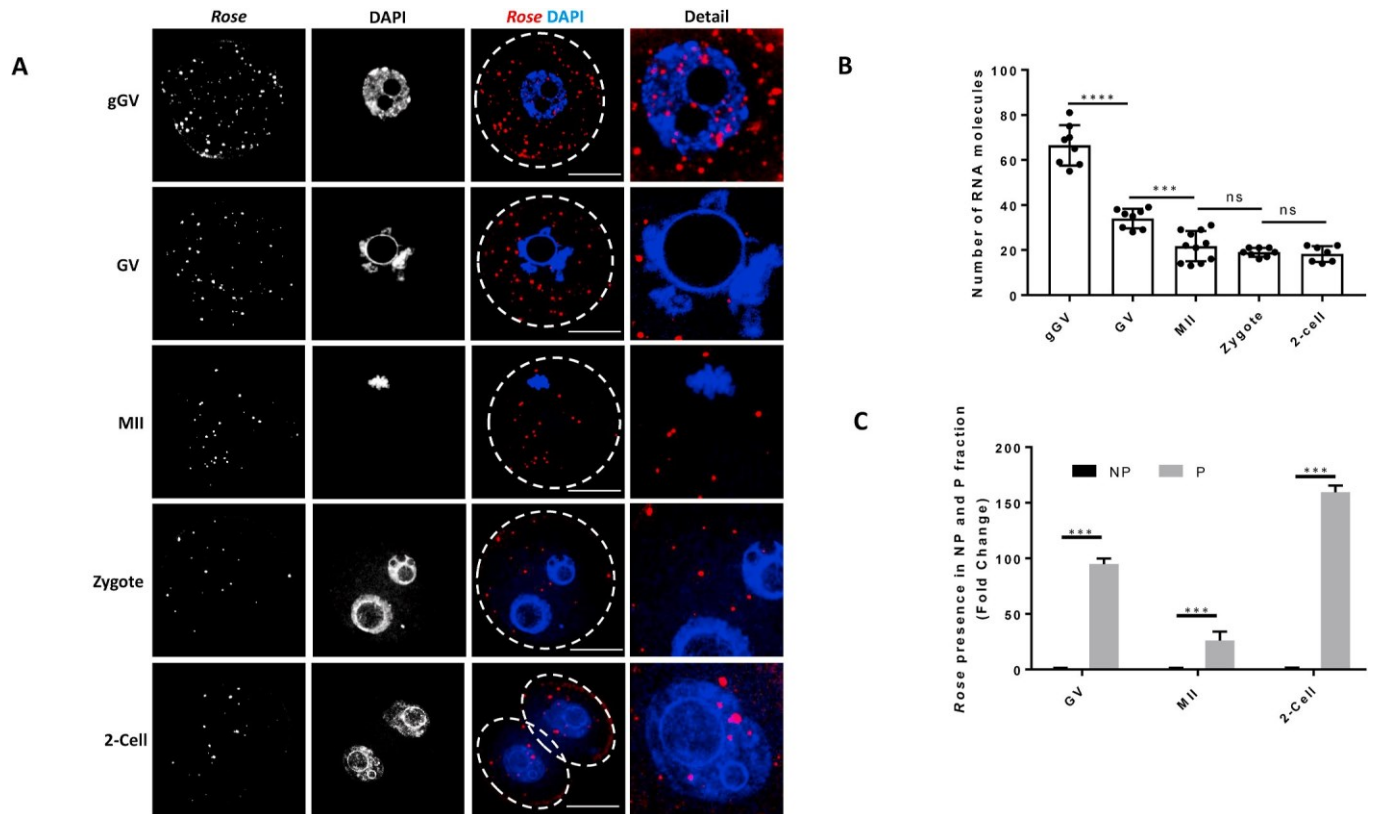


**Fig. 2.** Cytoplasmic localized *Rose* is present in the polysomal fraction in oocyte and early embryo. (A) Localization of *Rose* IncRNA detected by RNA FISH in growing and fully grown oocytes and early embryo. Combination of single equatorial optical section for *Rose IncRNA* and maximum intensity projections for DAPI. Representative images from three biological experiments. Scale bar = 25  $\mu$ m *Dab8* RNA was used as a negative control [Supplementary Fig. A and B](#). (B) Quantification of *Rose* IncRNA molecules in one Z section from RNA FISH. Mean  $\pm$  SD; One-way ANOVA:  $F(4, 37) = 99.15$ ,  $p < 0.0001$ . Tukey's multiple comparisons test: \*\*\*\* $p < 0.0001$ , \*\* $p < 0.01$ , ns - non-significant; from three biological replicates,  $n \geq 8$ . (C) qRT-PCR detection of *Rose* in the non-polyribosomal (NP) and polyribosomal (P) fractions in the oocyte and early embryo. Mean  $\pm$  SD; Student's t-test: \*\*\* $p < 0.001$ ;  $n = 3$ .

its polysomal occupancy. Thus we asked if *Rose* has coding potential. Analysis by the Coding Potential Assessment Tool (CPAT) produced a negative hexamer score ( $-0.187956336$ ; [Supplementary Table 2](#)), confirming the non-coding nature of *Rose*. As a positive control, *Xist* IncRNA and *Cyclin B1* mRNA were analysed with known noncoding *Xist* [18] and protein coding *Cenbl* [10] ([Supplementary Table 2](#)). Moreover *in silico* RNA-RNA interaction prediction analysis shows the positive interaction of *Rose* with noncoding and protein coding RNAs ([Supplementary Table 3](#)).

Here, we found that *Rose* is present in the nucleus of transcriptionally active growing oocytes and early embryos. Furthermore, despite *Rose* having no translational potential we detected it in the polysomal fraction.

### 3.3. Downregulation of *Rose* leads to aberrant meiotic progression and early embryo development

To further investigate the role of *Rose* in the oocyte and early embryo physiology, we performed overexpression of *Rose* by microinjection into the GV oocyte ([Supplementary Fig. 5A](#)) leading to its significant increase ([Supplementary Fig. 5B](#)). Following time lapse observation, no abnormalities were found in the oocyte meiotic progression ([Supplementary Figs. 5C and D](#)). Next, we performed knockdown (KD) of *Rose* in the GV oocyte ([Fig. 3A and B](#)). Here meiotic progression was quantified based on polar body extrusion. Time lapse imaging shows that 88.6% of the oocytes exhibited significant abnormal meiotic progression in response to *Rose* downregulation, which is 60.7% higher than the *dsRenilla* injected control (27.95%) ([Fig. 3C–E](#)). Oocytes in both groups underwent nuclear envelope breakdown normally, however in presence of

*dsRose* majority of oocytes failed to extrude a polar body which led to abnormal MI (red arrow head), abnormal polar body extrusion and symmetrical division ([Fig. 3D and E](#)). Moreover 64.7% of oocytes with extruded polar body showed irregularities in spindle and chromosome organisation ([Fig. 3E](#)). Finally, we investigated whether downregulation of *Rose* influences embryo development by *Rose* KD in the zygote ([Fig. 4A and B](#)). We found no significant differences in the progression to the 2-cell stage in either group ([Supplementary Fig. 6](#)) however the blastocyst rate was significantly lower (44.21%) in the *Rose* down-regulated group compared to control ([Fig. 4C and D](#)). In addition to this, we observed that embryos were arrested at the 2–8 cell stage ([Fig. 4C](#)).

In conclusion, we found that maternal *Rose* IncRNA has a significant role in the meiotic progression of the oocyte as well as in embryo development.

## 4. Discussion

Emerging RNA-seq technology and transcriptome analyses have uncovered a growing number of lncRNAs and their regulation over protein-coding in various cells and animal species. However, functional analysis of lncRNAs is still challenging, and so far the molecular role has only been explored for a small subset of lncRNAs. Majority of lncRNAs are just transcriptional noise only some contributing to cellular physiology. Annotation of mouse maternal lncRNAs has revealed a number of lncRNAs, but their roles still remain enigmatic.

The oocyte signature includes functionally recognized oocyte-specific mRNAs such as *Oogl* [19], *Dazl* [20], *ZPI-3* [21], *Figla* [22], and *Gdf-9* [23]. However, oocyte-specific lncRNAs are not well known and have no recognized role in the oocyte. We discovered *Rose* (*lncRNA*)



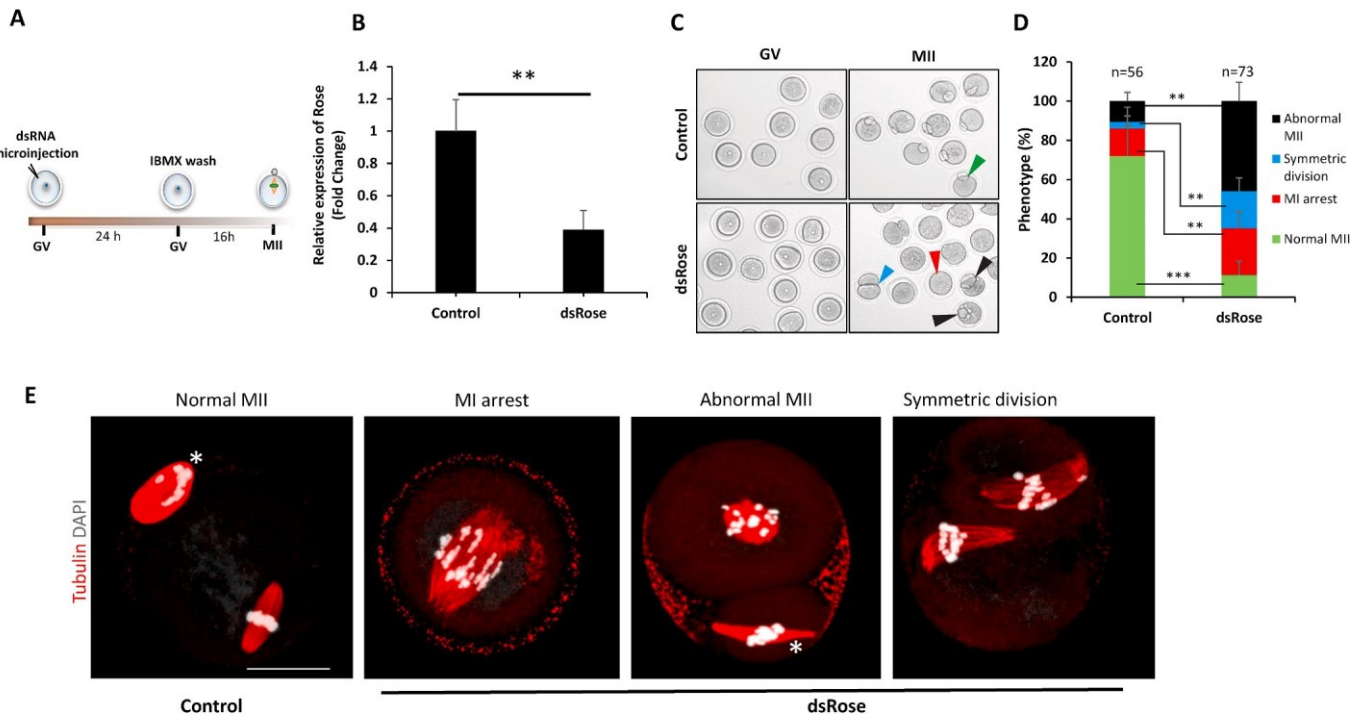


**Fig. 3.** Downregulation of *Rose* leads to aberrant meiotic progression. **(A)** Scheme of experimental approach for *Rose* downregulation in the oocyte. **(B)** qRT-PCR detection of knock down of *Rose* using dsRNA. Mean  $\pm$  SD; Student's t-test:  $^{**}p < 0.01$ ;  $n = 3$ . **(C)** Phenotype analysis of progression of GV oocytes to MII stage after downregulation of *Rose* lncRNA. Arrowheads (except green) depict aberrant meiotic progression. **(D)** Quantification of oocyte progression from GV to MII stage after downregulation of *Rose* lncRNA. Mean  $\pm$  SD; Student's t-test:  $^{****}p < 0.0001$ ,  $^{**}p < 0.01$ ; from three biological replicates with presented  $n$ . *dsRenilla* was used as a control. **(E)** Representative oocyte morphologies of oocytes microinjected with *dsRenilla* (control) and *dsRose*. Tubulin red and chromosomes labeled by DAPI (Gray); scale bar 10  $\mu$ m; asterisk depicts polar body. (For interpretation of the references to colour in this figure legend, the reader is referred to the Web version of this article.)

*in Oocyte Specifically Expressed*), a maternal lncRNA uniquely transcribed and processed in the mouse female germ cell. lncRNAs are poorly conserved compared to protein coding RNAs and most are expressed specifically in particular cells/species [24]. Similarly, *Rose* lncRNA did not share any detectable similarity with lncRNAs in other species, suggesting that *Rose* appeared after mouse split from its ancestor.

Interestingly, in transcriptionally silent fully grown oocyte, *Rose* is localized only in the cytoplasm, however, in transcriptionally active growing oocyte and 2-cell embryo, *Rose* exhibits in both nucleus and cytoplasm. For many lncRNAs subcellular location is directly linked to their function [7,25] and the nucleus and cytoplasm are well defined barriers for gene expression such redistribution of *Rose* is suggesting cell stage specific regulatory mechanisms. Nuclear localization of *Rose* in relation with transcriptional activity might contribute to transcription associated processes, epigenetic regulation and/or RNA transport. Detected *Rose* molecules in the nucleus do not constitute transcriptional hotspots which represent one or two large spots in the chromatin [26].

Moreover, previously was shown that lncRNA can regulate target genes on both epigenetic and translational levels [27,28]. This regulations often involve significant degree of complementarity between lncRNA and mRNAs which can link role of *Rose* with metabolism of target mRNAs leading to observed polysomal association and impact on translational regulation.

The specific spatio-temporal expression and localization can be linked to the establishment of both transcriptional and post transcriptional processes which might connect *Rose* with polysomal occupation or ribosomal protein maturation [29]. Similarly, *BCI* ncRNA was detected in the polysomal fraction from GV oocytes. *BCI* ncRNA is an example where the Fragile X Mental Retardation Protein (FMRP) is a co-player of ncRNA to promote translational repression in the cell [17]. Moreover, lncRNAs can physically interact with ribosomes or via recruitment of specific transcripts to the ribosome machinery [30]. Such

a versatile nature of lncRNAs, as evidenced in recent studies, is in close corroboration with *Rose*. We presume that the localization in the transcriptionally active nucleus combined with RNA-RNA interaction and polysomal presence indicate multi-mode action of *Rose* in RNA fate in the development of oocyte and early embryo.

Aberrant meiotic spindle in *Rose* downregulation, the one might predict the aberrancies in embryo cleavage. However, there was no arrest or malfunction in the cleavage from one-cell embryo to a two-cell embryo. Conversely, absence of *Rose* leads to detrimental effect on embryonic development post 2-cell stage. In addition, we discovered that the *Rose* is localized in the nucleus of the two-cell stage indicating role in the nucleoplasm of transcriptionally active cell. In conclusion *Rose* has possible different functions in oocyte maturation and early embryo development. Based on the observed phenotypes and oocyte-zygote expression, we hypothesize that *Rose* has a specific role in the female germ cell and consequently in the early embryo development. Diverse molecular and biological roles have been assigned to lncRNAs, although most of them probably did not acquire a detectable biological role under laboratory conditions e.g. *Neat2*, *Sirenal* [10,31]. Moreover, we found that maternal effect *Rose* lncRNA has an essential role in the achievement of meiotic and zygotic developmental competence.

Overall, *Rose* lncRNA has an important regulatory role in oocyte cytokinesis and the post maternal-to-zygotic transition in early embryo development. However, further study is required to explore the specific role of the *Rose* lncRNA in the development of the mouse oocyte and embryo.

#### Ethical approval

All animal work was conducted according to Act No 246/1992 for the protection of animals against cruelty; from 25.09.2014 number CZ02389, issued by the Ministry of Agriculture.

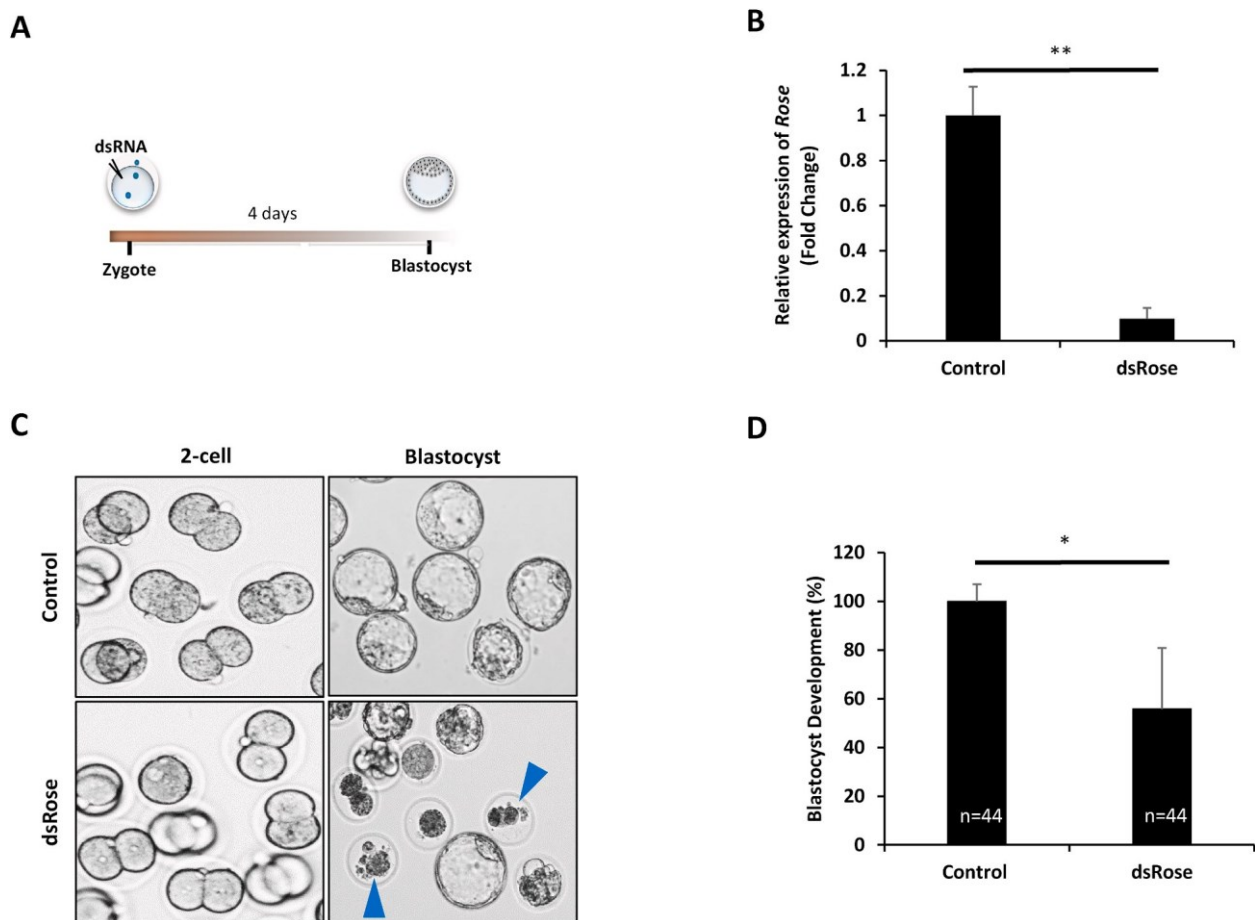


**Fig. 4.** Downregulation of *Rose* affects early embryo development. **(A)** Scheme of experimental approach for *Rose* downregulation in the embryo. **(B)** Knock down of *Rose* using dsRNA. qRT-PCR result of 2-cell embryos of control and dsRNA injected zygotes. Mean  $\pm$  SD; Student's t-test: \*\* $p < 0.01$ ;  $n = 3$ . **(C)** Phenotype analysis of progression of blastocyst stage after downregulation of *Rose* lncRNA. Arrowheads depict fragmented embryos after 2-cell stage. **(D)** Quantification of blastocyst development after downregulation of *Rose* lncRNA. Mean  $\pm$  SD; Student's t-test: \* $p < 0.05$ ; from three biological replicates with presented  $n$ .

## Funding

This research was funded by GACR18-19395S and Institutional Research Concept RVO67985904. Z.J. was supported by the funds from the NIH (R01HD102533) and USDA-NIFA (2019-67016-29863). The funders had no role in study design, data collection and analysis, decision to publish, or preparation of the manuscript.

## CRediT author statement

R.I. designed the experiments, carried out the data analysis and planned the project. carried out most of the experiments. wrote the manuscript. A.S. wrote the manuscript. designed the experiments, carried out the data analysis and planned the project; D.A. performed and analysed RNA FISH; L.Z. performed polysomal data analysis. Z.J. performed polysomal data analysis; V.K. designed and prepared dsRNA. All authors edited the manuscript.

## Declaration of competing interest

The authors have declared that no competing interests exist.

## Acknowledgements

We thank to Edgar Del Llano, Michal Dvoran, Jaroslava Supolikova and Marketa Hancova for their valuable assistance with experiments.

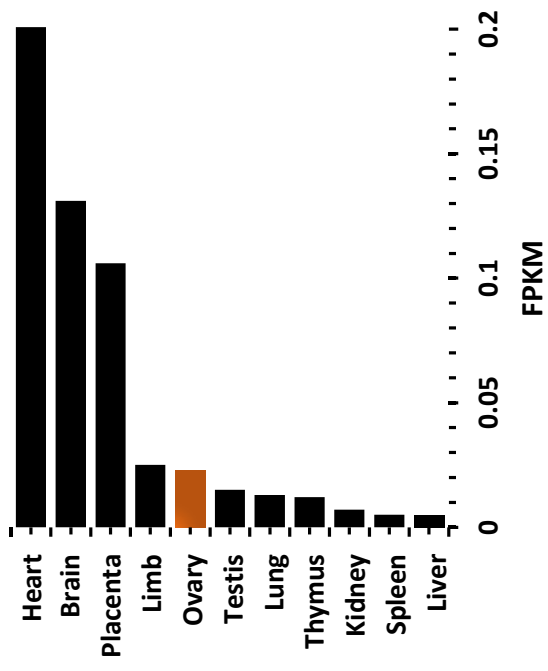
## Appendix A. Supplementary data

Supplementary data to this article can be found online at <https://doi.org/10.1016/j.ncrna.2021.06.001>.

## References

- [1] A. Breschi, T.R. Gingeras, R. Guigó, Comparative transcriptomics in human and mouse, *Nat. Rev. Genet.* 18 (2017) 425–440, <https://doi.org/10.1038/nrg.2017.19>.
- [2] J.S. Mattick, I.V. Makunin, Non-coding RNA, *Hum. Mol. Genet.* 15 (2006) R17–R29, <https://doi.org/10.1093/hmg/ddl046>.
- [3] X. Zhang, W. Wang, W. Zhu, J. Dong, Y. Cheng, Z. Yin, F. Shen, Mechanisms and functions of long non-coding RNAs at multiple regulatory levels, *Int. J. Mol. Sci.* 20 (2019) 5573, <https://doi.org/10.3390/ijms20225573>.
- [4] R.Z. He, D.X. Luo, Y.Y. Mo, Emerging roles of lncRNAs in the post-transcriptional regulation in cancer, *Genes Dis* 6 (2019) 6–15, <https://doi.org/10.1016/j.gendis.2019.01.003>.
- [5] C. Charon, A.B. Moreno, F. Bardou, M. Crespi, Non-protein-coding RNAs and their interacting RNA-binding proteins in the plant cell nucleus, *Mol. Plant* 3 (2010) 729–739, <https://doi.org/10.1093/mp/ssq037>.
- [6] I. Ulitsky, D.P. Bartel, XlincRNAs: genomics, evolution, and mechanisms, *Cell* 154 (2013) 26–46, <https://doi.org/10.1016/j.cell.2013.06.020>.
- [7] L.L. Chen, Linking long noncoding RNA localization and function, *Trends Biochem. Sci.* 41 (2016) 761–772, <https://doi.org/10.1016/j.tibs.2016.07.003>.
- [8] M. Joshi, S. Rajender, Long non-coding RNAs (lncRNAs) in spermatogenesis and male infertility, *Reprod. Biol. Endocrinol.* 18 (2020) 1–18, <https://doi.org/10.1186/s12958-020-00660-6>.
- [9] T.L. Lee, A. Xiao, O.M. Rennert, Identification of novel long noncoding RNA transcripts in male germ cells, *Methods Mol. Biol.* 825 (2012) 105–114, [https://doi.org/10.1007/978-1-61779-436-0\\_9](https://doi.org/10.1007/978-1-61779-436-0_9).
- [10] S. Ganesh, F. Horvat, D. Drutovic, M. Efenberkova, D. Pinkas, A. Jindrova, J. Pasulka, R. Iyyappan, R. Malik, A. Susor, K. Vlahovicek, P. Solc, P. Svoboda, The

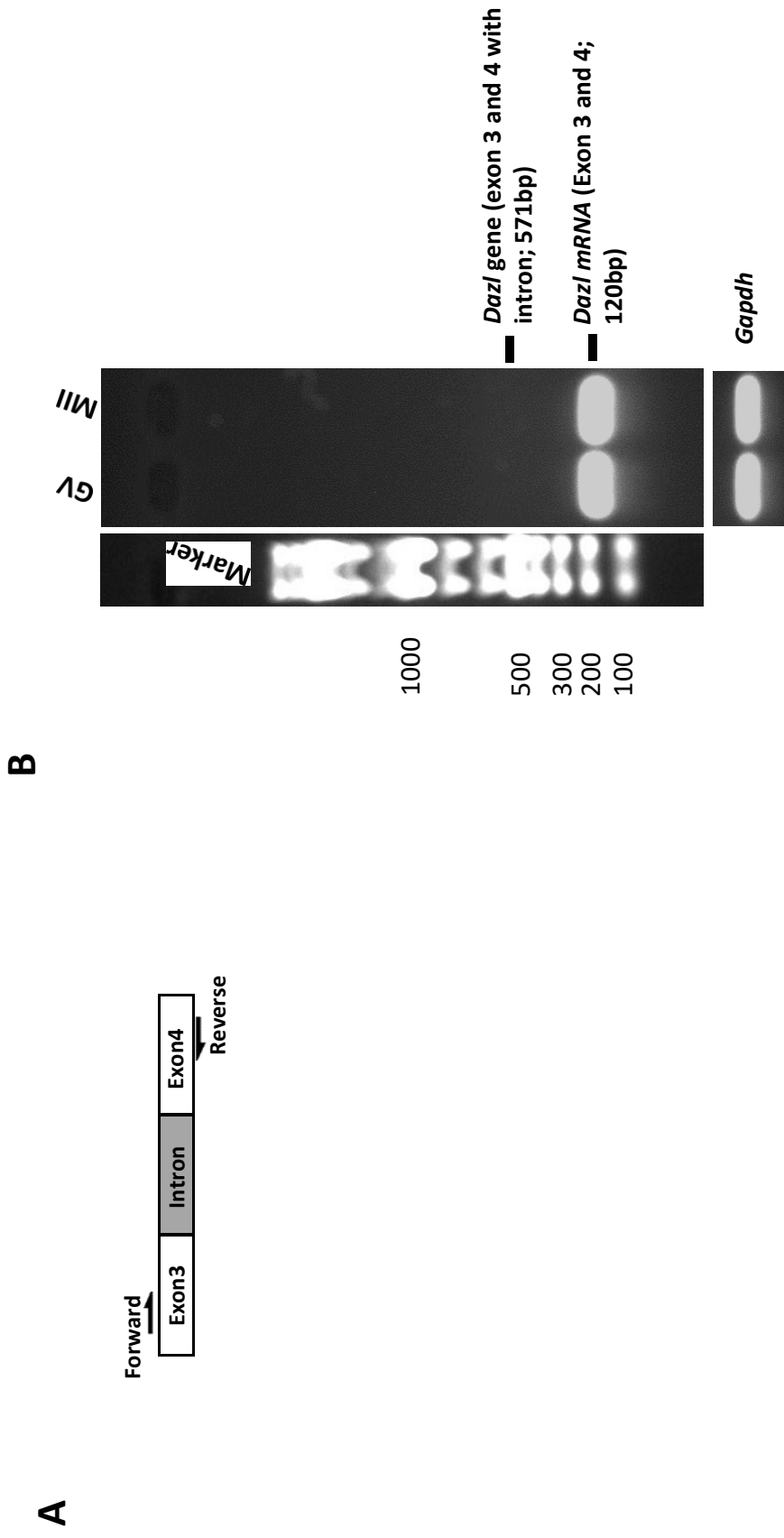
- most abundant maternal lncRNA Sirena1 acts post-transcriptionally and impacts mitochondrial distribution, *Nucleic Acids Res.* 48 (2020) 3211–3227, <https://doi.org/10.1093/nar/gkz1239>.
- [11] A. Tetskova, D. Jansova, A. Susor, Spatio-temporal expression of ANK2 promotes cytokinesis in oocytes, *Sci. Rep.* 9 (2019) 1–13, <https://doi.org/10.1038/s41598-019-49483-5>.
- [12] T. Masek, E. del Llano, L. Gahurova, M. Kubelka, A. Susor, K. Roucova, C.-J. Lin, A. W. Bruce, M. Pospisek, Identifying the translome of mouse NEBD-stage oocytes via SSP-profiling: A novel polysome fractionation method, *Int. J. Mol. Sci.* 21 (2020) 1254, <https://doi.org/10.3390/ijms21041254>.
- [13] A.-K. Heninger, F. Buchholz, Production of endoribonuclease-prepared short interfering RNAs (esiRNAs) for specific and effective gene silencing in mammalian cells, *Cold Spring Harb. Protoc.* (2007), <https://doi.org/10.1101/pdb.prot4824>.
- [14] M. Mann, P.R. Wright, R. Backofen, IntaRNA 2.0: enhanced and customizable prediction of RNA-RNA interactions, *Nucleic Acids Res.* 45 (2017) 435–439, <https://doi.org/10.1093/nar/gkx279>.
- [15] L. Wang, H.J. Park, S. Dasari, S. Wang, J.P. Kocher, W. Li, CPAT: coding-potential assessment tool using an alignment-free logistic regression model, *Nucleic Acids Res.* (2013), <https://doi.org/10.1093/nar/gkt006>.
- [16] E. Lecuyer, H. Yoshida, N. Parthasarathy, C. Alm, T. Babak, P. Tomancak, H. Krause, Global analysis of mRNA localization reveals a prominent role in the organization of cellular architecture and function, *Dev. Biol.* 131 (2008) 174–187, <https://doi.org/10.1016/j.ydbio.2008.05.012>.
- [17] D. Aleshkina, R. Iyyappan, C.J. Lin, T. Masek, M. Pospisek, A. Susor, ncRNA BC1 influences translation in the oocyte, *RNA Biol.* (2021), <https://doi.org/10.1080/15476286.2021.1880181>.
- [18] G. Pintacuda, A.N. Young, A. Cerase, Function by structure: spotlights on xist long non-coding RNA, *Front. Mol. Biosci.* 4 (2017) 90, <https://doi.org/10.3389/fmolb.2017.00090>.
- [19] S. Honda, Y. Miki, Y. Miyamoto, Y. Kawahara, S. Tsukamoto, H. Imai, N. Minami, Oocyte-specific gene Oog1 suppresses the expression of spermatogenesis-specific genes in oocytes, *J. Reprod. Dev.* 64 (2018) 297–301, <https://doi.org/10.1262/jrd.2018-024>.
- [20] D. Jansova, A. Tetskova, M. Koncicka, M. Kubelka, A. Susor, Localization of RNA and translation in the mammalian oocyte and embryo, *PLoS One* 13 (2018), e0192544, <https://doi.org/10.1371/journal.pone.0192544>.
- [21] C.C. Philpott, M.J. Ringuette, J. Dean, Oocyte-specific expression and developmental regulation of ZP3, the sperm receptor of the mouse zona pellucida, *Dev. Biol.* 121 (1987) 568–575, [https://doi.org/10.1016/0012-1606\(87\)90192-8](https://doi.org/10.1016/0012-1606(87)90192-8).
- [22] L.F. Liang, S.M. Soyak, J. Dean, FIG $\alpha$ , a germ cell specific transcription factor involved in the coordinate expression of the zona pellucida genes, *Development* 124 (1997) 4939–4947.
- [23] S.A. McGrath, A.F. Esquela, S.J. Lee, Oocyte-specific expression of growth/differentiation factor-9, *Mol. Endocrinol.* 9 (1995) 131–136, <https://doi.org/10.1210/mend.9.1.7760846>.
- [24] S. Washietl, M. Kellis, M. Garber, Evolutionary dynamics and tissue specificity of human long noncoding RNAs in six mammals, *Genome Res.* 24 (2014) 616–628, <https://doi.org/10.1101/gr.165035.113>.
- [25] B.L. Gudenias, L. Wang, Prediction of lncRNA subcellular localization with deep learning from sequence features, *Sci. Rep.* (2018), <https://doi.org/10.1038/s41598-018-34708-w>.
- [26] K. Tantale, F. Mueller, A. Kozulic-Pirher, A. Lesne, J.M. Victor, M.C. Robert, S. Capozzi, R. Chouaib, V. Bäcker, J. Mateos-Langerak, X. Darzacq, C. Zimmer, E. Basyuk, E. Bertrand, A single-molecule view of transcription reveals convoys of RNA polymerases and multi-scale bursting, *Nat. Commun.* (2016), <https://doi.org/10.1038/ncomms12248>.
- [27] H. Miao, L. Wang, H. Zhan, J. Dai, Y. Chang, F. Wu, T. Liu, Z. Liu, C. Gao, L. Li, X. Song, A long noncoding RNA distributed in both nucleus and cytoplasm operates in the PYCARD-regulated apoptosis by coordinating the epigenetic and translational regulation, *PLoS Genet.* (2019), <https://doi.org/10.1371/journal.pgen.1008144>.
- [28] A. Fatica, I. Bozzoni, Long non-coding RNAs: New players in cell differentiation and development, *Nat. Rev. Genet.* 15 (2014) 7–21, <https://doi.org/10.1038/nrg3606>.
- [29] Y. Verheyden, L. Goedert, E. Leucci, Control of nucleolar stress and translational reprogramming by lncRNAs, *Cell Stress* 3 (2019) 19–26, <https://doi.org/10.15698/cst2019.01.172>.
- [30] J. Carlevaro-Fita, A. Rahim, R. Guigó, L.A. Vardy, R. Johnson, Cytoplasmic long noncoding RNAs are frequently bound to and degraded at ribosomes in human cells, *RNA* 22 (2016) 867–882, <https://doi.org/10.1261/rna.053561.115>.
- [31] S. Nakagawa, T. Naganuma, G. Shioi, T. Hirose, Paraspeckles are subpopulation-specific nuclear bodies that are not essential in mice, *J. Cell Biol.* 193 (2011) 31–39, <https://doi.org/10.1083/jcb.201011110>.



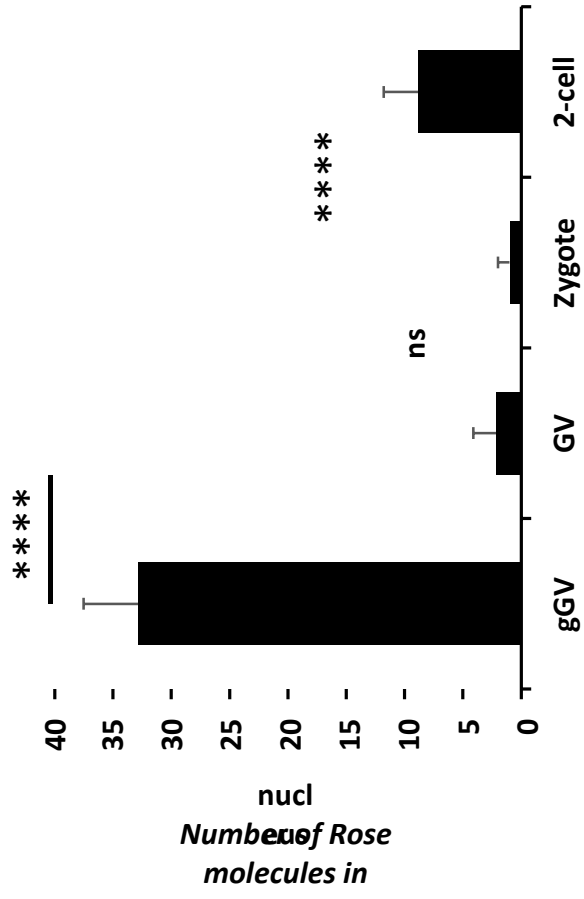
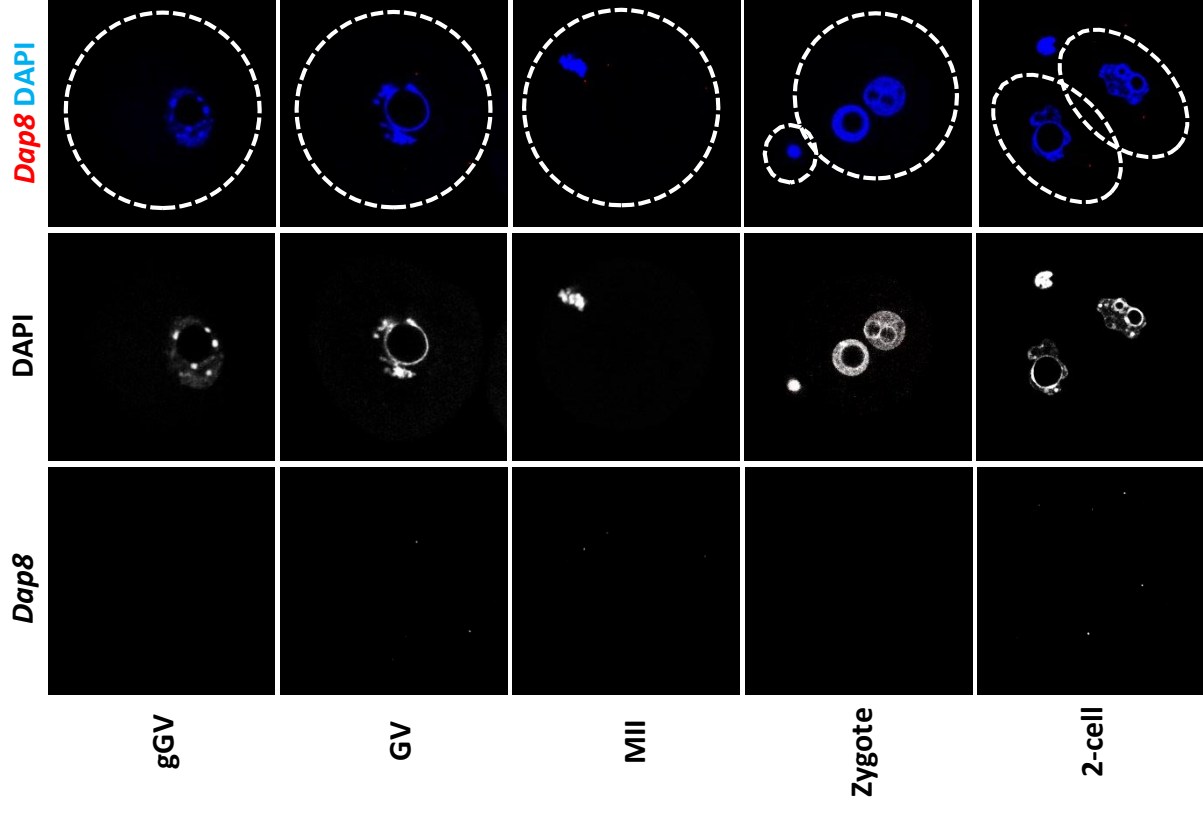
**Supplementary Fig. 1: *Gm32743* lncRNA expression in mouse tissues.** Expression estimated as FPKM from Mouse ENCODE transcriptome data.



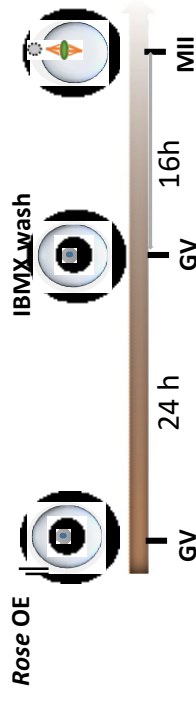
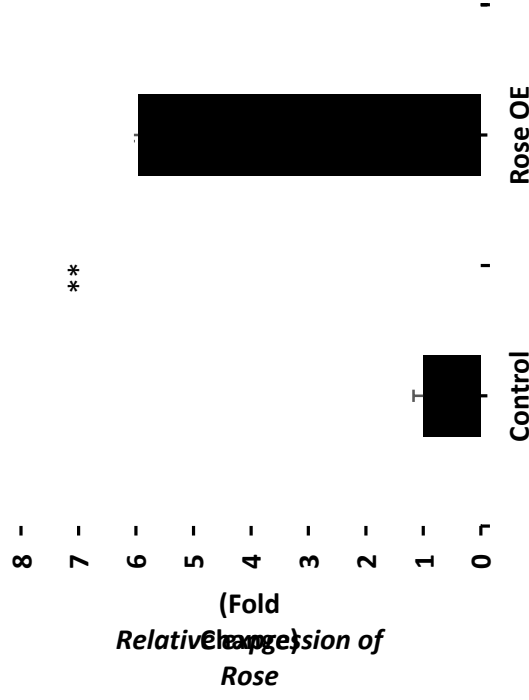
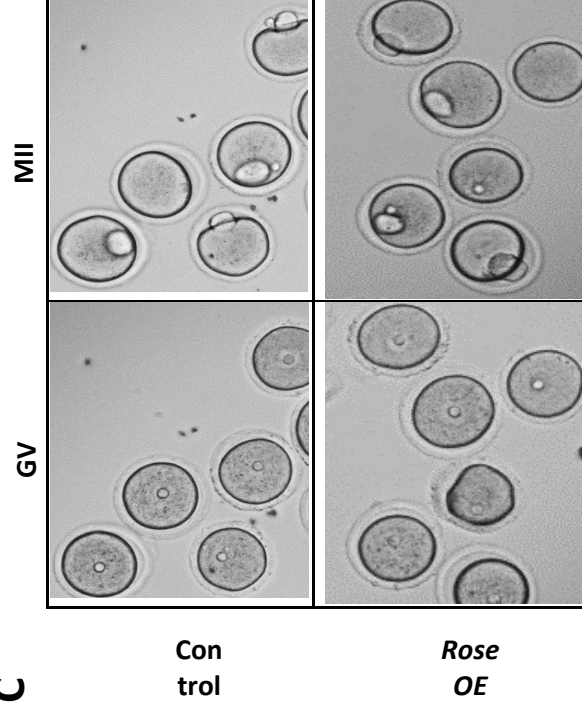
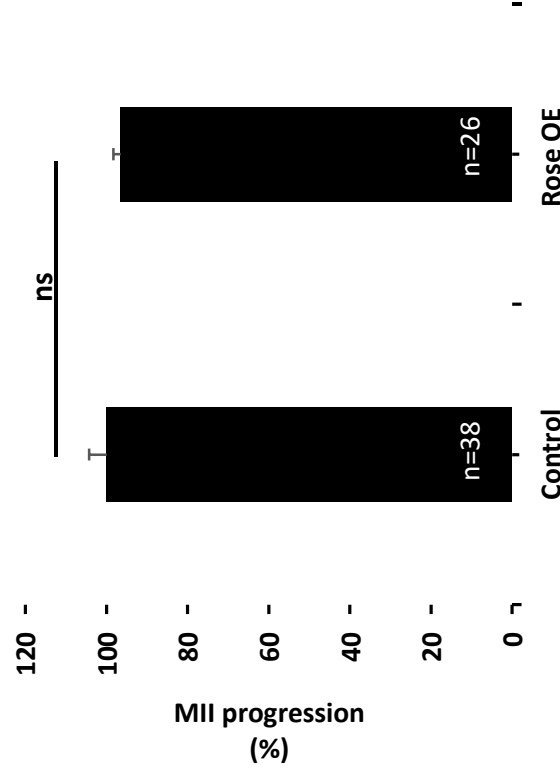




**Supplementary Fig. 3: Isolated RNA do not contain DNA contamination.** (A) Scheme of primer set up for detection of *Dazl* gene in the purified RNA sample of transcriptionally inactive GV and MII oocytes. (B) PCR analysis of processed *Dazl* mRNA showing absence of intron. *Gapdh mRNA* was used as a loading control.

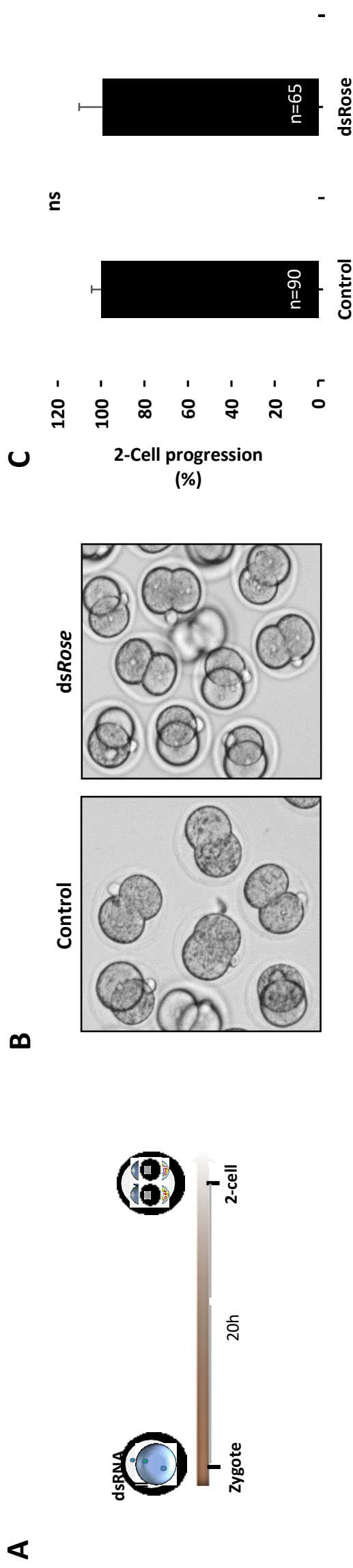
**A****B**

**Supplementary Fig. 4: Expression of *Rose* IncRNA significantly decreases during developmental stages and is localized to nucleus of growing oocyte and 2-cell embryo. (A)** Quantification of *Rose* IncRNA presence in the nucleus of growing and fully grown oocyte, zygote and 2-cell embryo. Mean  $\pm$  SD; One-way ANOVA: F (3, 38) = 246,1,  $p < 0.0001$ . Tukey's multiple comparisons test: \*\*\*\* $p < 0.0001$ , ns - non-significant; from three biological replicates,  $n \geq 7$ . (B) Bacterial *Dab8* RNA was used as a negative control for RNA FISH.

**A****B****C****D**

**Supplementary Fig. 5: Overexpression of *Rose* does not affect meiotic progression.** (A) Scheme of experimental approach for *Rose* overexpression. (B) qRT-PCR detection of overexpression of *Rose* lncRNA in GV oocytes. Mean  $\pm$  SD; Student's t-test:  $**p < 0.01$ ;  $n = 3$ . (C) Phenotype analysis of progression of GV oocytes to MII stage after overexpression of *Rose*;  $n \geq 18$ . (D) Quantification of oocyte progression from GV to MII stages after overexpression of *Rose*. Mean  $\pm$  SD; Student's t-test: ns – non-significant; from three biological replicates,  $n \geq 18$ .





**Supplementary Fig. 6: Downregulation of *Rose* does not affect 2-cell progression.** (A) Scheme of experimental approach for *Rose* downregulation. (B) Phenotype analysis of progression of zygote to 2-cell embryo after downregulation of *Rose* lncRNA. (C) Quantification of 2-cell progression from zygote after downregulation of *Rose* lncRNA. Mean  $\pm$  SD; Student's t-test: ns - non-significant;  $n \geq 12$ , from three biological replicates.

### Primers

Name	Sequence 5' ---- 3'	Amplicon Size (bp)
Upstream of NCE1 -F	AGTTGGTCCTTATAGAGGGC	682
Upstream of NCE1-R	GCATGAGATGATTCTGGTGT	
Downstream of NCE3 -F	CAGTTACCAGTGAACCAAGC	723
Downstream of NCE3 -R	CTTCAGAGCAAGGACACATA	
Rose NCE1-F	TCCAGGTTCTTCTTACAATG	482/594
Rose NCE3-R	CCAAAAACAGACTTGATGAG	
T7NCE1-F	CGAGTAATACGACTCACTATAGGTCAGGTTCTTACAATG	482/594
T7NCE3-R	CGAGTAATACGACTCACTATAGGCCAAAAACAGACTTGATGAG	
Rose-F	CTACGGCAGGAGTGACCCTA	256 (NCE1 region)
Rose-R	GGAGGGGGCTGTCTATGAAAAA	
Dazl exon 3-F	GTTTCTTTGCCAGATATGGCT	120
Dazl exon 4-R	CTACTATCTTCTGCACATCCAC	
18S-F	5'-CGCTCCACCAACTAAGAACG-3'	110
18S-R	5'-CTCAACACGGGAAACCTCAC-3'	
28S-F	5'-CTAAATACCGGCACGAGACC-3'	88
28S-R	5'-TTCACGCCCTCTTGAACCT-3'	
GAPDH-F	TGGAGAAACCTGCCAAAGTATG	130
GAPDH-R	GGTCCTCAGGTAGCCCAAG	

### RNA FISH Probes

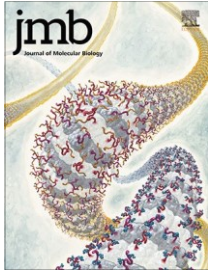
Gene name	Target region	No. of ZZ pairs	channel	Cat. No.
Gm32743 (XR_379793.2)	2092 - 3137	20	C1	320269
Dab8 (EF191515)	414 - 862	10	C1	310043

Name	Accession #	RNA size	ORF size	Ficket Score	Hexamer Score	Coding Probability	Coding Label
<i>Xist</i>	NR_001570.2	12250	519	0.4809	-0.601593733	0.043572362	no
<i>Ccnb1</i>	NM_172301.3	2316	1293	1.143	0.233312892	0.999193219	yes
<i>Rose</i>	XR_379793.3	1611	240	0.4575	-0.187956336	0.030229861	no

**Supplementary Table 2: Analysis of coding potential of *Rose* RNA using CPAT (<http://lilab.research.bcm.edu/cpat/>).**  
Known *Xist* lncRNA and *Ccnb1* mRNA candidates was used as a controls.

Serial No.	Sum of Energy	Min of Energy	Transcript ID	Transcript Name	Biotype
1	-456.31	-23.85	ENSMUST00000219061	AC160249.1-201	Noncoding
2	-330.44	-21.09	ENSMUST00000113862	Kcnj15-208	Protein Coding
3	-304.64	-18.83	ENSMUST00000208147	Olf2-203	Protein Coding
4	-259.72	-19.21	ENSMUST00000129791	Gm11373-201	Noncoding
5	-181.77	-18.28	ENSMUST0000053760	Utp14b-201	Protein Coding
6	-165.94	-21.30	ENSMUST00000110003	Eif4e1b-201	Protein Coding
7	-164.64	-17.70	ENSMUST0000095767	Etv1-201	Protein Coding
8	-147.66	-21.41	ENSMUST0000053880	Grin2b-201	Protein Coding
9	-135.67	-17.76	ENSMUST00000166353	Gm17402-201	Protein Coding
10	-128.84	-19.87	ENSMUST0000070342	Sertm1-201	Protein Coding

**Supplementary Table 3: The top 10 interaction with Rose analyzed by LncRRsearch web tool (<http://rtools.cbrc.jp/LncRRsearch/index.cgi>).**



# Single Molecule RNA Localization and Translation in the Mammalian Oocyte and Embryo

Denisa Jansova<sup>1</sup>†, Daria Aleshkina<sup>1</sup>, Anna Jindrova<sup>1</sup>, Rajan Iyyappan<sup>1</sup>, Qin An<sup>2</sup>, Guoping Fan<sup>2</sup> and Andrej Susor<sup>1</sup>†

<sup>1</sup> - Institute of Animal Physiology and Genetics, Czech Academy of Sciences, Libečov 277 21, Czech Republic

<sup>2</sup> - Department of Human Genetics, David Geffen School of Medicine, University of California, Los Angeles, CA 90095-7088, USA

Correspondence to Denisa Jansova and Andrej Susor: [jansova@iapg.cas.cz](mailto:jansova@iapg.cas.cz) (D. Jansova), [susor@iapg.cas.cz](mailto:susor@iapg.cas.cz) (A. Susor)

<https://doi.org/10.1016/j.jmb.2021.167166>

Edited by Sarah A. Teichmann

## Abstract

During oocyte growth the cell accumulates RNAs to contribute to oocyte and embryo development which progresses with ceased transcription. To investigate the subcellular distribution of specific RNAs and their translation we developed a technique revealing several instances of localized translation with distinctive regulatory implications. We analyzed the localization and expression of candidate non-coding and mRNAs in the mouse oocyte and embryo. Furthermore, we established simultaneous visualization of mRNA and *in situ* translation events validated with polysomal occupancy. We discovered that translationally dormant and abundant mRNAs *CyclinB1* and *Mos* are localized in the cytoplasm of the fully grown GV oocyte forming cloud-like structures with consequent abundant translation at the center of the MII oocyte. Coupling detection of the localization of specific single mRNA molecules with their translation at the subcellular context is a valuable tool to quantitatively study temporal and spatial translation of specific target mRNAs to understand molecular processes in the developing cell.

© 2021 Elsevier Ltd. All rights reserved.

## Introduction

Fully grown female gametes (oocytes) are transcriptionally inactive and dependent on the translation of mRNAs synthesized during the growth phase. Dynamic control of mRNA translation has a significant impact on oocyte<sup>1</sup> and early embryo development e.g. for nuclear envelope breakdown (NEBD) the oocyte requires translation of *Cyclin B1* mRNA<sup>2</sup> and on the other hand translation of *Mos* (V-Mos Moloney Murine Sarcoma Viral Oncogene Homolog) mRNA, is essential for meiotic arrest awaiting fertilization.<sup>3,4</sup>

Despite well-established knowledge about asymmetric localization and translation of various RNAs in oocytes of non-mammalian species,<sup>5,6</sup> RNA localization in the mammalian oocyte and

embryo is still not fully described and understood. The majority of mRNAs are distributed evenly throughout the cytoplasm, however, some transcripts localize in the nucleus or spindle area.<sup>7-9</sup> Cellular compartmentalization requires a semipermeable membrane described in mitotic cells<sup>10</sup> and meiotic oocytes<sup>11-13</sup> serving as a reservoir that locally sequester and mobilize chromosomes and spindle assembly factors within the cytoplasm which is essential for proper spindle assembly and cytokinesis.<sup>14-17</sup>

Instead of extracting RNA molecules from cells, direct visualization is beneficial to understand spatial distribution and fate within the single cell environment. RNA fluorescence *in situ* hybridization (FISH) is regularly used for studying single or multiple RNA localization in fixed

cells.<sup>18,19</sup> A combination of RNA FISH with other methods, such as immunocytochemical staining, qRT-PCR and proximity ligation assay (PLA)<sup>20,21</sup> provides more comprehensive and validated data about RNA localization. Recently, the advanced labeling MS2-GFP approach was established allowing the observation of mRNA dynamics in live cells.<sup>22,23</sup> Translation is a fundamental biological process by which ribosomes decode genetic information into proteins. Translational dynamics and localization in a cellular context are less well understood in mammalian oocytes and early embryo compared to other types of cells (e.g. neuronal cells) where a variety of techniques have been developed to analyze sites of specific protein synthesis in a subcellular context.<sup>24,25</sup> For protein synthesis study, it is important to distinguish newly synthesized proteins from pre-existing ones. A classical method for achieving this is through the pulse-chase approach, in which newly synthesized proteins are specifically tagged globally. Recently, a proximity ligation assay was combined with pulse-chase approaches (FUNCAT-PLA or Puro-PLA) to visualize local translation of specific proteins.<sup>20</sup> Another technique is Fluorescence Labeling System to Visualize Translation of Single mRNAs in live cells called SunTag.<sup>26,27</sup> SunTag usually requires the generation of a transgenic cell similar to the MS2 system, where both systems detect endogenous RNA. However, simple and time saving tools for the visualization of translation of specific mRNAs *in situ* are missing.

Here we present localization of various RNA candidates in the mammalian oocyte and zygote. Moreover, we have developed a novel system for simultaneous visualization of single mRNA with its translation event based on RNA FISH and the puromycilation proximity ligation assay (RNA-puro-PLA) that enables visualization of nascent translation of specific endogenous mRNAs in the spatial and biological context.

## Results

### Localization of selected ncRNAs and mRNAs in the mouse oocytes and zygotes

In order to visualize the intracellular localization of selected RNAs we used RNA FISH.<sup>19</sup> Firstly, we detected selected noncoding RNAs (ncRNA) in the oocyte (GV - oocyte with nucleus; MII - oocyte with second meiotic spindle formed) and zygote. All candidates, including *nuclear enriched abundant transcript 2 (Neat2)*, small nuclear RNA, *RNA Component of 7SK Nuclear Ribonucleoprotein (Rn7sk)* and *intracisternal A particle long terminal repeat RNA (IAPLtr1a)* are present in the nucleus of GV (Figure 1(A)-(C)) and dispersed in the cytoplasm of anuclear oocyte stage (MII). *Neat2* and *IAPLtr1a* are absent in the zygotic pronuclei (Figure 1(A) and (C)). On the other hand, *Rn7sk* shows a strong exclusive signal only in the pronuclei of the zygote

(Figure 1(B)). Candidate mRNAs, *Actin b (Actb)* and *Cyclins (Ccnb2, Ccnb3)* showed abundant signal in the cytoplasm of all developmental stages (Figure 1(D)-(F)). Oocyte absent bacterial RNA *DapB* was used as a negative control (Supplementary Figure 1(A)). Degradation of RNAs by RNase A showed an absence of *Ccnb2* mRNA (Supplementary Figure 1(B)). Here we used simplified quantification of RNA from a single equatorial Z-section to analyze the reliability of simplified scoring. *Ccnb3*, a candidate mRNA, was quantified from the entire oocyte and zygote volume (Supplementary Figure 1(C)). We found that relative expression pattern between two quantification methods has a positive correlation (Supplementary Figure 1(D)).

Furthermore, performed nuclei isolation from GV oocytes with subsequent PCR analysis of nuclear localized RNA showed a positive correlation with *in situ* detected RNA (Figure 1) and PCR (Supplementary Figure 2(A) and (B)), all analyzed ncRNAs exhibited exclusive localization to the nucleus of the GV oocyte (Figure 1(A)-(C) and Supplementary Figure 2(A)). From detected mRNAs only *Actb* showed a diminutive presence in the nucleus (Figure 1(D) and Supplementary Figure 2(B)).

Based on presented results, we were able to detect and validate specific RNAs in the oocyte and zygote in different subcellular compartments.

Trends of expression of selected ncRNAs and mRNAs in oocytes and zygotes.

To determine differential gene expression of candidate RNAs we used two approaches. We quantified RNA signals from RNA FISH imaging (Figure 1) and performed qRT-PCR on the isolated total RNA from oocytes and zygotes (Figure 2 and Supplementary Figure 3(A)). Describing trend lines for RNA FISH quantification and qRT-PCR we found a positive correlation between the two different methods (Figure 2). In general we detected a lower number of ncRNA molecules than mRNA (Supplementary Figure 3(B) and (C)). Quantification of RNA molecules from a single equatorial Z-section showed only 72 molecules for *Neat2* lncRNA however 332 molecules for *Ccnb2* mRNA (Supplementary Figure 3(B)). Quantification of the candidate mRNA, *Ccnb3*, from whole cellular volume of cells showed around 2150, 1410, and 1450 molecules in GV, MII oocytes, and zygotes, respectively (Supplementary Figure 1(C)). All RNA candidates showed a significant decrease of expression from GV to MII by both methods. ncRNAs showed a higher decrease from GV to MII than mRNA candidates (Figure 2 and Supplementary Figure 3). RNA FISH quantification showed mostly non-significant differences between MII and zygote stages for tested mRNA candidates (Supplementary Figure 3(B) and (C)), however qRT-PCR showed significant differences for *Actb*,

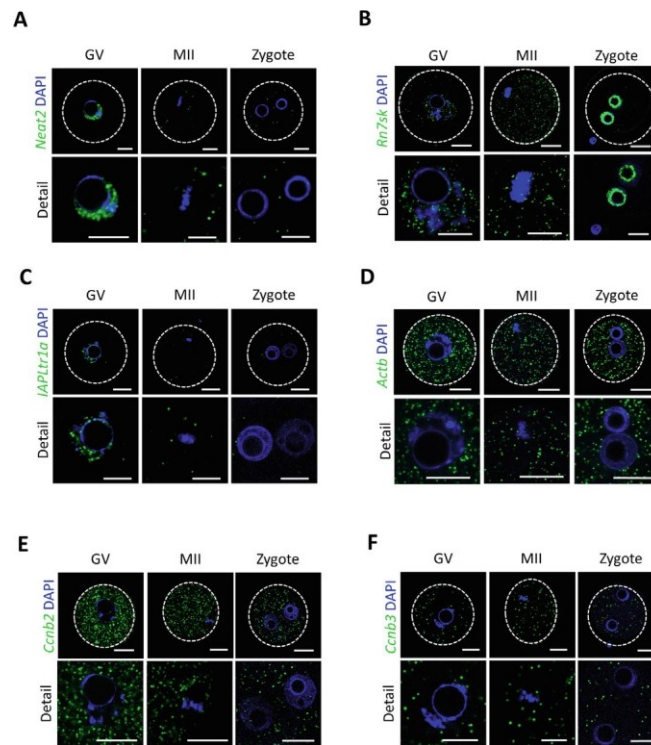


Figure 1. Localization of selected ncRNAs and mRNAs in mouse oocytes and zygotes. (A) Long noncoding RNA, *Neat2*. (B) Small nucleolar RNA, *Rn7sk*. (C) Long terminal repeat RNA, *IAPLtr1a*. (D) *Actin* bmRNA (*Actb*). (E) *Cyclin b2* mRNA (*Ccnb2*). (F) *Cyclin b3* mRNA (*Ccnb3*). Details show nuclear, chromosomal and pronuclear areas, DAPI (blue), dashed line shows cell cortex, scale bar 20  $\mu$ m. Controls are available in Supplementary Figure 1 and nuclear localization validation by PCR in Supplementary Figure 2.

*Ccnb2* and *Mos* mRNAs and a significant decrease in these stages (Figure 2 and Supplementary Figure 3). Despite this, simplified quantification of RNA expression using a single Z-section of RNA FISH imaging showed positive correlation pattern with qRT-PCR analysis (Figure 2).

In conclusion, comparison of commonly used qRT-PCR method for quantification or RNA expression positively correlate with simplistic *in situ* RNA quantification of expression by RNA FISH.

#### Simultaneous RNA and protein detection in oocytes and zygotes.

To analyze localization of two different mRNAs in the oocyte we performed RNA FISH for *Ccnb2* and *Ccnb3* using different color channels (Figure 3(A)). We found that both cyclins do not colocalize within the cell (Figure 3(A) and Supplementary Figure 4 (A)). Next we used oocytes from a transgenic *Actb*-MBS mouse (MBS<sup>+/+</sup>) to target two different sequences of *Actb* mRNA, ORF and 3'UTR containing 24 palindrome domains, MS2 Binding Site (MBS; Supplementary Figure 4(C)).<sup>22</sup>

We detected by RNA FISH both sequences on single *Actb* mRNA (Figure 3(B)) and observed colocalization signal in oocytes from MBS<sup>+/+</sup> female (Supplementary Figure 4(A)) however only

ORF of *Actb* mRNA was detected in the oocyte from MBS<sup>-/-</sup> female (Supplementary Figure 4(B)). To validate the localization of *Actb* mRNA from RNA FISH (Figure 1(D)) in the live oocyte (MBS<sup>+/+</sup>) we microinjected RNA coding for MS2 Coat Protein (MCP) tagged with GFP (Supplementary Figure 4(C)). We found a similar distribution of *Actb* mRNA labeled with MCP:GFP protein in the live oocyte (Supplementary Figure 4 (D)) as visualized by RNA FISH (Figure 1(D)).

Furthermore, we performed staining of specific RNA along with antibody detecting specific subcellular structures. Above we showed *Neat2* lncRNA localization in the nucleus (Figure 1 and Supplementary Figure 2(A)), and in addition to RNA FISH we used nuclear envelope marker, anti-lamin A/C (LMN A/C) (Figure 3(C)). In addition, we analyzed the localization of *Ccnb2* mRNA and spindle of MII oocyte simultaneously using tubulin antibody (Figure 3(D)). Here we detected and validated reliable localization of endogenous candidate RNAs in the cellular organelle context.

#### Simultaneous detection of translational event of specific mRNA in oocytes and zygotes.

Above we presented reliable localization of various RNAs in the oocyte and zygote (Figures 1



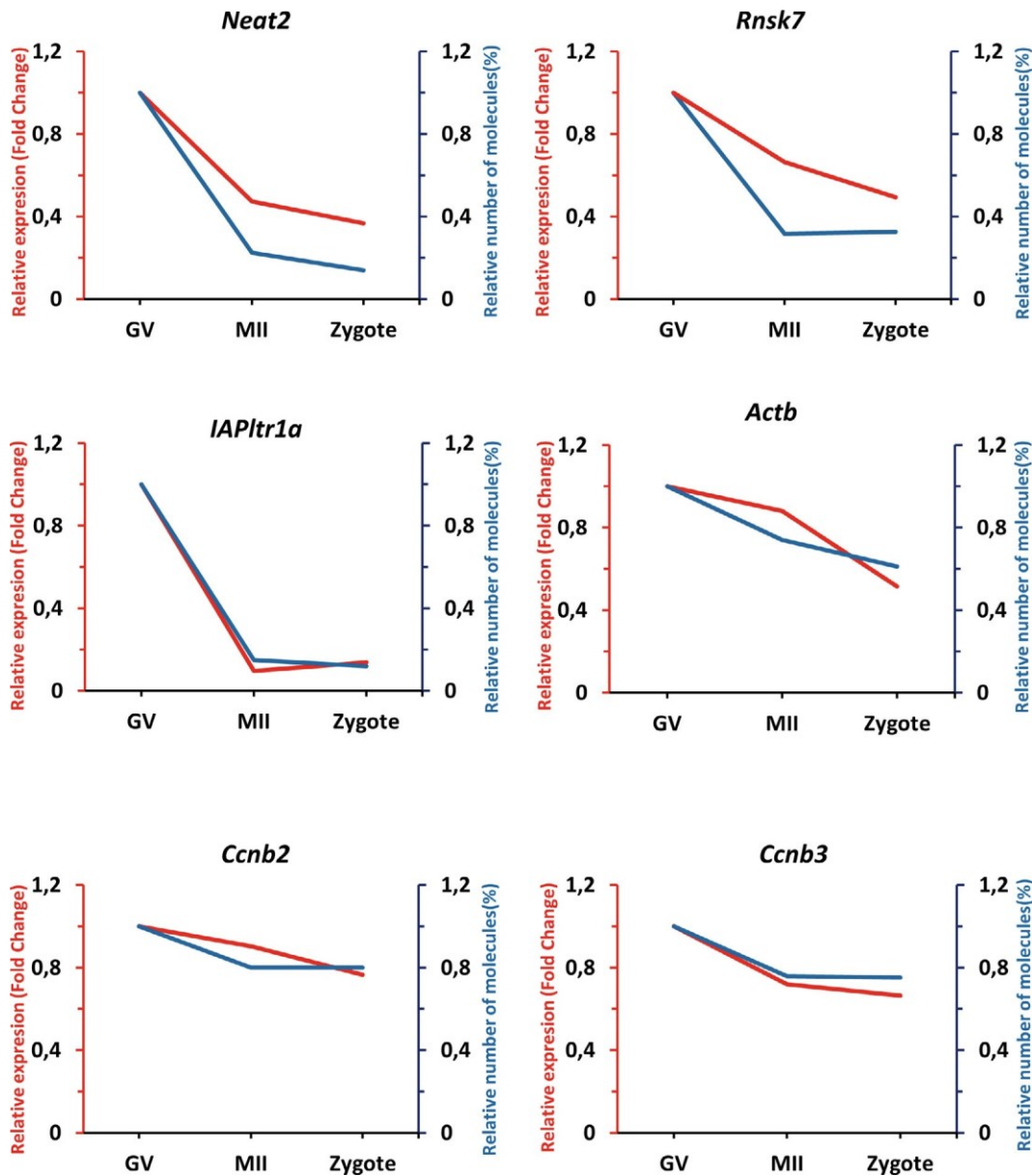


Figure 2. Trends of expression of selected ncRNAs and mRNAs in oocytes and zygotes. Graphs show trends of relative quantification of selected ncRNAs (*Neat2*, *Rn7sk*), *LTR RNA (IAPltr1a)* and mRNAs (*Actb*, *Ccnb2*, *Ccnb3*) from qRT-PCR (Y' axis, red; FC, fold change) and RNA FISH (Y axis, blue). Quantification of expression of selected RNAs is presented in Supplementary Figure 3.

and 3 and Supplementary Figures 1 and 4). Additionally, to localization of mRNA we added another dimension of mRNA life - the translation. We detected localization of *Actb* mRNA in the oocyte and embryo and to visualize *in situ* translational event on specific single mRNA, we performed a short (5 min) cell cultivation with 1 mM puromycin (Figure 4(A)). Then *Actb* mRNA was detected by RNA FISH (RNA) and its *in situ* translation was targeted by puromycylation (puro) and proximity ligation assay (PLA) using anti-puromycin and anti-ACTB antibodies (RNA-puro-PLA; Graphical Abstract). To validate the

RNA-puro-PLA method we quantified both *Actb* mRNA spots (single color channel-green) and dual channel spots (*Actb* mRNAs in translation-green and red). We found that *Actb* mRNA translation is increased in the GV stage (Supplementary Figure 5(A)) but decreased in the MII and zygote (Supplementary Figure 5(A)). Similarly we observed from genome wide RNA sequencing of the polysomal fraction where the majority of *Actb* mRNA has polysomal occupancy in the GV stage with a decrease in the MII and zygote (Supplementary Figure 5(B) and (C)). Importantly oocytes without puromycylation did not show



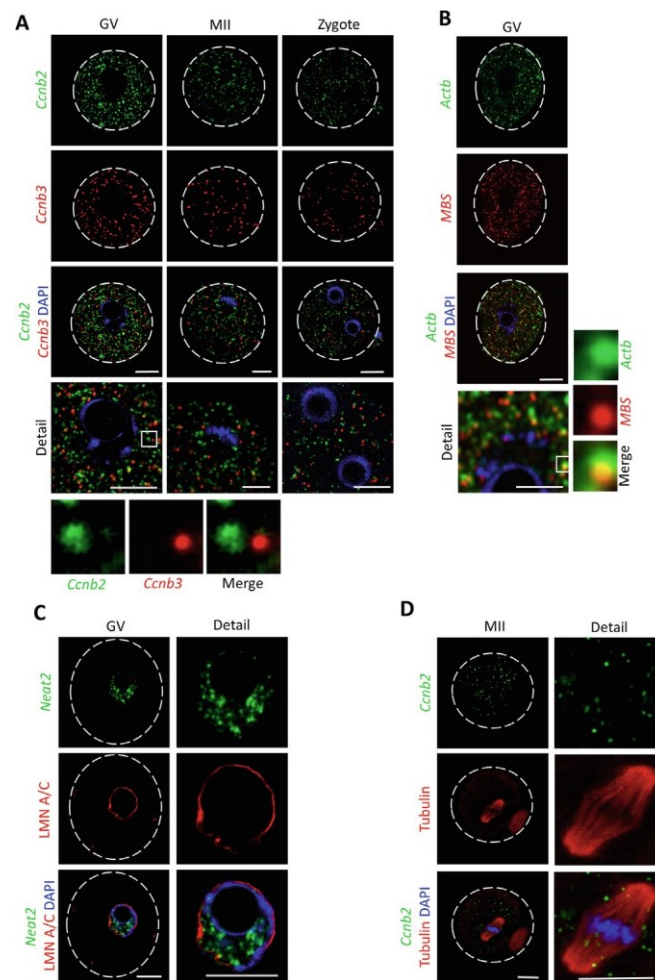


Figure 3. Simultaneous RNA and protein detection in oocytes and zygotes. (A) Simultaneous detection of *Ccnb2* (green) and *Ccnb3* (red) mRNAs. Details show nuclear, chromosomal and pronuclear areas, DAPI (blue), dashed line shows cell cortex, scale bars 20  $\mu$ m. Details show single mRNA molecules depicted by a white square. For quantification of the colocalization of *Ccnb2* and *Ccnb3* mRNAs see Supplementary Figure 4(A). (B) Simultaneous detection *Actb* mRNA (green) and *MBS* sequence at 3<sup>o</sup>UTR (red). Detail shows nuclear area, dashed line shows GV oocyte cortex, DAPI (blue), scale bar 20  $\mu$ m. Details depicted by white square (*Actb*, green and *MBS*, red). For quantification of colocalization of ORF *Actb* mRNA and its *MBS* 3<sup>o</sup>UTR domain see Supplementary Figure 4 (A). (C) Simultaneous detection of *Neat2* lncRNA (RNA FISH, green) and nuclear membrane marker Lamin A/C (Immunocytochemistry, red) in the GV oocyte. Detail of nucleus area, DAPI (blue); dashed lines shows cell cortex, scale bar 20  $\mu$ m. (D) Simultaneous detection of *Ccnb2* mRNA (green) and spindle protein marker, acetylated  $\alpha$ -tubulin (red) in the MII oocyte. Detail of spindle/chromosomal area, DAPI (blue); dashed line shows cell cortex, scale bar 20  $\mu$ m.

translation at *Actb* mRNA (Supplementary Figure 6 (A)). Additionally we labeled actin filaments (F-actin) with fluorescently labeled phalloidin and performed puro-PLA to visualize subcellular actin filaments and translation of *Actb* mRNA. We found partial colocalization of actin microfilaments with ACTB translation in oocytes (Figure 4(B) and Supplementary Figure 7).

Disruption of puromycylation by interference with the binding site for puromycin on the nascent peptide during translational elongation using 100  $\mu$ M Anisomycin<sup>28</sup> disrupts the detection of ACTB translational spots without influencing

the detection of actin filaments (Supplementary Figure 6 (B)). Furthermore, we performed another control to analyze the influence of protease Plus II used at initial step of RNA-puro-PLA. We found that addition of protease for 10 min post fixation do not negatively influence detection of translation by puro-PLA (Supplementary Figure 8).

Here we present a novel validated RNA-puro-PLA method which allowed us to obtain reliable visualization of the translational event of a specific endogenous single mRNA molecule at the subcellular context.

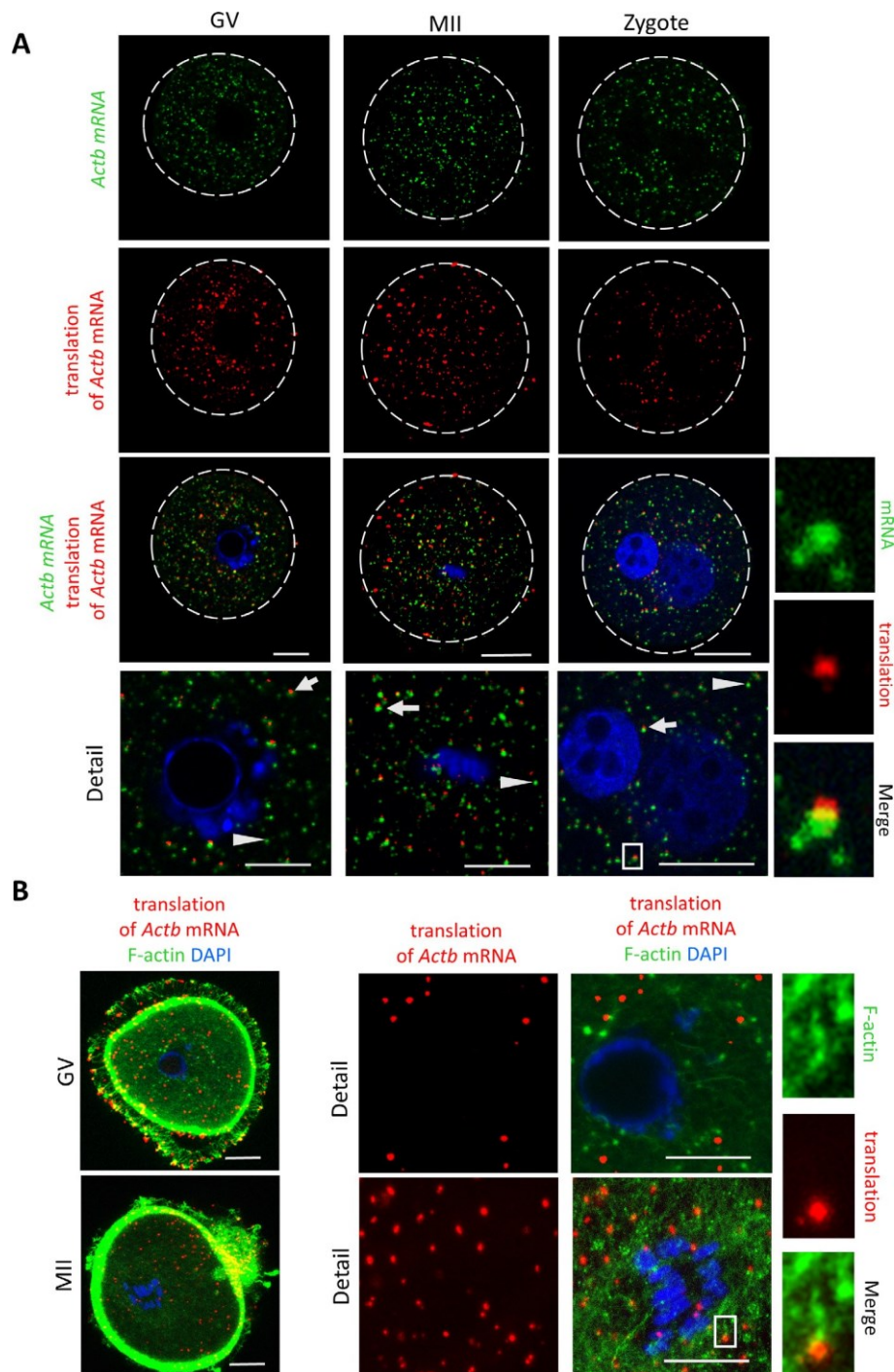


Figure 4. Simultaneous detection of translational event of specific mRNA in oocytes and zygotes. (A) Detection of *Actb* mRNA (RNA FISH, green) and its translational event (puro-PLA, red) in the oocyte and zygote. Details show nuclear, chromosomal and pronuclear area. Scale bar 20  $\mu$ m, DAPI (blue); arrowheads depict *Actb* mRNA and arrows translation of ACTB protein on mRNA, dashed line shows cell cortex. Details show translational event on *Actb* mRNA depicted by a white square. Quantification and validation of RNA-puro-PLA showed in Supplementary Figure 5. Controls showed in Supplementary Figure 6(A). (B) Detection of localization of ACTB translation (puro-PLA, red) and F-actin complex (phalloidin, green) in oocyte. Details show nuclear and chromosomal area, DAPI (blue), scale bar 20  $\mu$ m. Controls are showed in Supplementary Figure 6(B) and colocalization analysis in the Supplementary Figure 7.

Simultaneous detection of dormant maternal mRNAs and their translation in the oocyte.

To analyze *in situ* translation in the known biological context we selected specific candidate mRNAs *Ccnb1* and *Mos*. Both mRNAs are translationally dormant in the GV oocyte and actively translated in the MII oocyte.<sup>29</sup> Firstly, we found that pattern of *Ccnb1* and *Mos* mRNA in the cytoplasm of GV oocyte is different (Figure 5(A)) than *Actb* mRNA (Figure 4(A)). *Ccnb1* and *Mos* mRNA showed more an abundant mRNA signal forming cloud-like structures in the GV cytoplasm (Figure 5(A)). However, in the MII stage the mRNA spots become dispersed and the number of mRNAs decreased (Figure 5(A)). A reduced number of mRNA molecules positively correlated with qRT-PCR analysis where expression of both transcripts is significantly reduced between oocyte stages (Supplementary Figure 3(A)). Importantly we found that the rate of *in situ* translation of both *Ccnb1* and *Mos* mRNAs was minimal in GV oocytes (Figure 5), however translational activity elevated significantly during the MII stage (Figure 5). These data are consistent with results obtained from immunoblotting<sup>2,30</sup> and from polysomal occupancy analysis.<sup>29</sup> Moreover, quantification of mRNA molecules from a single Z-section of RNA-puro-PLA positively correlates with the RNA expression measured by qRT-PCR (Supplementary Figure 9). Next we asked if subcellular localization of translation of *Actb*, *Ccnb1* and *Mos* differs in the subcellular context. Quantification of translational events shows that *Actb* is translated evenly in the cell (Supplementary Figure 10) however translation of *Ccnb1* and *Mos* is significantly enriched in the center of the MII oocyte (Supplementary Figure 10).

In conclusion, we present a valuable tool for the detection of both single mRNA molecules and its translational event in one of the largest cell types in the body, the oocyte and zygote.

## Discussion

The heterogeneity of maternal RNA and its regulation is an essential driver of oocyte and early embryo development. Previous studies analyzed RNA localization in the germ cells of non-mammalian organisms e.g. *Drosophila*,<sup>31,32</sup> *Xenopus*<sup>5,33</sup> and zebrafish<sup>2</sup> using various techniques. However data about specific RNA localization in mammalian oocytes are scarce.<sup>19,34</sup>

Here, we showed the localization of selected RNA candidates in the mouse oocyte and zygote belonging to various classes e.g. lncRNA class (*Neat2*), small nuclear RNA (*Rn7sk*), retrotransposon RNA (*IAPLtr1a*) and mRNAs coding for ACTB, Cyclins B1, B2 and B3. Our data from RNA FISH and qPCR quantification for *Actb* mRNA correspond to qRT-PCR previously presented.<sup>3,35,47</sup> It is known that a number of

ncRNAs have nuclear localization<sup>36,37</sup> and similarly all ncRNAs and LTR RNA investigated in this study showed only nuclear localization. Both selected ncRNAs *Neat2* and *Rn7sk* have known localization to the nucleus,<sup>9,38</sup> however LTR retrotransposon RNA *IAPLtr1a* localization was not detected previously. Although all candidates showed a large decrease in expression in MII and zygote *IAPLtr1a* dropped to a minimal level. It is known that LTR retrotransposons have the highest expression during the embryonic genome activation period in mouse and human embryos.<sup>39</sup> We and others<sup>8,16,31,40-43</sup> have shown that the nucleoplasm contains large amounts of RNA which might serve as a mechanism for attenuation of their translation with consequent activation of the translation post nuclear envelope break down.<sup>9</sup> Despite the translational potential of *LTR RNA*, we showed that *IAPLtr1a* is retained in the nucleoplasm and minimal expression was detected in the MII oocyte, suggesting a mechanism of translational repression of *IAPLtr1a* in the oocyte and zygote or potentially nuclear localization protects RNA from decay. The GV oocyte nucleus contains a minor amount of *Actb* mRNA, possibly suggesting the presence of a mechanism to ensure translation of specific mRNA on the newly developing spindle post NEBD, as in the case of *Ank2* mRNA.<sup>9</sup>

Here we quantified RNA expression by two different methods showing similar trends for selected RNA candidates comparable to previous studies.<sup>19,35</sup> Xie et al. (2018) quantified mRNA molecules in the whole oocyte volume using confocal scanning, however we obtained a positive correlation of expression pattern using various quantifications approaches 1) simplistic RNA FISH quantification from single equatorial Z-section, 2) whole cellular volume and 3) qRT-PCR.

The level of *Ccnb3* mRNA declined during meiotic maturation. This is in agreement with the contribution of decay of *Ccnb3* to MII arrest.<sup>44</sup> The similar declining trend of *Ccnb2* implies a compensatory function of CCNB2 for CCNB1 in meiosis I.<sup>45</sup>

Oocytes of non-mammalian organisms<sup>5,46</sup> are highly RNA polarized, whilst polarity is unknown in mammalian oocytes. The presented visualization of RNA and organelle markers brings subcellular determinants which can aid the identification of the localization of potential polarization constituents. *Actb* mRNA localization by RNA FISH was confirmed and moreover was detected real-time in live oocytes using the MS2-GFP system on *Actb* mRNA.<sup>22</sup>

Furthermore, for the imaging of specific mRNAs we visualized another dimension of mRNA life, translation. By RNA-puro-PLA we distinguished translationally inactive and active candidate mRNAs in the oocyte and zygote. Previously detection of translation was based on western blotting or the polyadenylation status of *Actb*,<sup>47,48</sup> *Ccnb1*<sup>29</sup> and *Mos* mRNA, and the same trends in



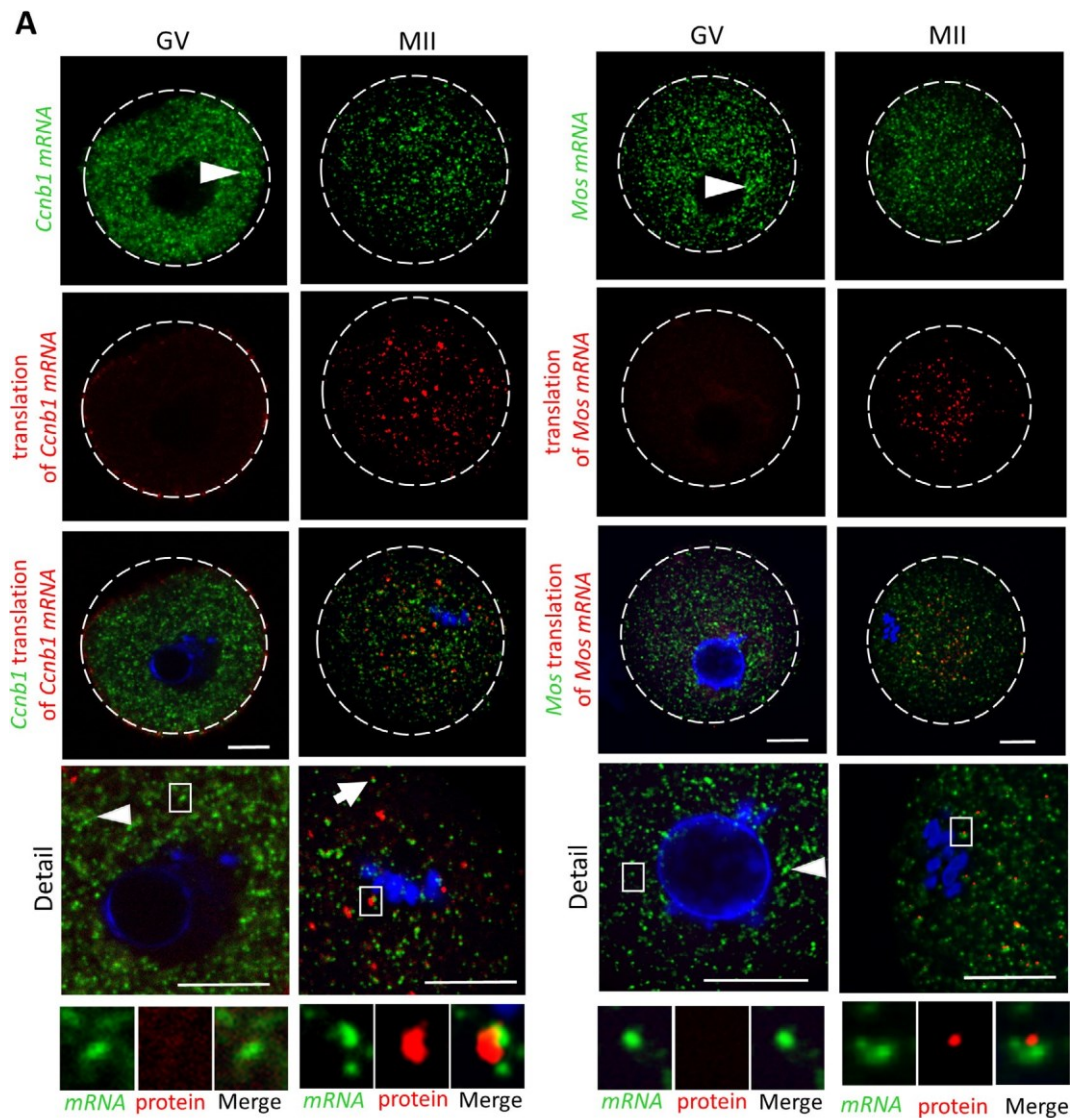


Figure 5. Detection of translation of candidate maternal mRNAs in the oocyte. (A) *In situ* detection of *Cyclin b1* and *Mos* mRNA (RNA FISH, green) and its translational event (puro-PLA, red). Details show nuclear and chromosomal area in GV and MII oocyte. DAPI (blue), scale bar 20  $\mu$ m, arrowheads depict mRNA clustering; dashed line shows cell cortex. Details show translational event (red) on single *Ccnb1* mRNA molecule (green) depicted by a white square. (B) Quantification of *Cyclin b1* and *Mos* mRNA (non-translated mRNA, black) and their translation (translated, grey) *in situ* in oocytes and zygotes. Graph show number of molecules in GV and MII oocytes. n 15; mean  $\pm$  SD, Student's *t*-test: \**p* < 0.05, \*\**p* < 0.01, \*\*\**p* < 0.001; *ns* for non-significant.

oocytes were confirmed by RNA-puro-PLA. We detected that subset of *Actb* mRNAs are translated directly on microfilament structures essential for the positioning of the nucleus, spindle migration and the cytokinesis of the oocyte.<sup>13,49</sup> Similarly *Rac1*, *ArpC2* and *Actb* mRNAs co-localize with actively translating ribosomes on lamellipodia.<sup>50,51</sup> Additionally, the cytoskeleton is crucial for the transport of specific mRNAs as well as their spatially localized translation in several organisms.<sup>52,53</sup> In connection to this, the actin cytoskeleton is associated with components of the translational machinery, including ribosomes.<sup>54,55</sup> Indeed, mRNA transcripts, polyosomes, eukaryotic initiation and elongation factors, and aminoacyl-tRNA synthetases have all been shown to associate with the cytoskeleton.<sup>56</sup> The translation of key meiotic players was observed here i.e. *CCNB1* and *Mos*.<sup>57,58</sup> Both candidate mRNAs are abundant in the translationally dormant GV oocyte.<sup>4</sup> Similarly, observed *Ccnb1* and *Mos* clustering in mouse and zebrafish GV oocytes.<sup>59</sup> We found that their abundant presence in the cytoplasm leads to cloud-like structures resembling cytoplasmic lattices,<sup>60</sup> structures containing mRNAs and ribosomes in translationally dormant state. Interestingly, candidate mRNAs *Actb*,<sup>61</sup> *Ccn- b2*<sup>62</sup> and *Ccnb3*<sup>44</sup> translated in the GV oocyte showed disperse mRNA localization similar to *Ccn- b1* and *Mos* mRNA in the MII stage. Our data indicate that mRNA cytoplasmic dispersion and decay might be prerequisite for translation of specific maternal mRNAs. Similarly *Oct4* RNA granules are dispersed in the MII oocyte or 2-cell embryo which leads to increased translation.<sup>63</sup> Interestingly the translation of *Ccnb1* and *Mos* mRNAs was increased in the central area of MII oocyte however *Actb* translation is distributed evenly. Importantly, localization of candidate RNAs or their translation did not show localization to subcortical maternal complex<sup>34</sup> which is in agreement with others.<sup>19,64,65</sup> Previously, it was demonstrated that fully grown oocyte neither forms P-bodies<sup>34</sup> nor stress granules after the induction of translational stress.<sup>61</sup> Translation of a single mRNA molecule was previously observed in live cells<sup>26</sup> however, it requires the implementation of reporter RNA sequence, which is complicated and time-consuming for primary cells. Thus, implementation of RNA-puro-PLA is a rather simple alternative to reporter RNAs and provides a comprehensive visualization of temporal and spatial translation of endogenous specific mRNA at single molecule resolution in different cellular developmental stages or treatments.

Here we revealed the reliable detection of the localization of endogenous RNA candidates and their translation within a biological context. The presented RNA-puro-PLA might be expanded by another dimension of translational regulation by adding visualization of additional translational players e.g. RNA or RNA binding proteins.

## Materials and methods

### Oocyte and zygote isolation and cultivation

Oocytes were acquired from 6-week-old CD1 and MBS<sup>+/-</sup> mice. The females were stimulated 46 h prior to oocyte isolation using 5 IU of pregnant mare serum gonadotropin (PMSG; Folligon; Merck Animal Health) per mouse. Selected oocytes were denuded and cultivated in M16 medium (Millipore) without IBMX at 37 °C, 5% CO<sub>2</sub> for 0 h (GV) or 16 h (MII). For embryo collection, the stimulated mice were again injected with 5 IU hCG before being mated overnight with males of the same strain. After 16 h, zygotes were recovered from the excised oviducts and cultured in M16 medium. All animal experiments were performed in accordance to guidelines and protocols approved by Laboratory of Biochemistry and Molecular Biology of Germ Cells at the Institute of Animal Physiology and Genetics in Czech Republic.<sup>66</sup> All animal work was conducted according to Act No. 246/1992 on the protection of animals against cruelty, issued by experimental project #215/2011, certificate #CZ02389, issued by the Ministry of Agriculture.

### RNA FISH

Fixed oocytes (20 min in 4% PFA) were pre-treated with protease PLUS from RNAScope H<sub>2</sub>O<sub>2</sub> and Protease Reagents kit (diluted 1:15 in nuclease free water; Cat. No. 322381, ACD) for 10 min. Each sample was incubated with a single RNAScope probe for 2 h at 40 °C to detect individual selected mRNA or two probes to detect two selected mRNAs (*Supplementary Table 2A*). RNA FISH protocol for amplification was followed using reagents in RNAScope Multiplex Fluorescent Detection Reagents v2 kit (Cat. No. 323110, ACD), with extended washing: 2 × 10 min washing after probe hybridization (1x wash buffer diluted in nuclease free water; RNAScope Wash Buffer Reagents, Cat. No. 310091, ACD); v2 Amp1 30 min, 40 °C, 2 × 5 min 1x wash buffer; v2 Amp2 30 min, 40 °C, 2 × 5 min 1x wash buffer; v2 Amp3 15 min, 40 °C, 2 × 5 min 1x wash buffer. After amplification, HRP-C1/C2/C3 was used on the corresponding channels of specific probe for 15 min at 40 °C. Oocytes were washed again 2 × 5 min in 1x wash buffer. TSA Cy5 dye (Perkin Elmer) diluted to 1:1500 in TSA buffer (ACD) was used for fluorescent labelling of the amplified signal. After washing and application of HRP blocker (30 min at 40 °C), samples were washed again and mounted in Prolong Gold Antifade with DAPI (Life Technologies) on epoxy coated slides. However for multiple labeling two mRNAs, samples were washed, HRP-C1/C2/C3 was used on the corresponding second channels

of second selected specific probe. TSA FITC dye (Perkin Elmer) diluted to 1:1500 in TSA buffer (ACD) was used for fluorescent labelling of the amplified signal. After washing and application of HRP blocker (30 min at 40 °C), samples were washed again. Samples were mounted in Prolong Gold Antifade with DAPI (Life Technologies) on epoxy coated slides.

#### RNA-Puro-PLA

Oocytes/zygotes were incubated 5 min with 1 mM puromycin in M16 prior fixation. Oocytes/zygotes were fixed for 20 min in 4% PFA. Fixed oocytes/zygotes were pre-treated with protease PLUS from RNAScope H<sub>2</sub>O<sub>2</sub> and Protease Reagents kit (diluted 1:15 in nuclease free water; Cat. No. 322381, ACD) for 10 min. In the control for protease treatment, protease was substituted by 0.5% TritonX in PBS for 10 minutes after fixation.

Each sample was incubated with a single RNAScope probe for 2 h at 40 °C to detect individual selected mRNA (*Supplementary Table 2A*). RNA FISH protocol for amplification was followed using reagents in RNAScope Multiplex Fluorescent Detection Reagents v2 kit (Cat. No. 323110, ACD), with extended washing: 2 × 10 min washing after probe hybridization (1x wash buffer diluted in nuclease free water; RNAScope Wash Buffer Reagents, Cat. No. 310091, ACD); v2 Amp1 30 min, 40 °C, 2 × 5 min 1x wash buffer; v2 Amp2 30 min, 40 °C, 2 × 5 min 1x wash buffer; v2 Amp3 15 min, 40 °C, 2 × 5 min 1x wash buffer. After amplification, HRP-C1/C2/C3 was used on the corresponding channels of specific probe for 15 min at 40 °C. Oocytes were washed again 2 × 5 min in 1x wash buffer. TSA Cy5 dye (Perkin Elmer) diluted to 1:1500 in TSA buffer (ACD) was used for fluorescent labelling of the amplified signal. After washing and application of HRP blocker (30 min at 40 °C), samples were washed again. Before mounting step, the cells were incubated with primary antibodies: rabbit anti-ACTB (1:150; 0061R, Bios) rabbit anti-CCNB1 (1:150; MS-338-PO, Thermo Fisher); rabbit anti-cMOS (1:150PA5-10108 Invitrogen); mouse anti-puromycin (1:200; MABE343, Millipore in TBS-BSA-PBS) at 4 °C overnight. PLA was performed according to instructions of PLA Duolink kits (DUO92006 and DUO92008, Sigma Aldrich). Briefly, the samples were washed using TBS-BSA-PBS and subsequently in Wash Buffer A (Sigma Aldrich) and incubated with 40 μL of the probe reaction mix for 1 h at 37 °C. Next the samples were washed in 1x Wash Buffer A for 2 × 5 min and the following ligation reaction was performed for 30 min at 37 °C. After washing 2 × 5 min in Wash Buffer A, 40 μL of amplification reaction reagent was added to each sample and incubated for 100 min at 37 °C. The samples were washed for 2 × 10 min in 1x Wash Buffer B (Sigma Aldrich) and for 2 min in 0.01x Wash

Buffer B, and then mounted on slides using Vectashield Mounting Medium with DAPI (H-1500, Vector Laboratories).

An inverted confocal microscope (Leica SP5) was used for sample visualization. Image quantification and assembly were performed using ImageJ and Adobe Photoshop CS3. Spindle area was defined by DAPI staining and number of interactions were analyzed in ImageJ software.

#### Nuclei isolation

Zona pellucida was removed by Tyrode acid solution (Sigma). The oocytes were disrupted by hand using a pulled glass pipette in PBS drop (cytoplasm) and nuclei were washed in three drops of PBS and transferred to microtubes (N). Negative control of the isolation was liquid used to wash pipette after oocyte disruption (NTC).

#### PCR and qRT-PCR

RNeasy Plus Micro kit (Qiagen) was used for RNA extraction according to the manufacturer's instructions. Reverse transcription was performed with qPCRBIO cDNA Synthesis Kit (PCR Biosystems). PCR was performed with PPP master mix (TOP-Bio). The following program was used: 94 °C 1 min; 94 °C 18 sec; 58 °C 15 sec; 72 °C. Annealing temperatures for selected genes are detailed in *Supplementary Table 3*. Products were separated on 1.5% agarose gel with GelRed (41003, Biotinum) staining. qRT-PCR was carried out using QuantStudio13 and Luna<sup>®</sup> Universal qPCR Master Mix (New England BioLabs) according to manufacturer's protocols with an annealing temperature of 60°C. Primers for selected candidates are listed in *Supplementary Table 3*. RT-qPCR results were normalized to exact number of cells in all samples and endogenous *Gapdh* mRNA expression.

#### Polysome fractionation and sequencing of fractions

Polysome fractionation followed by RNA isolation was carried out according to Scarce Sample Polysome profiling (SSP-profiling) method by Masek et al.,<sup>67</sup>. Then, non-polysomal (NP; fractions 1-5) and polysomal fractions (P; fractions 6-10) were pooled and subjected to qRT-PCR (QuantStudio 3 cycler, Applied Biosystems). Sequencing libraries were prepared using SMART-seq v4 ultra low input RNA kit (Takara Bio). Sequencing was performed with HiSeq 2500 (Illumina) as 150-bp paired-ends. Reads were trimmed using Trim Galore v0.4.1 and mapped onto the mouse GRCm38 genome assembly using Hisat2 v2.0.5. Gene expression was quantified as fragments per kilobase per million (FPKM) values in Seqmonk v1.40.0.



### RNA FISH - Immunocytochemistry

Oocytes were fixed for 20 min in 4% PFA. RNA FISH were performed according to Tetkova et al.<sup>9</sup> Oocyte were washed in PBS-TBS-BSA (Sigma Aldrich), incubated with primary antibodies (Supplementary Table 2B) diluted to 1:150 PBS-TBS-BSA overnight at 4 °C. Oocytes were washed 15 min in PBS-TBS-BSA and primary antibodies were detected using relevant HRP antibody conjugates with 488 or 594 dye (Perkin Elmer) diluted to 1:250 for 1 h at room temperature. Washed oocytes (15 min PBS-TBS-BSA) were mounted onto slides using Vectashield with DAPI. Inverted confocal microscope (Leica SP5) was used for sample visualization.

### Puro-PLA and labelling of filament actin

Oocytes were incubated for 5 min with 1 mM puromycin in M16 prior fixation. Oocytes were fixed for 20 min in 4% PFA and permeabilized by 0.5% TritonX/PBS for 10 minutes. Puro-PLA was performed according to Tetkova et al., 2019. One drop of ActinGreen probe Phalloidin 488 (Thermo Fisher) per 10 minute was then used for labelling filament actin in each sample (20-30 oocytes per group). Washed oocytes (15 min PBS/PVA) were mounted onto slides using Vectashield with DAPI. As negative control, oocytes were pre-incubated 45 min in 100 mM anisomycin in M16, then incubated 5 min with 1 mM puromycin prior fixation. Puro-PLA assay and labelling of actin filament was performed according protocol described above. An inverted confocal microscope (Leica SP5) was used for sample visualization. Rest of Puro-PLA assay was performed without changes. Experiments were repeated 3x with 20-30 oocytes per group/ experiment.

### Plasmid construct and mRNA microinjection and imaging

MCP-GFP was in vitro transcribed (IVT) from plasmid phage-ubc-nls-ha tdMCP-GFP (AddGENE 40649) and H2b:mCherry RNA from plasmid provided by Dr Martin Anger, Laboratory of Cell Division Control, IAPG CAS using mMACHINE™ Transcription Kit (Invitrogen, Carlsbad, CA, USA). MBS<sup>+/+</sup> oocytes were co-microinjected with 20 mM/ ml *tdMCP-GFP* mRNA and 20 ng/ml *H2B-m cherry* mRNA, using a Leica DMI 6000B inverted microscope, TransferMan NK2 (Eppendorf) and FemtoJet (Eppendorf). Microinjected oocytes were selected 1 h after microinjection and either washed from IBMX and cultivated to MII stage or stored at GV stage overnight. Microinjected oocytes were placed into 4-well culture chambers (Sarstedt) in 10 mL of equilibrated M16 media (37.5 °C, 5% CO<sub>2</sub>) covered with mineral oil (M8410; Sigma Aldrich). The cells were imaged using a Leica SP5

inverted confocal microscope with 488 nm excitation wavelength to detect single mRNP particles labeled with GFP. Time-lapse imaging of *Actb* mRNA sites was performed with an imaging interval of 60 s on 400 Hz. Experiments were repeated 3x with 20-30 oocytes per group/experiment.

### Post-imaging analysis

We analyzed images using ImageJ software with following plugins: FindFoci, ComDet, EzColocalization and Coloc2. Quantification of single RNA molecules from RNA FISH images was performed via FindFoci plugin, single Z- section image was converted to the binary 8-bit type. Spots of RNA were identified using the FindFoci algorithm<sup>68</sup> with Otsu thresholding to define the background parameter 5 and peak parameter 0.5 relative above the background minimum particle size 0.3. Whole oocyte volume analysis included 120-170 Z-section images. The Z- stack image was smoothed with Gaussians filter using sigma radius 2. Analysis was performed with FindFoci plugin with same parameters as used for single Z-section analysis. ComDet™ plugin was used for scoring colocalization of two different mRNA probes. Red channel was analyzed and minimum particle size was set as 5 pixels. Green channel was analyzed and minimum particle size was set as 3 pixels. Maximal distance between colocalized spots was 3 pixels. Intensity of spots was set for 5 times higher than background. Plugin scored number of colocalized spots. RNA-puro-PLA images were analyzed by “ComDet” plugin which included scoring of the colocalization of the RNA with its translation site. Green and red channels were analyzed and minimum particle size was set as 5 pixels. Maximal distance between colocalized spots was 4 pixels. Intensity of spots was set up for 5 times higher than background. To specify the localization of translation, two equal cellular areas were analyzed: cellular center (A, depicted by circle) and cellular cortex (B, depicted by dashed line). EzColocalization plugin was used to detect colocalization of F-actin and *Actb* translation site.<sup>69</sup> 8-bit format images with set parameters according to Otsu threshold. Particles were analyzed based on the signal intensity presented by heat maps. Filtered images were analyzed in Coloc2 plugin.

### Statistical analysis

Experiments were repeated at least 3 times. The statistical significance of the differences between the groups was analyzed by PrismaGraph8.3 software. The tool used to determine if the differences between groups were statistically significant was either Student's t-test on the averages and s.e.m.; the stated significance intervals were depicted as: Student's t-test: \*p < 0.05, \*\*p < 0.01, \*\*\*p < 0.001, ns for

non-significant; error bars denote calculated standard deviations.

## Ethical approval

All animal work was conducted according to Act No 246/1992 for the protection of animals against cruelty; from 25.09.2014 number CZ02389, issued by the Ministry of Agriculture.

## Acknowledgements

We thank Jaroslava Suplikova and Marketa Hancova for assistance with isolation of oocytes. We are also grateful to Dr Jeffery Chao, Timothee Lionnet and Robert Singer for advice and providing the b-actin-MBS mouse model and stdMCP-GFP plasmid (AddGENE 40649) [23]. Graphical abstract was created with BioRender.com. This research was funded by PPLZ (L200451901) for D.J., GAUK 389321 for D. A. and by GACR (18-19395S). The funders had no role in study design, data collection and analysis, decision to publish, or preparation of the manuscript.

## Author contribution

A.S. and D.J. designed and directed the project; wrote the manuscript. D.J. prepared the figures. D.J.; A.J.; D.A.; R.Y.; A.Q.; G.F. performed experiments and analyzed results. All authors discussed the results and edited manuscript. All authors read and approved the final manuscript.

## Declaration of Competing Interest

The authors declare that they have no known competing financial interests or personal relationships that could have appeared to influence the work reported in this paper.

## Appendix A. Supplementary material

Supplementary data to this article can be found online at <https://doi.org/10.1016/j.jmb.2021.167166>.

Received 22 April 2021;  
Accepted 13 July 2021;  
Available online 20 July 2021

**Keywords:**  
mRNA;  
translation;  
imaging;  
localization;  
subcellular

## Abbreviations used:

NEBD, nuclear envelope breakdown; FISH, fluorescence *in situ* hybridization; PLA, proximity ligation assay; MS2-GFP, a highly specific binding between the RNA stem-loop sequence and the coat protein of the MS2 bacteriophage with a green fluorescent protein; FUNCAT, fluorescent noncanonical amino acid tagging; Puro-PLA, puromycylation proximity ligation assay; RNA-puro-PLA, RNA fluorescence *in situ* hybridization and the puromycylation proximity ligation assay

## References

1. Takei, N., Sato, K., Takada, Y., Iyyappan, R., Susor, A., Kotani, T., (2021). Tdr3 regulates the progression of meiosis II through translational control of Emi2 mRNA in mouse oocytes 2021.02.17.431574 *Physiol. Genet.*, <https://doi.org/10.1101/2021.02.17.431574>.
2. Kotani, T., Yasuda, K., Ota, R., Yamashita, M., (2013). Cyclin b1 mRNA translation is temporally controlled through formation and disassembly of RNA granules. *J. Cell Biol.*, 202, 1041-1055. <https://doi.org/10.1083/jcb.201302139>.
3. Gebauer, F., Richter, J.D., (1997). Synthesis and function of Mos: The control switch of vertebrate oocyte meiosis. *BioEssays.*, 19, 23-28. <https://doi.org/10.1002/bies.950190106>.
4. Yoshida, N., Mita, K., Yamashita, M., (2000). Function of the Mos/MAPK pathway during oocyte maturation in the Japanese brown oocyte frog *Rana japonica*. *Mol. Reprod. Dev.*, 57, 88-98. [https://doi.org/10.1002/1098-2795\(200009\)57:1<88::AID-MRD12>3.0.CO;2-9](https://doi.org/10.1002/1098-2795(200009)57:1<88::AID-MRD12>3.0.CO;2-9).
5. Kloc, M., Bilinski, S., Chan, A.P., Allen, L.H., Zearfoss, N.R., Etkin, L.D., (2001). RNA localization and germ cell determination in xenopus. *Int. Rev. Cytol.*, 203, 63-91. [https://doi.org/10.1016/S0074-7696\(01\)03004-2](https://doi.org/10.1016/S0074-7696(01)03004-2).
6. Lou King, M., Zhou, Y., Bubunenko, M., (1999). Polarizing genetic information in the egg: RNA localization in the frog oocyte. *BioEssays.*, 21, 546-557. [https://doi.org/10.1002/\(SICI\)1521-1878\(199907\)21:7<546::AID-BIES3>3.0.CO;2-Z](https://doi.org/10.1002/(SICI)1521-1878(199907)21:7<546::AID-BIES3>3.0.CO;2-Z).
7. Romasco, E.J., Amarnath, D., Midic, U., Latham, K.E., (2013). Association of maternal mRNA and phosphorylated EIF4EBP1 variants with the spindle in mouse oocytes: localized translational control supporting female meiosis in mammals. *Genetics*, 195, 349-358. <https://doi.org/10.1534/genetics.113.154005>.
8. Jansova, D., Tetkova, A., Koncicka, M., Kubelka, M., Susor, A., (2018). Localization of RNA and translation in the mammalian oocyte and embryo. *PLoS One.*, 13 <https://doi.org/10.1371/journal.pone.0192544>.
9. Tetkova, A., Jansova, D., Susor, A., (2019). Spatio-temporal expression of ANK2 promotes cytokinesis in oocytes. *Sci. Rep.*, 9, 1-13. <https://doi.org/10.1038/s41598-019-49483-5>.
10. Schweizer, N., Pawar, N., Weiss, M., Maiato, H., (2015). An organelle-exclusion envelope assists mitosis and underlies distinct molecular crowding in the spindle region. *J. Cell Biol.*, 210, 695-704. <https://doi.org/10.1083/jcb.201506107>.
11. Schlaitz, A.L., Thompson, J., Wong, C.C.L., Yates, J.R., Heald, R., (2013). REEP3/4 ensure endoplasmic reticulum

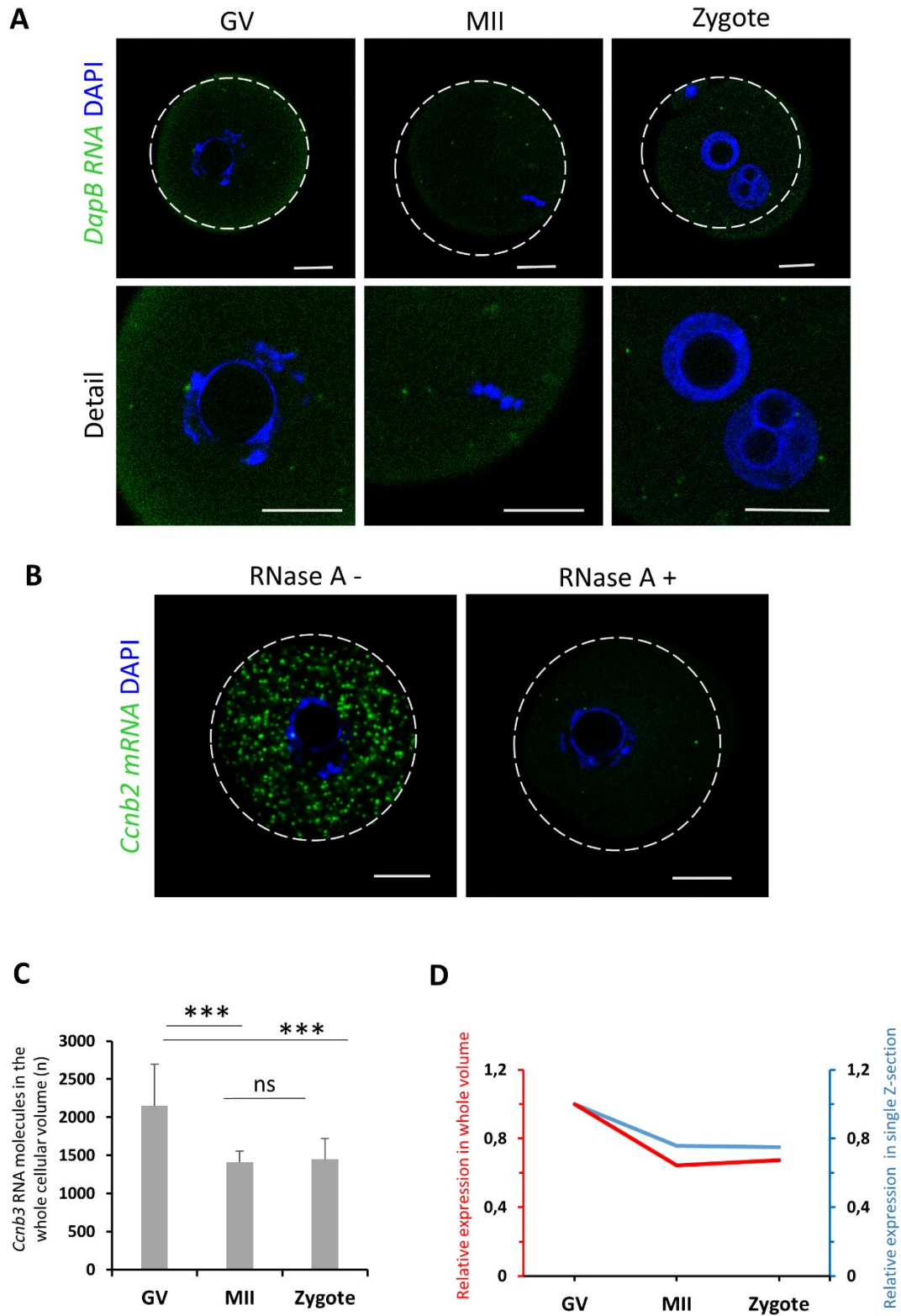


- clearance from metaphase chromatin and proper nuclear envelope architecture. *Dev. Cell.*, 26, 315-323. <https://doi.org/10.1016/j.devcel.2013.06.016>.
12. FitzHarris, G., Marangos, P., Carroll, J., (2007). Changes in endoplasmic reticulum structure during mouse oocyte maturation are controlled by the cytoskeleton and cytoplasmic dynein. *Dev. Biol.*, 305, 133-144. <https://doi.org/10.1016/j.ydbio.2007.02.006>.
  13. Yi, K., Rubinstein, B., Unruh, J.R., Guo, F., Slaughter, B.D., Li, R., (2013). Sequential actin-based pushing forces drive meiosis I chromosome migration and symmetry breaking in oocytes. *J. Cell Biol.*, 200, 567-576. <https://doi.org/10.1083/jcb.201211068>.
  14. So, C., Seres, K.B., Steyer, A.M., Mönlich, E., Clift, D., Pejkovska, A., Möbius, W., Schuh, M., (2019). A liquid-like spindle domain promotes acentrosomal spindle assembly in mammalian oocytes. *Science (80-)*, 364 <https://doi.org/10.1126/science.aat9557>.
  15. Lince-Faria, M., Maffini, S., Orr, B., Ding, Y., Florindo, C., Sunkel, C.E., Tavares, Á., Johansen, J., et al., (2009). Spatiotemporal control of mitosis by the conserved spindle matrix protein megorator. *J. Cell Biol.*, 184, 647-657. <https://doi.org/10.1083/jcb.200811012>.
  16. Susor, A., Jansova, D., Cerna, R., Danylevska, A., Anger, M., Toralova, T., Malik, R., Supolikova, J., et al., (2015). Temporal and spatial regulation of translation in the mammalian oocyte via the mTOR-eIF4F pathway. *Nature Commun.*, 6, 6078. <https://doi.org/10.1038/ncomms7078>.
  17. Jansova, D., Koncicka, M., Tetkova, A., Cerna, R., Malik, R., del Llano, E., Kubelka, M., Susor, A., (2017). Regulation of 4E-BP1 activity in the mammalian oocyte. *Cell Cycle*, 16, 927-939. <https://doi.org/10.1080/15384101.2017.1295178>.
  18. Raj, A., van den Bogaard, P., Rifkin, S.A., van Oudenaarden, A., Tyagi, S., (2008). Imaging individual mRNA molecules using multiple singly labeled probes. *Nature Methods*, <https://doi.org/10.1038/nmeth.1253>.
  19. Xie, F., Timme, K.A., Wood, J.R., (2018). Using single molecule mRNA fluorescent in situ hybridization (RNA-FISH) to quantify mRNAs in individual murine oocytes and embryos. *Sci. Rep.*, 8, 7930. <https://doi.org/10.1038/s41598-018-26345-0>.
  20. Tom Dieck, S., Kochen, L., Hanus, C., Heumüller, M., Bartnik, I., Nassim-Assir, B., Merk, K., Mosler, T., et al., (2015). Direct visualization of newly synthesized target proteins in situ. *Nature Methods*, 12, 411-414. <https://doi.org/10.1038/nmeth.3319>.
  21. Moissoglu, K., Yasuda, K., Wang, T., Chrisafis, G., Mili, S., (2019). Translational regulation of protrusion-localized RNAs involves silencing and clustering after transport. *Elife*, 8 <https://doi.org/10.7554/eLife.44752>.
  22. Lionnet, T., Czaplinski, K., Darzacq, X., Shav-Tal, Y., Wells, A.L., Chao, J.A., Park, H.Y., De Turrís, V., et al., (2011). A transgenic mouse for in vivo detection of endogenous labeled mRNA. *Nature Methods*, 8, 165-170. <https://doi.org/10.1038/nmeth.1551>.
  23. Wu, B., Chao, J.A., Singer, R.H., (2012). Fluorescence fluctuation spectroscopy enables quantitative imaging of single mRNAs in living cells. *Biophys. J.*, 102, 2936-2944. <https://doi.org/10.1016/j.bpj.2012.05.017>.
  24. Biswas, J., Liu, Y., Singer, R.H., Wu, B., (2019). Fluorescence imaging methods to investigate translation in single cells. *Cold Spring Harb. Perspect. Biol.*, 11 <https://doi.org/10.1101/cshperspect.a032722>.
  25. Broix, L., Turchetto, S., Nguyen, L., (2021). Coordination between Transport and Local Translation in Neurons. *Trends Cell Biol.*, <https://doi.org/10.1016/j.tcb.2021.01.001>.
  26. Tanenbaum, M.E., Gilbert, L.A., Qi, L.S., Weissman, J.S., Vale, R.D., (2014). A protein-tagging system for signal amplification in gene expression and fluorescence imaging. *Cell*, 159, 635-646. <https://doi.org/10.1016/j.cell.2014.09.039>.
  27. Enam, S.U., Zinshteyn, B., Goldman, D.H., Cassani, M., Livingston, N.M., Seydoux, G., Green, R., (2020). Puromycin reactivity does not accurately localize translation at the subcellular level. *Elife*, 9, 1-34. <https://doi.org/10.7554/ELIFE.60303>.
  28. Garreau De Loubresse, N., Prokhorova, I., Holtkamp, W., Rodnina, M.V., Yusupova, G., Yusupov, M., (2014). Structural basis for the inhibition of the eukaryotic ribosome. *Nature*, 513, 517-522. <https://doi.org/10.1038/nature13737>.
  29. Ganesh, S., Horvat, F., Drutovic, D., Efenberkova, M., Pinkas, D., Jandrova, A., Pasulka, J., Iyyappan, R., et al., (2020). The most abundant maternal lncRNA Sirena1 acts post-transcriptionally and impacts mitochondrial distribution. *Nucleic Acids Res.*, 48, 3211-3227. <https://doi.org/10.1093/nar/gkz1239>.
  30. Koncicka, M., Tetkova, A., Jansova, D., Del Llano, E., Gahurova, L., Kracmarova, J., Prokesova, S., Masek, T., et al., (2018). Increased expression of maturation promoting factor components speeds up meiosis in oocytes from aged females. *Int. J. Mol. Sci.*, 19 <https://doi.org/10.3390/ijms19092841>.
  31. Jambor, H., Surendranath, V., Kalinka, A.T., Mejkrik, P., Saalfeld, S., Tomancak, P., (2015). Systematic imaging reveals features and changing localization of mRNAs in Drosophila development. *Elife*, 2015 <https://doi.org/10.7554/eLife.05003>.
  32. Trcek, T., Lionnet, T., Shroff, H., Lehmann, R., (2017). mRNA quantification using single-molecule FISH in Drosophila embryos. *Nature Protoc.*, 12, 1326-1347. <https://doi.org/10.1038/nprot.2017.030>.
  33. Nakahata, S., Kotani, T., Mita, K., Kawasaki, T., Katsu, Y., Nagahama, Y., Yamashita, M., (2003). Involvement of Xenopus Pumilio in the translational regulation that is specific to cyclin B1 mRNA during oocyte maturation. *Mech. Dev.*, 120, 865-880. [https://doi.org/10.1016/S0925-4773\(03\)00160-6](https://doi.org/10.1016/S0925-4773(03)00160-6).
  34. Flemr, M., Ma, J., Schultz, R.M., Svoboda, P., (2010). P-body loss is concomitant with formation of a messenger RNA storage domain in mouse oocytes. *Biol. Reprod.*, 82, 1008-1017. <https://doi.org/10.1095/biolreprod.109.082057>.
  35. Jeong, Y.J., Choi, H.W., Shin, H.S., Cui, X.S., Kim, N.H., Gerton, G.L., Jun, J.H., (2005). Optimization of real time RT-PCR methods for the analysis of gene expression in mouse eggs and preimplantation embryos. *Mol. Reprod. Dev.*, 71, 284-289. <https://doi.org/10.1002/mrd.20269>.
  36. Cabili, M.N., Dunagin, M.C., McClanahan, P.D., Bialesch, A., Padovan-Merhar, O., Regev, A., Rinn, J.L., Raj, A., (2015). Localization and abundance analysis of human lncRNAs at single-cell and single-molecule resolution. *Genome Biol.*, 16, 1-16. <https://doi.org/10.1186/s13059-015-0586-4>.
  37. Hutchinson, J.N., Ensminger, A.W., Clemson, C.M., Lynch, C.R., Lawrence, J.B., Chess, A., (2007). A screen for

- nuclear transcripts identifies two linked noncoding RNAs associated with SC35 splicing domains. *BMC Genomics.*, 8, 1-16. <https://doi.org/10.1186/1471-2164-8-39>.
38. Eichhorn, C.D., Yang, Y., Repeta, L., Feigon, J., (2018). Structural basis for recognition of human 7SK long noncoding RNA by the La-related protein Larp7. *Proc. Natl. Acad. Sci. USA*, 115, E6457-E6466. <https://doi.org/10.1073/pnas.1806276115>.
  39. Grow, E.J., Flynn, R.A., Chavez, S.L., Bayless, N.L., Wossidlo, M., Wesche, D.J., Martin, L., Ware, C.B., et al., (2015). Intrinsic retroviral reactivation in human preimplantation embryos and pluripotent cells. *Nature*, 522, 221-246. <https://doi.org/10.1038/nature14308>.
  40. Herman, R.C., Williams, J.G., Penman, S., (1976). Message and non-message sequences adjacent to poly (A) in steady state heterogeneous nuclear RNA of HeLa cells. *Cell*, 7, 429-437. [https://doi.org/10.1016/0092-8674\(76\)90173-2](https://doi.org/10.1016/0092-8674(76)90173-2).
  41. Huang, S., Deerinck, T.J., Ellisman, M.H., Spector, D.L., (1994). In vivo analysis of the stability and transport of nuclear poly(A)+ RNA. *J. Cell Biol.*, 126, 877-899. <https://doi.org/10.1083/jcb.126.4.877>.
  42. Prasanth, K.V., Prasanth, S.G., Xuan, Z., Hearn, S., Freier, S.M., Bennett, C.F., Zhang, M.Q., Spector, D.L., (2005). Regulating gene expression through RNA nuclear retention. *Cell*, 123, 249-263. <https://doi.org/10.1016/j.cell.2005.08.033>.
  43. Bahar Halpern, K., Caspi, I., Lemze, D., Levy, M., Landen, S., Elinav, E., Ulitsky, I., Itzkovitz, S., (2015). Nuclear retention of mRNA in Mammalian tissues. *Cell Rep.*, 13, 2653-2662. <https://doi.org/10.1016/j.celrep.2015.11.036>.
  44. Meng, T.G., Lei, W.L., Li, J., Wang, F., Zhao, Z.H., Li, A., Wang, Z.B., Sun, Q.Y., et al., (2020). Degradation of Ccnb3 is essential for maintenance of MII arrest in oocyte. *Biochem. Biophys. Res. Commun.*, 521, 265-269. <https://doi.org/10.1016/j.bbrc.2019.10.124>.
  45. Li, J., Tang, J.X., Cheng, J.M., Hu, B., Wang, Y.Q., Aalia, B., Li, X.Y., Jin, C., et al., (2018). Cyclin B2 can compensate for Cyclin B1 in oocyte meiosis I. *J. Cell Biol.*, 217, 3901-3911. <https://doi.org/10.1083/jcb.201802077>.
  46. Kugler, J.M., Lasko, P., (2009). Localization, anchoring and translational control of oskar, gurken, bicoid and nanos mRNA during drosophila oogenesis. *Fly (Austin)*, 3, 15-28. <https://doi.org/10.4161/fly.3.1.7751>.
  47. Bachvarova, R., Cohen, E.M., De Leon, V., Tokunaga, K., Sakiyama, S., Paynton, B.V., (1989). Amounts and modulation of actin mRNAs in mouse oocytes and embryos. *Development*, 106
  48. Vieux, K.F., Clarke, H.J., (2018). CNOT6 regulates a novel pattern of mRNA deadenylation during oocyte meiotic maturation. *Sci. Rep.*, 8 <https://doi.org/10.1038/s41598-018-25187-0>.
  49. Schuh, M., Ellenberg, J., (2008). A new model for asymmetric spindle positioning in mouse oocytes. *Curr. Biol.*, 18, 1986-1992. <https://doi.org/10.1016/j.cub.2008.11.022>.
  50. Simpson, L.J., Tzima, E., Reader, J.S., (2020). Mechanical forces and their effect on the ribosome and protein translation machinery. *Cells*, 9, 650. <https://doi.org/10.3390/cells9030650>.
  51. Willett, M., Brocard, M., Pollard, H.J., Morley, S.J., (2013). MRNA encoding WAVE-Arp2/3-Associated proteins is co-localized with foci of active protein synthesis at the leading edge of MRC5 fibroblasts during cell migration. *Biochem. J.*, 452, 45-55. <https://doi.org/10.1042/BJ20121803>.
  52. Glotzer, J.B., Ephrussi, A., (1996). mRNA localization and the cytoskeleton. *Semin. Cell Dev. Biol.*, 7, 357-365. <https://doi.org/10.1006/scdb.1996.0045>.
  53. Martin, K.C., Ephrussi, A., (2009). mRNA localization: gene expression in the spatial dimension. *Cell*, 136, 719-730. <https://doi.org/10.1016/j.cell.2009.01.044>.
  54. Kim, S., Coulombe, P.A., (2010). Emerging role for the cytoskeleton as an organizer and regulator of translation. *Nature Rev. Mol. Cell Biol.*, 11, 75-81. <https://doi.org/10.1038/nrm2818>.
  55. Stapulionis, R., Kolli, S., Deutscher, M.P., (1997). Efficient mammalian protein synthesis requires an intact F-actin system. *J. Biol. Chem.*, 272, 24980-24986. <https://doi.org/10.1074/jbc.272.40.24980>.
  56. Silva, R.C., Sattlegger, E., Castilho, B.A., (2016). Perturbations in actin dynamics reconfigure protein complexes that modulate GCN2 activity and promote an eIF2 response. *J. Cell Sci.*, 129, 4521-4533. <https://doi.org/10.1242/jcs.194738>.
  57. Dupré, A., Haccard, O., Jessus, C., (2011). Mos in the Oocyte: How to Use MAPK Independently of Growth Factors and Transcription to Control Meiotic Divisions. *J. Signal Transduct.*, <https://doi.org/10.1155/2011/350412>.
  58. Lindqvist, A., van Zon, W., Karlsson Rosenthal, C., Wolthuis, R.M.F., (2007). Cyclin B1-Cdk1 activation continues after centrosome separation to control mitotic progression. *PLoS Biol.*, 5, <https://doi.org/10.1371/journal.pbio.0050123> e123.
  59. Takei, N., Nakamura, T., Kawamura, S., Takada, Y., Satoh, Y., Kimura, A.P., Kotani, T., (2018). High- sensitivity and high-resolution in situ hybridization of coding and long non-coding RNAs in vertebrate ovaries and testes. *Biol. Proced. Online*, 20, 6. <https://doi.org/10.1186/s12575-018-0071-z>.
  60. Yurttas, P., Vitale, A.M., Fitzhenry, R.J., Cohen-Gould, L., Wu, W., Gossen, J.A., Coonrod, S.A., (2008). Role for PADI6 and the cytoplasmic lattices in ribosomal storage in oocytes and translational control in the early mouse embryo. *Development*, 135, 2627-2636. <https://doi.org/10.1242/dev.016329>.
  61. Aleshkina, D., Iyyappan, R., Lin, C.J., Masek, T., Pospisek, M., Susor, A., (2021). ncRNA BC1 influences translation in the oocyte. *RNA Biol.*, <https://doi.org/10.1080/15476286.2021.1880181>.
  62. Han, S.J., Martins, J.P.S., Yang, Y., Kang, M.K., Daldello, E.M., Conti, M., (2017). The translation of cyclin B1 and B2 is differentially regulated during mouse oocyte reentry into the meiotic cell cycle. *Sci. Rep.*, 7 <https://doi.org/10.1038/s41598-017-13688-3>.
  63. Takada, Y., Iyyappan, R., Susor, A., Kotani, T., (2020). Posttranscriptional regulation of maternal Pou5f1/Oct4 during mouse oogenesis and early embryogenesis. *Histochem. Cell Biol.*, 154, 609-620. <https://doi.org/10.1007/s00418-020-01915-4>.
  64. Takei, N., Takada, Y., Kawamura, S., Sato, K., Saitoh, A., Bormann, J., Yuen, W.S., Carroll, J., et al. (2020). Changes in subcellular structures and states of pumilio 1 regulate the translation of target Mad2 and cyclin B1 mRNAs. <https://doi.org/10.1242/jcs.249128>.
  65. Trapphoff, T., Heiligentag, M., Dankert, D., Demond, H., Deutsch, D., Fröhlich, T., Arnold, G.J., Grümmer, R., et al.,

- (2016). Postovulatory aging affects dynamics of mRNA, expression and localization of maternal effect proteins, spindle integrity and pericentromeric proteins in mouse oocytes. *Hum. Reprod.*, 31, 133-149. <https://doi.org/10.1093/humrep/dev279>.
66. Tetkova, A., & Hancova, M. (2016). Mouse Oocyte Isolation, Cultivation and RNA Microinjection, BIO- PROTOCOL. <https://doi.org/10.21769/bioprotoc.1729>.
67. Masek, T., del Llano, E., Gahurova, L., Kubelka, M., Susor, A., Roucova, K., Lin, C.-J., Bruce, A.W., et al., (2020). Identifying the translome of mouse NEBD-stage oocytes via SSP-profiling; A novel polysome fractionation method. *Int. J. Mol. Sci.*, 21, 1254. <https://doi.org/10.3390/ijms21041254>.
68. Herbert, A.D., Carr, A.M., Hoffmann, E., Lichten, M., (2014). FindFoci: A focus detection algorithm with automated parameter training that closely matches human assignments, reduces human inconsistencies and increases speed of analysis. *PLoS One*, 9 <https://doi.org/10.1371/journal.pone.0114749>.
69. Stauffer, W., Sheng, H., Lim, H.N., (2018). EzColocalization: An ImageJ plugin for visualizing and measuring colocalization in cells and organisms. *Sci. Rep.*, <https://doi.org/10.1038/s41598-018-33592-8>.

## Supplementary Figures and Tables

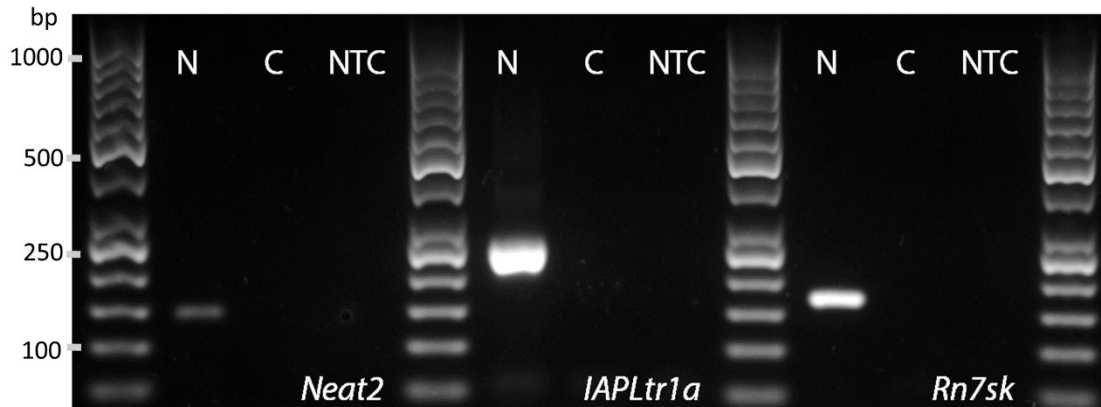


**Supplementary Fig. 1. Controls for RNA FISH.** (A) Negative control for RNA FISH. Detection of bacterial *DapB* RNA (*Bacillus subtilis*, EF191515.1, green) which is not expressed in mammalian cells. Details show nuclear, chromosomal and pronuclear areas, DAPI (blue), dashed line shows cell cortex, scale bars 20  $\mu\text{m}$ ,  $n \geq 15$ . (B) Negative control for RNA FISH.

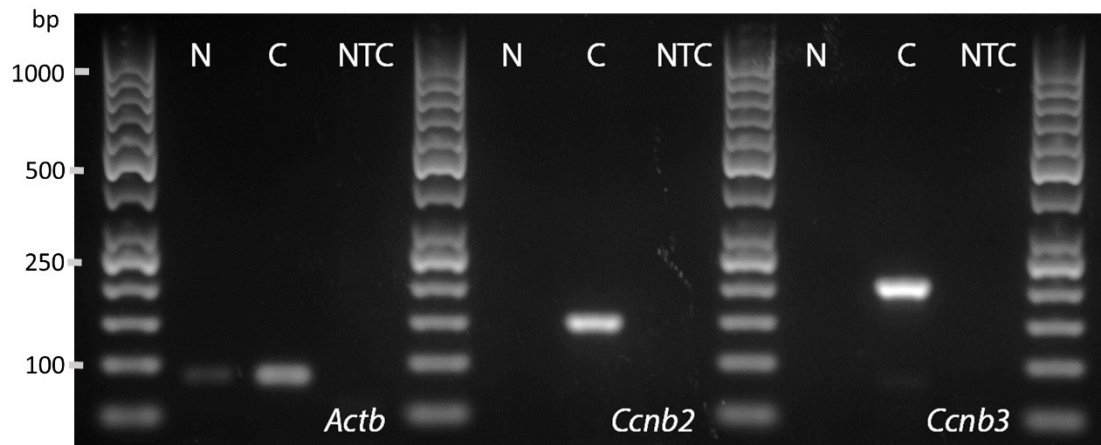


Detection of *Ccnb2* mRNA (green) with absence (-) and presence (+) of RNase A. DAPI (blue), dashed line shows cell cortex, scale bars 20  $\mu$ m,  $n \geq 15$ . (C) Average number of *Ccnb3* mRNA molecules from whole volume of oocytes and zygote. Mean  $\pm$  SD, Student's *t*-test: \*\*\* $p < 0.001$ ; *ns* for non-significant. (D) Graph shows trends of relative quantification of *Ccnb3* mRNA (Y axis, red) from whole cellular volume. Y' axis (blue) shows relative *Ccnb3* expression quantified from single equatorial Z-section axis, red) from whole cellular volume.

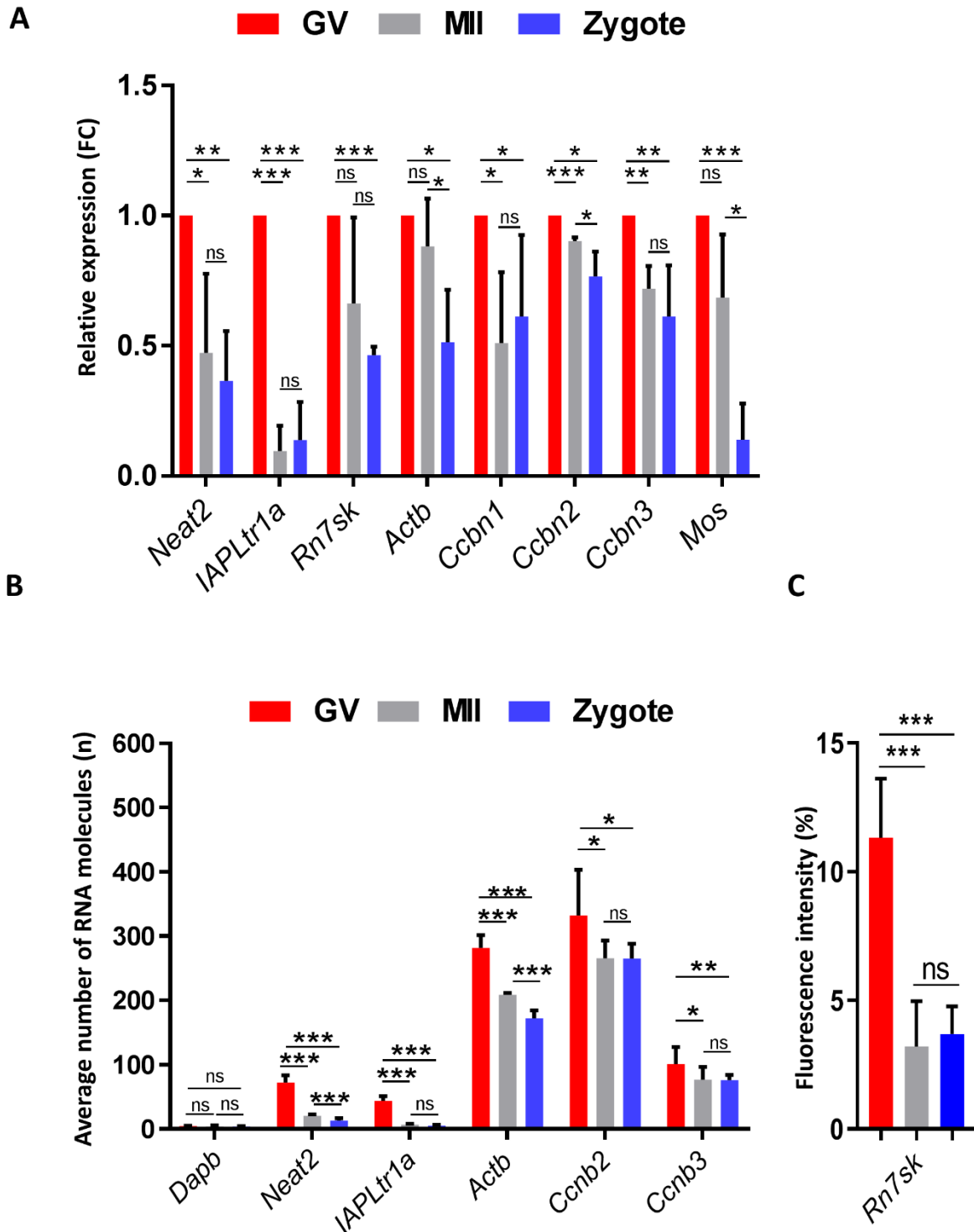
**A**



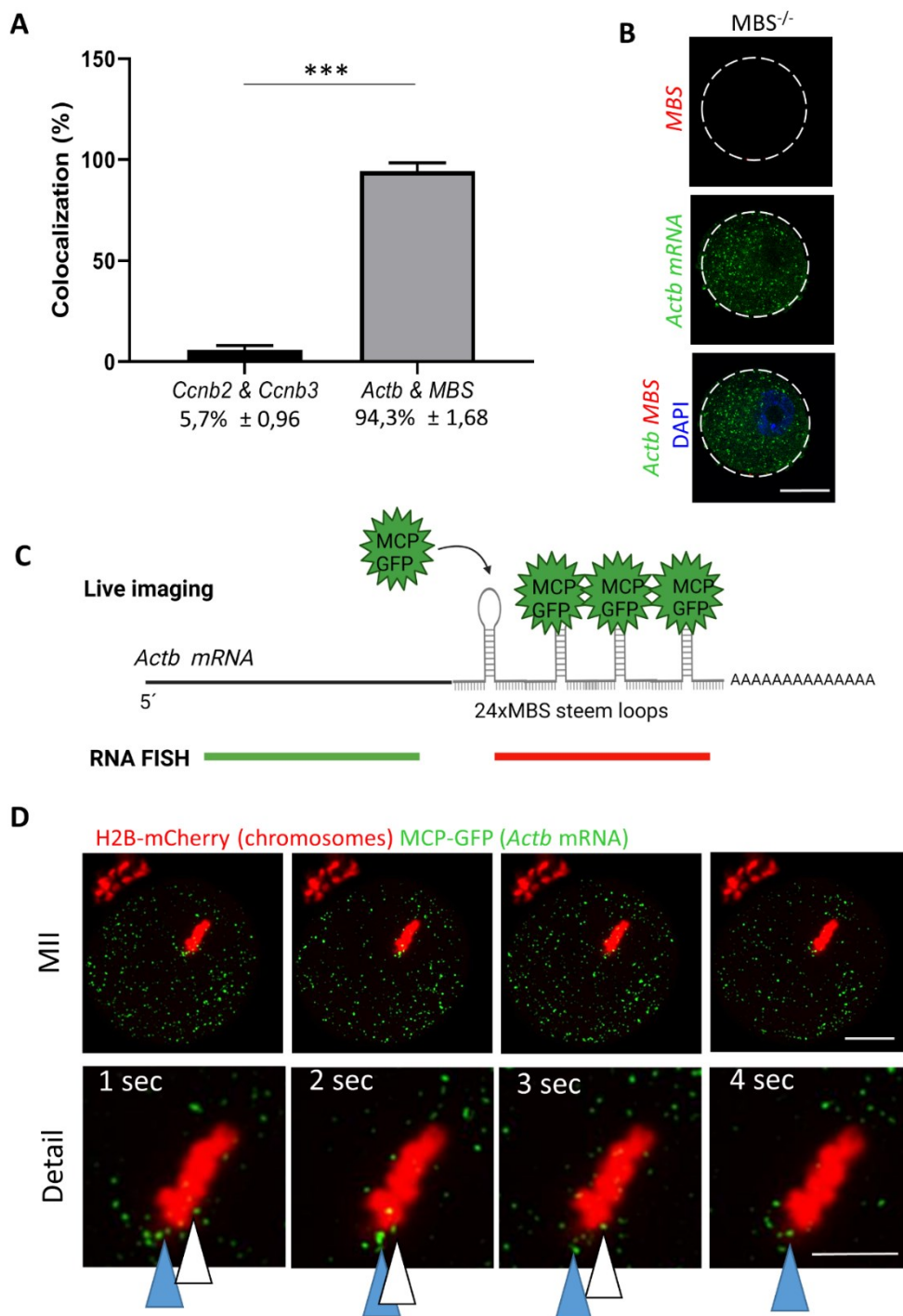
**B**



**Supplementary Fig. 2. Validation of RNA localization from nucleus and cytoplasmic fractions of the GV oocyte.** (A) PCR analysis of selected ncRNAs (*Neat2*, *IAPLtr1a*, *Rn7sk*). (B) PCR analysis of selected mRNAs (*Actb*, *Ccnb2*, *Ccnb3*). RNA isolated from nucleus (N) and cytoplasm (C) fractions. Negative technical control without template (NTC), marker 50 bp,  $n \leq 3$ .



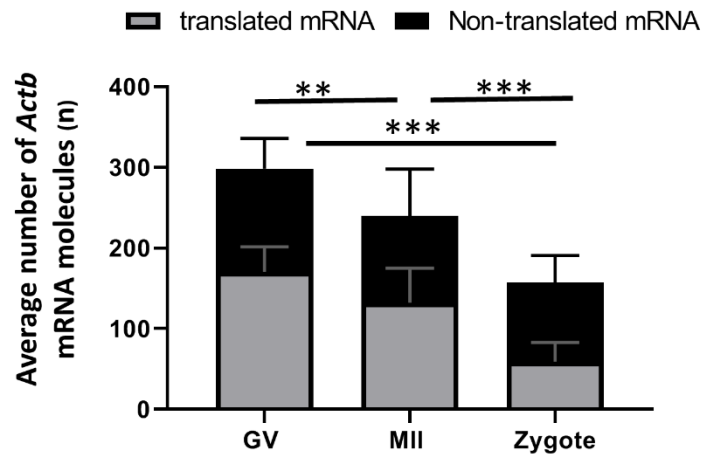
**Supplementary Fig. 3. Quantification of selected RNAs in oocytes (GV, MII) and zygotes.** (A) qRT-PCR quantification of expression of selected RNAs in the oocyte and zygote. Values obtained for GV oocyte were set as 1. Mean  $\pm$  SD, Student's *t*-test: \* $p < 0.05$ , \*\* $p < 0.01$ , \*\*\* $p < 0.001$ , ns for non-significant,  $n \geq 3$ . (B) Quantification of the number of RNA molecules in equatorial Z-section for *Neat2*, *IAPLtr1a*, *Actb*, *Ccbn2*, *Ccbn3*. Bacterial *DapB* RNA was used as a negative control. Values obtained for GV oocyte were set as 1. Mean  $\pm$  SD, Student's *t*-test: \* $p < 0.05$ , \*\* $p < 0.01$ , \*\*\* $p < 0.001$ , ns for non-significant,  $n \geq 15$ . *Ccbn1* and *Mos* mRNAs were quantified in the Fig.5B. (C) Quantification of *Rn7sk* snoRNA fluorescence. Value obtained for GV oocyte was set as 1. Mean  $\pm$  SD, Student's *t*-test: \*\*\* $p < 0.001$ , ns for non-significant,  $n \geq 15$ .



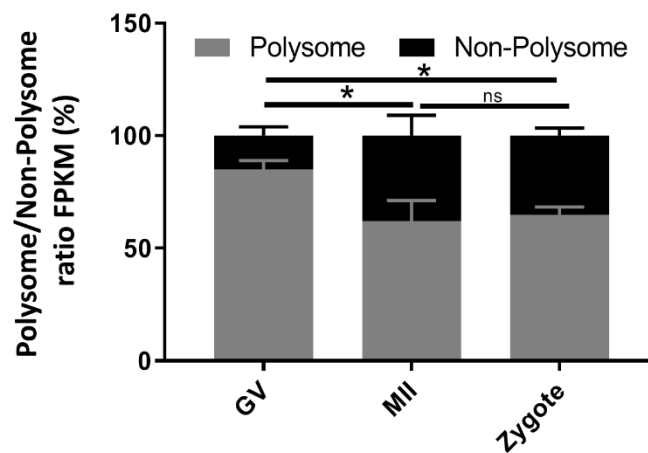
**Supplementary Fig. 4. Quantification of colocalization of RNAs from multiple staining. Detection of *Actb* mRNA in live oocyte. (A)** Quantification of colocalization of *Ccnb2* and *Ccnb3* mRNAs (black) from Fig. 3A and *Actb* mRNA with MBS on 3'UTR (grey) from Fig. 3B. Below values show mean  $\pm$  SD, Student's *t*-test Stat  $n \geq 20$ . (B) RNA FISH in GV oocyte from mouse without MBS 3'UTR sequence (*MBS*<sup>-/-</sup>). *Actb* mRNA (green), MBS sequence (red), DAPI (blue), dashed line shows cell cortex,  $n \geq 20$ , scale bars 20  $\mu$ m. (C) Scheme shows detection of *Actb* mRNA in the live cell and by dual colour RNA FISH presented in the Fig. 3B. (D) Time lapse imaging of endogenous *Actb* mRNA (green) labelled with MCP-GFP in live MII oocyte. H2B-mCherry (red), details show chromosomal area, arrowhead depicts movement of single mRNA molecule in time, scale bars 20  $\mu$ m.



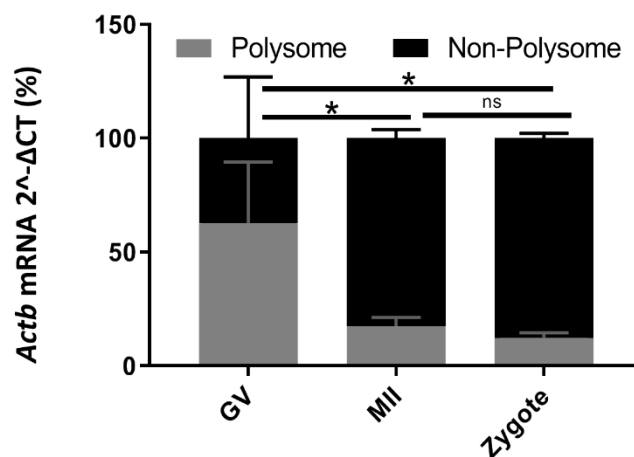
A



B

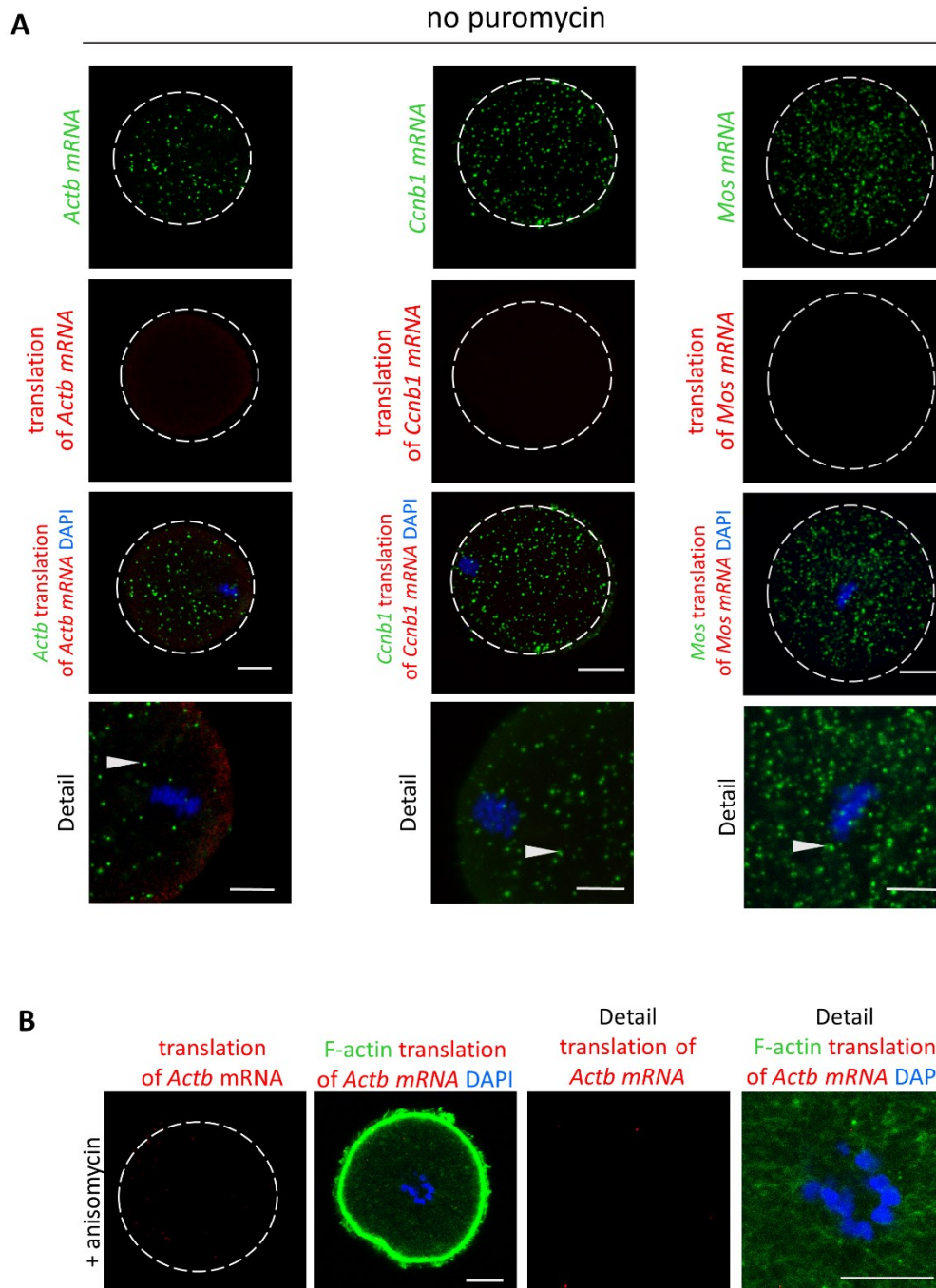


C



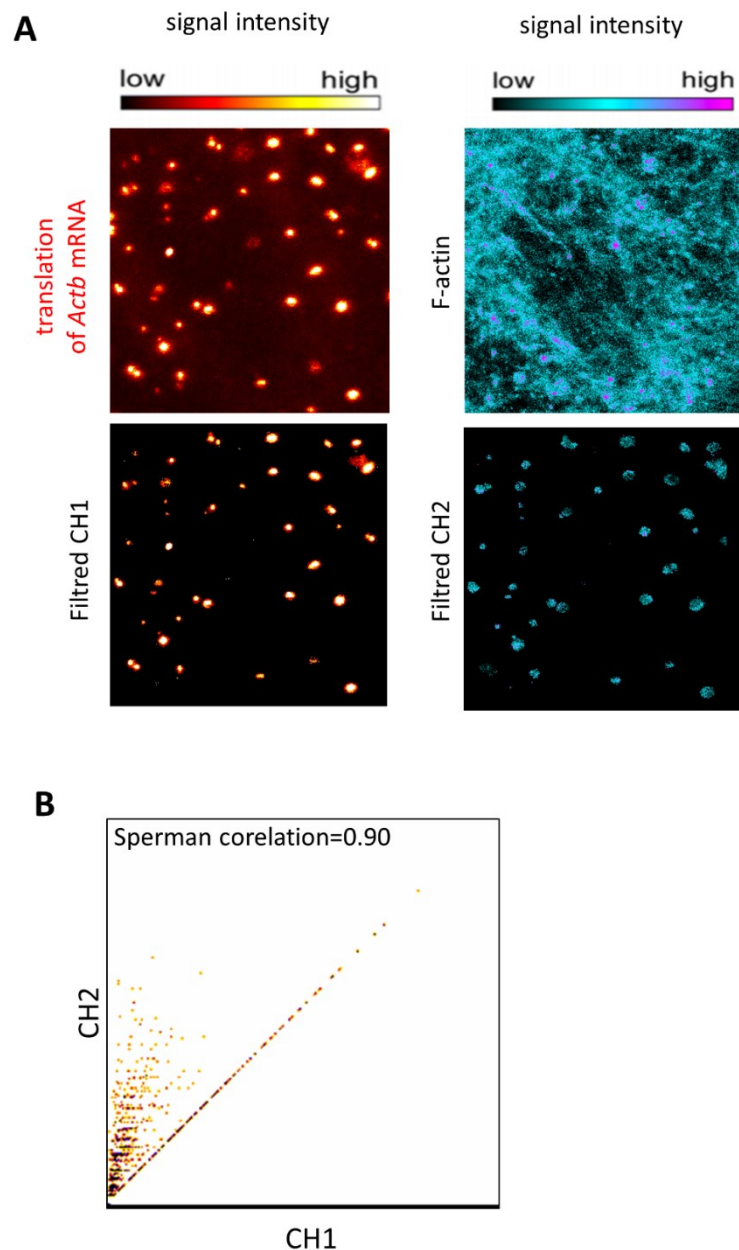
**Supplementary Fig. 5 Simultaneous detection of translational event of *Actb* mRNA in oocyte and zygote copies its polysomal occupancy.** (A) Quantification of *in situ* *Actb* mRNA (grey) and its translational event (puro-PLA, red) in oocytes and zygotes. From Fig. 4A.

n<sub>3</sub>; mean ± SD, Student's *t*-test: \**p* < 0.05, \*\**p* < 0.01, \*\*\**p* < 0.001; *ns* for non-significant. (B) Polysomal occupancy of *Actb* mRNA in oocytes and zygotes. Data from RNA seq, polysomal occupation (red) and non-polysomal (grey). Mean ± SD, Student's *t*-test: \**p* < 0.05, \*\**p* < 0.01, \*\*\**p* < 0.001; *ns* for non-significant. Raw data are presented in the Supplementary Table 1. (C) Validation of *Actb* mRNA sequencing results from polysomal and non-polysomal fractions by qRT-PCR. Mean ± SD, Student's *t*-test: \**p* < 0.05, \*\**p* < 0.01, \*\*\**p* < 0.001; *ns* for non-significant, n<sub>4</sub>.



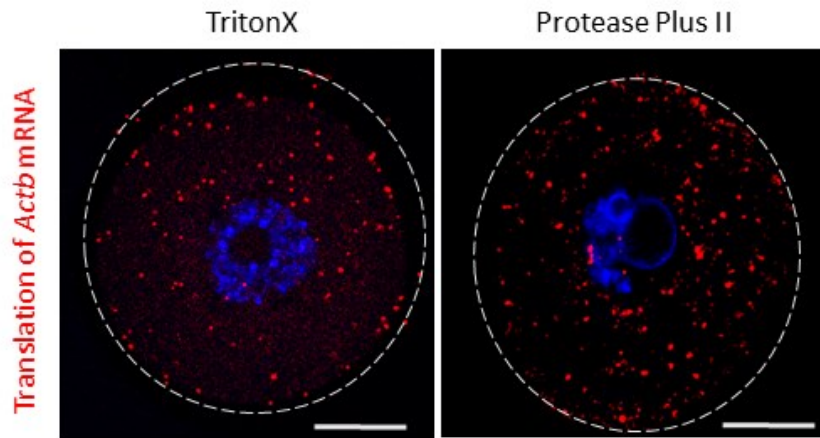
**Supplementary Fig. 6. Negative controls for simultaneous detection of specific mRNA and its translation in oocyte by RNA-puro-PLA assay. (A)** Negative control for RNA-puro-PLA assay without puromycin. Detection of specific mRNA (RNA FISH, green) and its translational event (puro-PLA, red) in the MII oocyte. n<sub>15</sub>, details show chromosomal area,

DAPI (blue), arrowheads depict single mRNA molecule, dashed line shows cell cortex, scale bar 20  $\mu\text{m}$ . **(B)** Depletion of elongation of translation by 100  $\mu\text{M}$  Anisomycin used as negative control for detection of ACTB translation by puro-PLA (red) and F-actin (green).  $n \geq 15$ , details show chromosomal area, DAPI (blue), scale bars 20  $\mu\text{m}$ .

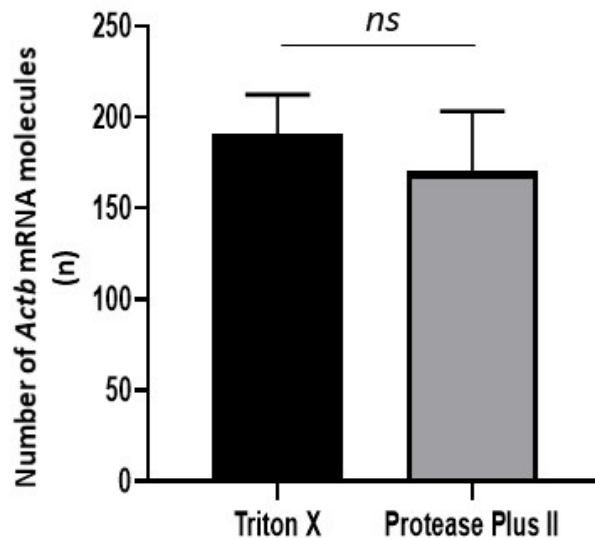


**Supplementary Fig. 7. Analysis of colocalization of *Actb* translation (red) with F-actin (blue).** **(A)** Representative images and relative magnitude of fluorescence intensity presented by heat maps show *Actb* translation (Channel 1, CH1, red) and F-actin (Channel 2, CH2, blue) by Ezcolocalization. **(B)** Both filtered areas measured in Colo2 plugin. Scatter plot of channel2/channel1 shows Spearman coefficient= 0.9; Coloc2 shows Pearson coefficient  $r = 0.57$ .

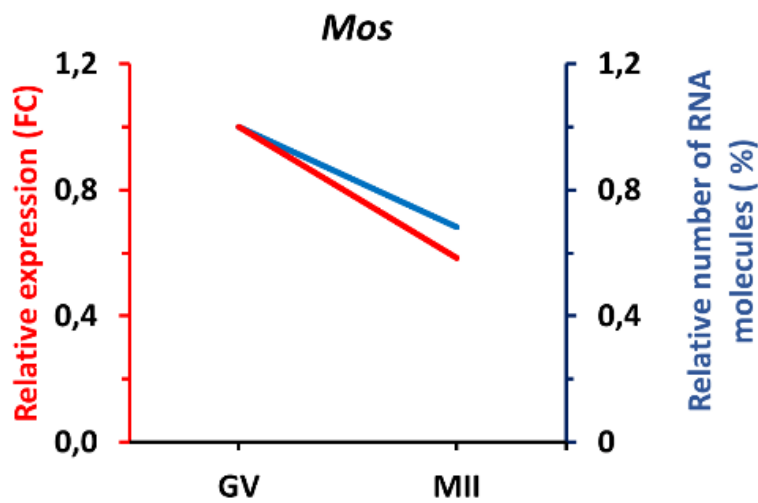
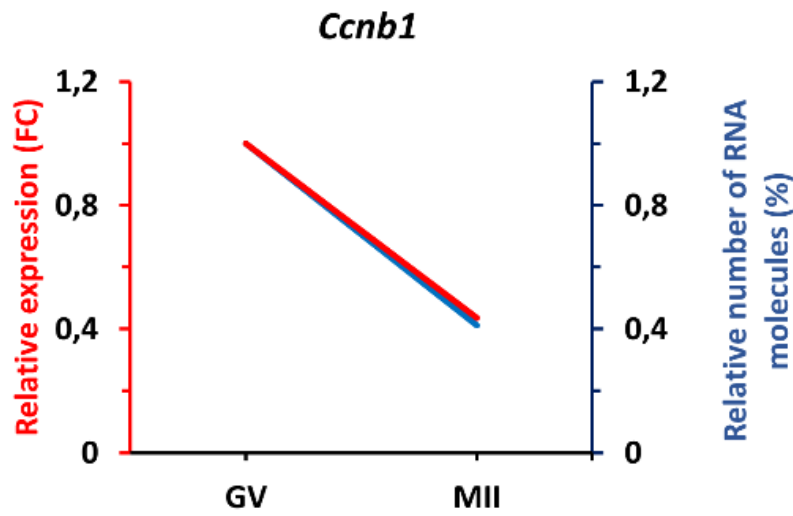
**A**



**B**

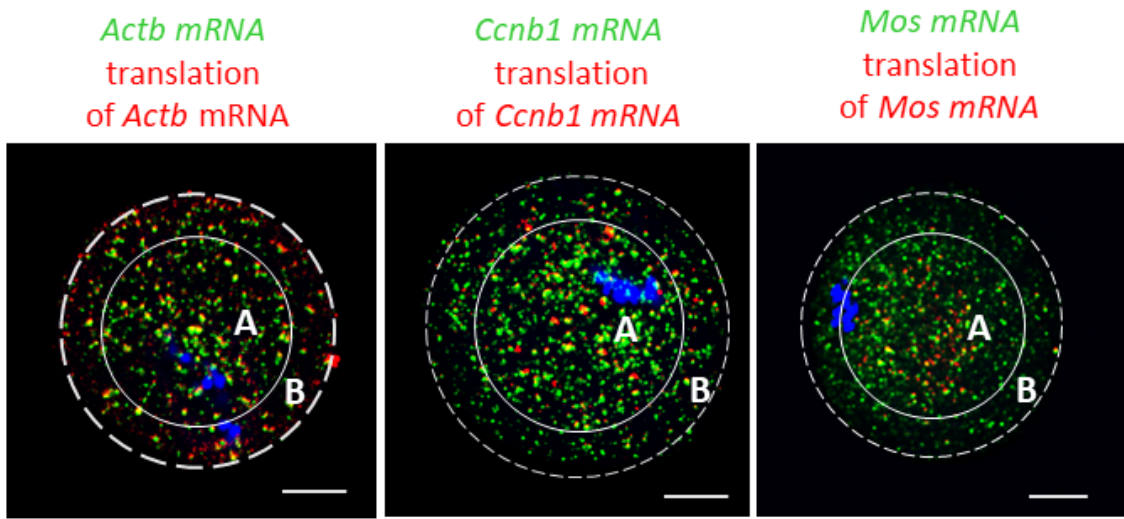


**Supplementary Fig. 8. Using of Protease Plus II do not influence detection of translation by puro-PLA assay in the cell. (A)** Representative images of puro-PLA of oocytes permeabilized with Triton X or protease Plus II for 10 min post fixation (puro-PLA, red), DAPI (blue), dashed line depicts cell cortex, scale bar 20  $\mu$ m. **(B)** Graph shows quantification of translational events in the cell under specific treatment, mean  $\pm$  SD, Student's *t*-test: *ns* for non-significant, from 3 biological experiments with  $n \geq 15$ .

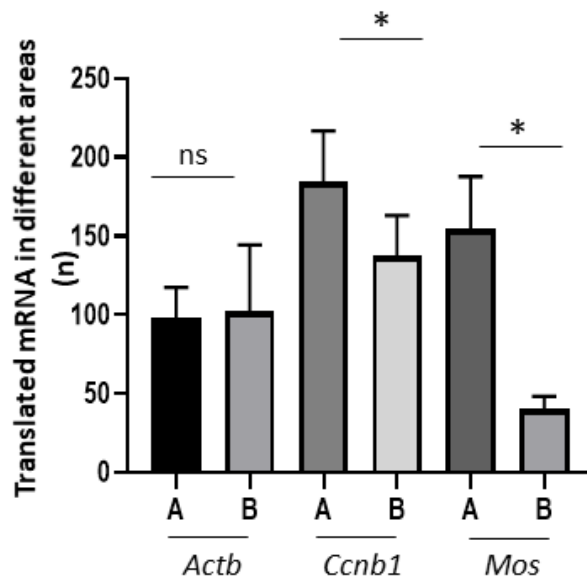


**Supplementary Fig. 9. Trends of expression of selected mRNAs in oocytes and zygote.** Graphs shows trends of relative quantification of *Ccnb1* and *Mos* mRNAs from qRT-PCR (Y axis, red) and RNA-puro-PLA (Y' axis, blue). Quantification of the number of RNA molecules per cell is presented in the Fig. 5B and expression measured by qRT-PCR Supplementary Fig. 3A.

A



B



**Supplementary Fig. 10. Quantification of translation in the subcellular context.** (A) Representative images with depiction of quantified areas, cellular center (A, depicted by circle) and cellular cortex (B, depicted with dashed line). Scale bar =20  $\mu$ m (B) Graph shows quantification of translational events in the above depicted subcellular areas A&B, mean  $\pm$  SD, Student's *t*-test: *ns* for non-significant; \**p*<0.05, from 3 biological experiment with *n* $\geq$ 5.

**Sequence of intracisternal A particle long terminal repeat RNA (IAPLtr1a)**

**IAPLTr1a\_I\_MM**

attaagaattggtccggaataatccgggacgagaaaaatccgggacgaaaaatacaagaaaactcgggaaccggcgcaaggaagatccctcattccaagaaccagaactcggg  
gtcgcggttaataaagttcccgtaaacgagactgtaagaaggattcaactgcatgaattcagaactttcagctggggaacgagagtaccagtgagtacagctttcaaggtaa  
gtctggtcttgaactttcaaggaattcaagacagctctatcagaagtaagtggaaaatagctttacaaggtatgtttgacctgaattttctagtgttaggagccctttgtcct  
ttccatgttatcaagtgattaagatagggctgaaaatctggatgaaatcagggcaatctatcagaagtaagcggggagagagtaggagcaagagaaaaataggtac  
acaaaataagtatacaggcctttcaagggtctgaaacccgaggaagaaatgtaggtcaggtagaatctctggggagagatagaaggaaggaaaaagaaaaagaaaa  
aaagatcaatagcggaggtctcagagatactgtaactagatgagctcaggaagccagctcttagtagctgaagcagatgaagaattcctctgaggaaaacagactggg  
aggaagaagcagccattaccagccagctaatggtcaagaaaaagcacaagcggctggcgaagccagcgtactgttcaacctcgggagctcggttcaaggtccgctcct  
atgcccggacccccccctgctgtagtgcgtcagcaatgcccagagaggcaatgcccagagaggcaatgcccagagaggcagtgcccagagaggcagtgcccagagaggcagt  
gcccagagaggcagtgcccagactcattcctccagagagaaacaaaggaatacaacaggcatttccagctttgaaggagcggagggtggcgctccacgctccggtag  
aatagctacagattaagaactgcccagctggtcgaataacggaaccaatgctaattttacctgggtcagttagacagggctccggcatggcactaactcctgctgactggc  
aaacgattgtaaaagcgcctccttagtagggcaaatatggaatggagagcctttggcacgaagctgcacaagcagggcccagcaaacgcagctgttactccag  
agcagagagattggactttgactgttaacgggtcagggagcttattctgctgacagaaaactaccattggggagcttatgcccataatctccacggcttagggcctgga  
aggcgtctcccagcaggtgaagccactgggagcttaacaaagataatcaggggacctcaggagctcttcagattttggtggcgaagatgacagaggcagcagagcgtat  
ggagagtcagagcaagccgctccttgtagaagcagctcatatgagcaagccacaaaggagtgcccagcggccatagccccaaagaaacaaaggttcaagactggc  
tcagggtttgtagagagctgggggacctctcagcaatgtaggttttagcgctccatcctcaatcccaaaaccgctccatgggcagaaataatcagaggacatgttttaactgcg  
gaaagcctgggcattttaagaaagattgcagagctccagataaacaggggagggactcactctttgctcaagtgtggcaagggttatcatagagccagcaggtgctgctg  
agggatataaaggcagaatcctcccacctgtagtaactagcttatgccaacaaaccgggtcatcgggcccctcggctccaggggcctcaagatagggaaccggtttgt  
caggaccagggaagcagtcagagaggcagccaggaaagcccaaggggtggacgtgctgcccctcagctcttataatgctcaaatgagttcagccggtgccagtg  
gagcctataccatccttgcgggggaacatgggcttattctggcggggttactcactcaccagggcttagtagccacctggagttatgattgcaacatcccctgaaa  
tacaggtcctgtgctcaagcccaaaaggcctttttcttagtaaaaggagataggatagctcagctgctgctcctccctgataataccagggagaaatgtaggacctgagata  
agaaaatgggctcctcaggaatgattctgctatttgggtatctttgtaagtagacctaagctccgcttaagatcaacgaaaagagttgaaggcatcctgataccggag  
cagataaaaagataattctacacattggtggcccaagcatggccaccacagagatctctcattacagggcctaggttatcaatcatgtcccataaagctccattgctt  
gacgtgggaatcctctgaagggcagcaagggaaatcataccttatgtgctccactccgggttaacctctggggaaggataattatgtagcattgggcttattttccaatga  
aaacgccccatcgggaggtattcagctaaagcaaaaatcatggaagatgggtataaagaaggaaggggttaggacatcaagaacaggggaaggatagagccatc  
tcacctaaggaacaaagacagagaggggtcgggtttcttagtggccattggggcagcagcaccataccatggaaaacaggggaccagtggtggttctcaatggccccct  
atcctctgaaaaaactagaagctgtgattcaactggtagaagcaataaaactaggccatattgaaacctcactcactcctggaatactcaatgtttgtaataagaaaaagtc  
aggaaaagtgagactgctccatgacctcagagccatgagcaaatgaaactatttggccagtagcagaggggtcctcctgactttccgcttaccagctggctggaat  
tattatagatataaagattgtttctttctatacctttgtccaaggataggccagatttgcctttaccatcccctcttataatcacatggaacctgataagaggtatcaatggaa  
ggtcttaccaggggaatgccaatgctcactatgtgtcaactttatgtgcaagaagctctttgtagcagtgaggaacaattcccctttaaatttgcctttcatgagatgacat  
cctcctgtccataaagacctaccatgctcaaaaaggcatatcctttctactaaaacttaagtcagtggggtttacagatagccagaaaaagtcacaatttctgatacagg  
acaattctgggctctgtggtgtcccagataagattgtgccccaaaaggtagagataagaagagatcactccataccttaaatgatttcaaaagctgttgggagatattaatg  
gtcagaccttttaaaagattcctcgtgagttaaagccttgggtttggtattttagaaggagatcctcactatctcctccctaggactcttactcagctgtaacccagggcttaca  
aaggtggaaaaaacctcagaaatgcaacatgtaggattgagccttgcagccttgcagcttgcctttaaagacagcaacaattgccaaccgagtttggcagaaatggg  
cattgttgggacatcaaacgtatcccagctaaaataatagattggtatctgtagcaattgcacagcttgccttaaaggcctaaaagcagcaatcaccactttggggca  
agtccatcttttaattgactttataccgctgcacaggttcaaacctggcagccacatcaatgattgggagttttagtacctctttcaggacaaaatagataaccattatcca  
aaacatccaattttacagtttgcacaaaatcaatctgttgggttccacaaaataagcaagaaacccactaaaaatgggattggtgataatactgtaggatacaaaactggcata  
ggtgctatgtggtaatgtaagtggtatcaaaaataatgaaaatcactcaagtgtagaattgtaggttttagaagttttaaacccttttagaacccttaaatat  
tgttcagattcctgttatgtggttaatgcaagtaacttttagaagtggtggagtgataagcctccagtagagttgccaatattttcagcagatacaatgattttgttatctag  
aagatttcctgtttatattactcatgttagagcccattcaggcctcagccctggcctgggaaatgattggcagataaggccactaaagtggtgctgctgctcctatc  
ccggtagaggctcaagaaaatttcatacaaatttcatgtgagcggctgaacattacgcagctgtttctccttgacaagaaaagggcccgtgacattgtactcaatgcaaaag  
ctgctgtgagttcttccagttcctatgtgggaatcaaccacgctgattcagctcctcagggctggcaaatggatgttacacatgtttctccttggaaaactcaatctcca  
tgtgtccattgacacatgttctggcatcatgttctcctcctgtaaccggagaaaaagcctcagatgattcaacattgtcttgaggatggagtgctgggggaaacccaaactc  
cttaagactgataatggaccagcttatacgtctcaaaaatccagcagttctgcctcagatggacgtaaccacctgactggactccatacaacctcaaggacagggatgtt  
gagcgtgcatcgcacccctcaaagcctatctataaaaacagaagggggaactttgaagagactttaccggagcacaagagtgctgtgctatggcacttttactactcaat  
tttttaaatattgctcattggccatactcggctgaacgtcattgtcagagccagataggcccaatgagatggttaaatggaataatgctcctgataataatggatggcccg  
gatcctatgttataagatccaggggagcgtctgtgtttccacagaatgaagcaacccatttggataccagaagactcaccgaaaaatccagactgaccaaggaata  
ctgatgctcctcgtctgtgtagtccagggcgtcaataaagaagagagcagcgttggggataatgtgacatttccactccaatgacggtgtagataatgctcaagattc  
tctcctttttaccactaaactaggaaactgggtttggccttgattcagacagcttggctgctgtagcaggtccagacgactgacaccattaaactttgtcagcctcagtgactac  
agtcatagataaaacaggcctcagctaatgtcaagatacagggaggtctcatgctggttaatacaactatagatctgtccagatacaactagatgattatggcaaatagctcagct  
gggatgtgacaaaagttccgggattgtgttacttccattcagtagttaaattactagggcagcctaattgtcaaaaagctttttcagtatatgttacagaattggacggctg  
aatttgaacagatcttcgggaattgagactcaggctcaactccacgctggacctgctcctgacccaagattaccaatggatctccagcattttcctctttaaagaatg  
ggtgggattgataattttggagatacactttgctggttagttgttcttctgattggtctgtaagcttaaggcccaaaactaggagagacaaggggttattgccaggccttg  
caggactagaactggagcttcccctgataatctatgcttaggcaataggtcgtggcactcagctcttatccatgaggctagctcattgcacgggatagagtgatgtg  
cttcagcagcccagagagttgacggtaagcactgagtagaagggctctcggcataatagcctatttagggagacatgctatcttcaagaaggttagtgccaagt  
gtccttctcaggcaaaacgacacgggagcaggtcaggggttctcgtgggttaaagcctgtagcctaagagtaactcctgtacatggctcctttacacactggggttga  
cctctatcctcactcattaatgggtggcctatttgccttataaaggaaagggggaga

**Supplementary Fig. 11. Sequence of intracisternal A particle long terminal repeat RNA (IAPLtr1a).**



Start	Stop	Strand	Gene Symbol	gene_biotype	gene_name	gene_source	gene_version	Havana gene_version	F1_GV_A	F1_GV_B	F1_GV_C	F1_MII_A	F1_MII_B	F1_MII_C	F1_zygote_B	F1_zygote_C	F1_zygote_D	F6_GV_A	F6_GV_B	F6_GV_C	F6_MII_A	F6_MII_B	F6_MII_C	F6_zygote_B	F6_zygote_C	F6_zygote_D
1.43E+08	1.43E+08		Actb	protein coding	Actb	ensembl_havana	14	5	108.845	60.8981	167.316	22.8961	34.7678	25.9893	85.6173	60.2325	93.1908	603.202	491.035	712.061	50.7782	37.2941	49.5436	134.902	128.102	175.935

Supplementary Table 1: Raw values obtained from RNA-seq of non-polysomal (F1) and polysomal fractions (F6)

A

RNA target	Accession No.	Target region	No. of ZZ pairs	Channel	Cat. No.
<i>Actb</i>	NM_007393.3	2 - 406	6	C1	316741
<i>Ccnb1</i>	NM_172301.3	697 – 1140	10	C1	316241
<i>Ccnb2</i>	Nm_007630.2	53-1531	18	C2	530761-C2
<i>Ccnb3</i>	NM_183015.3	2514 – 3537	18	C3	804331-C3
<i>DapB</i>	EF191515	404-862	10	C1	310043
<i>Mos</i>	NM_020021.2	2-965	20	C2	819361-C2
<i>IAPLTR1a</i>	IAP LTR sequence; Suppl. Fig. 8	3241-4258	20	C1	577641
<i>MS2</i>	(MS2 binding sequence from Lionnet 2011)	2-1100	20	C3	819401-C3
<i>Neat2</i>	NR_002847.2	712 - 2338	30	C2	313391
<i>Rn7sk</i>	NR_030687.1	21-323	7	C2	426741-C2

B

Primary antibodies	Cat. No., Company	Western Blot	Immunocytochemistry	puro-PLA
Acetylated Tubulin	T6793, Sigma Aldrich	not used	1:150	not used
Lamin A/C	SAB4200236, Sigma Aldrich	not used	1:150	not used
Puromycin	MABE334, Merck Milipore	not used	not used	1:150
Actin beta	0061R, Bios	not used	not used	1:100
<i>Mos</i>	PA5-101081, Invitrogen	not used	not used	1:100
Cyclin B1	MS-338-PO, Thermo Fisher	not used	not used	1:100

Supplementary Table 2.

A) Table of probes used for RNA FISH.

B) Table of used antibodies.

<b>RNA target</b>	<b>Forward 5'-3'</b>	<b>Reverse 5'-3'</b>	<b>Gene Bank ID</b>	<b>Product size (bp)</b>
<i>Actb</i>	TCCTTCTGGGTATGGAATCCT	GTCTTTACGGATGTCAACGTCA C	NM_007393.5	84
<i>Ccnb1</i>	TACAGCTGGTCGGTGTAACG	TGCACCATGTCGTAGTCCAG	NM_172301.3	282
<i>Ccnb2</i>	CCGACGGTGTCCAGTGATTT	AGGTTTCTTCGCCACCTGAG	NM_007630.2	141
<i>Ccnb3</i>	GAAAAGGAAGGCCAAGATCC	CAGGGTCTCATGGGTCATCT	NM_183015.3	198
<i>Gapdh</i>	TGGAGAAACCTGCCAAGTAT G	GGTCCTCAGTGTAGCCCAAG	NM_001289726.1	93
<i>IAPLTR1a</i>	CAAGGGTCTTGAACCCGAGG	GGTAATGGGCTGCTTCTTCCT	designed according sequence in S.Fig.8	224
<i>Mos</i>	GTATAAAGCCACTTACCACGG	CAATGTTTCAGTTCAGCCCA	NM_020021.3	107
<i>Neat2</i>	AGGGAAAAGGGGGAAAGC	AGGGGTGAAGGGTCTGTGAT	NR_002847.2	133
<i>Rn7sk</i>	AGGACGACCTTCCCCGAATA	GCGCCTCATTTGGATGTGTC	NC_000075.6	161

**Supplementary Table 3. Primers used for PCR.**

## **SGK1 is essential for meiotic resumption in mammalian oocytes**

Edgar del Llano<sup>1</sup>, Rajan Iyyappan<sup>1</sup>, Daria Aleshkina<sup>1</sup>, Tomas Masek<sup>3</sup>, Michal Dvoran<sup>1</sup>, Zongliang Jiang<sup>2</sup>, Martin Pospisek<sup>3</sup>, Michal Kubelka<sup>1</sup>, Andrej Susor<sup>1</sup>.

<sup>1</sup>Laboratory of Biochemistry and Molecular Biology of Germ Cells, Institute of Animal Physiology and Genetics, CAS, Libečhov, Czech Republic

<sup>2</sup>School of Animal Sciences, AgCenter, Louisiana State University, Baton Rouge, LA, 70803, United States

<sup>3</sup>Laboratory of RNA Biochemistry, Department of Genetics and Microbiology, Faculty of Science, Charles University, Viničná 5, 128 44, Prague, Czech Republic

### **ABSTRACT**

In mammalian females, oocytes are stored in the ovary and meiosis is arrested at the diplotene stage of prophase I. When females reach puberty oocytes are selectively recruited in cycles to grow, overcome the meiotic arrest, complete the first meiotic division and become mature (ready for fertilization). At a molecular level, the master regulator of prophase I arrest and meiotic resumption is the maturation-promoting factor (MPF) complex, formed by the active form of cyclin dependent kinase 1 (CDK1) and Cyclin B1. However, we still do not have complete information regarding the factors implicated in MPF activation.

In this study we document that out of three mammalian serum-glucocorticoid kinase proteins (SGK1, SGK2, SGK3), mouse oocytes express only SGK1 with a phosphorylated (active) form dominantly localized in the nucleoplasm. Further, suppression of SGK1 activity in oocytes results in decreased CDK1 activation via the phosphatase cell division cycle 25B (CDC25B), consequently delaying or inhibiting nuclear envelope breakdown. Expression of exogenous constitutively active CDK1 can rescue the phenotype induced by SGK1 inhibition. These findings bring new insights into the molecular pathways acting upstream of MPF and a better understanding of meiotic resumption control by presenting a new key player SGK1 in mammalian oocytes.

### **INTRODUCTION**

In women, oocyte quality is an essential factor for a successful fertilization, pregnancy and embryo development. Consequently, poor oocyte quality is one of the most common hindrances to natural and assisted reproduction (Homer, 2020; Keefe et al., 2015; Krisher, 2004). Unlike somatic cells, oocytes undergo a meiotic cell division instead of mitosis. Therefore, in order to tackle poor oocyte quality, a better understanding of the mechanisms orchestrating the oocyte meiotic divisions is needed. In mammals, oocyte formation and entry into meiosis occur during the early stages of development, meaning that mammalian females are born with a determined pool of oocytes in their ovaries. Interestingly, the reserve of oocytes in the ovaries are arrested at the diplotene stage of prophase of the first meiotic cell division (prophase I) (van den Hurk and Zhao, 2005). At this stage, also referred to as the germinal vesicle (GV) stage, the chromatin is still not fully condensed and the nuclear envelope is intact and visible. This arrest continues until the female reaches puberty. From that point onwards, oocytes are selected in cycles to develop further and ovulate, resuming their meiotic cell divisions and becoming able to be fertilized (Edson et al., 2009).

The maturation-promoting factor (MPF) complex is the master regulator of this release from the prophase I arrest and subsequent meiotic resumption. It is a heterodimer composed of Cyclin Dependent Kinase 1 (CDK1) and Cyclin B1 (Gautier et al., 1990; Sharma et al., 2018; Pan and Li, 2019). Up to date several other proteins have been identified as regulators of MPF activity during meiosis, mainly related to the inhibitory phosphosites of CDK1 (Thr14 and Tyr15) and the amount of Cyclin B1 in the cell. In order to activate MPF, Cyclin B1 levels increase during M phase and the above-mentioned residues must be dephosphorylated. The prophase I arrest is maintained by protein kinase A (PKA), which activates the WEE1 kinase (which phosphorylates Thr14 and Tyr15) and inactivates CDC25 (responsible for dephosphorylating these inhibitory sites). At the time of ovulation, a drop in cGMP levels allows PDE3A to reduce cAMP in the oocyte. With low cAMP, PKA becomes inactive which ultimately results in the activation of MPF (Tripathi et al., 2010). Active MPF triggers meiotic resumption and the release of oocytes from the prophase I block characterized by nuclear envelope breakdown (NEBD), chromosome condensation and the subsequent first meiotic division (MI) (Norris et al., 2009; Sharma et al., 2018).

The Phosphoinositide 3-kinase/ Protein Kinase B (PI3K/AKT) pathway is also involved in meiotic resumption. In mammals, PI3K/AKT has been reported to be involved in Cyclin B1 expression and CDK1 activation (Roberts et al., 2002). Specifically, when AKT activity is suppressed in mouse oocytes, their meiotic resumption potential is significantly diminished (Kalous et al., 2006). Interestingly, in starfish oocytes Hiraoka et al. (2016a) observed that the PI3K/AKT pathway alone may not be enough to activate CDK1 and therefore other pathways should be involved. Later, the same group discovered that serum-glucocorticoid-regulated kinase (SGK) was indispensable for CDC25 phosphorylation and Myt1 inactivation (Hiraoka et al., 2019).

Until now, studies on SGK function in oocytes have been performed only on starfish (Hiraoka et al., 2019; Hosoda et al., 2019) leaving the role of SGKs in mammalian oocytes largely unknown. As SGK proteins are evolutionary conserved in mammals it is highly possible that they also have functional roles in higher animal species. In this study using the mouse model, we have shown for the first time the role of SGKs for the resumption of meiosis in mammalian oocytes.

Our results show that only SGK1 isoform is expressed in fully grown oocytes. Moreover, we demonstrate that SGK1 inhibition delays NEBD via negative influence of CDK1 activation. Our findings strengthen the hypothesis that SGK (SGK1 in mammals) is essential for MPF activation and oocyte meiotic resumption.

## RESULTS

### **Of the SGK genes only SGK1 is expressed in the mouse oocyte and its inhibition hinders nuclear envelope breakdown.**

In mammals, there are three genes coding for different SGK proteins: SGK1, SGK2 and SGK3. Although all proteins have a very similar structure, they differ in specific regions and their expression are dynamic throughout various tissues (Bruhn et al., 2010; Kobayashi et al., 1999; Lang and Cohen, 2001). To determine which SGKs are expressed in the mammalian oocyte, we first performed RT-PCR to verify the presence or absence of their respective mRNAs. The results showed that mRNAs coding for all SGKs are present in the mouse kidney and brain while ovaries and oocytes contain only *Sgk1* and *Sgk3* (Figure S1A, B). Furthermore, we performed Western Blot (WB) to detect SGK protein expression in mouse oocytes. As expected, all SGK proteins were expressed in the mouse kidney while ovaries expressed SGK1 and SGK3. Interestingly, despite the presence of both *Sgk1* and

*Sgk3* mRNAs in oocytes, only the SGK1 protein was expressed at similar levels throughout all oocyte maturation stages (Figure 1A). Furthermore, polysomal datasets showed that *Sgk1* mRNA has the highest translation in the GV oocyte (Figure S1C) while mRNA coding for SGK3 is absent. However, SGK3 translation was significantly increased in the 2 cell embryo (Figure S1C).

The detection of SGK1 indicated its potential role in the oocyte. To unveil this role, we treated GV oocytes with a specific SGK1 inhibitor (GSK-650394, Merck, Darmstadt, Germany; Sherk et al., 2008) which restricts SGK1 activity (and SGK2 with less affinity) and has been already used in several fields of research (Berdel et al., 2014; Bomberger et al., 2014; Xiao et al., 2019). We applied concentrations of 0.01mM and 0.03mM of SGK1 inhibitor based on previously published results to keep cells viable for 48h (Alamares-Sapuay et al., 2013). Initially, we validated the effect of the SGK1 inhibitor on oocytes by checking the phosphorylation status of the known SGK1 substrate NDRG1 (Thr346) (Murray et al., 2004). The results confirmed that the inhibitor treatment suppressed SGK1 activity, as phosphorylation of NDRG was significantly reduced (Figure S2). When SGK1 was inhibited, 88 % of oocytes treated with 0.01mM concentration underwent nuclear envelope breakdown (NEBD), which was similar as the control group, however, when treated with the 0.03mM concentration, only 26 % of oocytes underwent NEBD (Figure 1B). Nonetheless, although most of the oocytes from the 0.01mM group underwent NEBD, there was a significant delay compared to the control oocytes ( $211 \pm 98$  minutes and  $67 \pm 15$  minutes, respectively) (Figure 1C). To analyse the reversibility of the SGK1 inhibitor, oocytes were cultured in the presence of the inhibitor (0.01mM) for one hour and then released. Those oocytes were able to undergo NEBD in  $97 \pm 14$  minutes, that is, 30 minutes later than the control.

Moreover, we noticed a significant delay in polar body extrusion (PBE) when SGK1 was inhibited (Figure 1D). To determine if this effect is due to the reported NEBD delay itself or whether SGK1 inhibition affects further meiotic stages, we introduced the SGK1 inhibitor at different time points during meiosis. The results show that SGK1 inhibition has a delaying effect on PB extrusion when oocytes were treated with the inhibitor up to four hours after IBMX removal (Figure 1D). However, the timing of PBE was not affected when SGK1 was inhibited later (Figure 1D).

In conclusion, our results show that only one member of the SGKs family (SGK1) is expressed in mouse oocytes and also suggest a role in the regulation of NEBD and PBE up to the first 4 h after meiotic resumption.

**The active form of SGK1 is concentrated in the oocyte nucleus and its expression decreases along the first meiotic division.**

SGK1 becomes active when phosphorylated at Thr256 (Kobayashi and Cohen, 1999; Chen et al., 2009). To better understand the role of SGK1 in the mammalian oocyte we further focused on the localization of its active form by immunocytochemistry (ICC) at different meiotic stages. We found that SGK1 (Thr256) is dominantly localized in the nucleus of the GV oocyte and at the subsequently newly forming spindle (Figures 2A and B). Similarly, the highest SGK1 phosphorylation levels were detected in the GV oocyte with a continuous significant decrease during meiotic progression to minimum in the MII stage (Figures 2A and B). These results are in accordance with the previous live cell experiments, which show that SGK1 inhibition has its strongest effect on meiotic GV-NEBD transition (Figures 1C and D).

### **Inhibition of SGK1 impairs CDK1 activation through CDC25B (Cell Division Cycle 25B) phosphatase in the oocyte prior to NEBD.**

The delay of NEBD caused by SGK1 inhibition pointed towards a possible effect of SGK1 on the master regulator of meiosis, CDK1. To test this hypothesis, we performed WB experiments to detect the inactive form of CDK1 (Tyr15) in oocytes in absence (control, DMSO 0.02%) or presence of SGK1 inhibitor (0.01mM) at different time points after an IBMX wash (0, 30 and 60 minutes) (Figures 3A and B). It is well known that the phosphorylation of CDK1 at Tyr15 must be removed to activate the kinase in order to resume meiosis (Coleman and Dunphy, 1994; Schmidt et al., 2017). The GV arrested oocyte group (0 minutes) was incubated for one hour in the presence of IBMX and treated with SGK1 inhibitor (or DMSO). Both groups showed maximal levels of CDK1 (Tyr15) as expected without any major differences. However, after 30 minutes post IBMX wash, inactive CDK1 levels (phosphorylated on Tyr 15) significantly decreased in non-treated oocytes while oocytes in SGK1 inhibitor continued to show high levels. After one hour, the differences were even more pronounced between the two groups, as non-treated oocytes were already at the NEBD stage and treated oocytes were still at the GV stage (Figures 3A and B).

As SGK1 is a protein kinase and CDK1 activation occurs through dephosphorylation (of Thr14 and Tyr15), we hypothesised that it must act through other proteins. Based on the literatures (Cazales et al., 2005; Pirino et al., 2009; Hiraoka et al., 2016b) and our *in silico* prediction interaction (Supplementary Table 1) the phosphatase CDC25B (which is known to dephosphorylate CDK1 on Tyr 15) proved to be a potential candidate as an SGK1 substrate. Therefore, we conducted a similar WB analysis to detect the activation of CDC25B phosphatase. The obtained results were in positive correlation with the previously detected activity of CDK1 (Figures 3A and B). Arrested GV oocytes (0 minutes) showed no difference between the control and SGK1 inhibition with regards to the level of total CDC25B nor to its phosphorylation state (represented by two shifted bands) (Figures 3C and D). However, when the oocytes were released from the IBMX block, differences became apparent. After 30 minutes, the lower band of control oocytes was fainter in comparison with SGK1 inhibited oocytes, indicating the activation of CDC25B. This shift was even more profound at 45 minutes after meiotic resumption, when a new higher band (representing the hyperphosphorylated CDC25B) appeared in control oocytes, while the lowest (hypophosphorylated) band disappeared. On the other hand, the oocytes cultured in the presence of SGK1 inhibitor still showed the presence of the lower hypophosphorylated band without any apparent hyperphosphorylated band visible (Figure 3C and D).

These results indicate that SGK1 plays a regulatory role in CDK1 activation and meiotic resumption upstream of CDC25B, and that CDC25B may in fact be its direct substrate.

### **The phenotype resulting from SGK1 inhibition can be reversed by activation of CDK1.**

Based on the above presented data which show that activation of CDK1 by SGK1 inhibition is negatively influenced (Figures 3A and B) and that CDK1 activation is a key event for the timing and promoting of NEBD (Koncicka et al., 2018), we sought to confirm that the SGK1 effect in oocytes is upstream of CDK1 activation. To that end, we microinjected oocytes with mRNA coding for CDK1-AF, a constitutively active CDK1 which cannot be phosphorylated on Tyr15 or Thr14 and therefore, allows oocytes to overcome meiotic arrest even in the presence of IBMX (Figure 4A) (Adhikari et al., 2016; Akaike and Chibazakura, 2020; Hagting et al., 1998). WB



of injected oocytes confirmed that the CDK1 protein was overexpressed compared to non-injected controls (Figure S3). First we expressed CDK1-AF in oocytes by microinjecting RNA coding for CDK1-AF + H2B-GFP in the presence of a higher concentration of SGK1 inhibitor (0.03mM) as seen in Figure 1B. The meiotically arrested phenotype caused by SGK1 inhibition was successfully overcome after CDK1-AF overexpression as 83% ( $\pm 0.35$ ) of these oocytes went through NEBD compared to only 27% ( $\pm 0.75$ ) of control oocytes (microinjected with RNA coding for H2B-GFP) (Figure 4A).

Next, we performed experiments with a smaller concentration of SGK1 inhibitor (0.01mM), which caused oocyte meiotic resumption delay (Figure 1C). For this experiment, one group of oocytes was microinjected with *H2b-gfp* RNA as a negative control and was cultivated in the presence of SGK1 inhibitor. The other two groups were microinjected with *Cdk1-AF + H2b-gfp* RNA; one group was cultivated in the presence of a solvent vehicle (0.02% DMSO) and another group in the presence of SGK1 inhibitor. All oocyte groups were arrested at the NEBD stage for 4h in the presence of IBMX after microinjection. After IBMX release, oocytes without expression of the constitutively active form of CDK1 showed a significant NEBD delay ( $214 \pm 15$  minutes) similarly as seen in Figure 1C. On the other hand, oocytes expressing CDK1-AF underwent NEBD significantly faster ( $127 \pm 8$  minutes) even in the presence of SGK1 inhibition (Fig.4B). Altogether, these results suggest a role of SGK1 in the regulation of NEBD in mammalian oocytes by influencing the regulatory pathway involved in CDK1 activation.

## DISCUSSION

Oocyte meiotic arrest and timely resumption are fundamental steps in mammalian meiosis. After much research, MPF has been accepted as a master regulator of such events. However, so far only a few key elements have been identified and described in detail as being involved in the MPF pathway (Edson et al., 2009; Sharma et al., 2018, Pan and Li, 2019). Data of the present study suggest SGK1 as a new player in mammalian oocyte meiotic resumption which is of great importance for the better understanding of the regulation of meiosis.

Up to now, no SGK protein has ever been linked to the process of meiosis (Bruhn et al., 2010; Lien et al., 2017; Di Cristofano, 2017). Only the recent studies by Hiraoka et al. (2019) have demonstrated that SGK protein was needed to overcome prophase I arrest at the GV stage in starfish oocytes (*Asterina pectinifera*). According to their work, SGK phosphorylates and activates CDC25, which in turn leads to the activation of MPF (cyclinB-CDK1) so the oocyte can proceed through the G2/M phase and continue meiosis. However, there are no reports on the matter outside of the starfish and, despite its advantages to study early reproduction, it is evolutionary far from vertebrates including humans. Therefore, our study provides much-needed information by focusing on the SGK role in mammals using the mouse model (*Mus musculus*).

Compared to the starfish whose genome codes for a single SGK protein, the mouse genome contains three different genes coding for three known SGK isoforms (SGK1, SGK2 and SGK3). These proteins share a sequence identity of 80% in their catalytic domain but only SGK3 contains an N-terminal phosphoinositide-binding Phox homology (PX) domain (Bruhn et al., 2010; Kobayashi et al., 1999; Lang and Cohen, 2001). Interestingly, despite their high similarity, SGKs have different tissue expression: SGK1 and SGK3 seem to be found in all tissues but tightly regulated, whereas SGK2 expression is dominant in the liver, pancreas, brain and kidney (Kobayashi et al., 1999). Accordingly, our results document the presence of *Sgk1* and *Sgk3* mRNAs in both ovaries and oocytes.

However, despite both SGK1 and SGK3 proteins being expressed in mouse ovaries, we detected only the SGK1 in mouse oocytes. These results correlate with previously published oocyte translome data (del Llano et al., 2020; Masek et al., 2020). Importantly, *Sgk3* mRNA is absent from oocyte polysomes but it starts to have a stronger polysomal presence after fertilization (Masek et al., 2020; Potireddy et al., 2006) and Figure S1C concomitantly with its transcription (Zeng et al., 2004). This suggests SGK1 as the sole isoform present in mouse oocytes and functioning in meiosis regulation while SGK3 is become translated after fertilization.

Hiraoka et al. (2019) speculated that SGK3 could be involved in mammalian oocyte meiosis based on the fact that it is the isoform most related to starfish SGK as both contain the N-terminal PX domain. In their experiments SGK was knocked-down from starfish oocytes causing a perpetually arrested GV phenotype which was later successfully reversed by exogenously expressing human SGK3. However, our findings suggest that SGK1 and not SGK3 is present in mouse oocytes. This seeming contradiction might be explained by the fact that only the catalytic domain may have a role in oocyte meiosis from both starfish and mammals, whereas the N-terminal PX domain would be irrelevant. This indicates that both SGK1 and SGK3 with 80% similarity of the catalytic domain can phosphorylate similar targets (Kobayashi et al., 1999; Bruhn et al., 2010). Therefore, it would be interesting to repeat Hiraoka et al. (2019) rescue experiments expressing human SGK1 or SGK2 instead of SGK3 and analyse the effect on oocyte meiosis. This could prove the conclusion that the N-terminal PX domain is not necessary for oocyte meiotic resumption.

To investigate the potential role of SGK1 in the fully grown mammalian GV oocyte, we decided to perform several experiments using a selective SGK1 inhibitor (GSK-650394). The inhibitor concentrations of 0.01mM and 0.03mM were selected according to a previously published study reporting them as being able to keep cells viable for 48h (Alamares-Sapuay et al., 2013). Surprisingly, our results after SGK1 inhibition at 0.03mM were similar to those obtained by Hiraoka et al. (2019): meiotic resumption (G2/M transition) was suppressed and most oocytes did not continue through NEBD. In other words, selective SGK1 inhibition in mammalian oocytes had a similar effect as inhibition of SGK in starfish oocytes. Our results reinforce the essential role of SGK in meiotic resumption in both starfish and mouse oocytes. Moreover, smaller amounts of SGK1 inhibitor (0.01mM) allowed oocytes to go through NEBD but at a much slower pace, pointing out that even small amounts of SGK1 can phosphorylate the necessary levels of G2/M transition key players if given enough time. The inhibitory effect was fully reversible for both concentrations as removing the inhibitor from the media allowed the oocytes to reach the MII stage. It is also noteworthy to mention that in our previous research we showed that these oocytes which underwent the first meiotic division in the presence of the inhibitor at 0.01mM suffered from significantly abnormal cytokinesis (del Llano et al., 2020). Whether these abnormalities are the result of SGK1 acting on the oocyte spindle itself or the result of a delayed meiotic resumption is not clear and needs further investigation, however, the new results presented here point towards the latter possibility.

Furthermore, we were able to uncover the time window of action of SGK1 in meiotic resumption thanks to the slower meiotic division caused by SGK1 inhibitor (0.01mM). By adding inhibitor at different time points and following the timing of PB extrusion we concluded that SGK1 activity is necessary up to 4 hours after meiotic resumption. Nonetheless, its role is most relevant at the beginning of the resumption of meiosis.

At the molecular level, we found that the cause of meiotic arrest (or delay) in GV oocytes treated with SGK1 inhibitor was caused by a failure in MPF activation, more specifically by impeding the removal of the inhibitory Tyr15 phosphorylation of CDK1. However, as a protein kinase, SGK1 cannot act directly to dephosphorylate CDK1. To that end, we further investigated and proved that SGK1 inhibition also had an effect on CDC25B activation, the upstream phosphatase of CDK1 at Tyr15 (Cazales et al., 2005; Pirino et al., 2009; Hiraoka et al., 2016b). This also positively correlated with the data on SGK in starfish oocytes, where it was proven that SGK inhibition blocked meiotic resumption by preventing the activation of CDC25 and therefore MPF remained inactive (Hiraoka et al., 2019). Surprisingly, we observed that fully-grown GV oocytes already displayed high levels of active SGK1 (phosphorylated at Thr256). At this stage, the activator phosphosites of CDC25B are not yet phosphorylated and it is not until oocytes are released from a high cAMP environment that they are “allowed” to be phosphorylated (Coleman and Dunphy, 1994; Norris et al., 2009). The fact that SGK1 is active already in the GV oocyte might seem contradictory at first glance as it could be able to keep CDC25B phosphorylated and active the whole time. However, we also noticed that at that stage SGK1 (Thr256) is strongly localized in the nucleus, while CDC25B is known to remain in the cytoplasm before meiotic resumption and it is not until PKA is inhibited (by low cAMP levels) that CDC25B is quickly translocated to the oocyte nucleus right before NEBD (Lincoln et al., 2002; Solc et al., 2008; Ferencova et al., under revision). Therefore, we hypothesize that SGK1 (Thr256) is active but restricted to the nucleus, which keeps it physically apart from CDC25B, which would further activate it. When cAMP levels decline CDC25B translocates to the nucleus, where SGK1 (Thr256) could phosphorylate and activate it, allowing the further dephosphorylation of CDK1 inhibitory sites. This makes MPF active and capable to induce meiosis resumption (Figure 5). Our hypothesis can be further strengthened by the fact that SGK1 and CDC25B display a high degree of interaction potential according to the online software PSOPIA. However, it must be taken into account that the evidence presented here together with the published data on starfish oocytes, are indirect and need to be addressed more specifically to be fully proven. Otherwise, despite the clear relation between SGK1 and CDC25B in oocytes, it is not possible to exclude the possibility that they do not interact directly but that there is a longer pathway, which connects them both through other proteins.

Furthermore, it is important to note that research groups studying SGK1 in kidneys reported that mouse homozygous knockouts for SGK1 are subfertile (Fejes-Tóth et al., 2008; Faresse et al., 2012). On one hand, this highlights the potential importance of this protein in female reproductive cells, adding support to our data. On the other hand, however, it is not possible to exclude that the effect on litter size was due to SGK1 absence affecting other reproductive tissues (testes, ovary, uterus, etc.) as the mice were full KO.

In summary, we present evidence that SGK1 has an important and previously unknown role in mammalian meiosis, specifically for the process of meiotic resumption. We suggest SGK1 acts through the phosphorylation of CDC25B, which ultimately leads to MPF activation. This role might be extrapolated to other species as it seems to be evolutionary conserved between the mouse and starfish. This research contributes to further understanding of the pathways controlling MPF, the master regulator of oocyte meiotic resumption.

## **MATERIAL AND METHODS**

### **Oocyte collection and culture**

ICR mice (bred in-house) were injected 46h prior to oocyte collection to be primed with 5 IU pregnant mare serum gonadotropin (PMSG HOR 272, ProSpec, Rehovot, Israel). All oocytes were collected at the GV stage from the mice ovaries in the presence of transfer media supplemented with 100  $\mu$ M 3-isobutyl-1-methylxanthine (IBMX, Sigma-Aldrich, Darmstadt, Germany) to block meiotic resumption (as described in Tetkova and Hancova, 2016). From the GV collected oocytes, only the fully grown were selected, denuded by pipetting and transferred to M16 media (Sigma-Aldrich, Darmstadt, Germany) with IBMX at 37°C, 5% CO<sub>2</sub>. For oocyte samples at further advanced meiotic stages than GV, the oocytes were placed in M16 media (Sigma-Aldrich, Darmstadt, Germany) at 37°C, 5% CO<sub>2</sub> without IBMX. For SGK1 inhibitor treatments, the oocytes were transferred in M16 media (without IBMX) supplemented with 0.02% or 0.06% Dimethyl Sulphoxide (DMSO) for solvent vehicle control or 0.01mM or 0.03mM GSK-650394 (Merck, Darmstadt, Germany) inhibitor.

All animal work was conducted according to Act No 246/1992 for the protection of animals against cruelty; from 25.09.2014 number CZ02389, issued by Ministry of Agriculture.

### **Live cell imaging**

Oocytes were transferred from M16 media to a 4-well culture chamber (Sarstedt, Prague, Czech Republic) in 15  $\mu$ l of M16 covered with mineral oil (M8410; Sigma-Aldrich) so they could be cultivated further under an inverted microscope Leica DMI 6000B (Leica Microsystems, Wetzlar, Germany) under the same culture conditions (Tempcontroller 2000–2 Pecon, and a CO<sub>2</sub> controller, Pecon, Erbach, Germany) and monitored live. The live cell time lapse images were taken using LAS X software (Leica microsystems, Wetzlar, Germany) every 5 and 15 minutes.

### **RNA isolation and RT-PCR**

RNA was extracted from oocytes using RNeasy Plus Micro kit (74034, Qiagen, Hilden, Germany) which includes a step for genomic DNA depletion using gDNA Eliminator columns. Afterwards, RT-PCR was performed using a qPCRBIO cDNA synthesis kit (PCR BIOSYSTEMS, London, UK). For regular PCR the PPP Mastermix kit (Top-Bio, Vestec, Czech Republic) was used. Primer sequences are listed in Table S2A.

### **Immunoblotting**

Oocyte samples were lysed using 10ul 1x Reducing SDS Loading Buffer (lithium dodecyl sulphate sample buffer NP 0007 and reduction buffer NP 0004 [Thermo Fisher Scientific, Waltham, MA, USA]) and heated at 100°C for 5 minutes. Separation of proteins was carried out in gradient precast 4–12% SDS–PAGE gels (NP 0323, Thermo Fisher Scientific) and transferred onto an Immobilon P membrane (IPVD 00010, Millipore, Merck group, Darmstadt, Germany) using a semidry blotting system (Biometra GmbH, Analytik Jena, Jena, Germany) for 25 min at 5 mA per cm<sup>-2</sup>. Blocking was done using 5% skimmed milk dissolved in 0.05% Tween-Tris buffer saline (TTBS) with pH 7.4 for 1 h. The membranes were then briefly washed with TTBS and incubated with 1% milk/TTBS diluted primary antibodies (see table S2B) at 4°C O/N. Secondary antibodies, Peroxidase Anti-Rabbit Donkey and Peroxidase Anti-Mouse Donkey (711-035-152 and 715-035-151, Jackson ImmunoResearch, West Grove, PA, USA) were diluted 1:7500 in 1% milk/TTBS. Membranes were incubated with secondary antibodies for 1 h at room temperature. Proteins were visualised by chemiluminescence using ECL (Amersham) and imaged

on Azure 600 Imager (Azure Biosystems) and acquired signals were quantified using ImageJ (<http://rsbweb.nih.gov/ij/>).

### **Immunocytochemistry**

Oocytes were fixed in 4% paraformaldehyde (PFA, Alfa Aesar, Thermo Fisher Scientific, Waltham, MA, USA) in PBS/PVA and left for 15 min followed by permeabilization in 0.1% Triton (X-100, Sigma-Aldrich) PBS/PVA for 10 min. The oocytes were then washed in PBS/PVA and incubated with primary antibodies (see Table S2B) at 4°C O/N. The next day, two washes in PBS/PVA were applied followed by incubation with the corresponding secondary antibody and conjugation with Alexa Fluor 488 or 647 (Invitrogen, Carlsbad, CA, USA) for 1 h at room temperature protected from light. Next, the oocytes were washed in PBS/PVA twice and mounted on glass slides using ProLong™ Gold antifade reagent with DAPI (Invitrogen, Carlsbad, CA, USA). Images of samples were taken with a Leica SP5 inverted confocal microscope (Leica Microsystems, Wetzlar, Germany). Images were assembled in software LAS X (Leica Microsystems) and signal intensity from the spindle area was quantified with ImageJ.

### **RNA synthesis and microinjection**

*Cdk1-AF* and *H2b:gfp* RNAs were in vitro transcribed by using the correspondent plasmid templates (*Cdk1-AF*: pcDNA3-CDC2-AF (718) was a gift from Jonathon Pines (Addgene plasmid # 39872; <http://n2t.net/addgene:39872> ; RRID: Addgene 39872); *H2B-GFP*: provided by Dr Martin Anger, Laboratory of Cell Division Control, IAPG CAS) and mMESSAGE mMACHINE™ Transcription Kit (Invitrogen, Carlsbad, CA, USA). In vitro transcribed RNA was then injected into GV oocytes at a final concentration of 50 ng/μl in the presence of transfer media and IBMX. Microinjection of GV oocytes was performed using FemtoJet (Eppendorf) and TransferMan NK2 (Eppendorf, Hamburg, Germany) using an inverted microscope Leica DMI 6000B (Leica Microsystems, Wetzlar, Germany). Afterwards, injected oocytes in IBMX were incubated at 37°C, 5% CO<sub>2</sub> for 6 hours to give them enough time to translate the injected RNAs.

### **Polysome fractionation and RNA sequencing**

Polysome fractionation followed by RNA isolation was carried out according to the Scarce Sample Polysome profiling (SSP-profiling) method from Masek et al., 2020. Then, polysomal fractions (P; fractions 6–10) were pooled and subjected to qRT-PCR (QuantStudio 3 cycler, Applied Biosystems). Sequencing libraries were prepared using SMART-seq v4 ultra low input RNA kit (Takara Bio). Sequencing was performed with HiSeq 2500 (Illumina) as 150-bp paired-ends. Reads were trimmed using Trim Galore v0.4.1 and mapped onto the mouse GRCm38 genome assembly using Hisat2 v2.0.5. Gene expression was quantified as fragments per kilobase per million (FPKM) values in Seqmonk v1.40.0.

### **Statistical Analysis**

Data are mean ± standard error of mean (SEM) of (n) replicates. All percentage data are first subjected to arcsine square-root transformation and then subjected to statistical analysis. Data were analyzed either by Student's t- test or One-way ANOVA using GraphPad Prism Software (San Diego, California, USA) with post-hoc analyses with a 95% confidence interval. \*p <0.05, \*\*p <0.01, \*\*\*p <0.001 considered as statistically significant.

## LEGENDS

### **Figure 1. Of the SGK genes only SGK1 is expressed in the mouse oocyte and its inhibition hinders nuclear envelope breakdown.**

A) WB analysis of the expression of the three SGK proteins in oocytes (30 or 100 per sample) and control tissue; GAPDH was used as loading control. The images are representative from at least three biological replicates. For mRNA expression see Figure S1.

B) Quantification of oocytes undergoing nuclear envelope breakdown (NEBD) in the control (0.06% vehicle, DMSO) and presence of SGK1 inhibitor (GSK-650394). Data are represented as the mean  $\pm$  SEM of at least three independent experiments;  $n \geq 44$  oocytes; ns, not significant; \*\*\* $p < 0.001$ ; \*\* $p < 0.01$  according to One-way ANOVA after arcsine transformation. For inhibitor validation see Figure S2.

C) Timing of oocyte NEBD after IBMX wash in absence (Control, 0.06% vehicle DMSO) or presence of SGK1 inhibitor (0.01mM) for 10 hours and 1 hour. Box plot displays mean, 25th and 75th percentile and  $\pm$  SD of at least three independent experiments;  $n \geq 45$  oocytes; ns, not significant; \*\* $p < 0.01$  according One-way ANOVA.

D) Timing of oocyte cytokinesis (polar body extrusion) in absence (control, 0.06% vehicle DMSO) or presence of SGK1 inhibitor (0.01mM) added at different time points post-IBMX wash. Box plot displays mean, 25th and 75th percentile and  $\pm$  SD of at least three independent experiments;  $n \geq 26$  oocytes; ns, not significant; \* $p < 0.05$ ; \*\*\*  $p < 0.001$ ; according One-way ANOVA.

### **Figure 2. Active SGK1 is concentrated in the oocyte nucleus and its expression decreases along the first meiotic division.**

A) Immunocytochemistry shows dominant localization of SGK1 phosphorylated at Thr256 in the oocyte nucleus (grey and red). DAPI (blue), scale bar 15  $\mu$ m.

B) Quantification of SGK1 (Thr256) fluorescence at different oocyte areas and stages of meiosis. Data are represented as the mean  $\pm$  SEM of at least three independent experiments normalized to the group with highest intensity (GV) as 100% fluorescence;  $n \geq 40$  oocytes; ns, not significant; \* $p < 0.05$ ; \*\* $p < 0.01$ ; \*\*\* $p < 0.001$  according to One-way ANOVA for comparing oocyte stages and Student's t test for comparing oocyte areas.

### **Figure 3. Inhibition of SGK1 impairs CDK1 activation through CDC25B in the oocyte prior to NEBD.**

A) WB analysis of CDK1 (Tyr 15) at different timing of oocyte meiotic resumption in absence (control, 0.02% vehicle DMSO) and presence of SGK1 inhibitor (GSK-650394; 0.01mM). GAPDH and CDK1 (total) were used as a loading control. The images are representative from at least three biological replicates of 30 oocytes per sample.

B) WB quantification of CDK1 (Tyr15) normalized to CDK1 (total). Data are represented as the mean  $\pm$  SEM from at least three independent experiments;  $n = 30$  oocytes per sample; ns, not significant, \* $p < 0.05$ , \*\*\* $p < 0.001$  according to Student's t test.

C) WB analysis of CDC25B at different timing of oocyte meiotic resumption in absence (control, 0.02% vehicle DMSO) and presence of SGK1 inhibitor (0.01mM). GAPDH was used as a loading control. The images are



representative from at least three biological replicates of 30 oocytes per sample. The arrowheads depict phosphorylated variants of CDC25B.

D) WB quantification of CDC25B protein normalized to GAPDH. Data are represented as the mean  $\pm$  SEM from at least three independent experiments; 30 oocytes per sample; ns = not significant, \* $p < 0.05$ , \*\*\* $p < 0.001$  according to Student's *t* test.

**Figure 4. The phenotype resulting from SGK1 inhibition can be reversed by activation of CDK1.**

A) Quantification of oocytes undergoing NEBD after microinjection with RNA coding for *H2b-gfp* RNA (control) in the presence of SGK1 inhibitor or microinjected with RNA coding for H2B-GFP + CDK1-AF RNA in the presence of SGK1 inhibitor or IBMX. Data are represented as mean  $\pm$  SEM of at least three independent experiments;  $n = 39$  oocytes per group; ns, not significant, \* $p < 0.05$ , \*\*\* $p < 0.001$  according to One-way ANOVA.

B) Timing of NEBD after IBMX wash in oocytes microinjected with H2B-GFP RNA (control) in the presence of inhibitor or microinjected with H2B-GFP+CDK1-AF RNA in absence and presence of SGK1 inhibitor. Box plot displays mean, 25th and 75th percentile and  $\pm$  SD of at least three independent experiments;  $n \geq 30$  oocytes per group; ns, not significant; \*\*\* $p < 0.001$  according to One-way ANOVA.

**Figure 5. Hypothesis of role of the SGK1 in the resumption of meiosis.**

At the GV stage, SGK1 (Thr256) is active enclosed in the oocyte nucleus without effect on meiotic resumption. PKA is active when cAMP levels are high, phosphorylating CDC25B (Ser321), inhibiting this phosphatase and keeping it in the cytoplasm. Prior to nuclear envelope breakdown (NEBD), cAMP levels decline, PKA becomes inactive and CDC25B is dephosphorylated. Consequently, CDC25B localizes to the nucleus where active SGK1 (Thr256) phosphorylates the activation sites of CDC25B, and thus promotes the NEBD process.

**Supplementary figures**

**S. Figure 1. Mouse oocytes contain mRNA coding for SGK1 and SGK3.**

A) Representative images of mRNA PCR products detected in mouse oocytes and tissues. Non-template control (NTC).

B) *Gapdh* mRNA was used as a loading control.

C) Polysomal occupation of mRNAs coding for SGK1 and SGK3 in the GV, MII oocytes and 2 cell embryo. Three polysomal isolations for each stage, mean  $\pm$  SD, Student's *t*-test: ns, not significant, \*\*  $p < 0.01$ .

**S. Figure 2. Validation of SGK1 inhibitor (GSK-650394) using a known specific substrate.**

A) WB analysis of NDRG1 (Thr346) on GV oocytes cultured in presence of IBMX and in absence (control, 0.1% vehicle DMSO) and presence of SGK1 inhibitor (GSK-650394; 0.1mM). GAPDH was used as a loading control. The images are representative from at least three biological replicates of 100 oocytes per sample. See also Table S2 for the list of antibodies.

B) WB quantification of NDRG1 (Thr346) normalized to GAPDH. Data are represented as the mean  $\pm$  SEM from at least three independent experiments;  $N = 100$  oocytes per sample; \* $p < 0.05$  according to Student's *t* test.

### **S. Figure 3. Validation of CDK1-AF expression in microinjected oocytes.**

A) WB analysis of CDK1 and CDK1 (Tyr15) expression in oocytes microinjected with *H2b-gfp* RNA (control) or *Cdk1-AF + H2b-gfp* RNAs (CDK1-AF). GAPDH was used as a loading control. The images are representative from at least three biological replicates of 37 oocytes per sample. See also Table S2 for the list of antibodies.

B) Quantification of CDK (Tyr15) expression normalized to CDK1. GAPDH was used a loading control. Data are represented as the mean  $\pm$  SEM of at three independent experiments; \*  $p < 0.05$ , according to Student's t test.

**Supplementary Table 1.** Values for protein-protein interactions between SGK1 and CDC25B calculated by PSOPIA (Prediction Server of Protein-protein Interactions; <https://mizuguchilab.org/PSOPIA/>). Probabilities are expressed in scores 0 ~ 1.0.

**Supplementary Table 2.** List of primers used for PCR (A) and list of antibodies used (B).

### **AUTHOR CONTRIBUTIONS**

EDL and AS designed the experiments. EDL, AS and MK drafted and revised the manuscript. EDL was involved in all experiments and performed most of them. RY and DA performed oocyte microinjections. RY, MD, TM and MP prepared samples and polysomal fractions. ZJ sequences and analysed polysome bound RNA. AS and MK supervised the study.

### **FUNDING**

This research was funded by MSMT (EXCELLENCECZ.02.1.01/0.0/0.0/15\_003/0000460 OP RDE), GACR (19-13491S) and by Institutional Research Concept VO67985904. ZJ was supported by the NIH (R01HD102533) and USDA-AFRI-NIFA (2019-67016-29863). The funders had no role in study design, data collection and analysis, decision to publish or preparation of the manuscript.

### **ACKNOWLEDGMENTS**

The authors acknowledge Marketa Hancova and Jaroslava Supolikova (Institute of Animal Physiology and Genetics, Libechov, Czech Republic) for their valuable help in collecting oocyte samples. Jaroslava Supolikova was also important in performing Western Blots. The plasmid containing *Cdk1-AF* (pcDNA3-cdc2-AF (718)) was a gift from Jonathon Pines (Addgene plasmid # 39872; <http://n2t.net/addgene:39872>; RRID: Addgene\_39872) and *H2b:gfp* was provided by Dr. Martin Anger (Laboratory of Cell Division Control, IAPG CAS).

### **ETHICS STATEMENT**

All animal work was conducted according to Act No 246/1992 for the protection of animals against cruelty; from 25.09.2014 number CZ02389, issued by the Ministry of Agriculture.

### **BIBLIOGRAPHY**

- Adhikari, D., Busayavalasa, K., Zhang, J., Hu, M., Risal, S., Bayazit, M.B., Singh, M., Diril, M.K., Kaldis, P., and Liu, K. (2016). Inhibitory phosphorylation of Cdk1 mediates prolonged prophase I arrest in female germ cells and is essential for female reproductive lifespan. *Cell Res* 26, 1212–1225.
- Akaike, Y., and Chibazakura, T. (2020). Aberrant activation of cyclin A-CDK induces G2/M-phase checkpoint in human cells. *Cell Cycle* 19, 84–96.
- Alamares-Sapuay, J.G., Martinez-Gil, L., Stertz, S., Miller, M.S., Shaw, M.L., and Palese, P. (2013). Serum- and glucocorticoid-regulated kinase 1 is required for nuclear export of the ribonucleoprotein of influenza A virus. *J Virol* 87, 6020–6026.
- Berdel, H.O., Yin, H., Liu, J.Y., Grochowska, K., Middleton, C., Yanasak, N., Abdelsayed, R., Berdel, W.E., Mozaffari, M., Yu, J.C., et al. (2014). Targeting Serum Glucocorticoid-Regulated Kinase-1 in Squamous Cell Carcinoma of the Head and Neck: A Novel Modality of Local Control. *PLOS ONE* 9, e113795.
- Bomberger, J.M., Coutermarsh, B.A., Barnaby, R.L., Sato, J.D., Chapline, M.C., and Stanton, B.A. (2014). Serum and Glucocorticoid-Inducible Kinase1 Increases Plasma Membrane wt-CFTR in Human Airway Epithelial Cells by Inhibiting Its Endocytic Retrieval. *PLOS ONE* 9, e89599.
- Bruhn, M.A., Pearson, R.B., Hannan, R.D., and Sheppard, K.E. (2010). Second AKT: The rise of SGK in cancer signalling. *Null* 28, 394–408.
- Cazales, M., Schmitt, E., Montembault, E., Dozier, C., Prigent, C., and Ducommun, B. (2005). CDC25B Phosphorylation by Aurora A Occurs at the G2/M Transition and is Inhibited by DNA Damage. *Cell Cycle* 4, 1233–1238.
- Chen, W., Chen, Y., Xu, B., Juang, Y.-C., Stippec, S., Zhao, Y., and Cobb, M.H. (2009). Regulation of a Third Conserved Phosphorylation Site in SGK1 \*. *Journal of Biological Chemistry* 284, 3453–3460.
- Coleman, T.R., and Dunphy, W.G. (1994). Cdc2 regulatory factors. *Current Opinion in Cell Biology* 6, 877–882.
- Di Cristofano, A. (2017). SGK1: The Dark Side of PI3K Signaling. *Curr Top Dev Biol* 123, 49–71.
- Edson, M.A., Nagaraja, A.K., and Matzuk, M.M. (2009). The mammalian ovary from genesis to revelation. *Endocr Rev* 30, 624–712.
- Ferencova, I., Vaskovicova, M., Drutovic, D., Knoblochova, L., Macurek, L., Schultz, R.M., and Solc, P. (under revision). CDC25B is required for the metaphase I-metaphase II transition in mouse oocytes. *Journal of Cell Science*.
- Gautier, J., Minshull, J., Lohka, M., Glotzer, M., Hunt, T., and Maller, J.L. (1990). Cyclin is a component of maturation-promoting factor from *Xenopus*. *Cell* 60, 487–494.
- Hagting, A., Karlsson, C., Clute, P., Jackman, M., and Pines, J. (1998). MPF localization is controlled by nuclear export. *The EMBO Journal* 17, 4127–4138.
- Hiraoka, D., Aono, R., Hanada, S., Okumura, E., and Kishimoto, T. (2016a). Two new competing pathways establish the threshold for cyclin-B–Cdk1 activation at the meiotic G2/M transition. *J Cell Sci* 129, 3153–3166.
- Hiraoka, D., Aono, R., Hanada, S., Okumura, E., and Kishimoto, T. (2016b). Two new competing pathways establish the threshold for cyclin-B–Cdk1 activation at the meiotic G2/M transition. *J Cell Sci* 129, 3153–3166.
- Hiraoka, D., Hosoda, E., Chiba, K., and Kishimoto, T. (2019). SGK phosphorylates Cdc25 and Myt1 to trigger cyclin B–Cdk1 activation at the meiotic G2/M transition. *Journal of Cell Biology* 218, 3597–3611.
- Homer, H.A. (2020). The Role of Oocyte Quality in Explaining “Unexplained” Infertility. *Semin Reprod Med* 38, 21–28.

Hosoda, E., Hiraoka, D., Hirohashi, N., Omi, S., Kishimoto, T., and Chiba, K. (2019). SGK regulates pH increase and cyclin B–Cdk1 activation to resume meiosis in starfish ovarian oocytes. *J Cell Biol* 218, 3612–3629.

van den Hurk, R., and Zhao, J. (2005). Formation of mammalian oocytes and their growth, differentiation and maturation within ovarian follicles. *Theriogenology* 63, 1717–1751.

Kalous, J., Solc, P., Baran, V., Kubelka, M., Schultz, R.M., and Motlik, J. (2006). PKB/AKT is involved in resumption of meiosis in mouse oocytes. *Biology of the Cell* 98, 111–123.

Keefe, D., Kumar, M., and Kalmbach, K. (2015). Oocyte competency is the key to embryo potential. *Fertility and Sterility* 103, 317–322.

Kobayashi, T., and Cohen, P. (1999). Activation of serum- and glucocorticoid-regulated protein kinase by agonists that activate phosphatidylinositide 3-kinase is mediated by 3-phosphoinositide-dependent protein kinase-1 (PDK1) and PDK2. *Biochem J* 339 (Pt 2), 319–328.

Kobayashi, T., Deak, M., Morrice, N., and Cohen, P. (1999). Characterization of the structure and regulation of two novel isoforms of serum- and glucocorticoid-induced protein kinase. *Biochem J* 344 Pt 1, 189–197.

Koncicka, M., Tetkova, A., Jansova, D., Del Llano, E., Gahurova, L., Kracmarova, J., Prokesova, S., Masek, T., Pospisek, M., Bruce, A.W., et al. (2018). Increased Expression of Maturation Promoting Factor Components Speeds Up Meiosis in Oocytes from Aged Females. *International Journal of Molecular Sciences* 19, 2841.

Krisher, R.L. (2004). The effect of oocyte quality on development. *Journal of Animal Science* 82, E14–E23.

Lang, F., and Cohen, P. (2001). Regulation and Physiological Roles of Serum- and Glucocorticoid-Induced Protein Kinase Isoforms. *Sci. STKE* 2001, re17.

Lien, E.C., Dibble, C.C., and Toker, A. (2017). PI3K signaling in cancer: beyond AKT. *Curr Opin Cell Biol* 45, 62–71.

Lincoln, A.J., Wickramasinghe, D., Stein, P., Schultz, R.M., Palko, M.E., De Miguel, M.P.D., Tessarollo, L., and Donovan, P.J. (2002). Cdc25b phosphatase is required for resumption of meiosis during oocyte maturation. *Nat Genet* 30, 446–449.

del Llano, E., Masek, T., Gahurova, L., Pospisek, M., Koncicka, M., Jindrova, A., Jansova, D., Iyyappan, R., Roucova, K., Bruce, A.W., et al. (2020). Age-related differences in the translational landscape of mammalian oocytes. *Aging Cell* n/a, e13231.

Masek, T., Del Llano, E., Gahurova, L., Kubelka, M., Susor, A., Roucova, K., Lin, C.-J., Bruce, A.W., and Pospisek, M. (2020). Identifying the Translatome of Mouse NEBD-Stage Oocytes via SSP-Profiling; A Novel Polysome Fractionation Method. *Int J Mol Sci* 21, E1254.

Murray, J.T., Campbell, D.G., Morrice, N., Auld, G.C., Shpiro, N., Marquez, R., Pegg, M., Bain, J., Bloomberg, G.B., Grahammer, F., et al. (2004). Exploitation of KESTREL to identify NDRG family members as physiological substrates for SGK1 and GSK3. *Biochem J* 384, 477–488.

Norris, R.P., Ratzan, W.J., Freudzon, M., Mehlmann, L.M., Krall, J., Movsesian, M.A., Wang, H., Ke, H., Nikolaev, V.O., and Jaffe, L.A. (2009). Cyclic GMP from the surrounding somatic cells regulates cyclic AMP and meiosis in the mouse oocyte. *Development* 136, 1869–1878.

Okumura, E., Fukuhara, T., Yoshida, H., Hanada, S., Kozutsumi, R., Mori, M., Tachibana, K., and Kishimoto, T. (2002). Akt inhibits Myt1 in the signalling pathway that leads to meiotic G2/M-phase transition. *Nat Cell Biol* 4, 111–116.

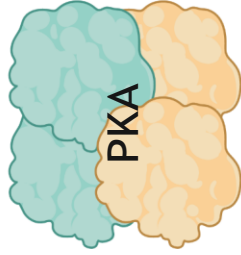
Pan, B., and Li, J. (2019). The art of oocyte meiotic arrest regulation. *Reproductive Biology and Endocrinology* 17, 8.

- Pirino, G., Wescott, M.P., and Donovan, P.J. (2009). Protein kinase A regulates resumption of meiosis by phosphorylation of Cdc25B in mammalian oocytes. *Cell Cycle* 8, 665–670.
- Potireddy, S., Vassena, R., Patel, B.G., and Latham, K.E. (2006). Analysis of polysomal mRNA populations of mouse oocytes and zygotes: Dynamic changes in maternal mRNA utilization and function. *Developmental Biology* 298, 155–166.
- Roberts, E.C., Shapiro, P.S., Nahreini, T.S., Pages, G., Pouyssegur, J., and Ahn, N.G. (2002). Distinct Cell Cycle Timing Requirements for Extracellular Signal-Regulated Kinase and Phosphoinositide 3-Kinase Signaling Pathways in Somatic Cell Mitosis. *Mol Cell Biol* 22, 7226–7241.
- Schmidt, M., Rohe, A., Platzer, C., Najjar, A., Erdmann, F., and Sippl, W. (2017). Regulation of G2/M Transition by Inhibition of WEE1 and PKMYT1 Kinases. *Molecules* 22, 2045.
- Sharma, A., Tiwari, M., Gupta, A., Pandey, A.N., Yadav, P.K., and Chaube, S.K. (2018). Journey of oocyte from metaphase-I to metaphase-II stage in mammals. *Journal of Cellular Physiology* 233, 5530–5536.
- Sherk, A.B., Frigo, D.E., Schnackenberg, C.G., Bray, J.D., Laping, N.J., Trizna, W., Hammond, M., Patterson, J.R., Thompson, S.K., Kazmin, D., et al. (2008). Development of a small-molecule serum- and glucocorticoid-regulated kinase-1 antagonist and its evaluation as a prostate cancer therapeutic. *Cancer Res* 68, 7475–7483.
- Solc, P., Saskova, A., Baran, V., Kubelka, M., Schultz, R.M., and Motlik, J. (2008). CDC25A phosphatase controls meiosis I progression in mouse oocytes. *Dev Biol* 317, 260–269.
- Tetkova, A., and Hancova, M. (2016). Mouse Oocyte Isolation, Cultivation and RNA Microinjection. *Bio-Protocol* 6, e1729.
- Tripathi, A., Kumar, K.V.P., and Chaube, S.K. (2010). Meiotic cell cycle arrest in mammalian oocytes. *Journal of Cellular Physiology* 223, 592–600.
- Xiao, L., Han, X., Wang, X., Li, Q., Shen, P., Liu, Z., Cui, Y., and Chen, Y. (2019). Spinal Serum- and Glucocorticoid-Regulated Kinase 1 (SGK1) Signaling Contributes to Morphine-Induced Analgesic Tolerance in Rats. *Neuroscience* 413, 206–218.
- Zeng, F., Baldwin, D.A., and Schultz, R.M. (2004). Transcript profiling during preimplantation mouse development. *Dev Biol* 272, 483–496.

Graphical abstract

GV

Cytoplasm

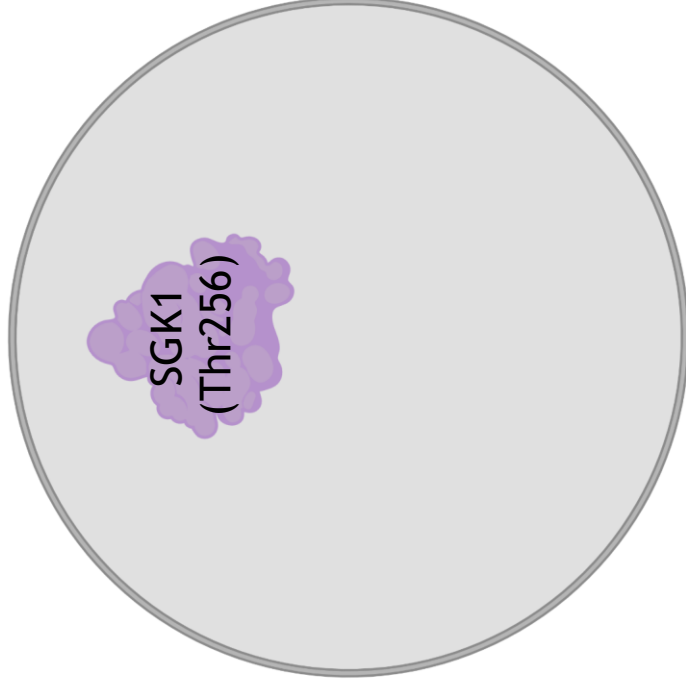


Ser321



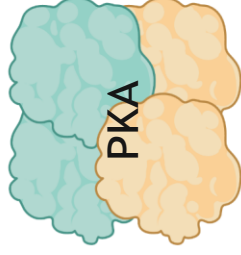
*Inactive*

Nucleus



NEBD

Cytoplasm



Ser321



*Inactive*

Nucleus

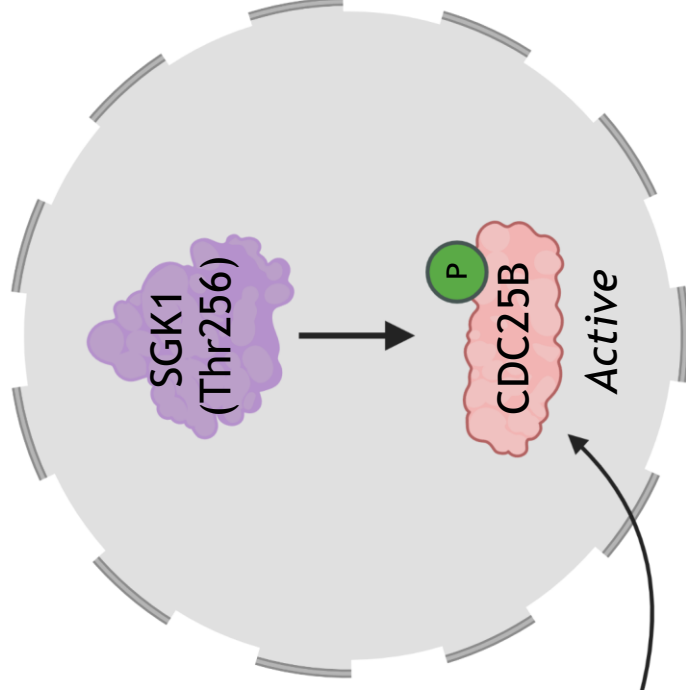
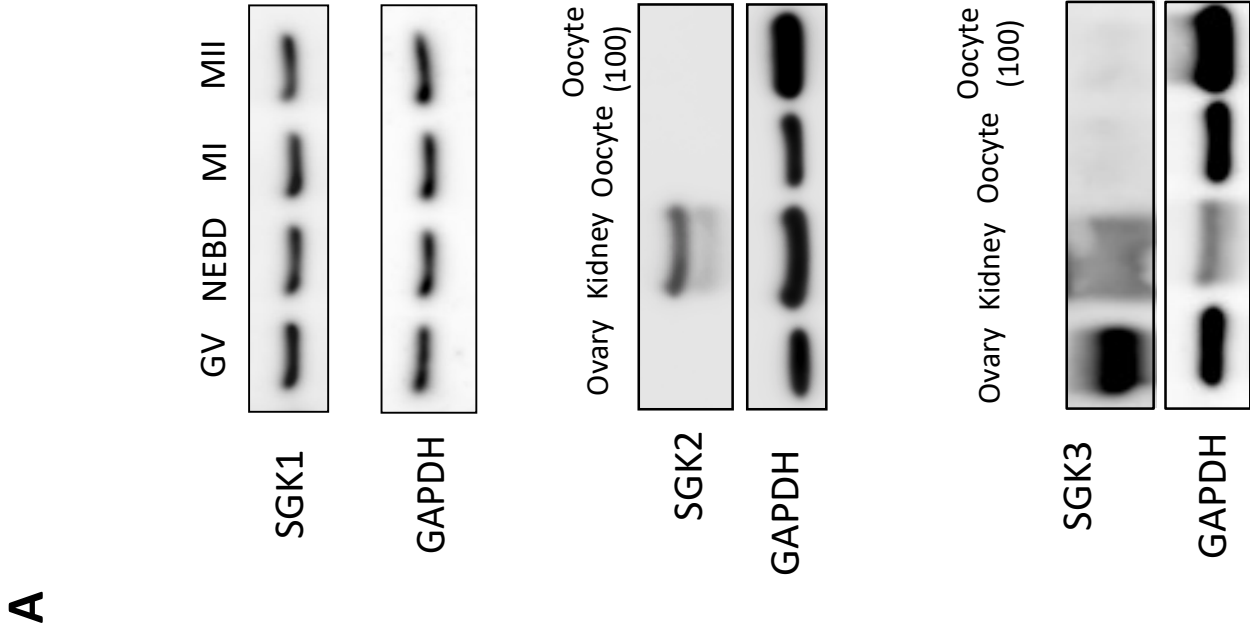
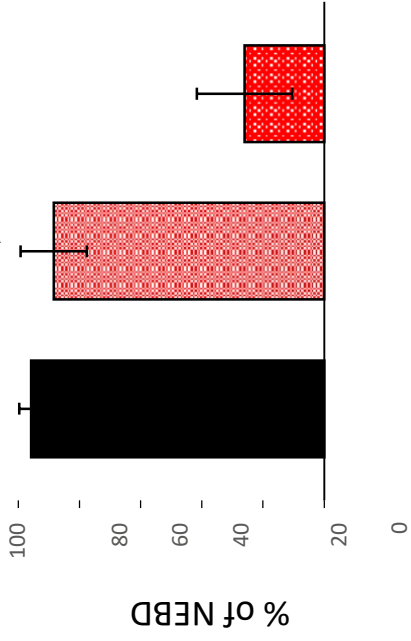




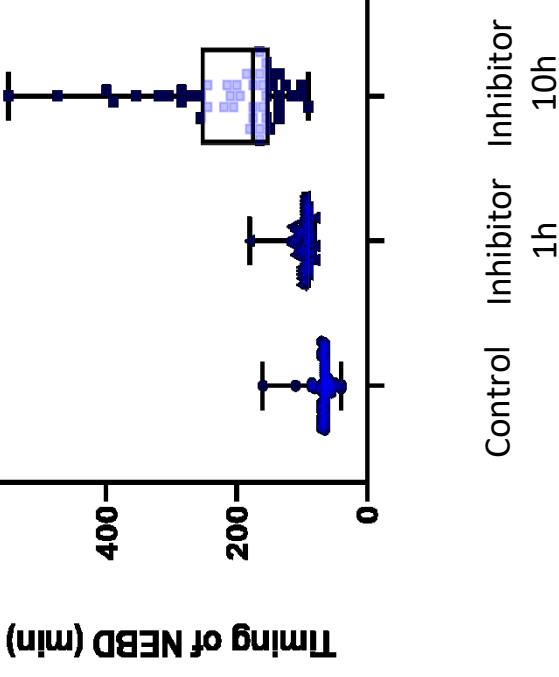
Figure 1



**B**



**C**



**D**

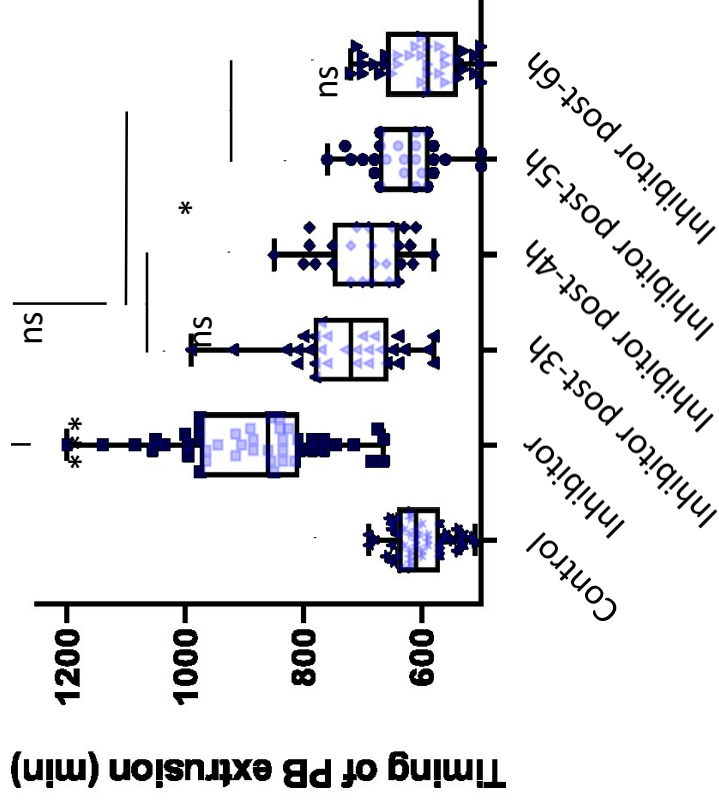
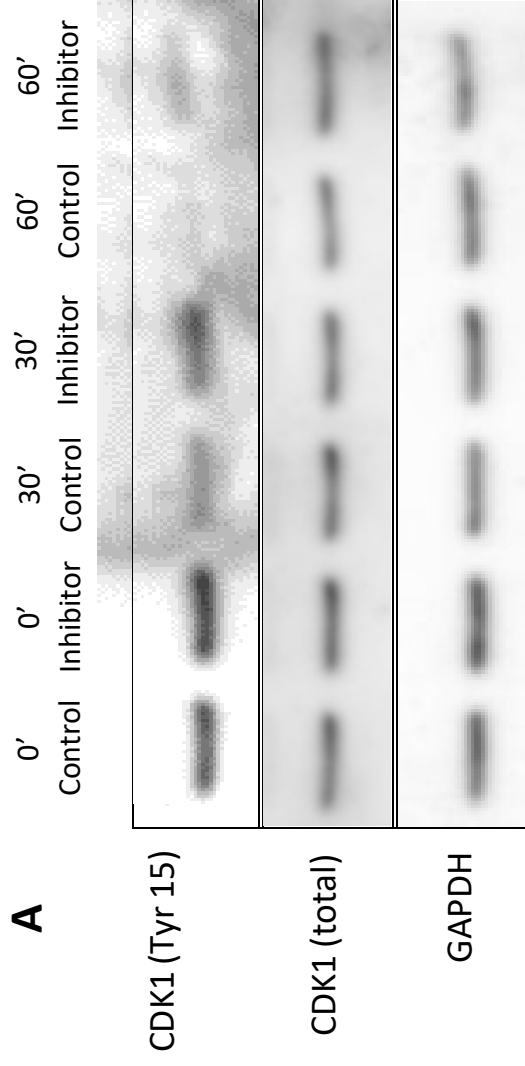
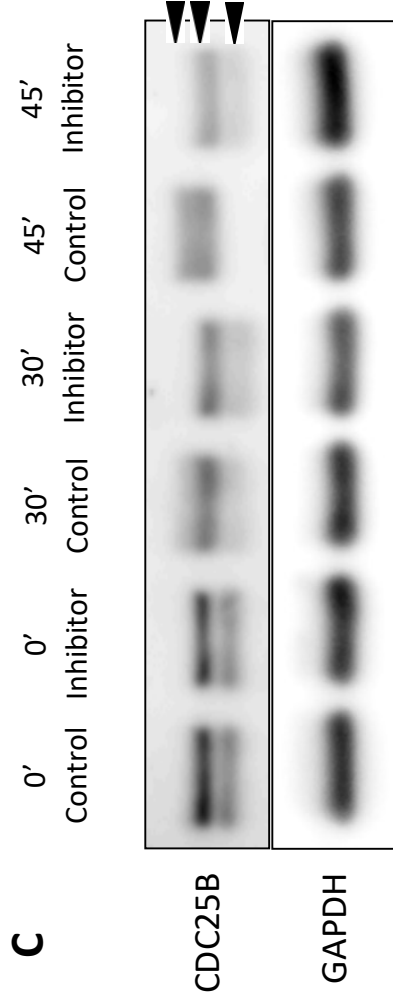
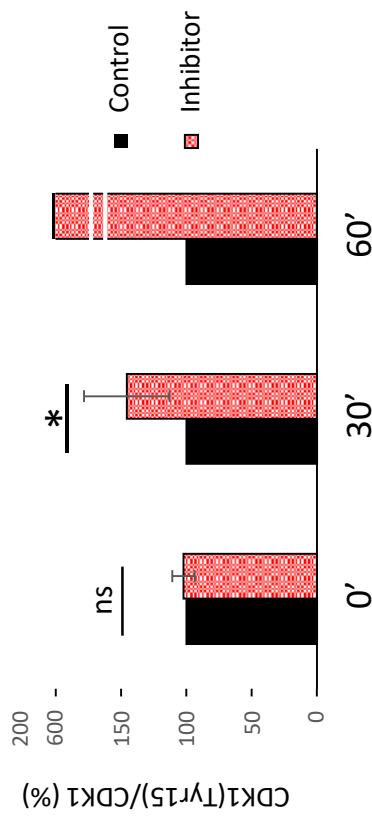




Figure 3



**B**



**D**

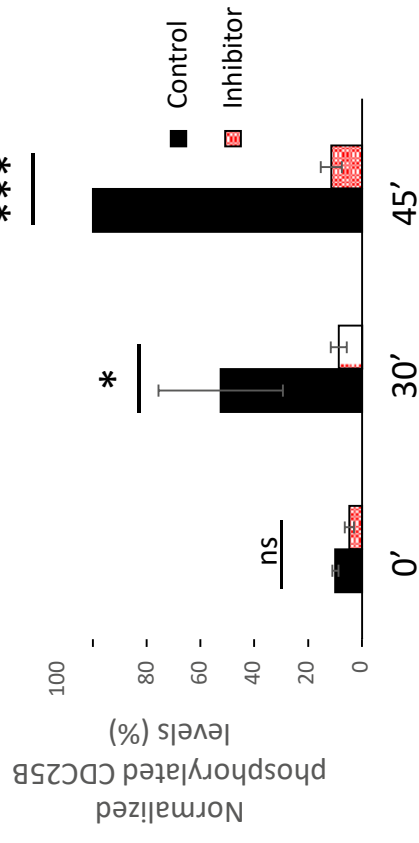
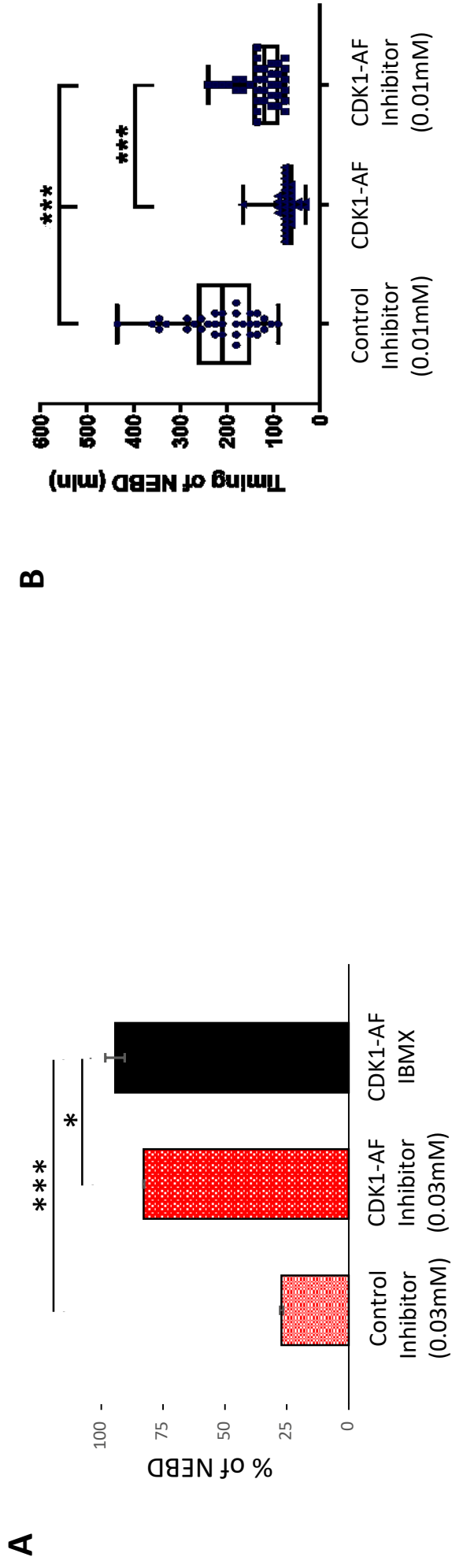
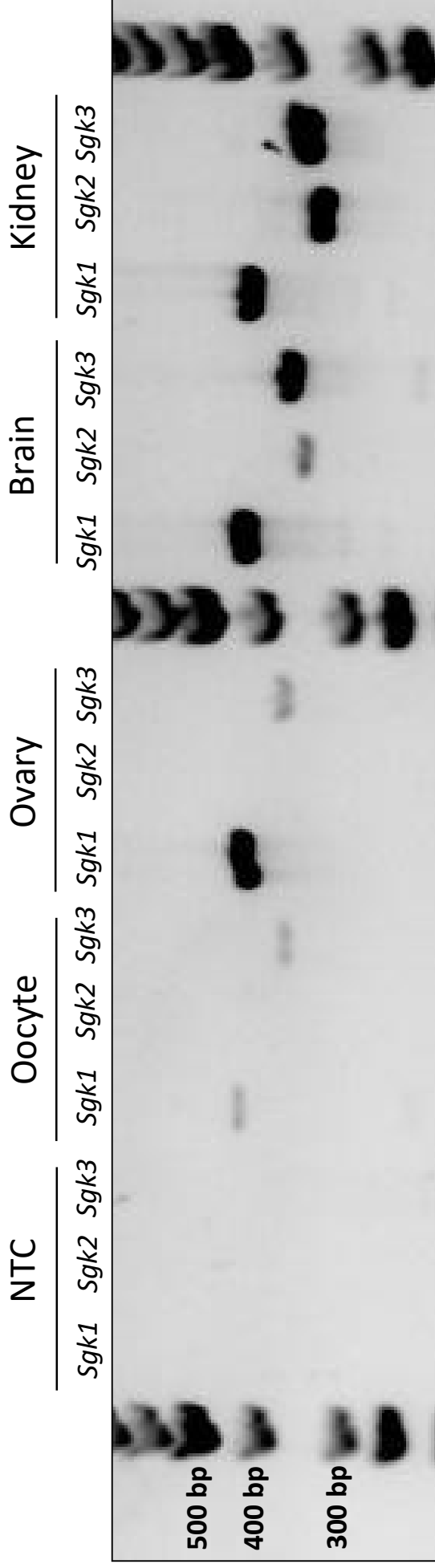


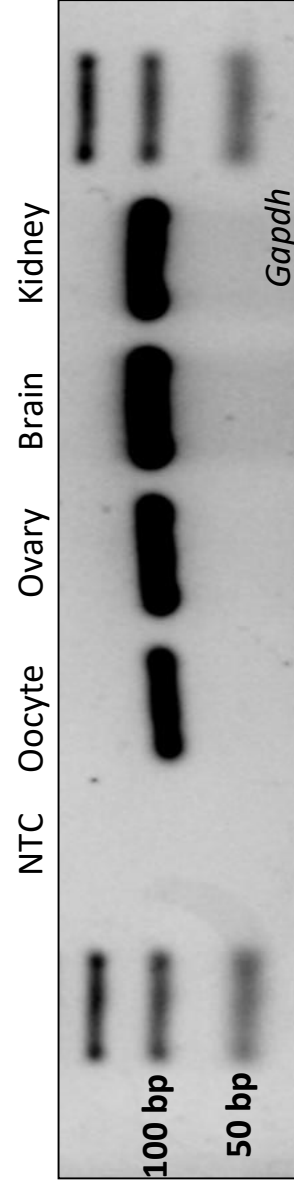
Figure 4



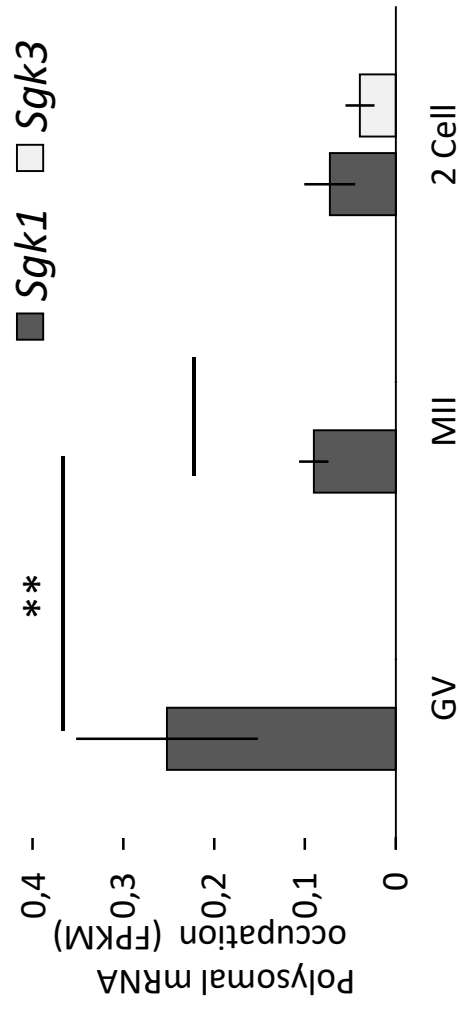
**A**

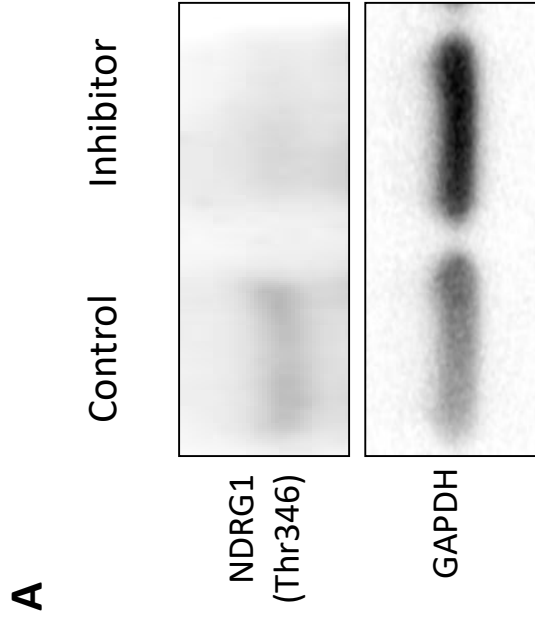


**B**

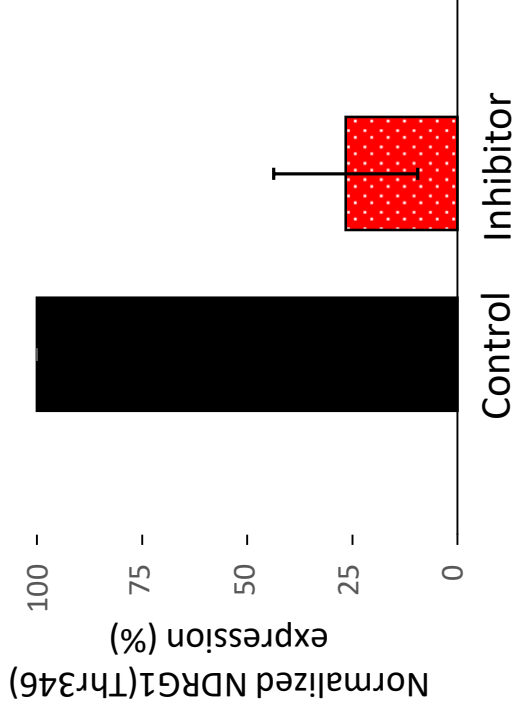


**C**

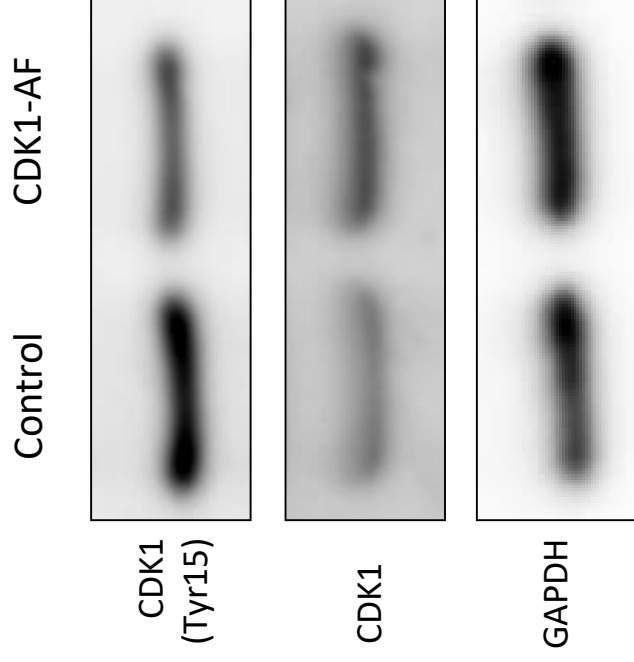




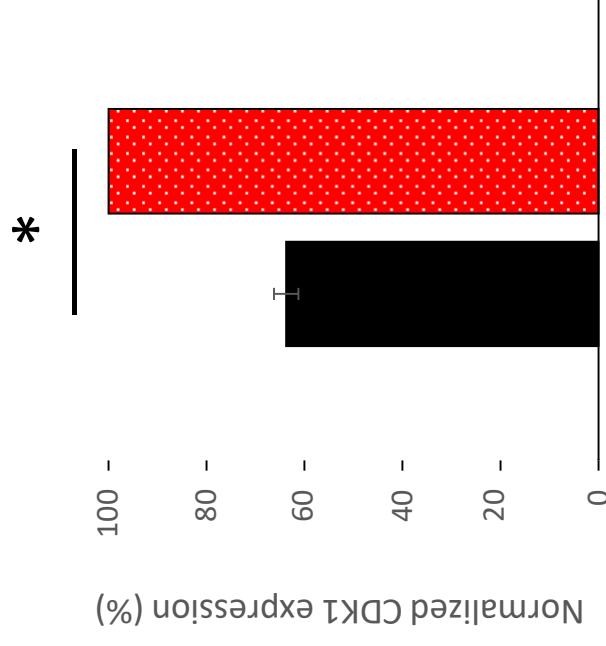
**B**



**A**



**B**





Supplementary Table 1

	Sseq (sequence similarities)	Sdom (domain interactions)	Snet (protein-protein homolog network)	Sall (score using all previous features)
SGK1 + CDC25B	0.9202	0.5146	0.8351	0.9357

**A**

Primers		
Name	Sequence	Accession number
Sgk1 - Forward	5'-GGTGCCAAGGATGACTTTATGG-3'	NM_001161845.2
Sgk1 - Reverse	5'-GGATCGAAGTGCCGAAGGTC-3'	
Sgk2 - Forward	5'-AGCCTTACGATCGAGCAGTG-3'	NM_013731.3
Sgk2 - Reverse	5'-AGCAGGTCCTTCCACGTTTG-3'	
Sgk3 - Forward	5'-GACCAACTGGAAATCCTCATGCT-3'	NM_133220.2
Sgk3 - Reverse	5'-CGGCATAAAACCTCGCTCTG-3'	
GAPDH - Forward	5'-TGGAGAAACCTGCCAAGTATG-3'	NM_001289726.1
GAPDH - Reverse	5'-GGTCCTCAGTGTAGCCCAAG-3'	

**B**

Antibodies		
Name (cat.#)	Company	Experiment
SGK1 (PA5-87746)	Thermo Fisher Scientific	WB
SGK2 (5595)	Cell Signalling	WB
Sgk3 (C-6; 166847)	Santa Cruz Biotechnology	WB
Sgk1(Thr256) (44-1260G)	Invitrogene	ICC
CDK1(Tyr15) (9111)	Cell Signalling	WB
CDC25B (326)	Santa Cruz Biotechnology	WB
NDRG1(Thr346) (3217)	Cell Signalling	WB
CDK1 (MA5-11472)	Thermo Fisher Scientific	WB
GAPDH (97166)	Cell Signalling	WB
GAPDH (G9545)	Sigma	WB